

**PREDICTIVE SIMULATION OF FLOW AND
SOLUTE TRANSPORT FOR MANAGING
THE COASTAL AQUIFER OF DAKSHINA
KANNADA DISTRICT, KARNATAKA, INDIA**

Thesis

**Submitted in partial fulfillment of the requirements for the
degree of**

DOCTOR OF PHILOSOPHY

By

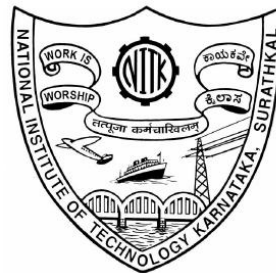
LATHASHRI. U. A

Under the guidance of

Dr. AMAI MAHESHA

Professor

Dept. of Applied Mechanics & Hydraulics
NITK, Surathkal



**DEPARTMENT OF APPLIED MECHANICS AND HYDRAULICS
NATIONAL INSTITUTE OF TECHNOLOGY KARNATAKA,
SURATHKAL, MANGALORE – 575 025**

MAY, 2016

D E C L A R A T I O N

By the Ph.D. Research Scholar

I hereby *declare* that the Research Thesis entitled **Predictive simulation of flow and solute transport for managing the coastal aquifer of the Dakshina Kannada district, Karnataka, India** which is being submitted to the **National Institute of Technology Karnataka, Surathkal** in partial fulfilment of the requirements for the award of the Degree of **Doctor of Philosophy in Applied Mechanics and Hydraulics Department** is a *bonafide report of the research work* carried out by me. The material contained in this Research Thesis has not been submitted to any University or Institution for the award of any degree.

AM11F07, LATHASHRI. U. A

(Register Number, Name & Signature of the Research Scholar)

Department of Applied Mechanics and Hydraulics

Place: NITK-Surathkal

Date:

C E R T I F I C A T E

This is to *certify* that the Research Thesis entitled **Predictive simulation of flow and solute transport for managing the coastal aquifer of the Dakshina Kannada district, Karnataka, India** submitted by LATHASHRI. U.A (Register Number: AM11F07) as the record of the research work carried out by her, is *accepted as the Research Thesis submission* in partial fulfilment of the requirements for the award of degree of **Doctor of Philosophy**.

Dr. Amai Mahesha

Professor

Research Guide

(Name and Signature with Date and Seal)

Chairman - DRPC

(Signature with Date and Seal)

ACKNOWLEDGEMENTS

I sincerely thank the Registrar and the Management of Manipal University for deputing me for doctoral research at NITK, Surathkal. I express my gratitude to the then Directors of MIT, Manipal, Dr. Kumkum Garg and Dr. Vinod V Thomas for giving me an opportunity to pursue higher studies. My thanks are due to the present Director Dr. G K Prabhu for his continuous encouragement.

I express my deep sense of gratitude to my supervisor, Dr. A Mahesha, Professor, Department of Applied Mechanics and Hydraulics, NITK Surathkal for his help and valuable suggestions throughout my research work. I also thank him for his in-time assessment and expert guidance in preparing the thesis and technical paper writing.

I am grateful to Research Progress Assessment Committee members, Prof. Kandasamy and Prof. Subba Rao, for their critical evaluation and useful suggestions during the progress of the work.

I thank the then Director of the NITK, Surathkal, Prof. Sawapan Bhattacharya, for granting me the permission to use the institutional infrastructure facilities, for the research work. I am greatly indebted to Prof. M. K. Nagaraj and Prof. Subba Rao, the former Heads of the Department of Applied Mechanics and Hydraulics, NITK, Surathkal, and Prof. Dwarakish G.S., the present Head of the Department, for granting me the permission to use the departmental facilities to the maximum extent, which was very vital for the completion of the this research.

I thank Mr. Jagadeesh, Foreman, Mr. Balakrishna, Programmer and all the teaching and non-teaching staff for their help. Also thanks to Mr. Ananda, Mr. Gopal and Mr. Harish, for their timely help in carrying out field work.

I sincerely acknowledge the assistance offered by technical support staff at support@aquaveo.com regarding the GMS software. I also thank Mr. S.K Chaurasia, Mr. Sachin M Patil and Mr. Kuldip Upasani from Aditi infotech, Nagpur for their timely help and service of the GMS software.

I wish to thank the reviewers of journals for their valuable and expert suggestions on the technical papers, which helped me in improving the presentation of my research findings in various aspects.

I express my gratitude to Mr. Kumar Raju B C, former research scholar for his help, particularly in carrying out DGPS survey. Thanks to all my friends at NITK for their co-operation and for making the moments spent at NITK memorable.

I sincerely thank Dr. Gicy M Kovoor, the then Head of the Department of Civil Engineering, MIT for facilitating me the provision granted by the Manipal University for higher studies. I also thank Dr. K Narayan Shenoy, the then Head of the Department and Dr. Mohandas Chadaga the present Head of the Department of Civil Engineering, MIT for their constant support during my studies.

Thanks are outstanding to all the teaching and non-teaching staff of MIT, Manipal for their help and co-operation. My special thanks to Dr. Balakrishna Rao and Dr. Asha U Rao, Professors at the Department of Civil Engineering, MIT Manipal for accelerating me towards the completion of my research work.

My heartfelt thanks are due to my beloved parents, brother and all the family members who always blessed and supported me to every success in life. My thanks are due to my mother-in-law for having very patiently taken care of my daughter and household during my research tenure. Special thanks are due to my husband, Shivaprasad for his moral support. Thanks to my little daughter Dhrithi for having missed my love and care during her special moments in her early childhood without complaints.

I thank my cousin brother Mr. Manish KV for helping me in formatting this thesis.

Thanks are to all those who directly or indirectly helped me during my research.

Finally, thanks to the almighty God for blessing me with good health and ability to work hard with lot of patience.

Lathashri. U.A

ABSTRACT

The present investigation is intended to simulate the response of an unconfined, shallow, tropical coastal aquifer to anticipated future stress scenarios due to developmental activities and climate change effect. The simulation of groundwater flow and solute transport are carried out using SEAWAT. The model is applied to the coastal basin of Dakshina Kannada district of Karnataka state, India having an areal extent of about 155 km² in. The study area is divided into four sub-basins for the simulation considering the natural boundaries. They are the basins between Shambhavi river and Pavanje river (sub-basin 1), Pavanje river and Gurpur river (sub-basin 2), Gurpur river and Netravathi river (sub-basin 3), Netravathi river and Talapady river (sub-basin 4).

It is learnt from the field investigations that, the basin is predominantly an unconfined aquifer with depth ranging from 12m to 30m. The region is mainly covered by the lateritic formation below the top soil. The aquifer profiling was plotted based on the vertical electrical sounding. The aquifer parameters are estimated based on pumping test results. Nine aquifer hydraulic parameter zones are mapped for each basin based on pumping tests evaluations. The transmissivity values range from 10 to 1440 m²/day.

The numerical simulation of groundwater flow was carried out by building a MODFLOW model to the basin and the transport parameters are assigned to execute the MT3DMS model. Finally, the SEAWAT model which is a coupled version of MODFLOW and MT3DMS designed to simulate three-dimensional, variable density groundwater flow and multi-species transport is developed. The model of each sub-basin has two dimensional grids in the horizontal plane with an approximate cell dimension of 100×100m with a single vertical layer. The digital elevation model (DEM) developed for the study area is interpolated to the top elevation of the model grid. The base of the model layer is set at -30m (with respect to mean sea level), which corresponds to the base of the shallow unconfined aquifer. The recharge is assigned on the upper-most active (wet) layer of the model during the monsoon

season (June to September). A total of 587, 730, 835 and 996 wells are introduced in the agricultural area of sub-basin 1, 2, 3 and 4 respectively, based on the village wise installation of irrigation pump set data. The draft per well is assigned based on the water requirement of crops, i.e. evapo-transpiration in the absence of actual data. A constant concentration of TDS 35kg/m^3 is specified to the model cells along the western boundary (Arabian sea). For rivers, TDS = 35 kg/m^3 and 17.5kg/m^3 are considered during the non-monsoon (October to May) and monsoon (June to September) respectively considering the quantum of mixing of freshwater and seawater.

The model is calibrated from September 2011 to August 2013 using observed groundwater heads and salinity data obtained from 29 observation wells. In the present study, PEST is used to calibrate the model. The total simulation period of two years has been divided into 24 stress periods. Daily time step has been considered for the transient simulation applying all the hydro-geologic conditions of the same period. The model is validated for the following year (2013-14). Both the flow and transport model performance during the monsoon (June to Sept) is not up to the mark, with all the three evaluation techniques (R^2 , RMSE and NSE) showing deviation from the desired levels. Overall, the model performance is satisfactory with $\text{NSE} \geq 0.5$.

The calibrated values of horizontal hydraulic conductivity and specific yield of the unconfined aquifer range from 1.85m/day to 49.50 m/day and 0.006 to 0.281. These values agree with the range established by the aquifer characterization studies carried out earlier. Also, recharge co-efficient of 20% of rainfall, porosity of 30% and river bed conductance of 10 m/day are obtained as appropriate parameters during the calibration process. The longitudinal dispersivity of 35m, transverse dispersivity of 3.5m and molecular diffusion co-efficient of $8.64 \times 10^{-5}\text{m}^2/\text{day}$ are achieved.

The spatial distribution map of groundwater table shows a gradually increasing trend from the coastline and the rivers towards the landward side (high elevated area). The water table rises to maximum elevation of about 43m (above msl) in sub-basin 1 and 3. The month of May is visibly drier than the month of August, with the lowest groundwater level contour moving towards inland by about 200m to 900m in comparison with that during the monsoon. Water balance study shows that, more than

75% of available water is being discharged to the sea during the wet season compared to that during the dry season throughout the coastline. The river Gurupur contributes hugely to the aquifer throughout the calibration period. This is due to the fact that the area surrounding the river is a low lying marshy land.

The management of freshwater aquifers within 1 km from the sea is of prime importance for sustainability against seawater intrusion. The salinity distribution across the study area for sub-basins 1, 2, 3 and 4 during the month of May 2013 shows a similar pattern in all the four sub-basins. An important outcome is that, the rivers that surround the system on the north and the south sides contribute equally as that of the sea in bringing in salinity into the aquifer. The TDS values are within 0.5 kg/m^3 throughout the year, except that for well nos. 1, 15 and 25. It is essential to note that, all these wells are very close to the rivers (less than 300 m).

The sensitivity analysis results clearly show that, the overall aquifer system is sensitive to hydraulic conductivity, groundwater draft and recharge rate. The model is sensitive to lower values of hydraulic conductivity (0.46 m/day to 12.40 m/day) and higher values of recharge rate (28 mm/day). The results also show that, the lateral movement of water from the river causes the adjoining area to respond differently to changes in the parameters than away from it. No significant influence of river bed conductance on the water table elevation was noticed over in the entire area except that in sub-basin 1 and zones adjacent to the river flow. The aquifer was found to be least sensitive to dispersivity, with the movement of salinity contour by just 10m for every increase in 25% of the dispersivity value.

The area under consideration is recently experiencing exponential growth in terms of urbanization, industrialization and other developmental activities. Hence, in order to understand the response of the coastal unconfined aquifer to varied overdraft and recharge scenarios, the SEAWAT is used to simulate over a considerably longer period of 20 years (2014 to 2034). The fresh water drafts considered are symbolic in nature and in this work, only electrically operated pumping units are accounted since data on other wells are not available. Also, to account for soils with low permeability, and decrease in rainfall, effect of decrease in recharge rate is also investigated. Accordingly, five scenarios are planned for investigation. Scenario 1 represents

existing abstraction rate, calibrated recharge rate and no sea level rise. Scenario 2 considers decrease in recharge rate by 50% with other parameters same as scenario 1. Scenario 3 simulates effect of varied freshwater draft of 50%, 100% and 150% of existing draft rate for the wells (case 1, 2 and 3 respectively). Scenario 4, is a combined case of scenarios 2 and 3. And finally, scenario 5 is scenario 4 with sea level rise of 1mm/year.

When all the scenarios are compared, the water table is estimated to fall by 0.3m to 0.6 m compared to scenario 1. The study shows that, the decrease in recharge rate (scenario 2) alone can raise the TDS to 5kg/m^3 in the first 8 years of simulation. However, with the present rate of groundwater utilization and recharge rate, the aquifer can be considered safe for the next 16 years with $\text{TDS} < 1.5 \text{ kg/m}^3$. Every 50% increase in groundwater utilization causes the salinity to increase steeply with every year of simulation till the end. Hence, except scenario 1 and scenario 3 (case 1), the remaining scenarios lead to the salinity above the drinking water standards ($\text{TDS} > 1.5 \text{ kg/m}^3$), by 6 years of operation.

To study the spatial effect on water table and advancement of salinity into the aquifer from the coastline, well hydrographs and salinity at every 200m distance from the coastline are investigated. As per the analysis, the aquifer beyond 200m from the sea is safe ($\text{TDS} < 1.5\text{kg/m}^3$) against seawater intrusion for scenarios 1, 2 and 3. Only due to scenario 4 (case 2 and 3), the seawater intrudes beyond 600 m up to 1200m making the aquifer unsafe for utilization. The percentage area affected by seawater intrusion due to different anticipated scenarios are estimated. Scenario 4 (case 3) is considered to be the most unfavourable condition, with water quality becoming unfit for drinking purpose over more than 35% area ($\text{TDS} > 1.5\text{kg/m}^3$). However, with the present stress conditions continuing for the next 20 years, less than 10% of the total area is predicted to be with $\text{TDS} > 1.5 \text{ kg/m}^3$. But, overdraft by three times the present rate i.e. scenario 3 (case 3) may increase the salinity beyond 10% for sub-basins 1 and 2. In the case of sub-basin 3, the water table falls by about 1.5m for every 50% increase in the groundwater utilization rate, which is less than 1 m for the rest of the basins. The simulation results for this basin show that, the wells within 500m from the sea and rivers are highly saline with $\text{TDS} > 3\text{kg/m}^3$ which was also confirmed with field

observations. In addition, simulations are carried out to estimate the effect of climate change on seawater intrusion by considering anticipated sea level rise. The anticipated sea level rise of 1mm/year along the coastline has negligible influence on groundwater and salinity of the study area.

Key words: Seawater intrusion, SEAWAT, Aquifer charecterization, Pumping tests, Coastal aquifer, Freshwater, MODFLOW, Solute transport, Groundwater modeling, Predictive simulation.

CONTENTS

ABSTRACT.....	i
CONTENTS.....	vi
LIST OF FIGURES.....	x
LIST OF TABLES.....	xvii
CHAPTER 1 INTRODUCTION.....	1
1.1 General	1
1.2 Mecahnism of saltwater intrusion	2
1.3 Groundwater modeling.....	3
1.4 Scope of the work.....	5
1.5 Research objectives	7
1.6 Overview of research work	7
1.7 Description of the study area.....	9
1.7.1 General	9
1.7.2 Topography	11
1.7.3 Climate and rainfall.....	13
1.7.4 Drainage characteristics	14
1.7.5 Soil	15
1.7.6 Land use and land cover.....	17
1.8 Organization of the thesis.....	19
CHAPTER 2 LITERATURE REVIEW.....	20
2.1 General	20
2.2 Aquifer charecterization.....	20
2.3 Groundwater modeling.....	22
2.4 Groundwater flow model	22
2.5 Solute transport model	30
2.5.1 General	30
2.5.2 Hypothetical models	31
2.5.3 Case specific models.....	33

2.6 Literature gap	39
CHAPTER 3 AQUIFER CHARACTERIZATION	40
3.1 General	40
3.2 Hydrogeology.....	40
3.2.1 Bore-log information.....	41
3.2.2 Lithology map	42
3.2.3 Vertical electrical sounding survey	44
3.3 Pumping tests	46
3.3.1 General	46
3.3.2 Methodology	46
3.3.3 Analysis of pumping test data	52
3.3.4 Results and discussion	59
3.4 Aquifer parameters	71
3.5 Closure	75
CHAPTER 4 GROUNDWATER FLOW MODEL.....	76
4.1 General	76
4.2 Overall program structure	77
4.3 Governing equation	80
4.4 Modeling approach.....	82
4.4.1 Data	83
4.4.2 Discretization of the basin.....	83
4.4.3 Hydrologic sources and sinks.....	84
4.4.4 Boundary conditions	89
4.4.5 Initial conditions	96
4.5 Model calibration	97
4.5.1 Observation wells.....	98
4.5.2 Steady state calibration	100
4.5.3 Transient calibration.....	101
4.6 Model validation	110
4.7 Model applications	111
4.7.1 Water balance.....	111

4.7.2 River aquifer interaction	114
4.8 Sensitivity analysis	119
4.8.1 General	119
4.8.2 Methodology	119
4.8.3 Results and discussion	120
4.8.3.1 Parameter sensitivities.....	125
4.8.3.2 Aquifer sensitivity to hydrological stresses	126
4.9 Closure	127
CHAPTER 5 SOLUTE TRANSPORT MODEL	129
5.1 General	129
5.2 Concepts and principles of SEAWAT approach.....	130
5.2.1 Basic description of the model	130
5.2.2 Generalized program structure of SEAWAT	132
5.2.3 Concept of equivalent freshwater head	133
5.2.4 Governing equation	135
5.3 Application to the study area.....	137
5.3.1 Similarity with the groundwater flow model	137
5.3.2 Boundary conditions	137
5.3.3 Initial conditions	138
5.3.4 Transport and density parameters	138
5.4 Model calibration	139
5.4.1 Calibration for flow parameters	139
5.4.2 Calibration for transport parameters	140
5.5 Model validation	145
5.6 Sensitivity analysis	146
5.7 Closure	148
CHAPTER 6 PREDICTIVE SIMULATIONS	149
6.1 General	149
6.2 Description of the scenarios	150
6.3 Results and Discussion.....	152
6.3.1 Temporal impacts of scenario simulation on the aquifer	152

6.3.2 Spatial impacts of scenario simulation on the aquifer	156
6.4 Variation of salinity and water table across the study area.....	169
6.5 Percentage area affected by seawater intrusion	174
6.6 Closure	175
CHAPTER 7 SUMMARY AND CONCLUSIONS.....	177
REFERENCES	184
APPENDIX	209
PUBLICATIONS	224
BIODATA	225

LIST OF FIGURES

Fig. 1.1 Flow chart of methodogoly in the present study	8
Fig. 1.2 Map of the study area	10
Fig. 1.3 Topography of the study area	12
Fig. 1.4 Monthly rainfall at NITK, Surathkal (1997-2012).....	13
Fig. 1.5 Drainage network of the study area.....	15
Fig. 1.6 Soil class map of the study area.....	16
Fig. 1.7 Land use land cover map of the study area	18
Fig. 3.1 Locations of borelog and VES survey.....	41
Fig. 3.2 Lithology of borelogs	42
Fig. 3.3 Lithology map of the study area	43
Fig. 3.4 Hydrogeological profile as per VES.....	45
Fig. 3.5 Photograph of pumping well no. PW1	47
Fig. 3.6 Photograph of pumping well no. PW2	48
Fig. 3.7 Photograph of pumping well no. PW3	48
Fig. 3.8 Measurements for determining the discharge (a) horizontal and (b) inclined pipe	49
Fig. 3.9 Discharge measurement in the field using (a) collecting tank (b) trajectory method.....	49
Fig. 3.10 Curves for determining C and F for estimation of flow through inclined and horizontal pipes.....	50

Fig. 3.11 Theis type curve for $W(u)$ verses u $W(u)$ verses $1/u$	54
Fig. 3.12 Type curve and data plot of t verses s of observation well for Theis method of analysis (Kruseman and de Ridder , 1994)	55
Fig. 3.13 Type curves for fully penetrating wells (Neuman, 1975).....	58
Fig. 3.14 Graph of drawdown and recovery versusu time for pumping well no.s PW1, PW2 and PW3	65
Fig. 3.15 Time-drawdown graph of well no. PW1 by Neuman(1974) method	67
Fig. 3.16 Time-drawdown graph of well no. PW1 by Theis (1935) method.....	67
Fig. 3.17 Time-drawdown graph of well no. PW1 by Tartakovsky-Neuman(2007) method	68
Fig. 3.18 Time-drawdown graph of well no. PW2 by Neuman(1974) method	68
Fig. 3.19 Time-drawdown graph of well no. PW2 by Theis (1935) method.....	69
Fig. 3.20 Time-drawdown graph of well no. PW2 by Tartakovsky-Neuman(2007) method	69
Fig. 3.21 Time-drawdown graph of well no. PW3 by Neuman(1974) method	70
Fig. 3.22 Time-drawdown graph of well no. PW3 by Theis (1935) method.....	70
Fig. 3.23 Time-drawdown graph of well no. PW3 by Tartakovsky-Neuman(2007) method	71
Fig. 3.24 Aquifer property zonation map of sub-basins 1 and 2.....	73
Fig. 3.25 Aquifer property zonation map of sub-basins 3 and 4.....	74
Fig. 4.1 Flow chart for the overall program structure of MODFLOW (McDonald and Harbaugh, 1988)	78
Fig. 4.2 Finite difference grid (Harbaugh, 2000).....	82

Fig. 4.3A Village map of sub-basin 1, and 2	88
Fig. 4.3B Village map of sub-basin 4.	89
Fig. 4.4 Model representation of sub-basin1	90
Fig. 4.5 Model representation of sub-basin 2	91
Fig. 4.6 Model representation of sub-basin 3	92
Fig. 4.7 Model representation of sub-basin 4	93
Fig. 4.8 Representation of river in MODFLOW	95
Fig. 4.9 Scatter plot of steady state calibration	101
Fig. 4.10 Simulated and observed groundwater heads (2011-13) for (A) post- monsoon, (B) pre-monsoon and (C) monsoon seasons for sub-basin 1 and that for sub-basin 2 (D), (E) and (F) respectively	105
Fig. 4.11 Simulated and observed groundwater heads (2011-13) for (A) post- monsoon, (B) pre-monsoon and (C) monsoon seasons for sub-basin 3 and that for sub-basin 4 (D), (E) and (F) respectively	106
Fig. 4.12 Simulated and observed groundwater heads during the calibration period for (A) well no.7 (B) well no.8 (C) well no.21 (D) well no.22 (E) well no.26 and (F) well no.28	107
Figure 4.13 Groundwater flow contours for (A) May 2013 and (B) August 2013 for sub-bainn 1.....	108
Figure 4.14 Groundwater flow contours for (A) May 2013 and (B) August 2013 for sub-bainn 2.....	109
Figure 4.15 Groundwater flow contours for (A) May 2013 and (B) August 2013 for sub-bainn 3.....	109

Figure 4.16 Groundwater flow contours for (A) May 2013 and (B) August 2013 for sub-basin 4.....	110
Fig. 4.17 Simulated and observed groundwater heads (2013-14) for (A) sub-basin 1 (B) sub-basin 2 (C) sub-basin 3 (D) sub-basin 4.....	111
Fig. 4.18 Schematic representation of water budget of the coastal aquifer of Dakshina Kannada.....	113
Fig. 4.19 Representation of river-aquifer interaction in MODFLOW.....	116
Fig. 4.20 River flow rate during the calibration period (2011-13) in sub-basin 1	117
Fig. 4.21 River flow rate during the calibration period (2011-13) in sub-basin 2	117
Fig. 4.22 River flow rate during the calibration period (2011-13) in sub-basin 3	118
Fig. 4.23 River flow rate during the calibration period (2011-13) in sub-basin 4	118
Fig. 4.24 Dot plot for zone 7 of sub-basin 1 considering (A) hydraulic conductivity (B) specific yield (C) recharge (D) river bed conductance	121
Fig. 4.25 Dot plot for zone 4 of sub-basin 2 considering (A) hydraulic conductivity (B) specific yield (C) recharge (D) river bed conductance	122
Fig. 4.26 Dot plot for zone 5 of sub-basin 3 considering (A) hydraulic conductivity (B) specific yield (C) recharge (D) river bed conductance	123
Fig. 4.27 Dot plot for zone 7 of sub-basin 4 considering (A) hydraulic conductivity (B) specific yield (C) recharge (D) river bed conductance	124
Fig. 4.28 Plot of sensitivity index (SI) as a function of percentage change in (A) hydraulic conductivity (B) specific yield (C) recharge rate	125

Fig. 5.1 Generalized flow chart of SEAWAT program (Guo and Langevin, 2002)	133
Fig. 5.2 Experimental set-up to illustrate the concept of equivalent freshwater head (Guo and Langevin, 2002).....	134
Fig. 5.3 Simulated groundwater heads at the end of the transient calibration by (a) MODFLOW (b) SEAWAT.....	140
Fig. 5.4 Simulated and observed TDS values (2011-13) for (A) post-monsoon, (B) pre-monsoon and (C) monsoon seasons for sub-basin 1 and that of sub- basin 2 (D), (E) and (F) respectively.....	142
Fig. 5.5 Simulated and observed TDS values (2011-13) for (A) post-monsoon, (B) pre-monsoon and (C) monsoon seasons for sub-basin 3 and that of sub- basin 4 (D), (E) and (F) respectively.....	144
Fig. 5.6 Plan view of the simulated salinity distribution in the study area during the month of May 2013.....	145
Fig. 5.7 Spatial distribution of saline concentration as simulated by SEAWAT along a part of the coastline during the year 2013 for increase of the longitudinal dispersivity by (A) 25% (B) 50% and (C) 75%.....	147
Fig. 6.1 Variation of groundwater table over 20 year period during the month of May.....	153
Fig. 6.2 Variation of groundwater table over 20 year period during the month of September.....	154
Fig. 6.3 Variation of water table elevation over 20 year period at a grid 700m from the coastline and 300m from river Shambhavi.....	154
Fig. 6.4 Variation of groundwater salinity over 20 year period for different scenario simulations.....	156

Fig. 6.5 Spatial distribution of water table in sub-basin 1 for (A) scenario 1 (B) scenario 2 (C) scenario 3 (case 3) and (D) scenario 4 (case 3) at the end of 20 year simulation	161
Fig. 6.6 Spatial distribution of water table in sub-basin 2 for (A) scenario 1 (B) scenario 2 (C) scenario 3 (case 3) and (D) scenario 4 (case 3) at the end of 20 year simulation	162
Fig. 6.7 Spatial distribution of water table in sub-basin 3 for (A) scenario 1 (B) scenario 2 (C) scenario 3 (case 3) and (D) scenario 4 (case 3) at the end of 20 year simulation	163
Fig. 6.8 Spatial distribution of water table in sub-basin 4 for (A) scenario 1 (B) scenario 2 (C) scenario 3 (case 3) and (D) scenario 4 (case 3) at the end of 20 year simulation	164
Fig. 6.9 Spatial distribution of salinity in sub-basin 1 for (A) scenario 1 (B) scenario 2 (C) scenario 3 (case 3) and (D) scenario 4 (case 3) at the end of 20 year simulation	166
Fig. 6.10 Spatial distribution of salinity in sub-basin 2 for (A) scenario 1 (B) scenario 2 (C) scenario 3 (case 3) and (D) scenario 4 (case 3) at the end of 20 year simulation	167
Fig. 6.11 Spatial distribution of salinity in sub-basin 3 for (A) scenario 1 (B) scenario 2 (C) scenario 3 (case 3) and (D) scenario 4 (case 3) at the end of 20 year simulation	168
Fig. 6.12 Spatial distribution of salinity in sub-basin 4 for (A) scenario 1 (B) scenario 2 (C) scenario 3 (case 3) and (D) scenario 4 (case 3) at the end of 20 year simulation	169
Fig. 6.13 Salinity profile at the end of 20 year simulation period along a horizontal cross section at every 200m interval from the coastline for simulation of (A) scenario 1 (B) scenario 2 (C) scenario 3 (case 1) and (D) scenario 3	

(case 2) (E) scenario 3 (case 3) (F) scenario 4 (case 1) (G) scenario 4
 (case 2) (H) scenario 4 (case 3) 171

Fig. 6.14 Water table profile at the end of 20 year simulation period along a horizontal cross section at every 200m interval from the coastline during the month of September for simulation of (A) scenario 1 (B) scenario 2 (C) scenario 3 (case 1) and (D) scenario 3 (case 2) (E) scenario 3 (case 3) (F) scenario 4 (case 1) (G) scenario 4 (case 2) (H) scenario 4 (case 3)... 172

Fig. 6.15 Water table profile at the end of 20 year simulation period along a horizontal cross section at every 200m interval from the coastline during the month of May for simulation of (A) scenario 1 (B) scenario 2 (C) scenario 3 (case 1) and (D) scenario 3 (case 2) (E) scenario 3 (case 3) (F) scenario 4 (case 1) (G) scenario 4 (case 2) (H) scenario 4 (case 3)... 173

Fig. 6.16 Bar graph of percentage area affected by seawater intrusion due to different anticipated scenarios in (A) sub-basin 1 (B) sub-basin 2 (C) sub-basin 3 and (D) sub-basin 4..... 174

LIST OF TABLES

Table 1.1 Soil type classification	17
Table 3.1 Lithological classification.....	43
Table 3.2 Details of the pumping wells	47
Table 3.3 Time-drawdown and recovery data for well no.PW1	59
Table 3.4 Time-drawdown and recovery data for well no.PW2.....	61
Table 3.5 Time-drawdown and recovery data for well no.PW3.....	63
Table 3.6 Transmissivity and storage parameters obtained from pumping test analysis	66
Table 3.7 Initial aquifer parameters	72
Table 4.1 The MODFLOW packages used for groundwater flow simulation	79
Table 4.2 Availability of water table and salinity data in the study area.....	83
Table 4.3 Model discretization	84
Table 4.4 Village-wise details of pumping rates	87
Table 4.5 Details of observation wells.....	99
Table 4.6 Optimal parameter values obtained after seasonal calibration	102
Table 4.7 Zonewise optimal parameter values obtained after seasonal calibration....	102
Table 4.8 Groundwater flow model efficiency values on monthly basis during 2011- 13.....	104
Table 4.9 Groundwater flow model efficiency values on monthly basis during 2013- 14.....	111

Table 4.10 Volumetric water budget	113
Table 4.11 Ranking of sensitivity classes (Lenhart et al.,2002)	120
Table 5.1 The MT3DMS packages used for transport simulation in the study	131
Table 5.2 Solute transport parameters	142
Table 5.3 SEAWAT model efficiency values on monthly basis during 2011-13	143
Table 6.1 Water table elevation (with resepect to mean sea level) and groundwater salinity due to different scenario simulations for sub-basin 1 at the end of simulation	157
Table 6.2 Water table elevation (with resepect to mean sea level) and groundwater salinity due to different scenario simulations for sub-basin 2 at the end of simulation	158
Table 6.3 Water table elevation (with resepect to mean sea level) and groundwater salinity due to different scenario simulations for sub-basin 3 at the end of simulation	159
Table 6.4 Water table elevation (with resepect to mean sea level) and groundwater salinity due to different scenario simulations for sub-basin 4 at the end of simulation	160

CHAPTER 1

INTRODUCTION

1.1 GENERAL

During the last few decades, groundwater has become an important source of freshwater and hence, the stress on groundwater resources has increased tremendously. Groundwater provides about one-third of the world's freshwater consumption. However, overdraft is distorting the natural recharge-discharge equilibrium and thereby resulting in declining groundwater levels leading to freshwater scarcity, saltwater intrusion and land subsidence worldwide. According to World Health Organisation (WHO) guidelines for drinking water quality, 1% of seawater (approx.250 mg/l) renders freshwater unfit for drinking (Adrian et al., 2012). It is estimated that, if the current trend continues, about two-thirds of global population will face moderate to severe water stress by 2025. According to the Ministry of Water Resources, Government of India, the groundwater level in the 16 states of India has dropped to more than 4 m during the 1981–2000 period. Karnataka is one among those states. Therefore, in order to avoid such consequences of overdraft, it is important to understand the behaviour of an aquifer system subjected to artificial stresses.

Groundwater in coastal regions is of major concern due to the fact that, more than 60% of the world population lives within 30km of shorelines and about 20% (205 million people) of the population of India lives in the coastal areas (INCCA, 2010). Coastal groundwater systems are sensitive to impacts such as reduced recharge, contamination from natural and manmade sources and over-exploitation (Essink, 2001). The coastal areas are often densely inhabited, especially the river deltas, where good soil and abundant water availability have been able to support large population centres (Volker, 1983). However, overuse of groundwater in many places has resulted in saltwater intrusion as far as up to 15 km inland (Geyh and Soefner, 1996).

Saltwater intrusion occurs in many of the coastal aquifers around the globe (Amer, 1995) due to over abstraction of groundwater.

Saltwater intrusion into aquifers and groundwater quality degradation by salinization is the most serious threat to coastal fresh groundwater resources, which constitute an essential supply for human needs in the coastal areas (Custodio and Galofre, 1992). This occurs when the hydrostatic balance that exists between the seawater and freshwater along the coastal tract is disturbed due to various reasons such as overdraft, land reclamation, climate changes, sea level rise etc. This can significantly hamper the quality of fresh groundwater over a long term and may prevent the use of groundwater for various purposes such as drinking, agricultural use, and so on. A good understanding of the coastal dynamics and detailed knowledge of the variability of their parameters is essential to carryout studies on coastal aquifers (Carrera et al., 2010).

1.2 MECHANISM OF SALTWATER INTRUSION

The migration of saltwater into freshwater aquifers under the influence of groundwater development is termed as saltwater intrusion (Freeze and Cherry, 1979). There is a likelihood of intrusion of salt both into freshwater aquifers and surface water bodies in low lying coastal areas. Saline water originates mainly from sea into open estuaries. Penetration of sea water into rivers is induced by the density difference between fresh and saline water and also due to head differences during low river flow. Normally, the denser saline water forms a deep wedge that is separated from freshwater by a transition zone. Under perturbed conditions, the saline water body remains stationary, its position being defined by the freshwater potential and hydraulic gradient. But, when the aquifer is disturbed by activities like pumping of freshwater or reduced recharge conditions, the saline water body may gradually advance until a new equilibrium state is reached. Problem arises when saline water from deep saline wedge enters the well fields there by affecting the water quality. Freshwater aquifers in coastal areas may become saline due to overdraft of freshwater pockets, tidal effects and sea level changes.

Saltwater intrusion is driven mainly by transport of saltwater due to advection and dispersion. The process by which solutes are transported by the bulk motion of flowing groundwater is termed as advection. However, there is tendency for the solutes to spread out from the path called hydrodynamic dispersion (Freeze and Cherry, 1979). The dispersion is due to combined action of both a purely mechanical phenomenon and a physio-chemical phenomenon. The mechanical dispersion is produced by non-uniform velocity distribution of fluid flow, due to boundary effects acting in three different ways; (i) the velocity is zero on the solid surface, which creates a velocity gradient in the fluid phase (ii) the variation of pore spaces cause discrepancies between the maximum velocities along the pore axes and (iii) the streamlines fluctuate with respect to the mean direction of flow. The physio-chemical dispersion is the molecular dispersion resulting from the chemical potential gradient which is correlated to the concentration (Fried and Combamous, 1971).

Mathematical models which simulate saltwater intrusions through advection only are known as sharp interface models, whereas, models that take into account both the processes of advection and hydrodynamic dispersion are called dispersed interface or transport models. In the former case, it is assumed that the saltwater and freshwater are immiscible fluids separated by a sharp interface, while in the later, a transition zone of mixed salt and freshwater is considered to be present at the interface (Ashtiani et al., 1999). Obviously, the latter only can simulate real life field conditions effectively.

1.3 GROUNDWATER MODELING

Groundwater modeling is a tool which can simulate the complexities involved in understanding the groundwater movement. Groundwater models, which replicate the groundwater flow process at the site of interest, can be used to complement monitoring studies in evaluating and forecasting groundwater flow and transport. However, every reliable groundwater model is based on accurate field data and decent prior knowledge of the site. We use groundwater models to integrate our hydrogeological understanding with the available data, to develop a predictive tool for evaluating groundwater systems, subject to assumptions and limitations.

Mathematical models of groundwater flow have been used since the late 19th century. A mathematical model consists of differential equations developed from analyzing groundwater flow or solute transport in groundwater and are known to govern the physics of flow and transport in porous media. The reliability of model predictions depends on how well the model approximates the actual situation in the field. Inevitably, simplifying assumption must be made in order to construct a model, because the field situation is usually too complicated to be simulated exactly. In general, the assumptions necessary to solve a mathematical model analytically are very restrictive. For example, many analytical solutions are developed for homogeneous, isotropic, and infinite geological formations, where, flow is also steady state (hydraulic head and groundwater velocity do not change with time). To deal with the more realistic situations (e.g., heterogeneous and anisotropic aquifer, in which, groundwater flow is transient), the mathematical model is commonly solved approximately using numerical techniques. Ever since the 1960s, when computers became widely available, numerical models have been the most preferred.

Fate and transport models estimate the concentration of a chemical in groundwater beginning at its point of introduction to the environment to locations down gradient of the source. Fate and transport models require the development of a calibrated groundwater flow model or, at a minimum, an accurate determination of the velocity and direction of groundwater flow that has been based on field data. When the complexities involved in the model make it difficult to solve the equations analytically, numerical methods can be adopted where the domain of interest is discretized into distinctive cells. The solution is obtained in both the space and time by using numerical approximations of the governing partial differential equation.

Finite difference method and finite element methods are widely used numerical solution techniques in groundwater modeling. In finite difference method, the computational domain is discretized by rectangular or quadrilateral elements. The unknown value is defined at the nodes, which are placed at centre of the cells or at the intersection points of cell boundaries. The groundwater heads or concentrations are calculated at these nodes. The finite element model differs from the finite difference model by approximating the flow equation by integration rather than differentiation.

The choice between the methods is done based on the objective of the study and data availability.

Groundwater models allow hydrogeologists and engineers to bring available information and estimates on aquifers together to see how this information interacts with itself. The intricacies involved in modeling density dependent groundwater flow and transport are overcome by computer modeling, which has emerged as a powerful tool for understanding and investigating the groundwater hydrology of coastal aquifers in the recent years. Seawater intrusion is one such subsurface flow and transport processes, which can be addressed using the modeling technique.

1.4 SCOPE OF THE WORK

As per (INCCA, 2010) Karnataka coast has a population of 200 people / km². Groundwater is a prominent source of water supply accounting to about 40% of domestic and agricultural water use in the study area. This requirement is met mainly through the open wells.

This coastal region of Karnataka is also a fast developing area in terms of industries, commercial complexes and academic institutions. The Dakshina Kannada district is known as Cradle of Indian Banking and one of the most industrialized districts in the coastal region. Investments in information technology (IT) sector are gaining momentum in the district and the presence of major IT companies has seen a constant rise. The region is considered as one of the biggest centres for fisheries. According to the economic survey of Karnataka 2010-11, the Dakshina Kannada is recognised as the third largest contributor to the state economy (4.6%). The freshwater requirements of the region even though partially met by surface water supply, greater thrust would be on groundwater resources during the drier months. The projected water demand of Mangaluru city in the year 2026 is estimated to be about 0.25 Million m³/day. The present supply level is less than 0.09 Mm³ per day whereas the demand has already exceeded to 0.1 Mm³ per day causing severe stress on the existing water supply system (Shetkar and Mahesha, 2011). Hence, the quantity and quality deterioration of groundwater, which is the only dependable source for irrigation, industries and

domestic purposes during the summer months, may have a great impact on human settlement and their socio-economic conditions of this region.

The Dakshina Kannada district, one among the 3 coastal districts of Karnataka state spreads along the west coast of India covering coastal track of about 60 km. The district receives more than 3,900 mm rainfall annually. However, in spite of a good amount of rainfall, acute freshwater shortage is experienced in the non-monsoon months (December to May). The major problems, that need immediate attention are i) Flooding and coastal erosion ii) Salinity ingress into coastal aquifers and along the river courses. According to the CGWB (2012), the water draft (exploitation) for domestic and industrial uses is set to increase sharply in Dakshina Kannada, and its availability for irrigation will decrease drastically by 2025. The report points out that, the consumption of groundwater by the district's households and industries will register a 42 per cent increase (up from 3,792 ha.m. in 2004 to 5,370 ha.m. by 2025). The groundwater available for irrigation will come down by more than 8,600 ha.m. or about 31 per cent. In 2004, the district consumed 27,623 ha m of groundwater for irrigation. This is set to decline to 18,997 ha. m by 2025.

In this context, an attempt is made to integrate all the existing database on Dakshina Kannada coastal aquifer for better understanding of the aquifer dynamics and groundwater mass balance. At present, a scientific assessment is yet to be established on seawater intrusion into the present basin which has tremendous growth rate potential in the near future. Also, the problem of saltwater intrusion along the coastal Dakshina Kannada district has not been attempted yet through numerical simulation. This research is a step forward in understanding the hydrodynamics of coastal aquifer of the Dakshina Kannada district in addressing the saltwater intrusion problems using numerical modeling approach. A three dimensional variable density model SEAWAT ver.4 (Langevin et al., 2008) is used in the study to resolve the spatio temporal variation of groundwater level and salt concentrations in the basin.

1.5 RESEARCH OBJECTIVES

The present investigation is intended to simulate the seawater intrusion phenomena for the existing and anticipated future developments in the area. The simulation is three-dimensional using SEAWAT to identify the spatial and temporal distribution of the groundwater flow and salinity. With the above vision, the present investigation has the following objectives:

1. To develop a representative three dimensional numerical groundwater flow and solute transport model using SEAWAT.
2. To apply the calibrated model to predict the groundwater flow dynamics considering future developments.
3. To simulate groundwater solute transport of the region for the present and future stress scenarios.
4. Sensitivity analysis of the hydrological stresses and aquifer parameters on coastal groundwater flow and transport model.

1.6 OVERVIEW OF THE RESEARCH WORK

The steps involved in the present research work are depicted in the form of a flow chart in fig.1.1. The database generation is the first and foremost requirement of any model development. The toposheets number 48K/16/SW, 48L/13/NW, 48L/13/SW and 48L/13/SE with a scale 1:25,000 having a contour interval of 10m are procured from the Geological Survey of India. They are processed using ArcMap[®] (version 9.3) software to delineate the study area boundary and to create digital elevation model (DEM) and generation of drainage network map. The toposheets are geo-referenced and projected to UTM coordinate system. The meteorological, hydrological and hydro-geological data for the model are obtained from the government and private

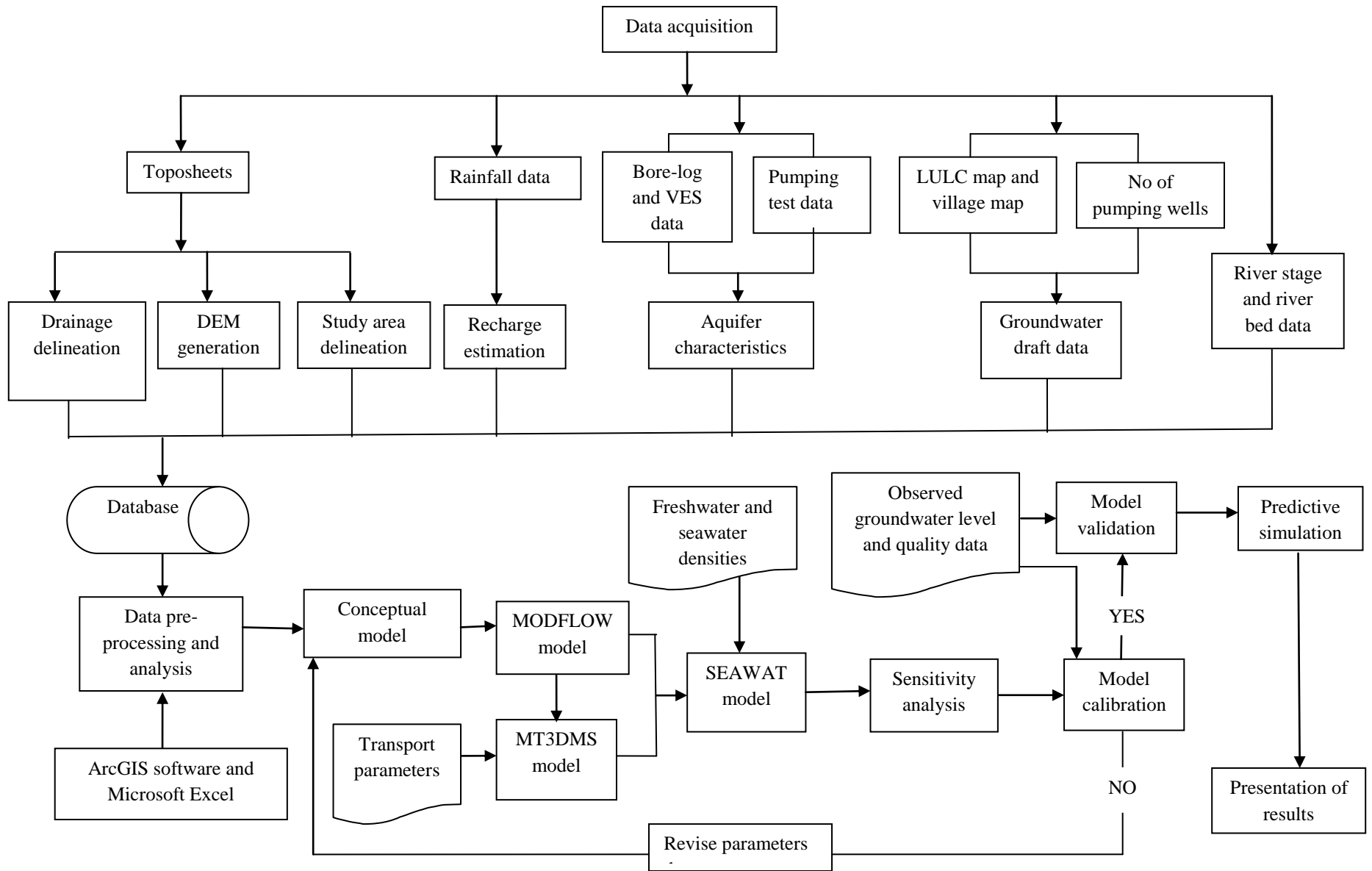


Fig. 1.1 Flow chart for methodology in the present study

agencies. The aquifer characterization of the area is carried out by previous researches in the area, with vertical electrical sounding (VES) survey and pumping tests.

For the present research, conceptual modeling approach is used for the simulation which simplifies the field problem and stacks the required field data for better understanding of the behaviour of the aquifer system. The database is used to develop a conceptual model, which is introduced into SEAWAT. In the process, initially, the MODFLOW is executed, and then the transport parameters are introduced to execute a MT3DMS model. These models are combined with additional input of density parameters to execute the SEAWAT model. Sensitivity analysis is performed to learn the parameter importance in the model calibration. Besides, the calibration is performed using the observed water level and water quality data. The aquifer parameters are revised within the appropriate range to obtain better calibration results. The model is then validated to assess the model performance.

1.7 DESCRIPTION OF STUDY AREA

1.7.1 General

The state of Karnataka situated in the west coast of India consists of three coastal districts, namely Dakshina Kannada, Udupi and Uttara Kannada. The Dakshina Kannada district is one of the fast growing districts of Karnataka. It is a maritime district located in the south-western part of Karnataka adjoining the Arabian sea. Mangalore city is the district headquarters. Administratively, the district is divided into five taluks viz. Bantwal, Belthangady, Mangalore, Puttur and Sulya. Administratively, the study area comes under Mangalore taluk. The present investigation focuses on a typical tropical, coastal aquifer that may experience seawater intrusion due to groundwater development. In this regard, a conceptual model of a coastal basin in the west coast of India is considered. The study area for the investigation is the coastal aquifer extending from Mulki to Talapady of Dakshina Kannada district. Geographically, the area is between 12°45'30"N to 13°06'00"N and 74°54'30"E to 74°46'30"E as shown in fig.1.2. The areal extent of the region is about 155 km² having a coastline of about 40 km.

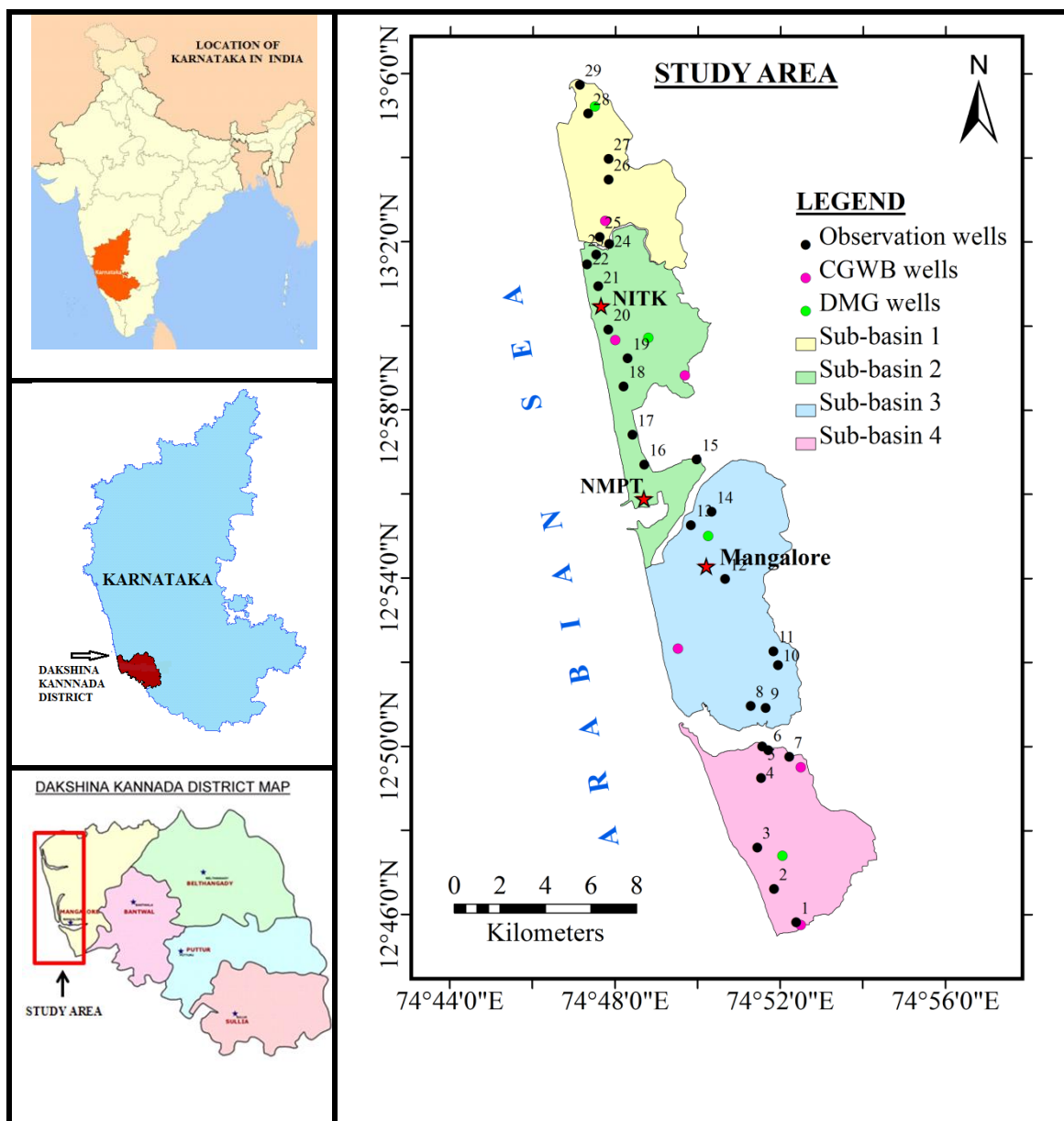


Fig 1.2 Map of the study area

Major industries such as Mangalore Chemicals and Fertilizers Ltd (MCF), New Mangalore Port Trust (NMPT) and other smaller units comprising of industrial estate, small scale industries are located in the region. Besides, academic institutes like the National Institute of Technology Karnataka (NITK), Srinivas College of Engineering etc. are located in the region. The Oil and Natural Gas Corporation (ONGC) is exploring various options for diversification of its activities including setting up of special economic zones (SEZ) and storage of crude oil near Mangalore. The study area has a population of about more than 2,00,000, which is expected to grow with a decennial growth rate of about 12.1% as per 2011 population census of

India. Coconut, arecanut and paddy are the main crops grown in the area. Fishing is also a major source of income to a large community. The population is dependent on both surface water and groundwater resources for irrigation and domestic water requirements. Since the surface water is scarce during January to May, greater thrust is on the groundwater resources during this period.

The entire study area is divided into four sub-basins, for the convenience of hydro-geologic modeling since they are separated by natural boundaries. All the basins have Arabian sea on the west and ridge line boundary towards east.

Sub-basin-I: It is an area between Mulki river on the northern side and Pavanje river on the southern side. The area is about 25 km². The slope of the area is ranging from 0 to 20.35°.

Sub-basin-II: It is an area stretched between Pavanje river in the north and Gurupur river in the south. The area is about 38 km². The slope of the area is ranging from 0 to 20.50°.

Sub-basin-III: It is a basin between Gurupur river in the north and Nethravati river in the south. The area is about 56 km² covering the central portion of Mangaluru city. The average slope of the terrain is ranging from 0 to 30.07°.

Sub-basin-IV: Starting from Nethravati river in the north, the area extending up to Talapady river in the south is coming under this sub-basin. The area is about 36 km². The slope of the area ranges from 0 to 22.03°.

1.7.2 Topography

India is a peninsular country bounded by ocean on its three sides, of which the western India has a long coastline. The coastal plain with low elevation spreads to an extent of 30 to 50 km inland. The topography of the study area is shown in fig.1.3.

The coastal region here has high mountain ranges called the Western Ghats towards the east and the Arabian sea on the west. Physiographically, the western coast consists of upland Western Ghats hill slopes (high elevation), the mid-land region with undulating topography (medium elevation) and the coastal plains (low elevation).The

study area has a gradual westerly sloping low-lying terrain with elevation ranging from 0 to 90 m above mean sea level (msl). The topography of the region is from plain to undulating with hilly regions and natural valleys.

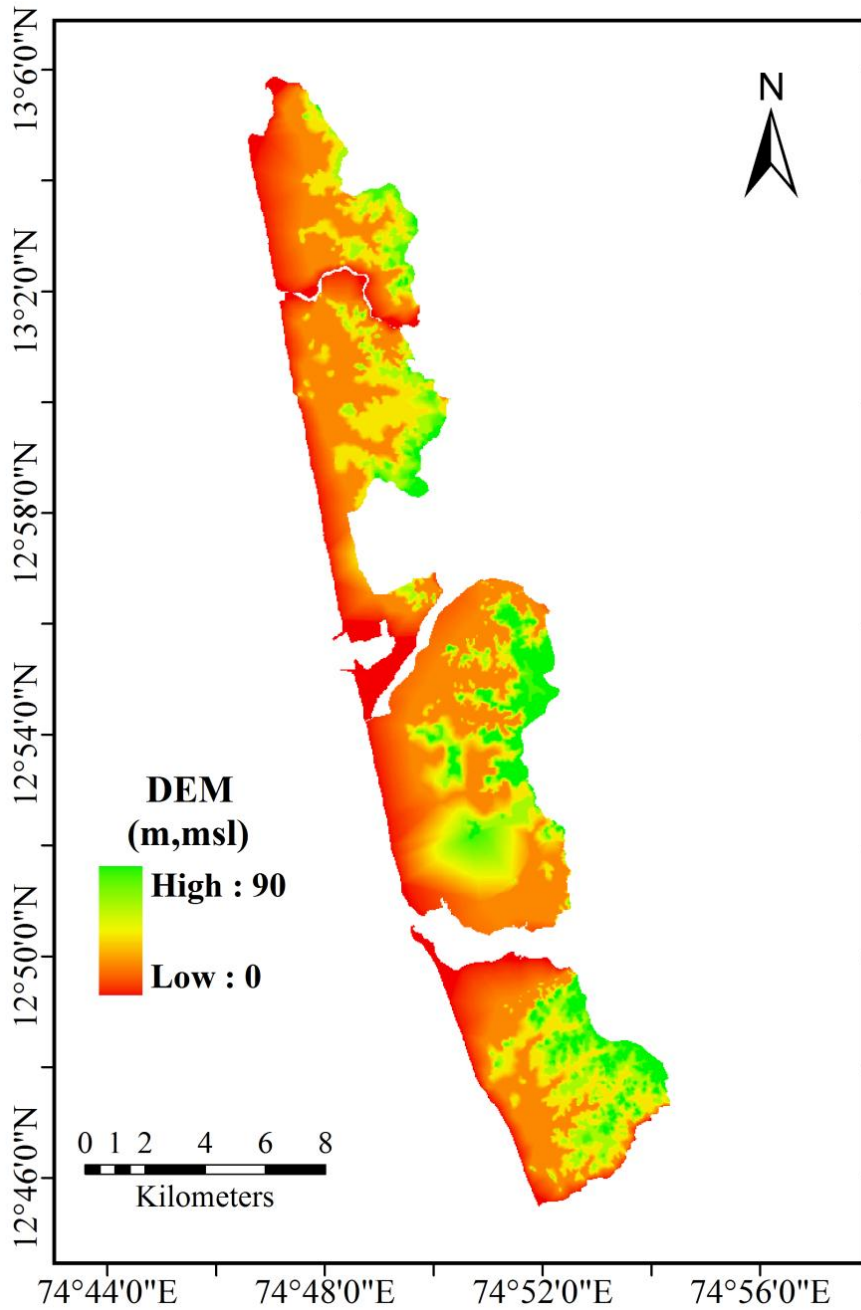


Fig.1.3 Topography of the study area

1.7.3 Climate and rainfall

The climate of the area is tropical humid type with moderate air temperatures of 36°C (May) and 21°C (December) during extreme seasons of the year and high levels of relative humidity ranging between 65% and 100%. The India Meteorological Department (IMD) has classified a year into four seasons as the monsoon (June to September), post-monsoon (October to November), winter (December to January), and pre-monsoon or summer (February to May) seasons. The average annual rainfall of the region is about 3,500 mm, with the greater part (about 85%) occurring during the months of June through September due to the phenomenon of the southwest monsoon. This is evident in Fig.1.4, where the monthly rainfall during 1997-2012 observed at the National Institute of Technology Karnataka, Surathkal, India is shown.

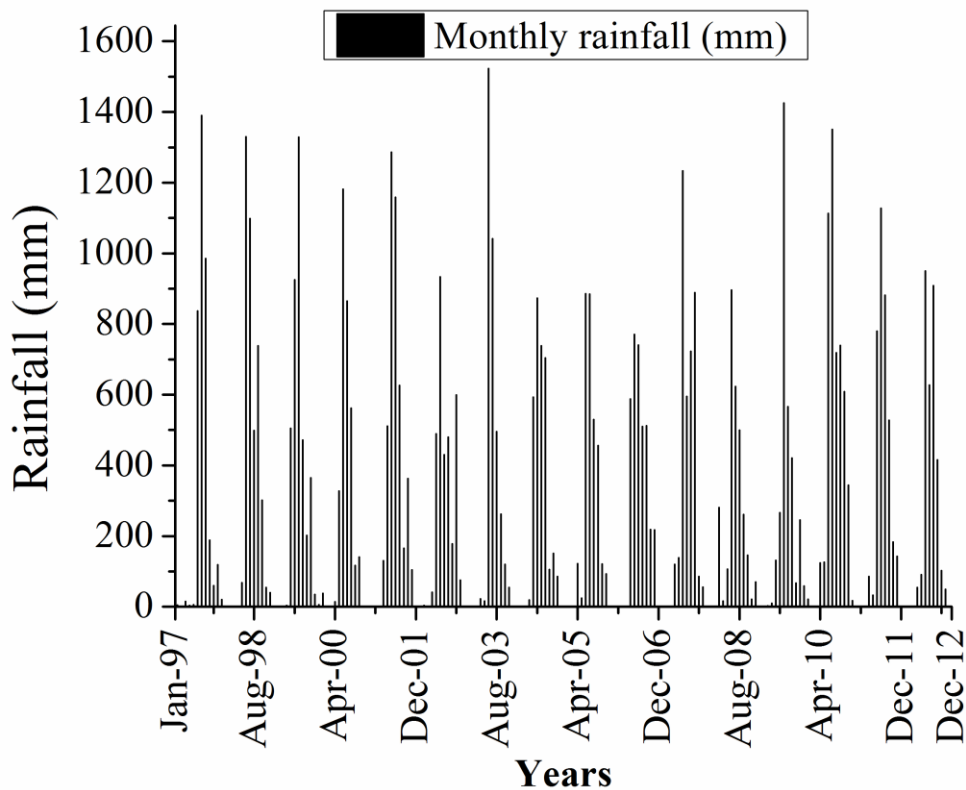


Fig. 1.4 Monthly rainfall at NITK, Surathkal (1997-2012)

1.7.4 Drainage characteristics

Fig 1.5 shows the drainage network of the study area which is drained by the rivers, viz., Shambhavi, Pavanje, Gurupur, Nethravati and Talapdy. Among them, Gurupur and Nethravati are the major rivers. About 80% of the total annual river flow is confined to 3 to 4 months in a year (June to September) and they almost run dry during the months of January to May. However, during these months, seawater intrudes into the river up to distance of about 20km during high tides. Hence, these rivers are tidal in nature and carry saline water contaminating adjoining well fields up to a few hundred meters on either side.

The sea waves approach the shore line of this area from west-northwest and northwest during post-monsoon season with maximum wave heights of 2 to 2.5 meter. The first and second order streams dry quickly as both surface and subsurface flows recede very fast. The rivers flow through the undulating terrain of the middle land and then through a narrow stretch of coastal plains.

The river Pavanje has a total length of 33 km, it joins the Mulki river before draining into the sea. The river Pavanje meanders along the coastline for about 6 kms at a distance of about 500m from the sea to form the river mouth along with the river Shambhavi (fig. 1.5). The Nethravati and Gurupur rivers originate in the Western Ghats and flow for a distance of 148 km and 87 km respectively before joining the Arabian sea together at Mangalore. They cover a drainage area of about 4260 km². The Gurupur river meanders along the coastline for about 8kms to form the river mouth along with the river Nethravati. As per Kumar (2011), the river profile of Gurupur is at higher level than that of Nethravati at the origin. However, the Nethravati river flows at higher elevation than Gurupur river when distance versus elevation is taken into consideration. The river beds have 1° to 2.5° gradients which are flanked by thin gravelly terraces.

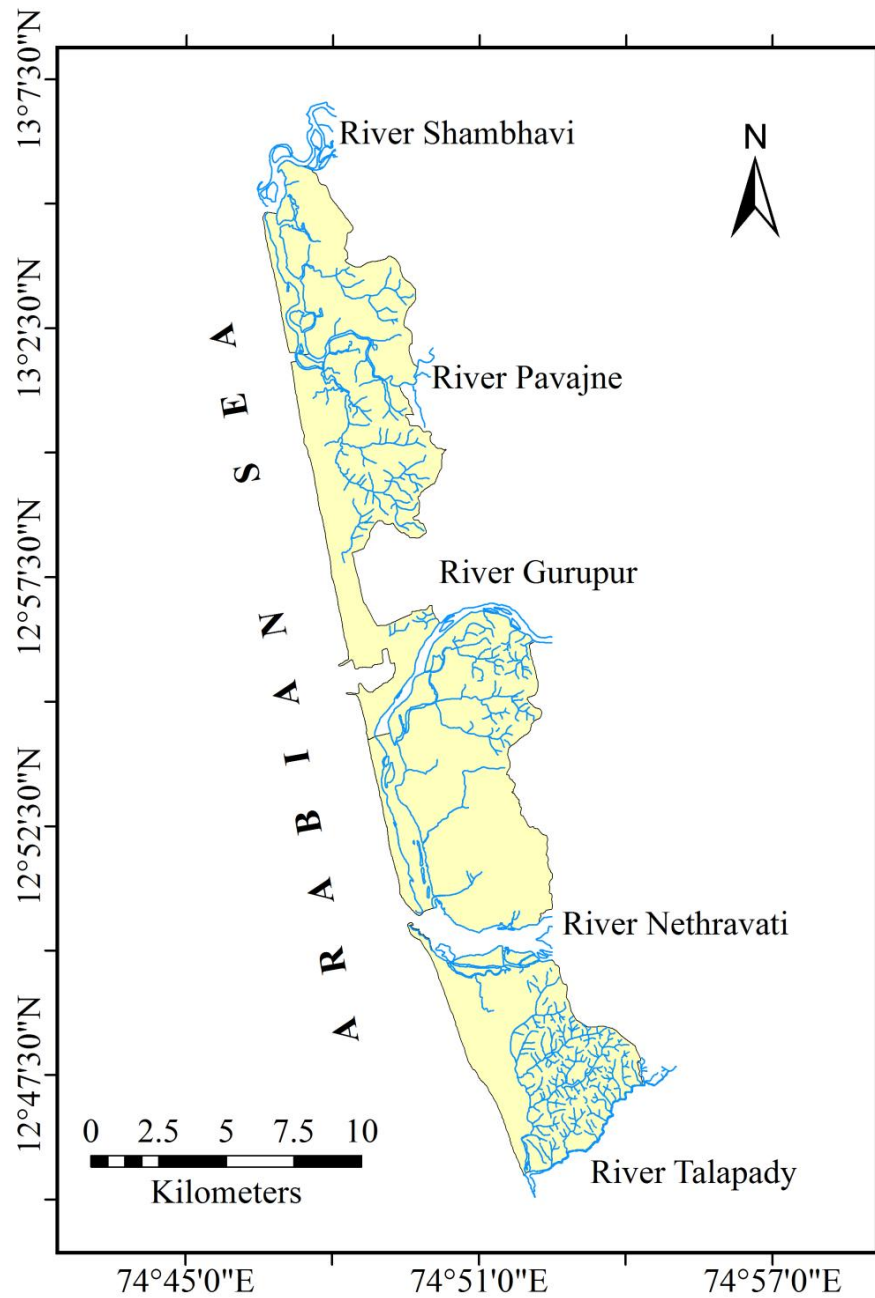


Fig. 1.5 Drainage network of the study area

1.7.5 Soil

The study area consists of two types of soil, viz. coastal alluvium and laterite soils. The coastal alluvium exists along with silt and clay as evident from laboratory tests (Jayappa, 1991). The lateritic deposits belong to recent and sub-recent formations of the parent rock, granitic gneiss. The lateritic soil is generally fine grained and composed of hydrated aluminium and iron oxides. The soil map prepared by the

NBSS&LUP (1998) is extracted for the present study area using Arc GIS to understand the spatial soil type distribution. Fig.1.6 reveals the spatial distribution of these soil types sampled at depths varying from 8m to 18m and each soil class is described in table 1.1. Soil type 5 covers the vast portion (68%) of the study area with almost the entire stretch of sub-basin 3 and major portion of the remaining sub-basins. The soil type 2 envelopes 25% of the study area having present predominantly in sub-basins 2 and 4.

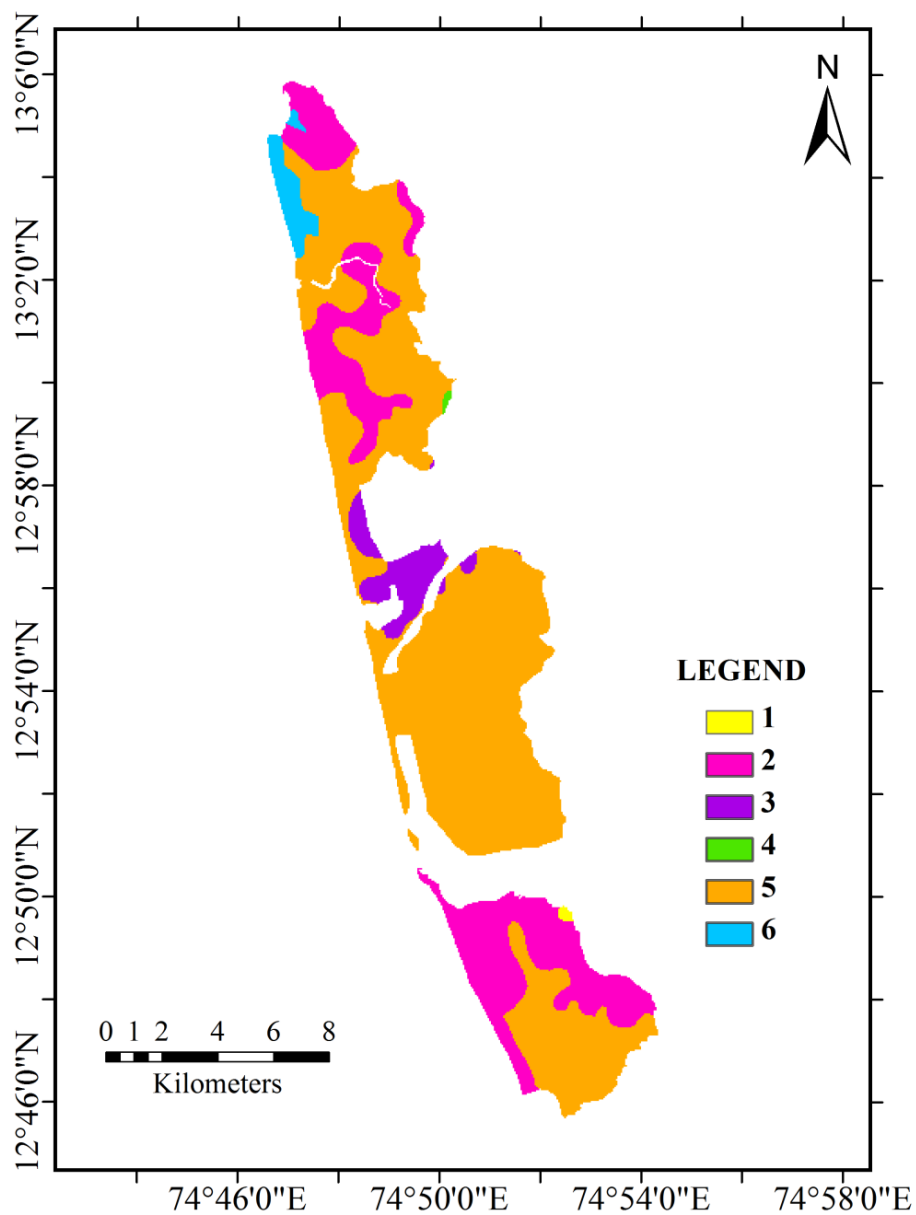


Fig. 1.6 Soil class map of the study area

Table 1.1. Soil type classification

Soil class	Description
1	Moderately shallow, somewhat excessively drained, gravelly clay soils with hard ironstone on coastal plateau summits, with moderate erosion
2	Moderately deep, well drained, gravelly clay soils with low AWC and surface crusting on undulating uplands, with moderate erosion
3	Deep, imperfectly drained, sandy over loamy soils of valleys, with shallow water table
4	Very deep, well drained, gravelly clay soils with low AWC on laterite mounds, with slight erosion
5	Very deep, well drained, gravelly clay soils with surface crusting and compaction on undulating uplands, with moderate erosion.
6	Very deep, moderately well drained, sandy soils with very low AWC on bars and ridges

1.7.6 Land use and land cover

The land use/ land cover distribution over the area is presented in fig.1.7. The LULC data of scale 1:2,50,000 derived from Resourcesat-1 satellite's Linear Imaging Self scanning Sensor (LISS) -III data (2011-12) is downloaded from Bhuvan-Thematic services website (<http://bhuvannoeda.nrsc.gov.in/theme/thematic/theme.php>). This data consists of 19 classes which are then merged to get 5 required classes for the study area, namely built-up (class-1), agricultural (class-2), forest (class-3), barren/waste land (class-4) and water bodies (class-5). According to the classification, 53.21% of the total area is covered by agricultural land, 33.61% by forest land, 6.14% by built-up area, 6.77% by water bodies and only 0.27% as wasteland.

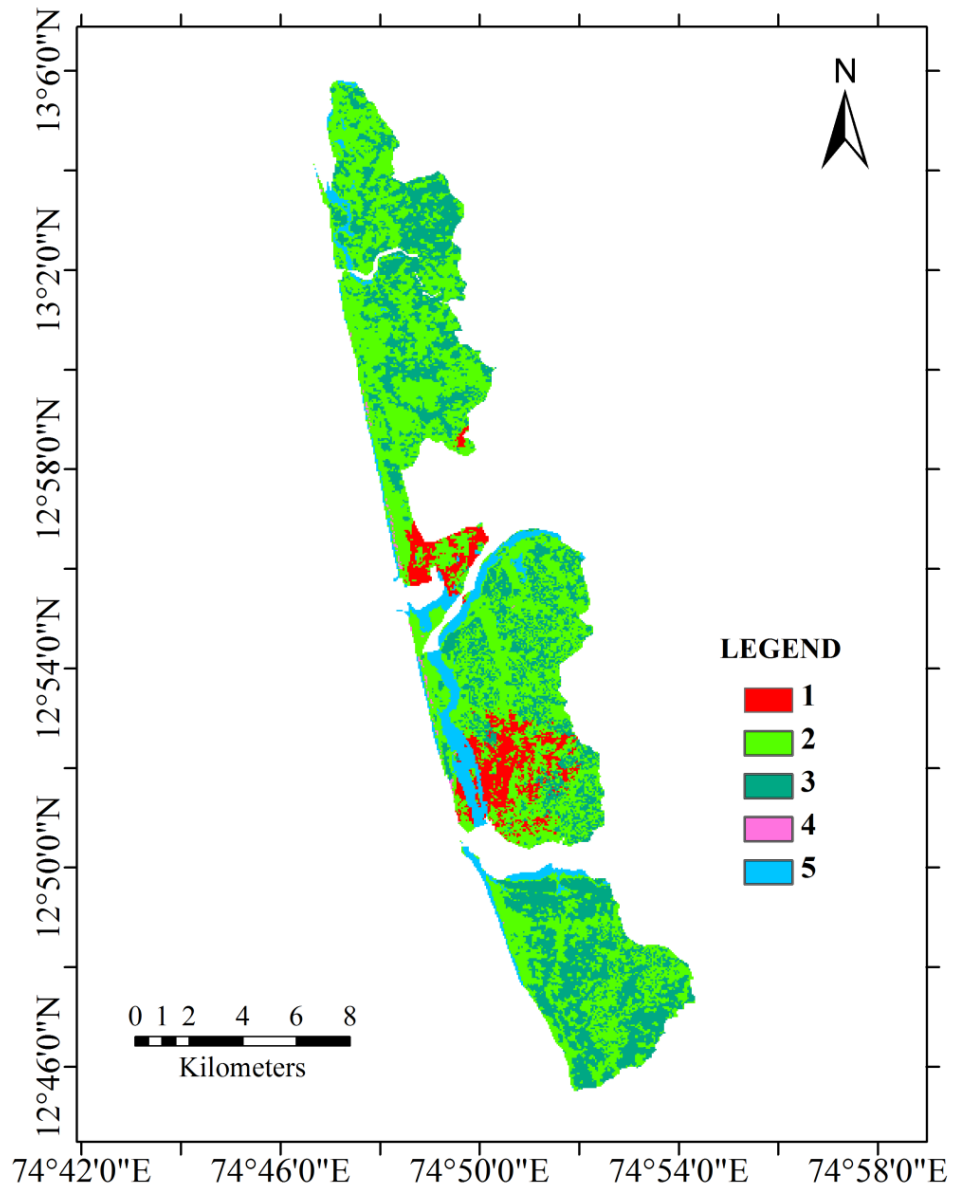


Fig. 1.7 Land use land cover map of the study area

1.8 ORGANIZATION OF THE THESIS

The thesis comprises of seven chapters, list of references and annexure. A brief description of the each chapter is presented here.

Chapter 1 provides an introduction to the problem and the objectives of the study, overview of the research methodology adopted and description of the study area.

Chapter 2 presents the literature review of the groundwater parameter estimation, groundwater flow and solute transport models.

Chapter 3 provides an insight on the various studies carried out to characterize the aquifer.

The development of a groundwater flow model for the coastal aquifer system located in the Dakshina Kannada district, Karnataka, India using MODLFOW, its application pertaining to the study area and sensitivity analysis are detailed in **Chapter 4**.

Chapter 5 presents the investigations on solute transport model for the coastal aquifer system located in the Dakshina Kannada district, Karnataka, India using SEAWAT, its application pertaining to the study area and sensitivity analysis.

Chapter 6 illustrates the application of developed models for the region to simulate the impacts of increased groundwater utilization and climate change scenarios.

Finally, **Chapter 7** lists out the conclusions, limitations and scope for further research.

CHAPTER 2

LITERATUREREVIEW

2.1 GENERAL

Modeling of coastal groundwater systems is a challenging problem due to their highly dynamic boundary conditions and the coupling between the equations for groundwater flow and solute transport (Post, 2011). Groundwater flow models are appropriate tools to assess the effect of foreseen future human activities on groundwater dynamics (Xu et al., 2011). Over the years, many models have been developed to represent and study the problem of sea water intrusion. They range from relatively simple analytical solutions to complex numerical models.

The characteristics of transition zones between freshwater and saltwater in coastal aquifers and the dynamics of their movements have been understood for several decades (Todd, 2005; Cooper et al., 1964). With the advent of digital computers, numerical algorithms and solution methods were developed to solve the equations for variable-density groundwater flow and transport that represent seawater intrusion (Pinder and Cooper, 1970; Segol and Pinder, 1976). Computer codes then became available to simulate seawater intrusion for user-specified aquifer geometries and characteristics in the two dimensions of a cross-sectional profile (Voss, 1984; Sanford and Konikow, 1985). The availability of mathematical tools has promoted a growing interest in the study and forecasting of seawater intrusion hazards (Bear et al., 1999).

2.2 AQUIFER CHARACTERIZATION

Groundwater modeling of an area depends largely on the aquifer characteristics, e.g., transmissivity, hydraulic conductivity and storage co-efficient. Pumping test is one of the methods to evaluate these parameters. Almost all the well hydraulics models are based on the assumption that the pumped well is a line source. This assumption proposed by Theis (1935) may not be valid if the well bore storage effects are

significant. Effects of well bore storage become important when the aquifer transmissivity and storage coefficient are small or the pumped well diameter is large.

A semi-empirical, mathematical model capable of reproducing all three segments of the time drawdown curve in an unconfined aquifer was introduced by Boulton (1954, 1963). In this method, Boulton assumed that the amount of water released from storage per unit horizontal area of the aquifer is the sum of volume of water instantaneously released and another volume of water, the release of which is delayed due to the aquifer characteristics. This method was later extended by Boulton (1970) and Boulton and Pontin (1971) to account for anisotropy and the effect of vertical flow components in the aquifer. The classical solutions developed by Boulton(1954), Dagan (1967) and Neuman (1972,1974) assume the pumped well to be infinitesimal in diameter. These solutions cannot be used to correctly interpret early time drawdown in pumped.

Kipp (1973) developed a solution that accounts for the finite diameter of the pumped well but assumed the water to be incompressible and the porous matrix to be rigid. Consequently, although well bore storage is included, the aquifer specific storage is not. Boulton and Streltsova (1976) also have presented an analytical solution for flow to a partially penetrating large diameter well in an unconfined aquifer. The very complexity of the solution allows too many options to be selected for the curve matching process. There is no easily found unique solution. This method also requires relatively long pumping periods before a curve matching technique can be applied. Their solution allows for aquifer compressibility but, because they assume the water table to be a constant head boundary, the effect of specific yield cannot be properly accounted.

It has been demonstrated in the literature (Moench,1995) that, the Neuman (1972, 1974) model when properly applied, can be used to estimate the most important water table aquifer parameters with reasonable accuracy. However, accurate estimates of specific storage are often not possible with the Neuman (1974) model because they require use of early time drawdown data.

Several investigators have developed numerical models to account for effects of a finite-diameter pumped well (Sridharan et.al., 1990; Narasimhan and Zhu, 1993). Narasimhan and Zhu (1993) used their model to demonstrate that the effect of well storage in the pumped well can mask large parts of the early time and intermediate time responses as seen in Neuman's (1975) type curves. Singh (2006) proposed a simplified semi-analytical model for the drawdown due to pumping a large diameter, partially penetrated well which can take into account pumping and recovery phases. The model yields transient drawdown in the well, well storage and aquifer storage contributions including from the well bottom.

2.3 GROUNDWATER MODELING

Water resource managers are charged with the task of maintaining water supplies and quality standards in the face of increasing demand, changing land use, weather variability, and long-term climate changes. The effects of these factors and management actions can be difficult to assess because of the complex and interrelated nature of a watershed's hydrology. A computer model that is able to simulate possible scenarios and their effects on a watershed will be a useful management tool to investigate the watershed's sensitivity to change with respect to a variety of factors (Perkins and Sophocleous, 1999). Physical-based numerical groundwater flow models are commonly used for refining hydro-geologic characterization and making informed groundwater management decisions. The numerical flow models are powerful simulation tools because, they can represent high spatial and temporal variability of aquifer properties and conditions inherent to natural systems (Coppola et al., 2005).

2.4 GROUNDWATER FLOW MODEL

A number of commercial groundwater software with GIS capabilities like Visual MODLOW, GMS, Groundwater Vista etc are being widely used for this purpose. These models have been used to understand and manage various type of groundwater issues, such as management of coastal aquifer system (Shammas et al., 2009); simulation of the effect of subsurface barrier on groundwater flow (Senthilkumar and Elango, 2011); groundwater resource management (Rejani et al., 2008; Kushwaha et al., 2009; Sudhir Kumar, 2011); groundwater flow modeling (Ahmed and Umar,

2009); modeling flow and salt transport in a salinity threatened irrigated valley (Gates et al., 2002). Several investigators adopted different methods for groundwater flow and transport modeling, some of which are discussed here.

A three dimensional modular model (MODFLOW) was used by Varni and Usunoff (1999) to simulate groundwater flow in the Azul River basin, Buenos Aires Province, Argentina, in order to assess the correctness of the conceptual model of the hydrogeological system.

Dufresne and Drake (1999) constructed a regional groundwater flow model (MODFLOW) using existing hydro-geologic data from state and federal agencies in order to simulate the existing hydrologic conditions of a karst area, in Lake City Florida, USA and to predict withdrawal impacts. The model was calibrated by matching potentiometric surface maps and spring flows to within reasonable ranges. The drawdowns in the Floridian and surficial aquifers predicted by the model showed minimal impacts to existing legal users and only a 5% reduction in the flow at 21km away in the Ichetucknee Springs, Florida, USA. Abdulla et al. (2000) applied three dimensional MODFLOW to simulate water level change in the complex multi-aquifer system (the Upper and Middle aquifers) of the Azraq basin, Jordan. To predict the aquifer system responses for the period of 1997-2005, 4 different pumping schemes (scenarios) have been investigated. If the pumping rate was increased to 1.5 times the present rate, an approximate 39m drop in the water level by 2050 was revealed. Three dimensional groundwater modeling experiments were carried out by Reeve et al. (2001) to test the hypothesis that regional groundwater flow is an important component of the water budget in the Glacial Lake Agassiz Peatlands of northern Minnesota, USA encompassing an area of 10,160 km².

Asghar et al. (2002) used MODFLOW and MT3D to simulate the interface movement in an unconfined aquifer of Punjab, Pakistan. The results indicated that skimming wells of 10–18 l/s can be installed and operated successfully with 60–70% well penetration ratio for an operating time of 8–24 h/day from an unconfined aquifer having 15–18 m thick having relatively fresh groundwater lens. Sakiyan & Yazicigil (2004) studied the aquifer system of the Küçük Menderes basin for sustainable

development and management of an aquifer system. The spatial distributions of the hydrogeological parameters and recharge were estimated by geostatistical methods and hydrologic simulations. Alternative groundwater management scenarios were developed by them to determine the safe yield for the Küçük Menderes aquifer system. Declining groundwater levels caused by irrigation is the main problem for agricultural development in northern China. Mao et al. (2005) investigated the effect of future irrigation patterns on the decline of the groundwater table with the aid of MODFLOW. The simulated results showed that, the groundwater decline would be decreased, and perhaps halted, by decreasing the use of irrigation. MODFLOW has been used by Aggarwal et al. (2005) to simulate groundwater behaviour of south-west Punjab for Kharif and Rabi seasons from June 1986 to June 1998. The sensitivity analysis showed that, the model is more sensitive to specific yield than hydraulic conductivity values. They opined that, the best practice is to maintain water levels at predetermined depth while opting for sustainable crop production.

Juckem et al. (2006) devised a methodology for estimating a critical basin size, above which base flow appears to be relatively less sensitive to the spatial distribution of recharge and hydraulic conductivity in Coon Creek watershed, Wisconsin, USA. The results of three dimensional steady state model showed that, there is a scale effect that influences the relative importance of recharge and hydraulic conductivity such that at some scale, the influence of spatial parameter variability on base flow diminishes and can be approximated using a simplified representation. Abdulla and Al-Assad (2006) used MODFLOW to simulate the behaviour of the flow system under different stresses for Mujib aquifer, Jordan. The results of the sensitivity analysis showed that, the model is highly sensitive to horizontal hydraulic conductivity, specific yield and anisotropy and with lower level to the recharge rates. Rojas and Dassargues (2007) developed a groundwater flow model using MODFLOW for Pampa del Tamarugal aquifer, northern Chile. It was observed that, the groundwater heads would continue to decrease with the present pumping rates.

To reconstruct the transient character of yearly recharge using MODFLOW for Yargon-Taninim aquifer, Israel, Weiss & Gvirtzman (2007) studied 20 to 30 years of precipitation and spring discharge records. Best fit between measured and computed

spring hydrograph data allowed to develop a set of empirical functions relating measured precipitation to recharge to the aquifer. Palma & Bentley (2007) constructed Visual MODFLOW which was simulated using transient and steady-state numerical models for the Leon- Chinandega aquifer in Nicaragua to assess the potential of the aquifer as a source of water for irrigation. The simulations indicated that groundwater from deep wells is recharged at high elevations, corresponding to the deep flow system. The shallow wells mostly capture groundwater that was recharged locally, but there was also an indication that mixing of the regional and local system can occur.

Pisinaras et al. (2007) developed MODFLOW for the stream-aquifer system of Ismarida plain, north eastern Greece. The simulated groundwater budget indicated that, there must be approximately 33% decrease of withdrawals to stop the dramatic decline of groundwater levels. Wang et al. (2008) constructed MODFLOW for north China Plain. The authors used GIS for analyzing spatial data and computer languages such as Visual C and Visual Basic to define the relationship between the original data and the model data. The results indicated a negative budget in the Plain. Suresh Babu et al. (2008) analysed a coastal plain falling within the watershed limits of Pereque stream in Parana state, Brazil using MODFLOW to assess the surface and subsurface water components under different stress conditions. The three dimensional model of the groundwater reserve helped to visualize the hydro geologic changes and to formulate management plans.

Martinez-Santos et al. (2008) described an interdisciplinary exercise of scenario design and modeling through finite difference code for providing a methodology to couple hard science numerical modeling approaches with the involvement of key water sectors. Given the long-standing conflicts in the area, modeling work largely focused on carrying out a vulnerability assessment rather than on trying to find solutions. Ayenew et al. (2008) developed a three dimensional steady-state finite difference groundwater flow model and used to quantify the groundwater fluxes and analyse the subsurface hydrodynamics in the Akaki catchment, Central Ethiopia by giving particular emphasis to the well field that supplies water to the city of Addis Ababa. The calibrated model was used to forecast groundwater flow pattern, the

interaction of groundwater and surface water, and the effect of pumping on the well field under different scenarios.

Zume and Tarhule (2008) used Visual MODFLOW, a numerical groundwater flow model to evaluate the impacts of groundwater exploitation on stream flow depletion in the Alluvium and Terrace aquifer of the Beaver-North Canadian River (BNCR) in north western Oklahoma, USA. The simulation results indicated that, groundwater pumping had reduced base flow to streams by approximately 29% and had also increased stream leakage into the aquifer by 18% for a net stream flow loss of 47%. Takounjou et al. (2009) carried out steady state groundwater flow and particle tracking modeling using Visual MODFLOW to determine in detail the groundwater flow and particle migration in the shallow unconfined aquifer of the Upper Anga's river watershed, Cameroon. The results indicated that, the topography controls groundwater flow in the watershed and that, base flow to the river is an important factor moderating groundwater movement in the Anga's river watershed.

Kushwaha et al. (2009) applied MODFLOW for the northern part of Mendha sub-basin in the semi-arid region of north-eastern Rajasthan, employing conceptual groundwater modeling approach. The model was run to groundwater scenario for a 15 year period from 2006 to 2020 considering the existing rate of groundwater draft and recharge. El-Bihery (2009) applied MODFLOW for designing the model of the RasSudr area in Egypt. The groundwater flow model was used to recognize the groundwater potential as well as exploitation plan of the most prospective aquifer in the area. The groundwater flow model applied to Yamuna–Krishni interstream, a part of central Ganga Plain, Uttar Pradesh (Ahmed and Umar, 2009) showed that, the model is most sensitive to hydraulic conductivity and recharge parameters. Abdalla (2009) used MODFLOW as a groundwater modeling technique to interpret the hydrologic system in arid to semi-arid central Sudan and to simulate the future influence of the project on the hydro-geologic system. It was concluded that, a total of $3.5 \times 10^7 \text{ m}^3/\text{year}$ could be continually extracted from the deep aquifer to supply El Obeid city without endangering the groundwater resources in the region.

The groundwater level variations of the Ejina basin, north-western China on a large-scale was analysed (Xi et al., 2010) by using MODFLOW and GIS software to evaluate a conceptual groundwater model. The model simulated the regional hydrologic regime in recent 10 years and compared with various delivery scenarios from midstream and determined which one would be the best plan for maintaining and recovering the groundwater levels and increasing the area of Ejina Oasis. Liu et al. (2010) formulated a management strategy to rationally reduce the groundwater level declining trend and sustainable utilization of groundwater resources in the Taipei Basin. A hydro-geologic model of Taipei Basin using MODFLOW-96 was setup to evaluate water budget and safe yield of the aquifer. Sanz et al. (2011) ventured to characterize the river–aquifer relationship and to determine the influence that groundwater abstraction has on the river discharge in south eastern Spain using MODFLOW. It is demonstrated that, although groundwater abstraction increased considerably from the early 1980s to 2000, the depletion of water stored in the aquifer was lower than might be expected.

An integrated methodology was developed by Xu et al. (2011) adopting loose coupling of the groundwater flow model MODFLOW with ArcInfo Geographic Information System. The investigation assessed the impacts of irrigation water-saving practices and groundwater abstraction foreseen for the year of 2020 on the groundwater dynamics of the Jiefangzha Irrigation System (JFIS) in Hetao Irrigation District, upper Yellow River basin, China. A module package, GWF, was developed by Li et al. (2011) to simulate the groundwater fall, which can be embedded directly into MODFLOW. A theoretical example was presented, to show how the package GWF is used to simulate perched water. This package was also applied successfully to build a regional groundwater model of the Urumqi River Basin, Xinjiang, China, and the simulation results showed good agreement with the local hydro-geologic conditions. Al-Salamah et al. (2011) investigated groundwater modeling of Saq Aquifer in Buraydah Al Qassim, Saudi Arabia to estimate the impact of overdraft using MODFLOW model. The model results indicated that, pumping from the Saq Aquifer in Buraydah area will result into significant cones of depression if the existing excessive pumping rates prevail.

Rahnama and Zamzam (2011) investigated on groundwater development in Rafsanjan plain, southeast Iran by MODFLOW and MT3DMS. The results indicated that, water elevation decreased approximately 15m over a period of 10 years and the electrical conductivity would reach a value of 16,000 μ s/l in the next 5 years. Surinaidu et al. (2011) developed a hydrological and a hydrogeological model for the Katni area, Madhyapradesh, India, using USGS flow code, MODFLOW 2000. The water budget estimation showed that, the total groundwater flow into the aquifer system due to interaction with river was 14,783 m³/day. Infiltration from precipitation was 1,600 m³/day of the groundwater supply, while 1,446 m³/day came from lateral inflow and the remaining, through the inflow into mine pit area ie. 15,725 m³/day. The result of this study was also used to predict the required amounts of pumping and the possible locations to dewater the groundwater in the mining pits.

Sudhir Kumar et al. (2011) developed a groundwater management model for Nadia district, West Bengal in India using Visual MODFLOW software. The groundwater flow pattern of the study area indicated the occurrence of base flow which fed both the rivers Bhagirathi and Jalangi throughout the year. The outcome of modeling showed that the model can be used for prediction purpose in the future by updating input boundary conditions and hydrologic stresses during the preceding year. Senthil Kumar and Elango (2011) assessed the effect of a sub-surface barrier on groundwater flow in the Palar river basin, Tamilnadu, southern India using a numerical model. The model predicted that with the sub-surface barrier in place, additional groundwater requirement of approximately 13,600 m³/day can be met with minimum decline in regional groundwater head.

Yang et al. (2011) developed a groundwater flow model in Tongliao city, China by using Visual MODFLOW. The calibrated parameters were very useful to identify the aquifer properties and to analyse the groundwater flow dynamics, the changes of groundwater levels in the study area. Manghi et al. (2012) developed a three-dimensional groundwater flow model using MODFLOW for the Arlington basin, southern California, USA to investigate different water management strategies. Five groundwater management scenarios were run for a 30-year time period. The model

results showed that, long-term groundwater pumping from the existing Desalter wells is not sustainable without artificial recharge.

Panagopoulos (2012) used MODFLOW for simulating groundwater flow in the Trifilia Karst aquifer, Greece. The steady and transient state calibrations gave encouraging results for the equivalent porous media approach, which does not consider pipe flow or turbulence. Lachaal (2012) developed an integrated methodology to investigate hydrological processes in Zéramdine–Béni Hassen Miocene aquifer (east-central Tunisia) and to validate the groundwater properties deduced from the geological, geophysical, hydrodynamic and hydro-chemical studies using the coupling of groundwater flow model MODFLOW with Geographic Information System tools. It was concluded that, the model can be regarded as a useful tool for analyzing the hydrological processes for complex groundwater problems.

The Rajshahi city is the fourth largest metropolitan city in Bangladesh on the bank of the river Padma (Ganges). Here an upper semi-impervious layer overlies aquifer – the source for large-scale groundwater development. The groundwater resource study adjoining the river Ganges using Visual MODFLOW (Haque et al., 2012) showed that, the total groundwater abstraction in 2004 (15000 million litres) was lower than total input to aquifer through river induced recharge. Groundwater resources assessment, modeling and management are hampered considerably by a lack of data in semi-arid and arid environments with a weak observation infrastructure especially in Dar-es-Salaam aquifer of Tanzania (Brunner et al., 2006). This issue was well addressed by Camp et al. (2013) later using MODFLOW by creating additional database through field tests. From the calibrated model, it was estimated that, the annual recharge in the area is in the range 80–100mm/year.

Louwyck et al. (2014) outlined a procedure to simulate axisymmetric groundwater flow in radially heterogeneous and layered aquifer systems using the unmodified version of MODFLOW. Several test cases were presented, which compare the calculated results with existing analytical solutions, the analytic element solver TTim, and the axisymmetric, finite-difference model MxSym. It is concluded that the

MODFLOW procedure is capable of simulating accurately axisymmetric flow in radially heterogeneous multi-aquifer systems. Yang et al. (2015) used MODFLOW as one of the three steps carried to prioritizing feasible locations for permeable pavement, taking into account environmental, economic, and social aspects in Mokgamcheon watershed, central Korea. Visual MODFLOW software is used to simulate groundwater levels with and without permeable pavement. The results showed that, by considering anthropogenic factors and hydrological effectiveness, the study effectively prioritizes feasible alternatives that can be implemented into comprehensive hydrological cycle rehabilitation plans.

Kelbe et al. (2016) used a groundwater model (MODFLOW) to simulate 10 year water table fluctuations on the Maputaland coastal plain in northern KwaZulu-Natal, South Africa from January 2000 to December 2010, to contrast the conditions between wet and dry years. Remote sensing imagery was used to map “permanent” and “temporary” wetlands in dry and wet years to evaluate the effectiveness of identifying the suitable conditions for their formation using numerical modeling techniques. The results confirm that, topography plays an important role on a sub-regional and local level to support wetland formation.

2.5 SOLUTE TRANSPORT MODEL

2.5.1 General

The studies on seawater intrusion are carried out through analogous models, physical models, and mathematical models. Because of the limitations in the analogous and physical models, the last few decades have witnessed developments in numerical groundwater models and their application for different aquifer systems. A number of numerical models capable of modeling three dimensional groundwater flow and solute transport are available, such as 3DFEMFAT, FEFLOW, AQUA3D, FEMWATER, HST3D, MOCDENS3D, and SEAWAT. These models play an important role as an enhancement over field studies, leading to more accurate results. To simulate the groundwater problems in coastal regions, numerical tools prove to be the best compared with others because of their flexibility in handling complex boundary conditions. The SEAWAT program was developed to simulate variable-

density, transient groundwater flow problems in coastal aquifers. A detailed review of SEAWAT 2000 model is presented by Simpson (2004). The major advantages of SEAWAT over other programs include formulation of flow equation based on conservation of mass and implicit coupling between the flow and solute transport equations. This leads to more accurate results and wide ranging applicability for hydrogeological problems. The performance of SEAWAT was verified with a number of bench mark problems and is capable of accurately simulating variable density groundwater flow (Langevin and Guo, 1999).

Two dimensional and three dimensional numerical models on the sharp interface approach and the transition zone approach have been developed to simulate the seawater intrusion problem worldwide. Both finite element and finite difference methods of numerical modeling techniques are being practiced to mitigate problems related to seawater intrusion in the coastal aquifers. The numerical models have been used for various management and planning activities, especially in the coastal aquifers during the past decade. Researchers have addressed the seawater intrusion problem either by modeling a hypothetical boundary or case specific for a coastal aquifer. The most recent studies involving different numerical models are included in the following sections.

2.5.2 Hypothetical models

A hypothetical two dimensional model was developed by Ataie- Ashtiani et al. (1999) using SUTRA (Voss 1984) to analyse the effects of tidal fluctuations on seawater intrusion in an unconfined aquifer. Langevin and Guo (2006) present an approach for coupling MODFLOW and MT3DMS for the simulation of variable-density groundwater flow. The approach was tested by simulating the Henry problem and two of the saltpool laboratory experiments (low and high density cases). For the Henry problem, the simulated results compared well with the steady state semi-analytic solution and also the transient iso-chlor movement as simulated by a finite element model. For the saltpool problem, the simulated breakthrough curves compared better with the laboratory measurements for the low density case than for the high density case, but, showed good agreement with the measured salinity iso-surfaces for both cases. The

results from the test cases indicated that, the MODFLOW/MT3DMS approaches provide accurate solutions for problems involving variable density groundwater flow and solute transport.

A management model was presented by Rao et al. (2005) for planning groundwater development in coastal deltas with paleo channels. A simulation-optimization model was used to determine the optimal locations and pumpages for groundwater development for a group of production wells, while limiting the salinity below desired levels. A three dimensional, density-dependent flow and transport model SEAWAT was used in combination with, trained Artificial Neural Network (ANN). The applicability of the model was demonstrated on a hypothetical, but near-real delta system. The model was used to determine the optimal draft locations for a group of production wells, limiting the salinity below desired levels. It was demonstrated that paleo channels are the best locations for locating the wells for large-scale pumping.

A two dimensional hypothetical model in a representative cross section perpendicular to the coastline was developed (Feseker, 2007) using numerical model to analyse the key processes that control the seawater intrusion in the coastal aquifer in Germany. Narayan et al. (2007) developed a two dimensional vertical cross sectional model using SUTRA to define the current and potential extent of seawater intrusion in the Burdekin delta irrigation area in Australia under various pumping and recharge conditions. Webb and Howard (2011) developed a series of fixed inland head, two dimensional seawater intrusion hypothetical models using SEAWAT in order to assess the impact of rising sea levels on the transient migration of saline intrusion in coastal aquifers under a range of hydrogeological properties. Park et al. (2012) performed a series of three dimensional numerical simulations using a multi-dimensional hydrodynamic dispersion numerical model, 3DFEMFAT (Yeh et al. 1994) to analyse various seawater intrusion extraction schemes for mitigating seawater intrusion attributed to groundwater pumping in a coastal aquifer system.

The seasonal variation in natural recharge of coastal aquifers through two dimensional hypothetical SEAWAT models was studied by Mollema and Antonellini (2013). As per the study, the discrepancy between models with continuous and discontinuous recharge is relatively small in areas where the total annual recharge is low. But, in

places with monsoon dominated climate, the difference in freshwater lens thickness between the continuous and discontinuous model is larger. A conceptual, unconfined aquifer with a sub-surface barrier subjected to simultaneous freshwater pumping at single/multiple locations perpendicular to the coast is considered to analyse the effect of freshwater pumping on saltwater intrusion in coastal aquifers in the presence of a semi-pervious subsurface barrier along the coast by Mahesha and Lakshmikanth (2014). The numerical model predicted the behaviour of the saltwater-freshwater interface and the piezometric surface due to simultaneous pumping at single/multiple wells across the sea coast. The results showed that, the barrier is effective in checking the progress of saltwater for freshwater pumping on the landward side of the barrier compared to no barrier condition.

2.5.3 Case specific models

Sherif (1999) presented the seawater intrusion mechanisms through various numerical simulations for the seawater intrusion in the vertical and aerial views of the Nile delta coast, Egypt. The study came out with recommendations for the mitigation of the seawater intrusion problem. Gates et al. (2002) applied a finite difference model developed using the Groundwater Modeling System (GMS), to analyse and predict water table elevations, flow of water and salinity in the salinity threatened lower Arkansas River basin of Colorado, USA. The preliminary steady state modeling indicated that, only limited improvement can be expected from vertical drainage derived from increased pumping, or from decreased recharge brought about by reduced over irrigation.

Langevin (2003) applied the SEAWAT code to estimate the rates of submarine groundwater discharge to a coastal marine estuary in Florida, USA. The model demonstrated that, regional scale variable density models are potentially useful tools for estimating rates of submarine groundwater discharge. Lin and Medina (2003) incorporated the transient storage concept in modeling solute transport in the conjunctive stream-aquifer model. Three widely used USGS models were coupled to form the core of this conjunctive model: MODFLOW, DAFLOW and MOC3D. Rao et al. (2004) developed a density dependent groundwater flow and transport model

using SEAWAT for simulating the dynamics of seawater intrusion and the simulated annealing algorithm for solving the optimization problem. Bauer et al. (2006) used SEAWAT for coupled flow/transport simulations for the Shashe river valley in Botswana. They found that, the salinity distribution in and around the area as well as its temporal dynamics can be satisfactorily reproduced if the transpiration is modelled as a function of groundwater salinity. Qahman and Larabi (2006) used SEAWAT for simulating the spatial and temporal variations of hydraulic heads and solute concentrations of groundwater for the Gaza aquifer in the Palestine. Their predictive simulation for 17 years showed that, the seawater intrusion would worsen in the aquifer if the current rates of groundwater pumping are continued.

Feseker (2007) concluded from his studies that, rising sea level causes rapid progression of saltwater intrusion in coastal north-western Germany, whereas the drainage network compensates changes in groundwater recharge. The numerical model, MOCDENS3D (Essink 1998) was used by Giambastiani et al. (2007) to simulate the seawater intrusion in the unconfined coastal aquifer of Ravenna, Italy. The simulation results showed that, over the last century, artificial subsidence and heavy drainage started the salinization process in the study area and a relative sea level rise will accelerate the seawater water intrusion process. Moustadraf et al. (2008) developed a numerical transient model which related the intensive pumping during the periods of drought to the seawater intrusion in the aquifer of the Chaouia Coast of Morocco. The results indicated that, the severe degradation of the resource was primarily related to intensive pumping which was 7 meters during periods of drought.

Studies were carried out by Vyshali (2008) in the rural coastal areas between the rivers Gurupur and Pavnaje in Dakshina Kannada district, Karnataka to characterize the aquifer and to assess the vulnerability of the basin to seawater intrusion using SUTRA. The study revealed that, the area consists of shallow unconfined aquifer with thickness ranging from 18m to 30m. The area was found to be having moderate to high vulnerability to seawater intrusion during non-monsoon season. The groundwater simulation in a micro-basin of Pavanje river in Dakshina Kannada district, Karnataka (Santhosh, 2011) using the MODFLOW and MT3MDS combination software

confirmed the severity of saltwater intrusion during the months of April and May. Rejani et al. (2008) developed a 2-D groundwater flow and transport model using Visual MODFLOW for analysing the aquifer response to various pumping strategies in Balasore basin of Orissa, India. The results of the sensitivity analysis indicated that, the Balasore aquifer system is more susceptible to the river seepage, recharge from rainfall and interflow than the horizontal and vertical hydraulic conductivities and specific storage. Based on the modeling results, salient management strategies are suggested for the long-term sustainability of vital groundwater resources of the basin.

Lin et al. (2009) developed a variable-density groundwater flow and miscible salt transport model (SEAWAT) to investigate the extent of seawater intrusion in the Gulf coast aquifers of Alabama, USA. Using the calibrated model and assuming all the hydrogeologic conditions remain the same as those in 1996, a predictive 40-year simulation run predicted that, further seawater intrusion into the coastal aquifers could occur in the study area. Vandenbohede et al. (2009) developed three dimensional model using MOCDENS3D (Essink 1998), for sustainable management of a phreatic aquifer in the Belgian plain that faces the problem of decline in groundwater head and seawater intrusion because of overdraft of groundwater. Kopsiaftisa et al. (2009) developed flow and transport model for an unconfined aquifer in Thira Island, Greece using FEFLOW. Two potential cases of aquifer replenishment, with natural and artificial recharge are also simulated. The results showed that advancement of seawater intrusion depends on the initial and boundary conditions prevailing on the seaside boundary of the aquifer.

Shammas and Thunvik (2009) used a three dimensional numerical model for flow and solute transport for the management of the Salalah aquifer, Oman. The established simulation model was used to predict the distribution of the piezometric surface, salinity distribution and mass balance under various water management scenarios for the period 2006-2020. Gholami et al. (2010) presented a linear model and a non-linear model for estimating groundwater salinity on the Caspian southern coasts. The model efficiency was evaluated by applying them in the sites that their data were not used for presenting the models. The electrical conductivity of groundwater map was developed using the non-linear model and Geographic Information System in the

Eastern part of Mazandaran province. Rozzel and Wong (2010) found in their study conducted for Shelter Island, New York that the effects of sea level rise on the fresh water volume would be relatively minor.

The Korba aquifer, Tunisia was numerically simulated by Kerrou and Tarhouni (2010) to understand the current aquifer situation. The model building process was difficult because of data required on groundwater discharge from thousands of unmonitored private wells. To circumvent that difficulty, indirect exhaustive information including remote sensing data and the physical parameters of the aquifer has been used in a multi-linear regression framework. The results showed that, the aquifer was over-exploited. Sedki and Ouazar (2011) constructed a transient simulation model characterizing groundwater flow in the coastal aquifer of Rhis-Nekor, Morocco using MODFLOW. The flow model was then used in conjunction with a genetic algorithm based optimization model to explore the optimal pumping schemes that meet current and future water demands while minimizing the risks for saltwater intrusion, excessive drawdown, as well as waterlogging and salinity problems.

A three dimensional, finite element model of the coastal aquifer in California was constructed using FEFLOW (Diersch, 2006) by Loaiciga et al. (2012) to study the effect of groundwater extraction and sea level rise on the seawater intrusion. The simulation results showed that, groundwater extraction is the predominant driver of seawater intrusion in the study area. Sindhu et al. (2012) developed Visual MODFLOW and SEAWAT for Karikkakom to Pozhiyur region towards south of the coastal belt of Trivandrum, Kerala, India. The effect of 1% increase in pumping on intrusion was studied and it was predicted that, groundwater heads in most of the observation wells are decreasing. The author found that the lateral extent of saltwater intrusion was more at Karikkakom pumping well location when compared to all other well locations due to 1% increase in pumping.

Cobaner et al. (2012) used SEAWAT to develop a model to control seawater intrusion in the coastal aquifer of Goksu deltaic plain along the Mediterranean coast of Turkey. They evaluated the hydraulic and hydro-geologic parameters of the aquifer and

estimated the spatial variation of seawater intrusion in the aquifer for increase and decrease in groundwater extraction. Allow (2012) developed a three dimensional model using SEAWAT to study the groundwater volume and quality for the purpose of planning and management of water resources in the coastal aquifer in Syria. Sherif et al. (2012) used MODFLOW to simulate the groundwater flow and assess the seawater intrusion in the coastal aquifer of Wadi Ham, UAE. Due to the lack of natural replenishment from rainfall and the excessive pumping, groundwater levels had declined significantly causing an intrusion of seawater in the coastal aquifer.

Nowbuth et al. (2012) first developed a groundwater flow model for the southern aquifer of Mauritius. The model has predicted the pathways for contaminants from source pollutants. If there is excessive abstraction of groundwater, then the radial flow towards the sea may decrease or even the flow pattern is reversed, thereafter causing seawater movement inland. Chaaban et al. (2012) coupled GIS and GMS, in order to find the possible scenarios which could lower the piezometric surface in south of Hardelot area, France. The model created in GMS was calibrated against the historical and observed water level data for 1995–2006. Then a hydro-dispersive model (MT3D code) was launched for evaluating seawater intrusion. Langevin and Zygnerski (2013) used SEAWAT to evaluate the relative importance of sea level rise compared to the other dominant hydrologic processes for a municipal well field in south-eastern Florida, USA. The model was used to predict the impact of future rises in sea level on seawater intrusion near the well field.

(Kerrou, 2013) presented a stochastic study of long term forecasts of seawater intrusion with an application to the Korba aquifer, Tunisia using a geo-statistical model of the exploitation based on a multi-linear regression model combining incomplete direct data and exhaustive secondary information and the density dependent transient model. The forecasts of the impacts of two different management scenarios on seawater intrusion in the year 2048 were performed by means of Monte Carlo simulations, accounting for uncertainties in the input parameters as well as possible changes of the boundary conditions. The results of the stochastic long term forecasts showed that, most probably, the Korba aquifer will be subject to important losses in terms of regional groundwater resources.

SEAWAT was used by Zhou et al. (2014) to simulate tide-induced groundwater flow and the groundwater flow dynamics and the effect of beach slope on groundwater table in the unconfined aquifer of Donghai Island, China. The analysis indicated that, the water table fluctuation was especially sensitive to the hydraulic conductivity and specific yield, and the horizontal length of the model domain could affect the amplitude of the water table fluctuation. Moreover, it was found that, the variation of the amplitude is more evident when the beach slope angle changes in the range from 1.5 to 45°, especially in the range from 1.5 to 5°. Comte et al. (2014) concluded from their studies on coral island using SEAWAT model that long term changes in mean sea level and climatic conditions (rainfall and evapotranspiration) are responsible for an average increase in salinity. Green and MacQuarrie (2014), investigated the relative importance of sea level rise and climate change effects on recharge and groundwater extraction on seawater intrusion in the coastal aquifer of Atlantic Canada. The authors developed a three dimensional model of the aquifer using SEAWAT for the investigation and concluded that sea level rise has the least significant effect on the future seawater intrusion.

A salinization of groundwater by oilfield brine and seawater intrusion was detected in the plain of Wadi Al Ayn and Darouda in CapBon, northeast of Tunisia. The historical trends of saltwater distribution (Chekirbane et al., 2015) and the future dynamics were predicted. Based on the developed model with SEAWAT, it was concluded that, the oilfield brine plume needs at least 5 years to be naturally reduced to less than the half of its actual size, while the seawater–freshwater interface can reach inland to the extent of 1.3 km with a TDS of 10 g/L if, no counter measures will be taken until the next three decades. The tested remediation plan by model demonstrated that the artificial recharge with treated wastewater is the best solution to stop seawater intrusion just after 2 years of percolating 1 m/day with TDS of 1.5 g/L of recharge water.

Many coastal areas historically were inundated by seawater, but have since undergone land reclamation to enable settlements and farming. The coastal unconfined aquifer in the Po Plain near Ravenna, Italy, consists of freshwater present as isolated thin (1–5 m) lenses on top of brackish to saline water. Antonellini et al. (2015) used

SEAWAT to simulate a 200 year freshening history, starting with a model domain that is saturated with seawater, and applying recharge across the top model layer. The modeling results showed that, the current distribution of freshwater is largely controlled by the drainage network. Within and adjacent to the drains, the groundwater has high salinity due to up-coning of salt water. Between drains, the surface layers of the aquifer are fresh due to the flushing action of recharge.

2.6 LITERATURE GAP

A review of literature related to past studies of seawater intrusion in coastal aquifers have been presented in this chapter. It is brought out from the literature review that, intricate numerical modeling studies are not attempted in the study area, though a good number of geophysical and field studies have been performed.

The studies on shallow fresh groundwater are necessary as they are equally threatened by salinization (Giambastiani et al., 2007, Vandenbohede et al., 2014, De Louw et al., 2011) as are deeper freshwater resources. Most of the seawater intrusion studies are carried out to examine the impact of seawater intrusion in the deeper aquifer, and hence, each layer of the aquifer is uniformly assigned the aquifer properties. Therefore, the spatial variability of the aquifer parameters is often not accounted. The present study is taken up with a keen interest in understanding the response of an unconfined shallow coastal aquifer to future stress and climate change scenarios existing in tropical climatic conditions considering the spatial (zonal) variability of hydro-geologic parameters. The river aquifer interaction is not well addressed in many earlier investigations. Testing the seasonal performance of the calibrated model is another important criterion to be fulfilled to get a better confidence on the model, which is lacking in the previous studies. This gap has been taken care in the present study by carrying out a monthly model evaluation of a coastal, shallow aquifer system.

CHAPTER 3

AQUIFER CHARACTERIZATION

3.1 GENERAL

The hydrogeological investigation and pumping test are important attributes that is necessary to characterise an aquifer. The aquifer parameters are estimated based on the material property underneath. The pumping tests are imperative in determining aquifer parameters, such as transmissivity and specific yield. A particular method for the pumping test data analysis is chosen based on the knowledge of the groundwater system and conformance of the site hydraulic conditions to the assumptions of the test method. The purpose of the pumping test and the hydro-geological conditions present at the test site are the two important factors based on which the optimal well location, depth, pumping rate, test duration and analysis method are selected. Nine aquifer hydraulic parameter zones are mapped for each basin based on pumping tests evaluations.

3.2 HYDROGEOLOGY

The necessary data in this regard was obtained by the interpretation of test results for the study area. The locations where bore log and vertical electrical sounding (VES) studies are carried out are shown in fig.3.1. The Surface electrical resistivity surveying is based on the principle that, the distribution of electrical potential in the ground around a current carrying electrode depends on the electrical resistivity and distribution of the surrounding soils and rocks. Vertical electrical sounding (VES) is a geophysical method for investigation of a geological medium by Schlumberger method. The method is based on the estimation of the electrical conductivity or resistivity of the medium. The estimation is performed based on the measurement of voltage of electrical field induced by the distant grounded electrodes (current electrodes).

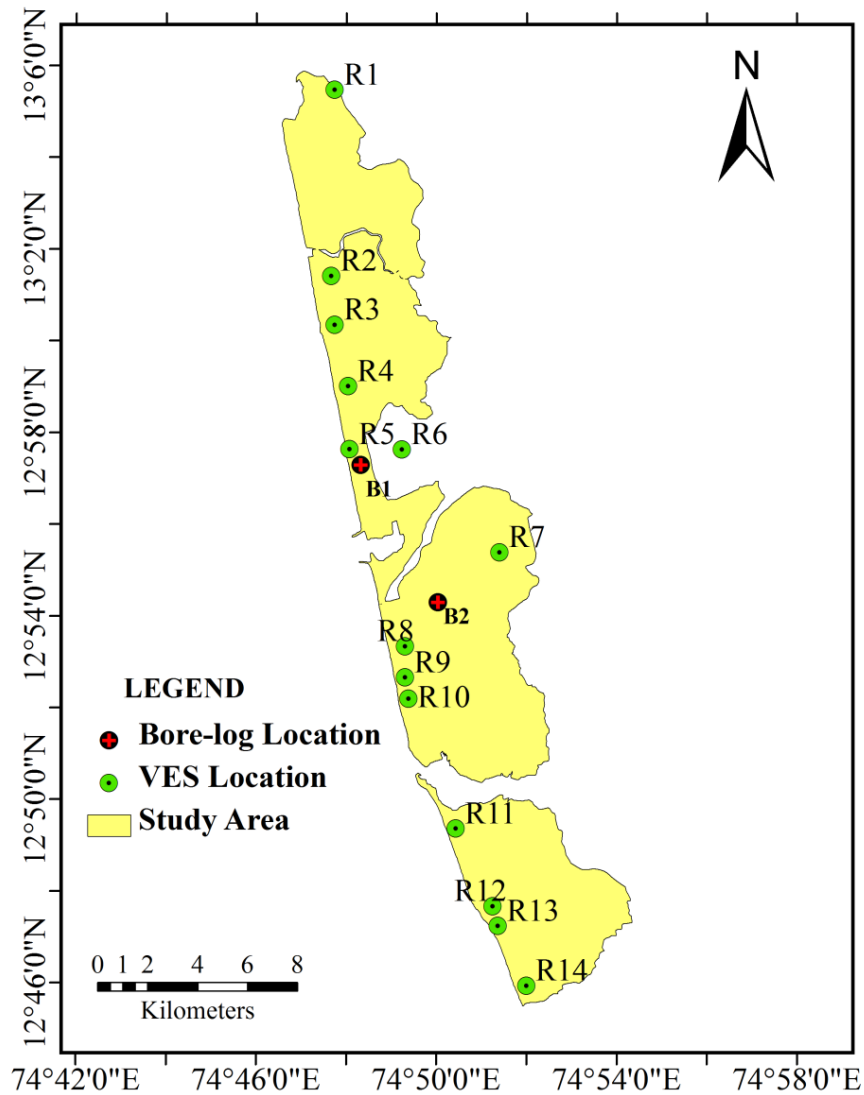


Fig.3.1 Locations of bore log and VES survey

3.2.1 Bore- log information

The lateritic formation in the region is underlain by a thin bed of clay, granites, gneisses, and coastal alluvium along the coast. It is evident from the earlier investigations (Rao, 1974; Srikantiah, 1987; Lokesh, 1997 and Mahesha et al., 2012) that, the basin is predominantly an unconfined aquifer with depth ranging from 12 to 30 m. The lithology of the bore log investigation carried out by the Central Ground Water Board (CGWB, 2008) at B1 and B2 (fig. 3.1) is presented in fig. 3.2. At least one clay layer was found to be covered by several non-cohesive sand layers in these

locations of the coastal belt. In the interior part, laterite mainly covers the subsurface with depth of lateritic formation varying from 5 to 20 m.

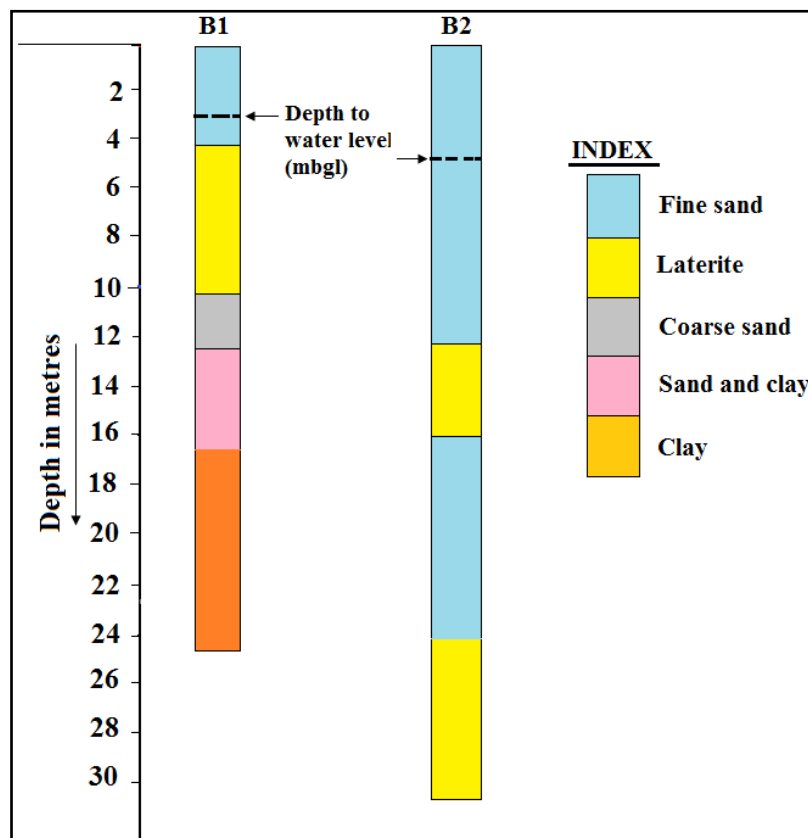


Fig. 3.2 Lithology of bore logs

3.2.2 Lithology map

In the absence of dense bore log data pertaining to the area, the lithological unit map prepared by the KRSAC (Karnataka State Remote Sensing Applications Centre) for the district is extracted for the area of interest and is presented in fig.3.3. The related description is given in table 3.1. The map shows an alluvial unit running parallel to the coastline up to about 2- 4 km stretch perpendicular to the coast. The laterite is seen adjacent to coast occurring as capping on ridges and hillocks and as sheet like masses at elevated terrains. The thickness of the laterite cover is found to vary generally from 5 to 20m.

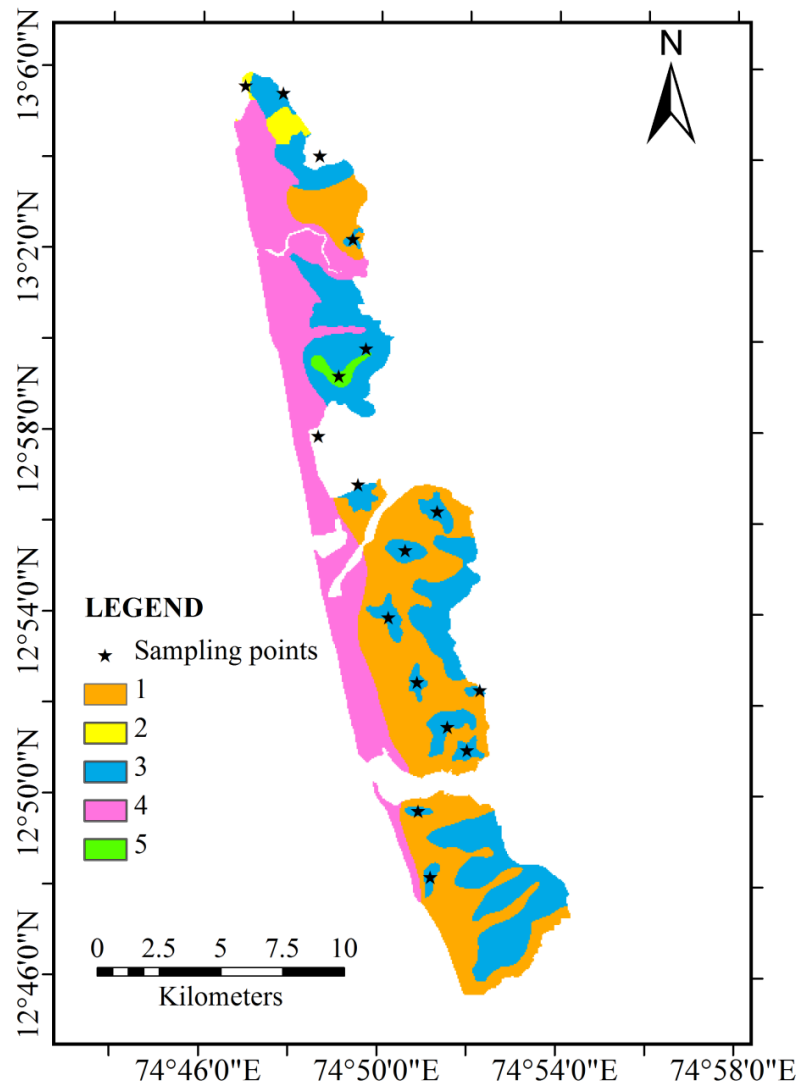


Fig.3.3 Lithology map of the study area

Table 3.1. Lithological classification

Litho-class	Description
1	Magmatites and granodiorite –Tonalitic gneiss
2	Pink hornblende granite
3	Laterite
4	Alluvium / beach sand, alluvial soil
5	Hornblende-biotite gneiss

3.2.3 Vertical electrical sounding survey

A vertical electrical sounding survey is carried out (Shivanagouda, 2015) at 14 locations (fig. 3.1) in the area. Among them, the lithological variation at 11 locations situated along the coastline within 1km distance is interpreted as shown in fig.3.4. This observation matches well with the bore log and lithology maps agreeing to the fact that, the region is underlain by shallow lateritic formation as a key aquifer material in the region. Laterites are generally coarse grained and are composed of vermicular tube like structure. The thickness of the lateritic formation ranges from about 18 to 25m. The lateritic formation is topped by sand and top soil and beneath the laterite a huge mass of hard rock material (gneiss) is detected upto a depth of about 90m.

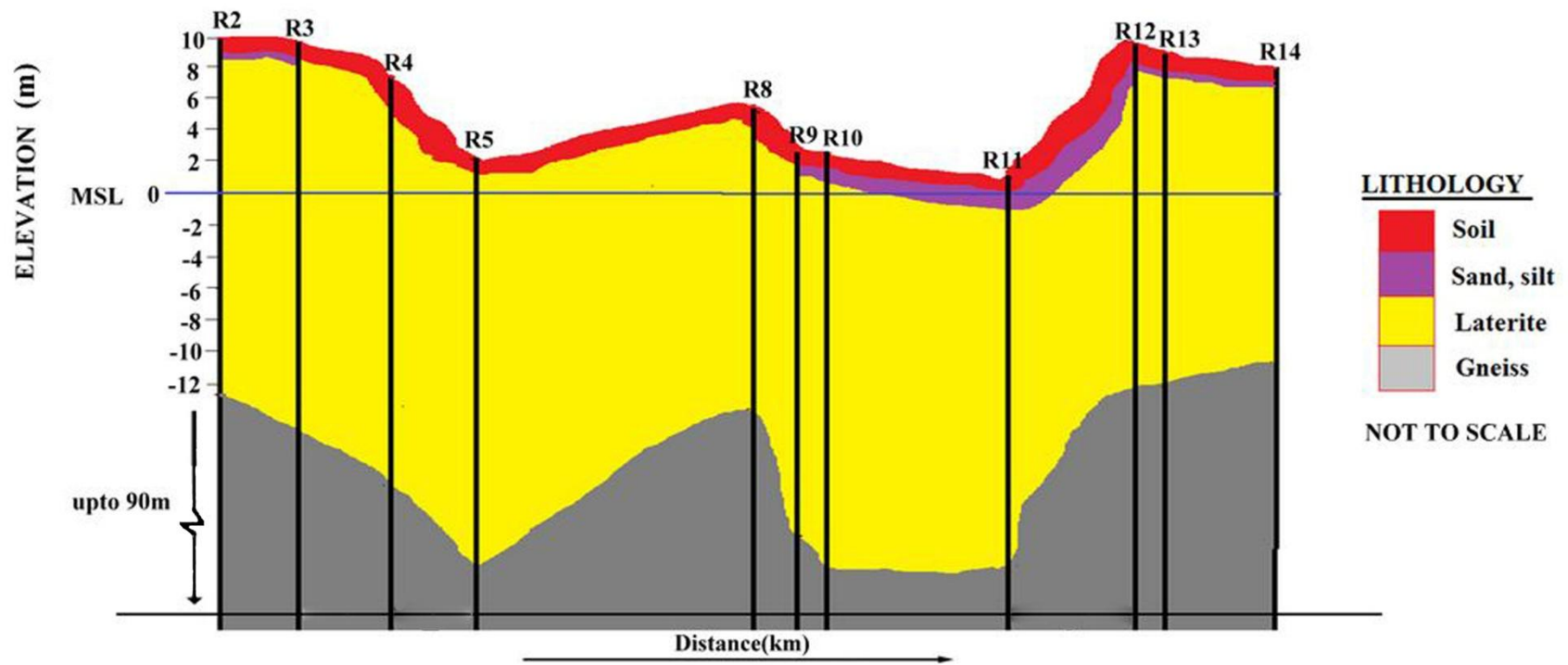


Fig. 3.4 Hydrogeological profile as per VES

3.3 PUMPING TESTS

3.3.1 General

The hydraulic properties of aquifers can be determined by the ‘pumping test’ which is also termed as ‘aquifer test’. It involves pumping of water from a well at a controlled rate and observation of water level at the observation well with respect to time. Pumping tests also provide information on the yield and drawdown of water table (Karanth, 1987). Better and more reliable results are obtained if pumping continues till the cone of depression has reached a stabilized position and does not seem to expand further as pumping continues. In fact, the cone of depression will continue to expand until the recharge of the aquifer equals the pumping rate (Rajagopalan, 1983). Initial knowledge of the lithological profile of the study area would be of great help in planning the tests and interpreting the data. It is therefore necessary to carry out adequate subsurface investigations prior to undertaking aquifer tests.

3.3.2 Methodology

In the study area, pumping tests are conducted in 3 open wells located in and around sub-basin 3. These data are in addition to the data already available from aquifer characterization. The details and photographs of the pumping wells are given in table 3.2 and figs.3.5 to 3.7 respectively. The wells selected for the analysis are of shallow depth (<10m). The locations of these wells are shown in fig.3.25 of section 3.4.

Before starting the pumping test, it is to be ensured that, the initial water level in the well is in steady state. In the present study, the maximum pumping duration possible was about 2 hours due to drying up of well, erratic power supply etc. After the pumping is started, drawdown is measured at every minute till first 10 minutes, thereafter the frequency of measurement goes on decreasing till the pumping is stopped. After the pumping is stopped, the recovery of water level is measured with decreased frequency with time. The initial recovery is faster which gets stabilized later depending on the aquifer characteristics.

Table 3.2 Details of the pumping wells

Well No	Well location	Place	Dia. of the well (m)	Total depth of the well (m)	Depth to water level before test (m)	Discharge (m ³ /sec)
PW1	12°55'54.83"N	Marakada	5.10	4.70	0.90	0.00571
	74°51'39.08" E					
PW2	12°52'9.06" N	Adyar	2.50	5.53	2.12	0.00203
	74°53'47.08"E					
PW3	12°54'22.29" N	Konchadi	2.30	7.30	2.98	0.00182
	74°51'05.40"E					



Fig.3.5 Photograph of pumping well no PW1



Fig.3.6 Photograph of pumping well no PW2



Fig.3.7 Photograph of pumping well no PW3

Pumping rate

The discharges of wells are usually measured at the well head. When this is not possible, they can be measured some distance away after ensuring that water is not

lost during transit. The pumping rate is measure by a variety of ways and in the present study, two methods are adopted depending on the suitability. In the first method, suitable for small pumping rates, the time required to fill a collecting tank of known volume is noted using a stop watch and discharge rate is calculated as follows:

$$Q(\text{m}^3/\text{sec}) = \frac{\text{Volume of collecting tank (m}^3\text{)}}{\text{Time required to fill the collecting tank (seconds)}} \quad (3.1)$$

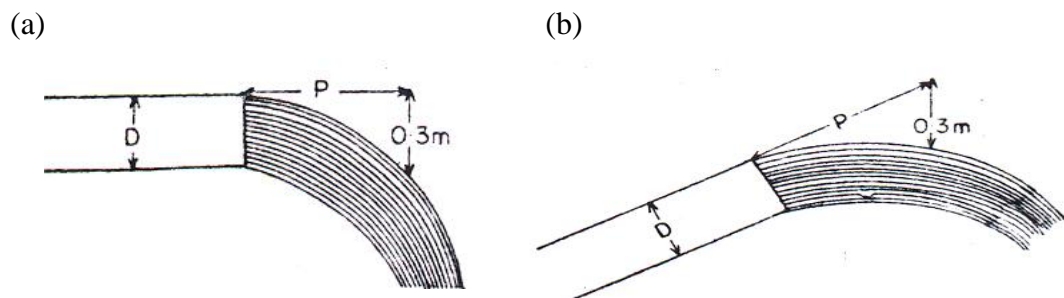


Fig. 3.8 Measurements for determining the discharge: (a) horizontal and (b) inclined pipe



Fig. 3.9 Discharge measurement in the field using (a) collecting tank (b) trajectory methods

In the second method, the horizontal distance travelled by the trajectory of water out of the horizontal (fig.3.8a) or inclined pipe (fig.3.8b) for a vertical fall of 30cm is measured. Both the methods carried out in the field for discharge measurements are depicted in fig.3.9. The discharge rate for trajectory method is calculated using the following relation:

$$Q = 0.017CP \tag{3.2}$$

Where, Q = flow of water in m^3/s

C = constant to be determined from the graph (fig.3.10A)

P = distance travelled by the stream, in m, measured parallel to the pipe for a 30 cm vertical drop.

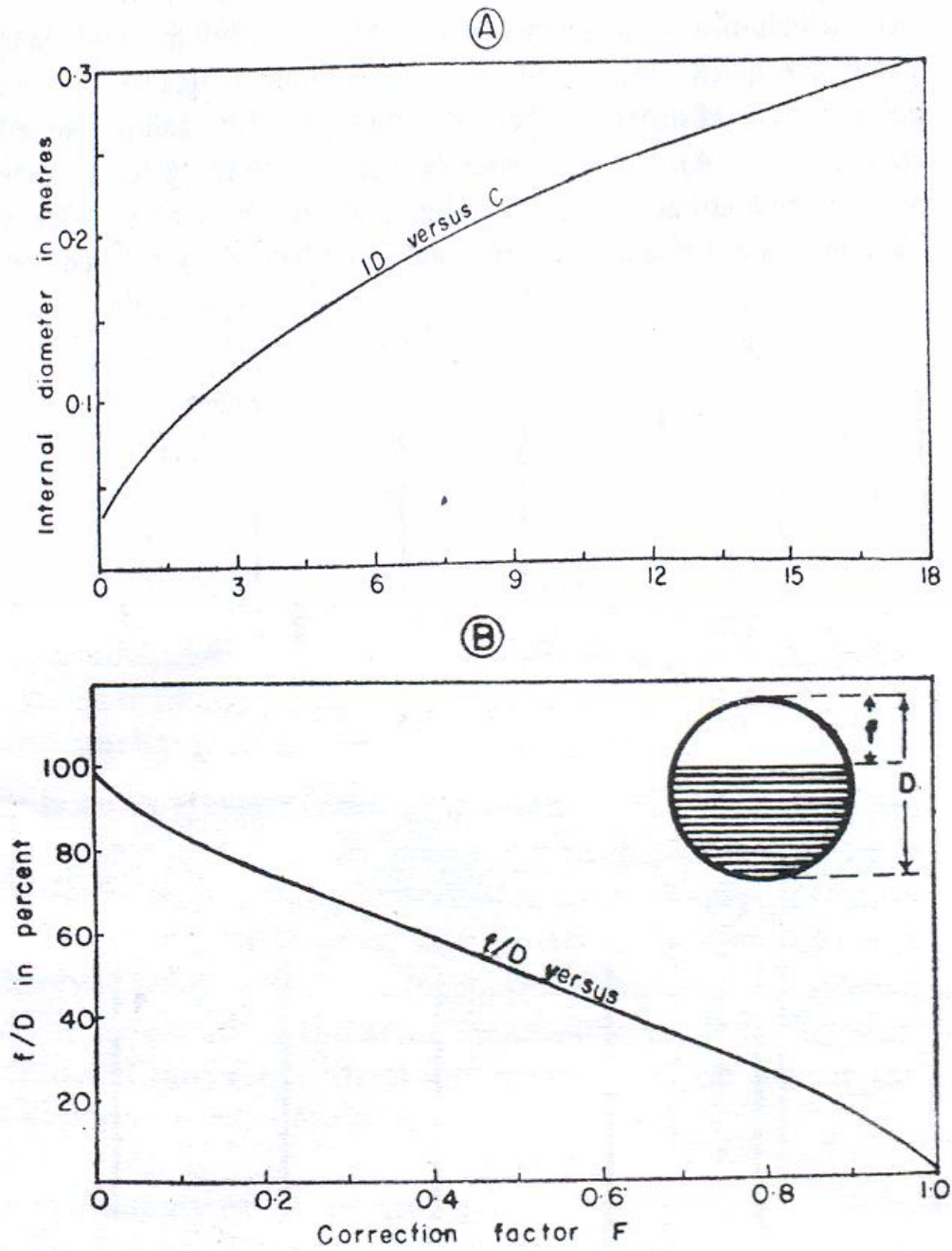


Fig. 3.10 Curves for determining C and F for estimation of flow through inclined and horizontal pipes

When the pipes are only partially filled, the freeboard (f) and the internal diameter (D) are measured and the ratio f/D calculated as a percentage. The discharge is calculated as in the method for full pipes and a correction factor to be read from the curve in Fig.3.10 B is applied to obtain the appropriate discharge.

Hydraulic properties

The important hydraulic properties of aquifers are the hydraulic conductivity, transmissivity, coefficient of storage, specific yield and the specific capacity.

(i) Hydraulic conductivity (K)

The hydraulic conductivity, also known as the permeability is as measure of the ease with which fluid moves through a formation and is defined as the amount of flow per unit cross sectional area under the influence of a unit gradient. It has the dimensions of velocity and is usually expressed as m/day. The hydraulic conductivity depends upon the properties of the fluid as well as the aquifer.

(ii) Transmissivity (T)

Transmissivity is a hydraulic characteristic of the aquifer which is defined as the rate of flow of water at the prevailing field temperature under a unit hydraulic gradient through a vertical strip of aquifer of unit width and extending through the entire saturated thickness of the aquifer. It is therefore the product of the average hydraulic conductivity (K) and the thickness (b) of the aquifer ($T = Kb$, m^2/day). The concept of transmissivity holds good in confined aquifer but in unconfined aquifer, as the saturated thickness of the aquifer changes with time, the T will also change accordingly.

(iii) Coefficient of storage (S) and specific yield (S_y)

Each aquifer, whether under the water table or in a confined condition, has the capacity to store water which is expressed as a coefficient. The storage coefficient of an aquifer is defined as the volume of water it releases from or it takes into storage per unit surface area of the aquifer per unit change in the head. In the case of an unconfined aquifer, the concept of storage is analogous to that of specific yield. In

confined aquifer, the storage coefficient depends on the compressibility of the aquifer and the expansion of water. Since the unconfined aquifer is not bounded by confining layers, the specific yield or storage coefficient does not depend upon the compressibility of either the aquifer or the fluid. The specific yield for all practical purposes is same as effective porosity or drainable porosity, because in the unconfined aquifer the effects of elasticity of the aquifer material or fluid are generally negligible.

(iv) Specific capacity

It is a measure of both effectiveness of a well and of the aquifer characteristics. It is defined as the ratio of the pumping rate and the drawdown and is usually expressed in liters per minute per meter of drawdown for a specific period of pumping.

3.3.3 Analysis of pumping test data

A frequently used method for estimating the hydraulic properties is the graphical type-curve analysis in which dimensionless type curves derived from an assumed analytical model of ground water flow to a pumped well are used to analyse the time-drawdown measurements of hydraulic head in the observation wells. These analyses are done to estimate the hydraulic conductivity and specific yield of water table (unconfined) aquifers. Three methods adopted for the present study are described in the following sections.

Theis (1935) method

Theis (1935) was the first to develop a formula for unsteady state flow that introduces the time factor and storativity. He noted that when a well penetrating an extensive confined aquifer is pumped at a constant rate, the influence of discharge extends outward with time. The rate of decline of head, multiplied by the storativity and summed over the area of influence, equals the discharge.

The unsteady state (or Theis) equation, which was derived from the analogy between the flow of groundwater and the conduction of heat, is written as

$$s = \frac{Q}{4\pi T} \int_u^\infty \frac{e^{-u}}{u} du = \frac{Q}{4\pi T} W(u) \quad (3.3)$$

Where $u = r^2S/4Tt$ and consequently $S = 4Tu/r^2$ (3.4)

s = drawdown, in metres

$T = KD$ = transmissivity, in m^2/day

Q = constant rate of discharge of well in m^3/day

S = storage coefficient, dimensionless

t = time, in days, since pumping started

e = base of natural logarithm

r = radial distance from discharge well to the point of observation, in metres

In the above equation the exponential integral expression is symbolically expressed as $W(u)$ for ‘well function of u ’

$$W(u) = -0.5772 - \ln u + u - \frac{u^2}{2.2!} + \frac{u^3}{3.3!} - \frac{u^4}{4.4!} + \dots \dots \dots \quad (3.5)$$

The formula is based on the following assumptions: (1) the aquifer is isotropic and homogeneous. (2) The aquifer has infinite areal extent. (3) The discharge well penetrates and receives water from the entire thickness of the aquifer. (4) The transmissivity is constant at all times and at all places. (5) The well has infinitesimal diameter. (6) Water removed from storage is discharged instantaneously with decline in the head.

Implied in the assumptions are other limiting conditions – the aquifer is horizontal and confined; has a constant coefficient of storage, is not recharged; the pumped well is fully penetrating and screened in the entire aquifer; the piezometric surface is horizontal and the storage in the well can be neglected.

From equation 3.3, it will be seen that, if s can be measured for one or more values of r and several values of t , and if the well discharge Q is known, S and T can be determined. The presence of two unknowns and nature of exponential integral make it

impossible to effect an explicit solution. Using equations 3.3 and 3.4, Theis devised the ‘curve-fitting method’ to determine S and T. The equation 3.3 can also be written as

$$\log s = \log (Q/4\pi T) + \log (W(u)) \quad (3.6)$$

and equation 3.4 as

$$\log (r^2/t) = \log (4T/S) + \log(u) \quad (3.7)$$

Since $Q/4\pi T$ and $4T/S$ are constant, the relation between $\log s$ and $\log (r^2/t)$ must be similar to the relation between $\log W(u)$ and $\log(u)$. This curve fitting method is based on the fact that if s is plotted against r^2/t and $W(u)$ against u on the same log-log paper (Fig.3.11), the resulting curves (the data curve and the type curve, respectively) will be of the same shape, but will be horizontally and vertically offset by the constants $Q/4\pi T$ and $4T/S$. The two curves can be made to match. The coordinates of an arbitrary matching point are the related values of s , r^2/t , u , and $W(u)$, which can be used to calculate T and S with equations 3.3 and 3.4.

Instead of using a plot of $W(u)$ (normal type curve) in combination with a data plot of s versus r^2/t , it is frequently more convenient to use a plot of $W(u)$ versus $1/u$ (reversed type curve) and a plot of s versus r^2/t (Fig.3.12).

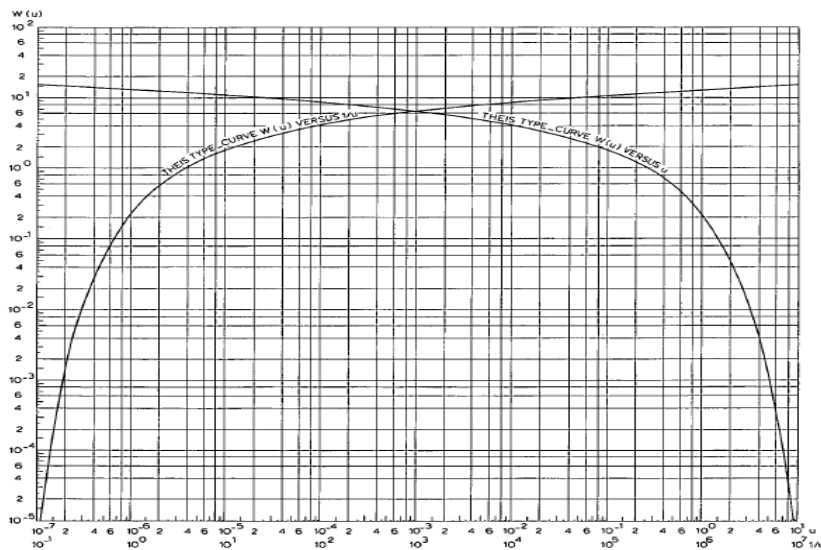


Fig. 3.11 Theis type curve for $W(u)$ versus u and $W(u)$ versus $1/u$

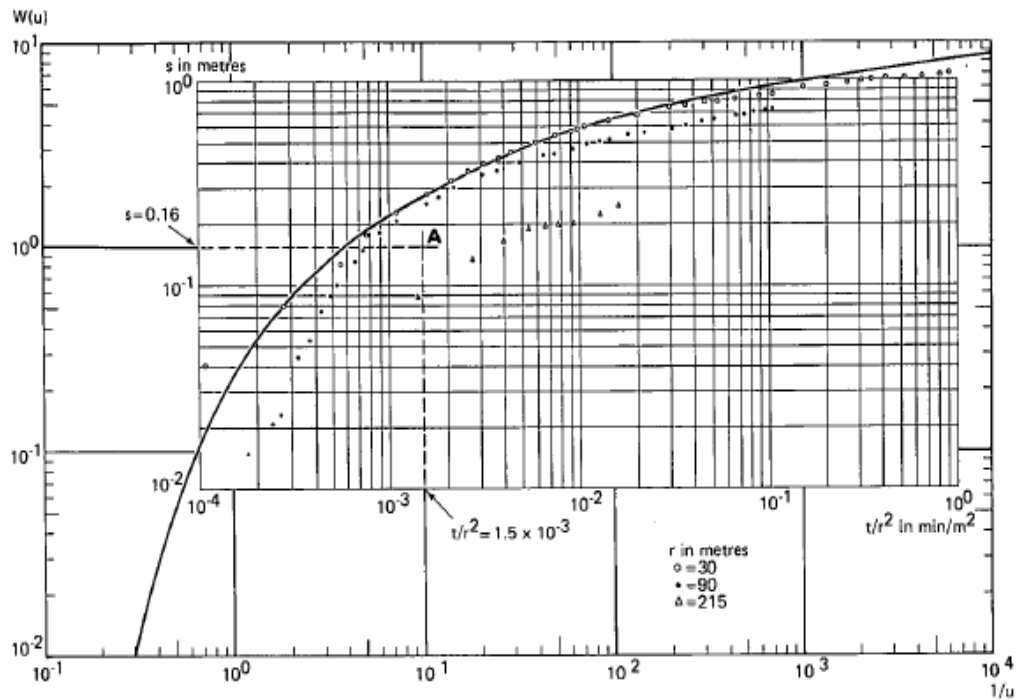


Fig.3.12 Type curve and data plot of t versus s of observation well for Theis method of analysis (Kruseman and de Ridder, 1994)

Theis (1935) approximation for unconfined aquifers

When a well screened in a thick unconfined aquifer without delayed yield is pumped, the flow pattern around the well is nearly identical to that in a confined aquifer so that the Theis non-equilibrium formula is applicable under the same limiting conditions except the one regarding the confined condition of the aquifer. If the aquifer is thin, a correction has to be made to the drawdown to account for partial desaturation and consequent reduction during the course of pumping, in the transmissivity of the aquifer. In such a situation the observed drawdown would be more than what it would have been had the transmissivity not decreased, appreciably, progressively, during pumping. Jacob (1963) showed that equations based on the assumption of negligible dewatering and radial flow can be used for aquifer test data analysis if the drawdown observed in thin unconfined aquifers is adjusted as follows:

$$s_c = s - (s^2/2b) \quad (3.8)$$

where, s_c = drawdown that would have occurred in a confined aquifer

s = observed drawdown under water table conditions

b = initial saturated thickness of the aquifer

where the adjustment for dewatering of the aquifer is considered significant, $s - (s^2/2b)$ should be plotted against t and not s versus t . Such corrections are applicable if the flow is essentially radial and the corrections cannot be relied upon where vertical flow components are dominant, as in the case of partially penetrating wells. When the drawdowns are adjusted, the non-equilibrium formula can be used with fair assurance even when the dewatering is as much as 25 percent of the initial saturated thickness.

The values of S can be determined by the equation (Jacob, 1963)

$$S = \left(\frac{b-s}{b}\right) S' \quad (3.9)$$

Where S = corrected storage coefficient

b = thickness of the aquifer

s = drawdown

S' = apparent coefficient of storage

Neuman (1974) method

When the pumping well and the observation well is perforated throughout the entire saturated thickness of the aquifer, the drawdown in the observation well is given by Neuman (1974) for unconfined aquifers as:

$$s(r,t) = \frac{Q}{4\pi T} \int_0^\infty 4yJ_0(y\beta^{1/2}) \left[u_0(y) + \sum_{n=1}^\infty u_n(y) \right] dy \quad (3.10)$$

where,

$$u_0(y) = \frac{\{1 - \exp[-t_s \beta(y^2 - \gamma_0^2)]\} \tanh(\gamma_0)}{\{y^2 + (1 + \sigma)\gamma_0^2 - [(y^2 - \gamma_0^2)^2 / \sigma]\} \gamma_0} \quad (3.11)$$

$$u_n(y) = \frac{\{1 - \exp[-t_n \beta(y^2 + \gamma_n^2)]\} \tanh(\gamma_n)}{\{y^2 - (1 + \sigma)\gamma_n^2 - [(y^2 + \gamma_n^2)^2 / \sigma]\} \gamma_n} \quad (3.12)$$

and the terms γ_0 and γ_n are the roots of the equations

$$\begin{aligned} \sigma \gamma_0 \sinh(\gamma_0) - (y^2 - \gamma_0^2) \cosh(\gamma_0) &= 0 \\ \gamma_0^2 &< y^2 \end{aligned} \quad (3.13)$$

$$\begin{aligned} \sigma \gamma_n \sin(\gamma_n) + (y^2 + \gamma_n^2) \cos(\gamma_n) &= 0 \\ (2n - 1)(\pi/2) < \gamma_n < n\pi \quad n \geq 1 \end{aligned} \quad (3.14)$$

The formula is based on the following assumptions: (1) the aquifer has a seemingly infinite areal extent. (2) The aquifer is homogeneous and of uniform thickness over the area influenced by the test. (3) Prior to pumping, the water-table is horizontal over the area that will be influenced by the test. (4) The aquifer is pumped at a constant discharge rate. (5) The well does not penetrate the entire thickness of the aquifer. (6) The aquifer is isotropic or anisotropic. (7) The flow to the well is in an unsteady state. (8) The influence of the unsaturated zone upon the drawdown in the aquifer is negligible. (9) An observation well screened over its entire length penetrates the full thickness of the aquifer. (10) The diameters of the pumped and observation wells are small, i.e. storage in them can be neglected.

The three independent dimensionless parameters σ , β and t_s or t_y , are related to each other by $t_y = \sigma t_s$. The curves lying to the left of the values of β in fig. 3.13 are called type A curves and correspond to the top scale expressed in terms of t_s . The curves lying to the right of the values of β in the figure are called type B curves and correspond to the bottom scale expressed in terms of t_y . The Theis curves with respect to both dimensionless time parameters t_s and t_y have been included in the figure for reference purposes. Type A curves are intended for use with early drawdown data and type B curves with late drawdown data.

The field data, plotted on a logarithmic paper (drawdown, s versus time, t) is superimposed on the type B curves, keeping the vertical and the horizontal axes of both graphs parallel to each other and matching as much of the latest time-drawdown data to a particular type curve. The value of β corresponding to this type curve is noted and a match point is chosen anywhere on the overlapping portion of the two sheets of paper. The coordinates of this match point are s^* and s_d^* along the vertical axis and t^* and t_y^* along the horizontal axis. Hence, transmissivity

$$T = c_1(Qs_d^*/s^*) \quad (3.15)$$

and the specific yield

$$S_y = c_2(Tt^* / r^2 t_y^*) \quad (3.16)$$

where c_1 and c_2 are constants and are equal to $1/4\pi$ and 1.0 in CGS units respectively.

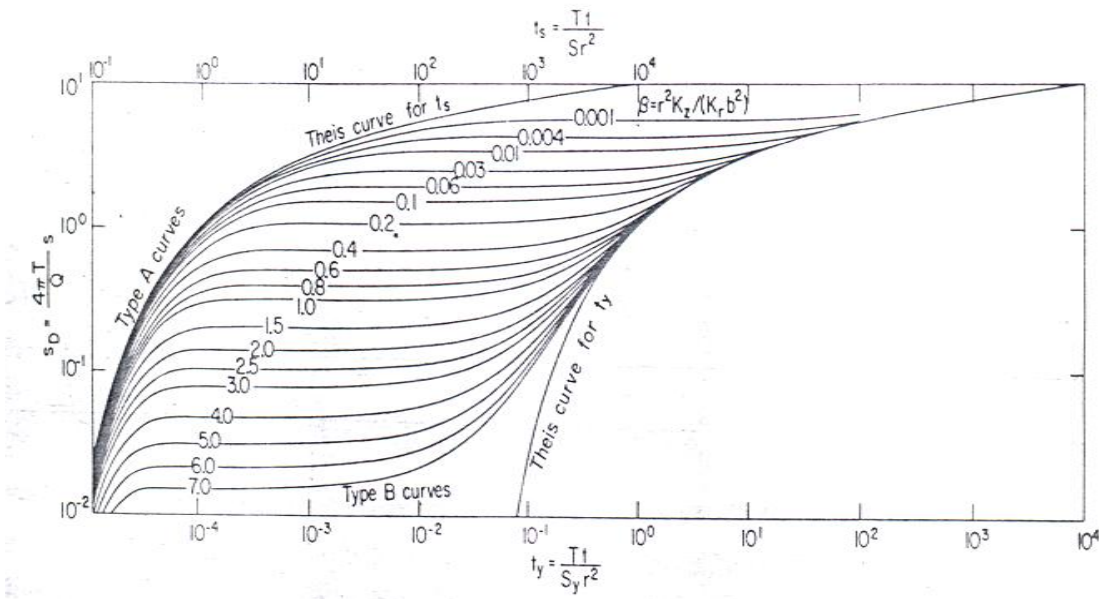


Fig.3.13. Type curves for fully penetrating wells (Neuman, 1975)

The transmissivity value is again calculated by superimposing the field data on the type A curve and its value should be approximately equal to that calculated from the late drawdown data.

Tartakovsky Neuman method

Tartakovsky and Neuman (2007) developed an analytical solution for flow to a partially penetrating well pumping at a constant rate from a compressible unconfined aquifer considering an unsaturated zone of infinite thickness. In their solution three dimensional, axially symmetric unsaturated flow was described by a linearized version of Richards' equation in which both relative hydraulic conductivity and water content vary exponentially with incremental capillary pressure head relative to its air entry value, the latter defining the interface between the saturated and unsaturated zones. Both exponential functions were characterized by a common exponent 'k'

having the dimension of inverse length, or equivalently a dimensionless exponent 'kd=kb', where b is initial saturated thickness. A solution admitting two separate values of k, one characterizing relative hydraulic conductivity and the other water content, was developed by Mathias and Butler (2006). Whereas their solution allowed the unsaturated zone to have finite thickness, it considered flow in the unsaturated zone to be strictly vertical and the pumping well to be fully penetrating.

3.3.4 Results and discussion

The aquifer test data analysis by graphical type-curve method is most frequently used, where dimensionless type curves derived from an assumed analytical model of groundwater flow to a pumped well are used. The pumping test analysis of unconfined aquifer should consider saturated thickness, reduction and vertical flow since the pumping from an unconfined aquifer leads to dewatering of the aquifer. In the present study, Theis (1935) method, Nueman (1974) method and Tartakovsky Nueman (2007) methods are used for the analysis which are applicable for unconfined aquifer system. The time-drawdown and recovery data for the test conducted in pumping well number PW1, PW2 and PW3 are listed in Table 3.3, 3.4 and 3.5 respectively.

Table 3.3 Time-drawdown and recovery data for well no.PW1

Time (mins)	During pumping		After pumping is stopped		Residual drawdown (m)
	Depth to water level(m)	Drawdown (m)	Depth to water level(m)	Recovery (m)	
0	0.9	0	2.38	0	1.48
1	0.92	0.02	2.36	0.02	1.46
2	0.94	0.04	2.34	0.04	1.44
3	0.96	0.06	2.32	0.06	1.42
4	0.98	0.08	2.3	0.08	1.4
5	1.01	0.11	2.29	0.09	1.39

6	1.03	0.13	2.27	0.11	1.37
7	1.06	0.16	2.24	0.14	1.34
8	1.07	0.17	2.22	0.16	1.32
9	1.09	0.19	2.2	0.18	1.3
10	1.11	0.21	2.18	0.2	1.28
12	1.15	0.25	2.15	0.23	1.25
14	1.19	0.29	2.11	0.27	1.21
16	1.23	0.33	2.08	0.3	1.18
18	1.27	0.37	2.05	0.33	1.15
20	1.29	0.39	2.02	0.36	1.12
25	1.37	0.47	1.95	0.43	1.05
30	1.44	0.54	1.88	0.5	0.98
35	1.53	0.63	1.83	0.55	0.93
40	1.58	0.68	1.74	0.64	0.84
45	1.64	0.74	1.63	0.75	0.73
50	1.7	0.8	1.62	0.76	0.72
55	1.76	0.86	1.56	0.82	0.66
60	1.81	0.91	1.51	0.87	0.61
70	1.91	1.01	1.44	0.94	0.54
80	2.02	1.12	1.37	1.01	0.47
90	2.12	1.22	1.32	1.06	0.42
100	2.2	1.3	1.26	1.12	0.36
110	2.3	1.4	1.22	1.16	0.32
120	2.38	1.48	1.18	1.2	0.28
130			1.15	1.23	0.25
140			1.11	1.27	0.21
150			1.1	1.28	0.2
160			1.08	1.3	0.18
170			1.05	1.33	0.15
180			1.05	1.33	0.15
190			1.03	1.35	0.13

200			1.02	1.36	0.12
210			1	1.38	0.1
225			0.99	1.39	0.09
240			0.98	1.4	0.08
255			0.98	1.4	0.08
270			0.96	1.42	0.06

Table 3.4 Time-drawdown and recovery data for well no.PW2

Time (mins)	During pumping		After pumping is stopped		Residual drawdown (m)
	Depth to water level(m)	Drawdown (m)	Depth to water level(m)	Recovery (m)	
0	2.12	0	3.55	0	1.43
1	2.16	0.04	3.54	0.01	1.42
2	2.21	0.09	3.53	0.02	1.41
3	2.21	0.09	3.53	0.02	1.41
4	2.24	0.12	3.52	0.03	1.4
5	2.26	0.14	3.52	0.03	1.4
6	2.29	0.17	3.51	0.04	1.39
7	2.32	0.2	3.5	0.05	1.38
8	2.35	0.23	3.5	0.05	1.38
9	2.37	0.25	3.49	0.06	1.37
10	2.4	0.28	3.48	0.07	1.36
12	2.44	0.32	3.47	0.08	1.35
14	2.49	0.37	3.46	0.09	1.34
16	2.54	0.42	3.45	0.1	1.33
18	2.59	0.47	3.44	0.11	1.32
20	2.64	0.52	3.43	0.12	1.31
25	2.76	0.64	3.39	0.16	1.27
30	2.88	0.76	3.36	0.19	1.24

35	3.02	0.9	3.33	0.22	1.21
40	3.12	1	3.31	0.24	1.19
45	3.23	1.11	3.28	0.27	1.16
50	3.34	1.22	3.25	0.3	1.13
55	3.45	1.33	3.23	0.32	1.11
60	3.55	1.43	3.2	0.35	1.08
70			3.15	0.4	1.03
80			3.11	0.44	0.99
90			3.06	0.49	0.94
100			3.02	0.53	0.9
110			2.98	0.57	0.86
120			2.96	0.59	0.84
130			2.9	0.65	0.78
140			2.88	0.67	0.76
150			2.83	0.72	0.71
165			2.79	0.76	0.67
180			2.75	0.8	0.63
195			2.7	0.85	0.58
210			2.67	0.88	0.55
225			2.61	0.94	0.49
240			2.59	0.96	0.47
255			2.55	1	0.43
270			2.51	1.04	0.39
285			2.48	1.07	0.36
300			2.46	1.09	0.34
315			2.43	1.12	0.31
330			2.42	1.13	0.3
345			2.4	1.15	0.28
360			2.38	1.17	0.26
375			2.37	1.18	0.25
390			2.35	1.2	0.23

405			2.33	1.22	0.21
420			2.31	1.24	0.19
435			2.31	1.24	0.19
450			2.3	1.25	0.18
465			2.29	1.26	0.17

Table 3.5 Time-drawdown and recovery data for well no.PW3

Time (mins)	During pumping		After pumping is stopped		Residual drawdown (m)
	Depth to water level(m)	Drawdown (m)	Depth to water level(m)	Recovery (m)	
0	2.98	0	3.19	0	0.21
1	3.01	0.03	3.16	0.03	0.18
2	3.03	0.05	3.14	0.05	0.16
3	3.04	0.06	3.13	0.06	0.15
4	3.05	0.07	3.12	0.07	0.14
5	3.06	0.08	3.11	0.08	0.13
6	3.07	0.09	3.1	0.09	0.12
7	3.07	0.09	3.09	0.1	0.11
8	3.08	0.1	3.09	0.1	0.11
9	3.09	0.11	3.085	0.105	0.105
10	3.1	0.12	3.08	0.11	0.1
12	3.1	0.12	3.075	0.115	0.095
14	3.11	0.13	3.07	0.12	0.09
16	3.12	0.14	3.065	0.125	0.085
18	3.12	0.14	3.06	0.13	0.08
20	3.12	0.14	3.06	0.13	0.08
25	3.14	0.16	3.05	0.14	0.07
30	3.15	0.17	3.04	0.15	0.06
35	3.16	0.18	3.035	0.155	0.055
40	3.16	0.18	3.03	0.16	0.05

45	3.16	0.18	3.03	0.16	0.05
50	3.17	0.19	3.03	0.16	0.05
55	3.17	0.19	3.025	0.165	0.045
60	3.17	0.19	3.02	0.17	0.04
70	3.17	0.19	3.02	0.17	0.04
80	3.18	0.2	3.01	0.18	0.03
90	3.19	0.21	3.01	0.18	0.03
100			3.005	0.185	0.025
110			3	0.19	0.02
120			3	0.19	0.02
130			3	0.19	0.02
140			2.995	0.195	0.015
150			2.99	0.2	0.01
160			2.99	0.2	0.01
170			2.99	0.2	0.01
180			2.99	0.2	0.01
195			2.99	0.2	0.01
210			2.99	0.2	0.01
225			2.99	0.2	0.01
240			2.99	0.2	0.01

Also, a graph of drawdown and recovery versus time is shown in fig.3.14 for pumping well nos. PW1, PW2 and PW3. Pumping well PW2 was having faster drawdown compared to other wells. The recovery was maximum in well nos. 1 and 3 with about 95% recovery in 260 minutes.

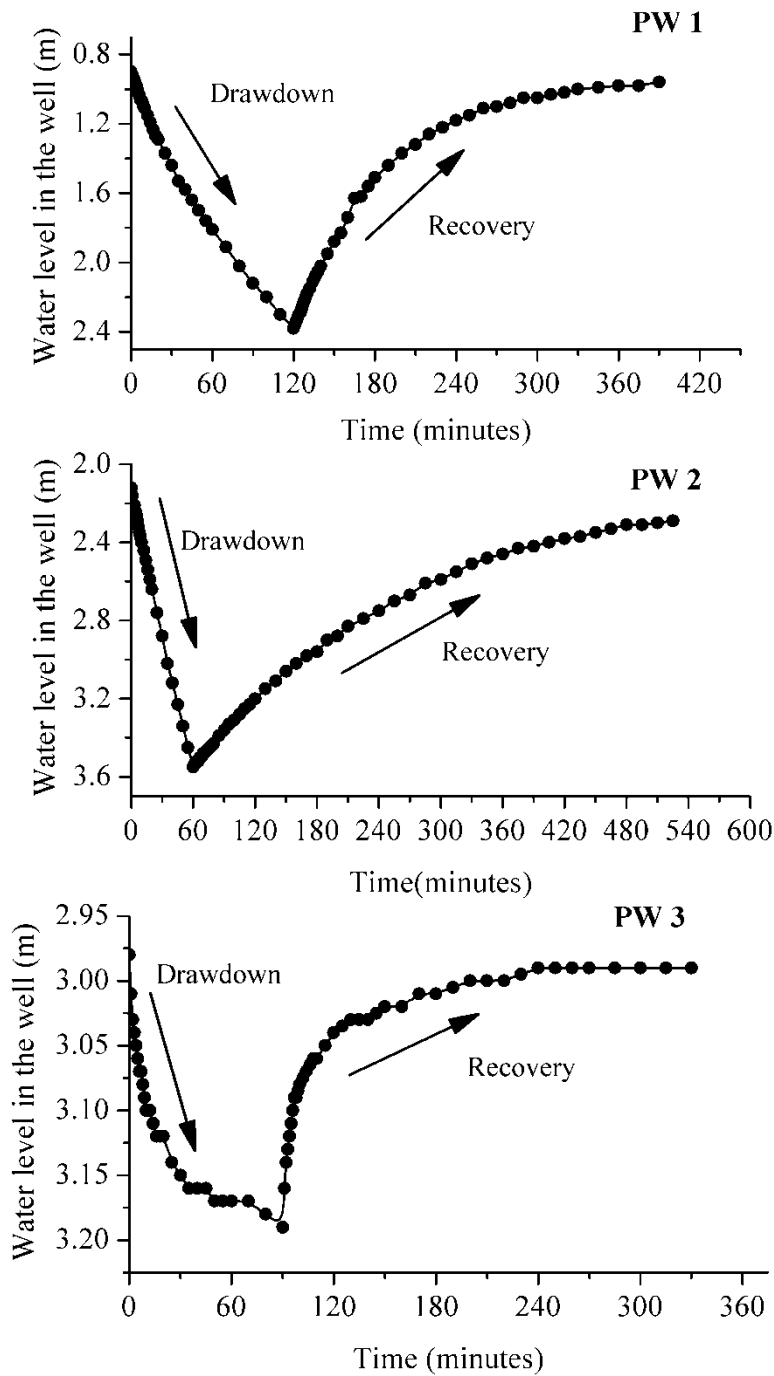


Fig.3.14 Graph of drawdown and recovery versus time for pumping well nos. PW1, PW2 and PW3

The results of the pumping test conducted for the 3 open wells in the sub-basin 3 are discussed in this section. The pumping test data is analysed using AQTESOLV ver.4.5 (Duffield, 2007) software for windows developed. This software is a package

for the analysis of aquifer tests with analytical solutions, curve matching tools and report graphics. AQTESOLV applies the principle of superposition in time to simulate variable rate test including recovery by various methods. The data is entered for the pumping or recovery tests using the data set wizard and the results are obtained by choosing an appropriate method for confined, unconfined or leaky aquifer. The aquifer properties are obtained using visual or automatic curve matching. The final output is available in graphical or report formats. The graphical solutions including displacement versus time curves from the analysis are presented in figures 3.15 to 3.23. The results are also presented in table 3.6.

Table. 3.6 Transmissivity and storage parameters obtained from pumping test analysis

Well No.	Theis(1935) method		Nueman (1974) method		TartakovskyNueman (2007) method	
	T (m/day)	Specific storage	T(m/day)	Specific yield	T (m/day)	Specific yield
PW1	60.88	0.2375	36.48	0.2432	56.22	0.0273
PW2	16.23	0.2463	15.44	0.001	39.6	0.1
PW3	275.8	0.2836	271.40	0.214	244.60	0.50

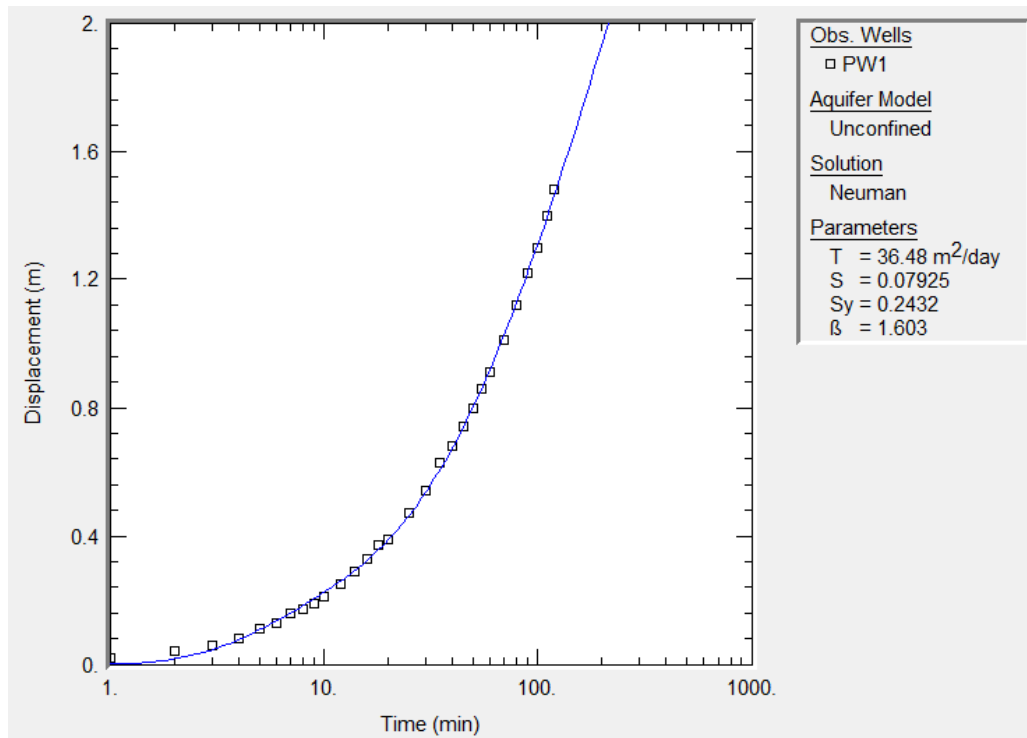


Fig.3.15 Time–drawdown graph of well no PW1 by Neuman(1974) method

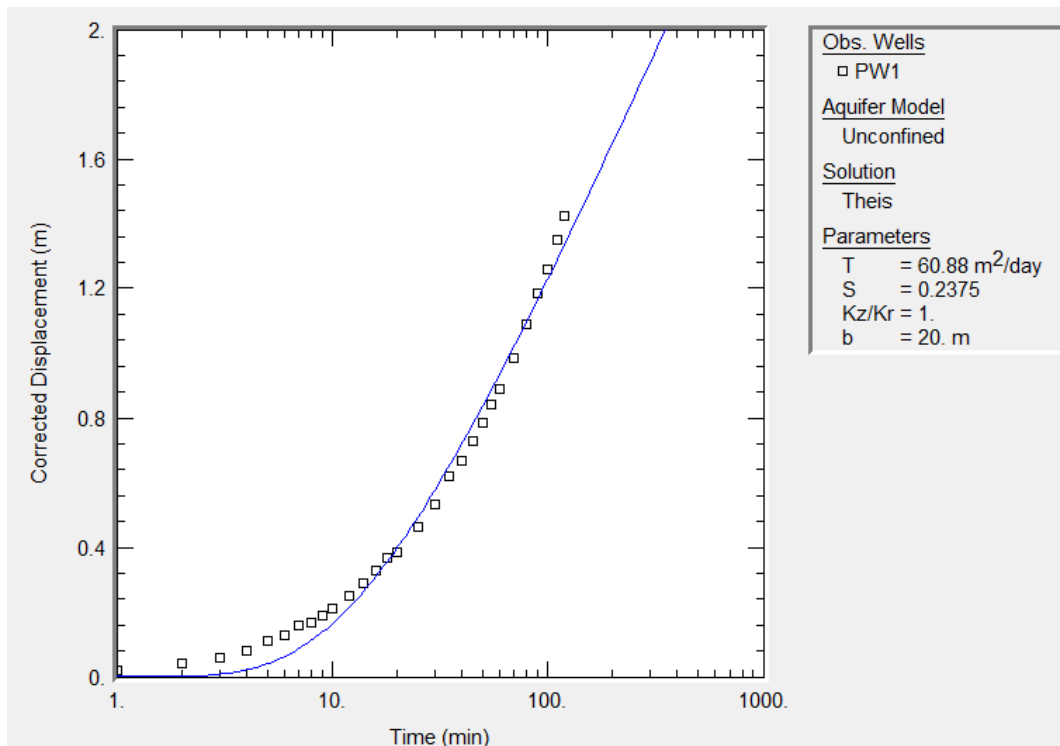


Fig.3.16 Time–drawdown graph of well no PW1 by Theis (1935) method

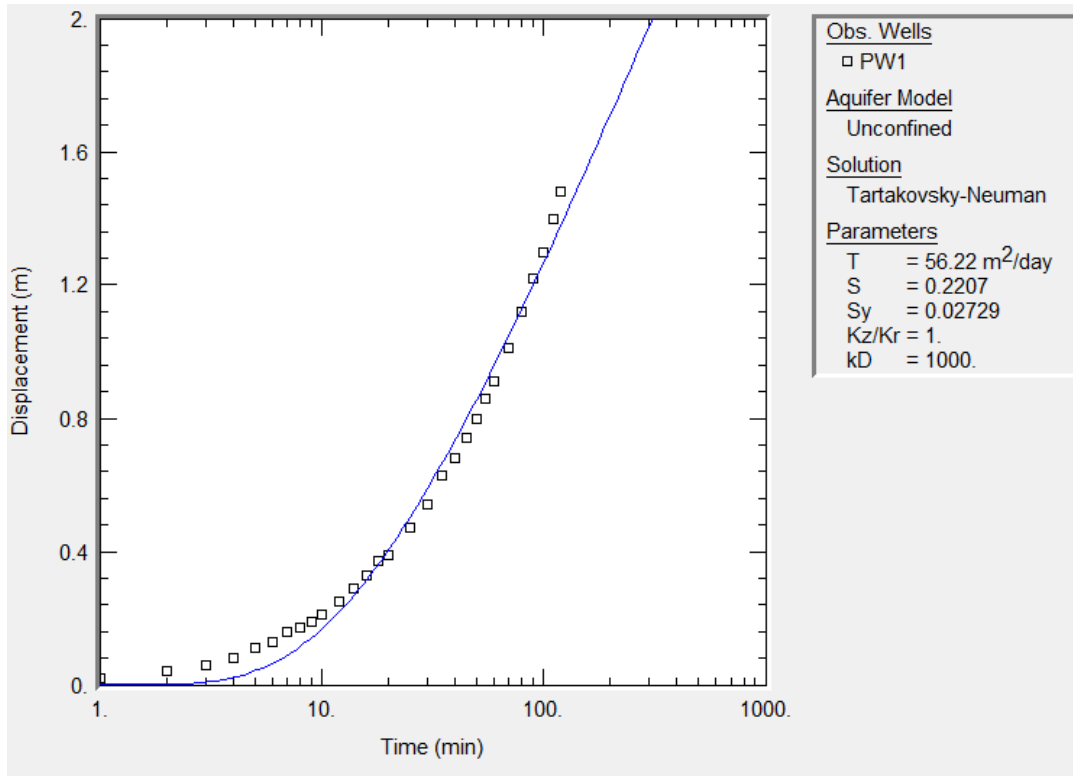


Fig.3.17 Time–drawdown graph of well no PW1 by Tartakovsky-Neuman (2007) method

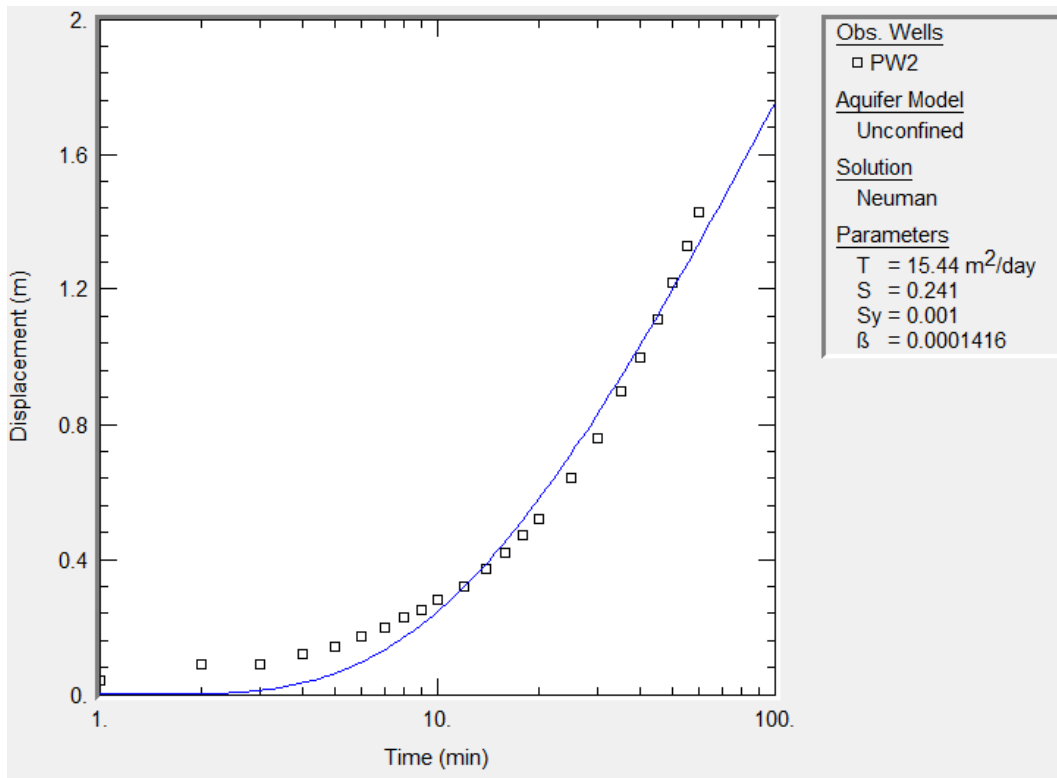


Fig.3.18 Time–drawdown graph of well no PW2 by Neuman(1974) method

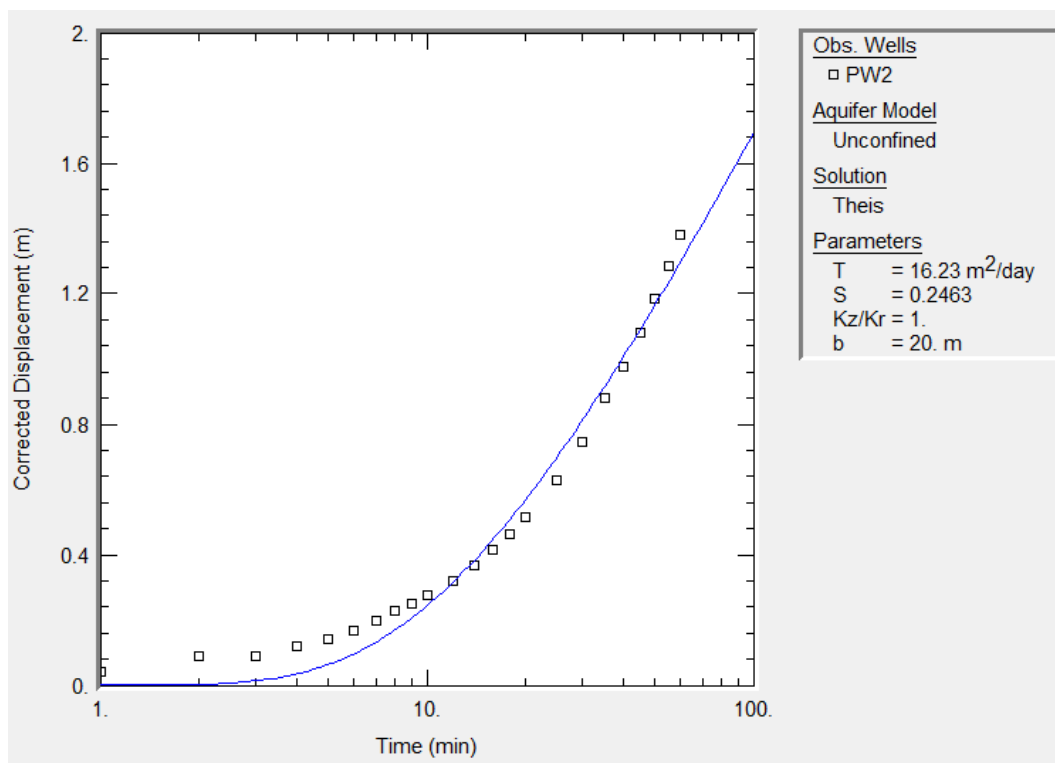


Fig.3.19 Time–drawdown graph of well no PW2 by Theis (1935) method

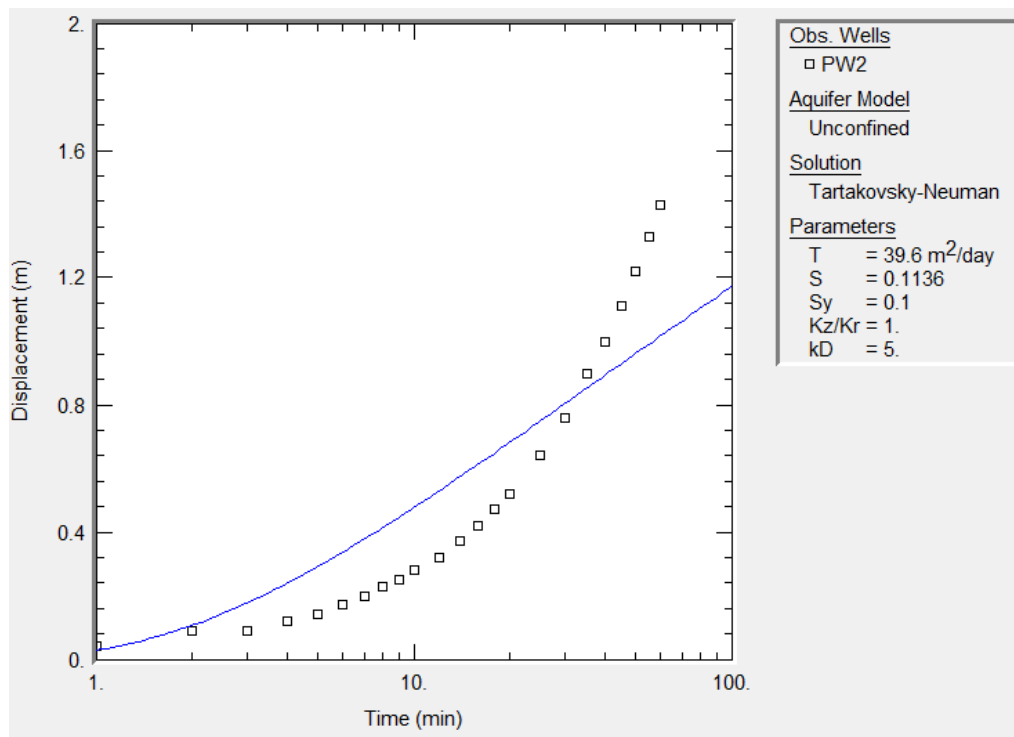


Fig.3.20 Time–drawdown graph of well no PW2 by Tartakovsky-Neuman (2007) method

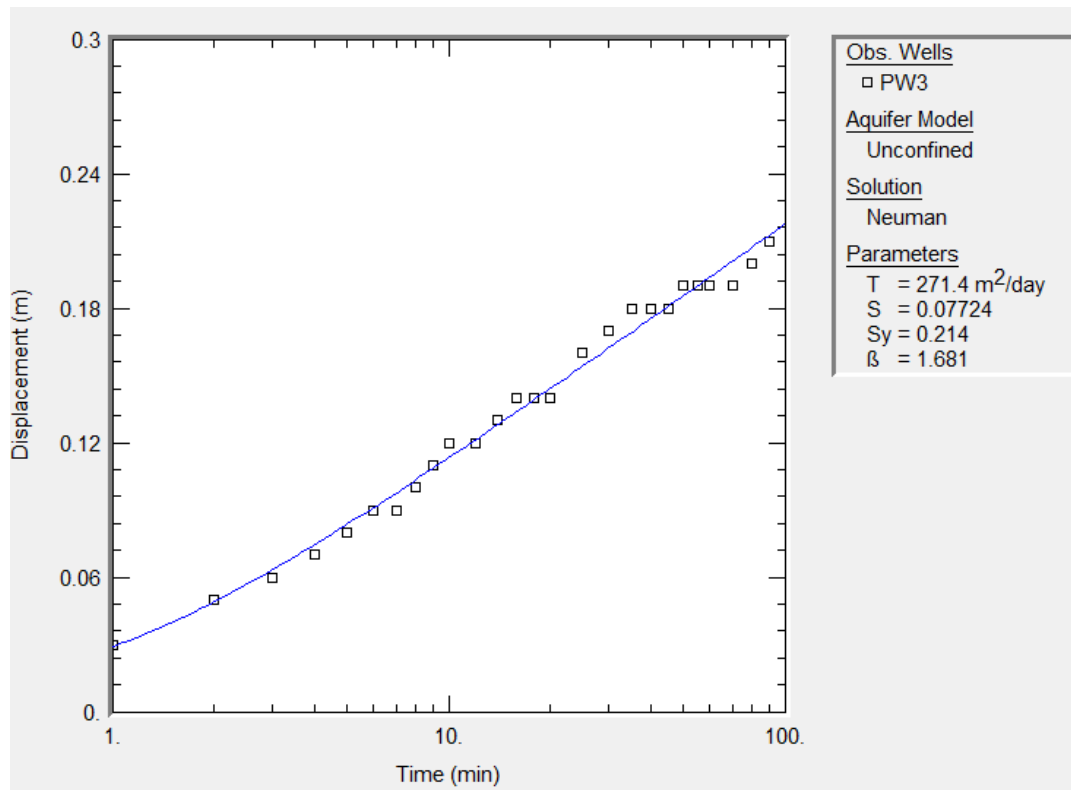


Fig.3.21 Time–drawdown graph of well no PW3 by Neuman(1974) method

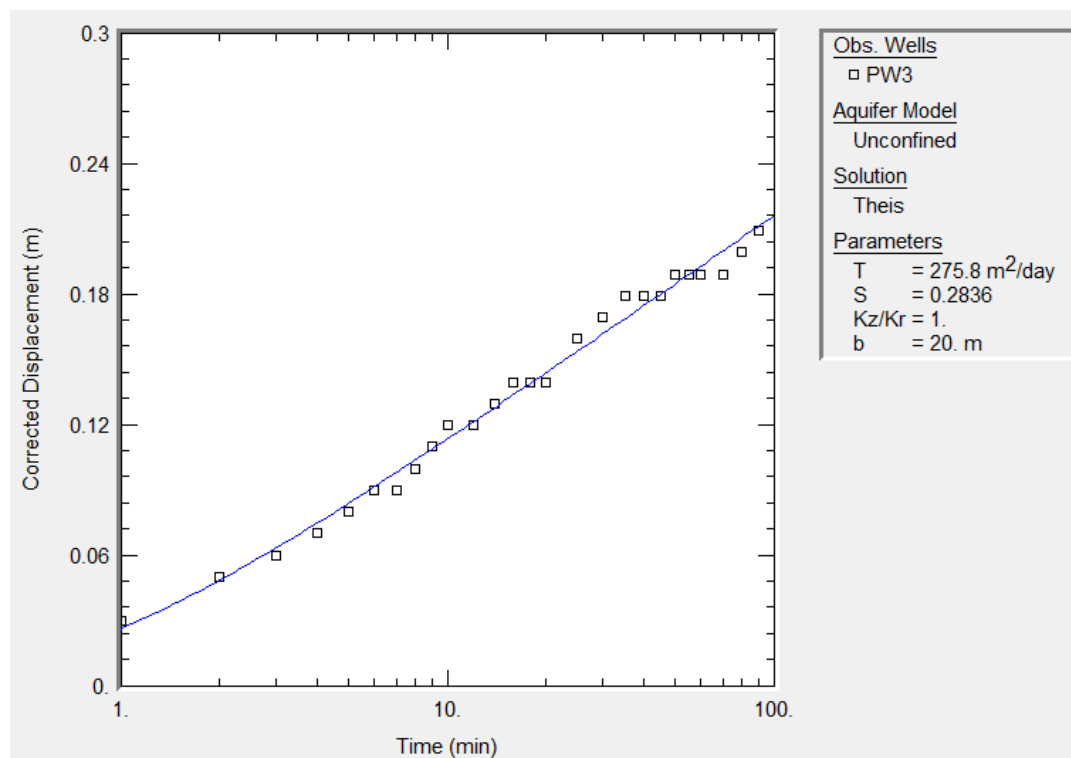


Fig.3.22 Time–drawdown graph of well no PW3 by Theis (1935) method

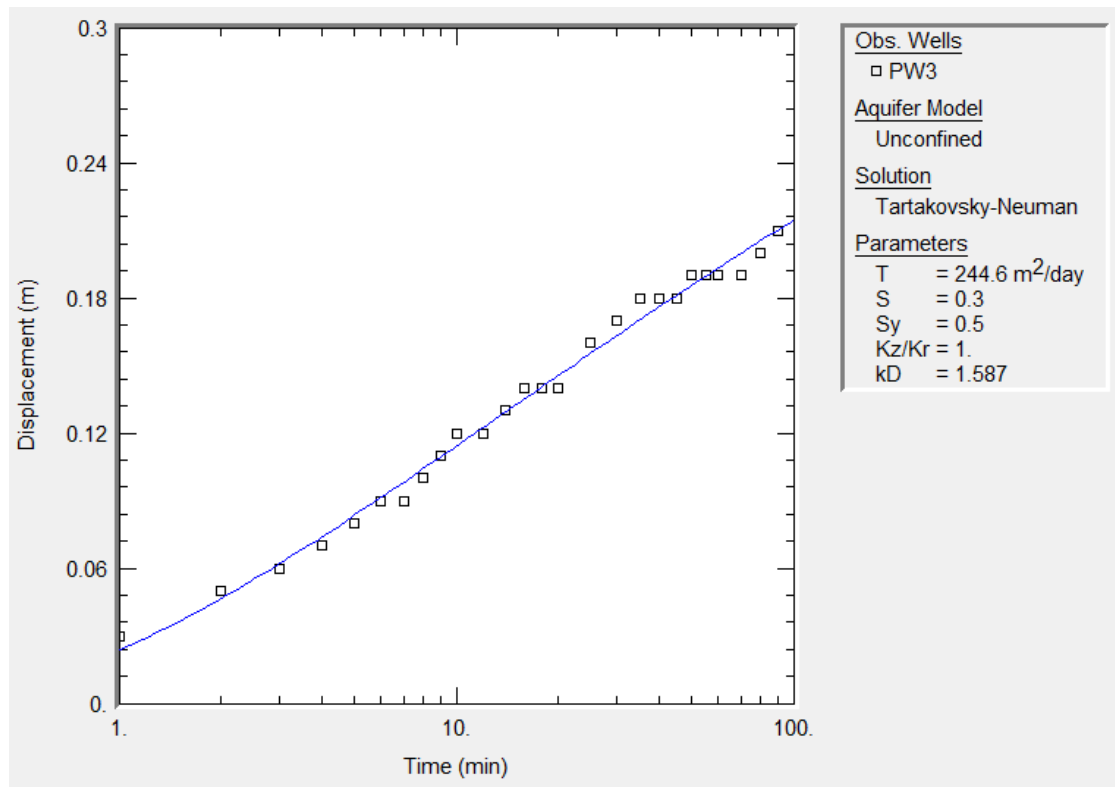


Fig.3.23 Time–drawdown graph of well no PW3 by Tartakovsky-Neuman (2007) method

3.4 AQUIFER PARAMETERS

Extensive pumping tests and laboratory tests were carried out in sub-basin-2 by previous investigators (Harshendra, 1991; Vyshali, 2008 and Udaykumar, 2008) to explore the hydraulic parameters of the aquifer. Three pumping tests are carried out in the present study as a part of aquifer characterisation in sub-basin 3 to add to the earlier studies (Shivanagouda, 2015 and Shetkar, 2008).

Based on the data available for the study area (about 40 locations), transmissivity is spatially mapped throughout all the four sub-basins using krigging interpolation technique available in ArcGIS 9.3, resulting into nine aquifer hydraulic parameter zones for each basin. Zones 1 and 9 represent the low and high transmissivity zones respectively. The corresponding hydraulic conductivity values are obtained by dividing the transmissivity values by an approximate saturated aquifer thickness for each aquifer zone as initial guess during the calibration of the model. The aquifer

property zones mapped for each of the sub-basin are shown in fig.3.24 and 3.25 along with the data points. The range of initial values of hydraulic conductivity and specific yield that is assigned for each of the sub-basin is presented in table3.7. The table shows that, transmissivity ranges between 10 and 1440 m²/day in the entire study area.

Table 3.7 Initial aquifer parameters

Sub-basin	Transmissivity (m ² /day)	Specific yield	Source	No. of point data
1	10 - 810	0.0008 – 0.0122	Harshendra, 1991	8
2	69 – 461	0.0008 – 0.2805	Harshendra, 1991, Vyshali, 2008 and Udaykumar, 2008	18
3	16 -1440	0.00058 –0.2432	Shivanagouda, 2015, Shetkar, 2008 and present study	5
4	100 - 256	0.0008 – 0.1131	Ranganna et al. 1986 and Shivanagouda, 2015	6

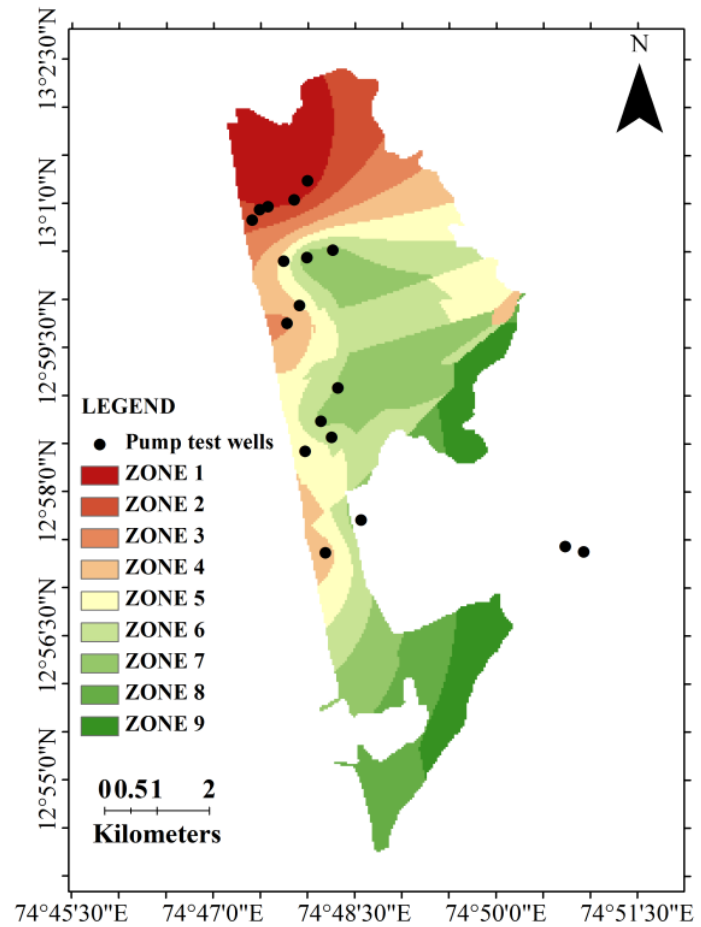
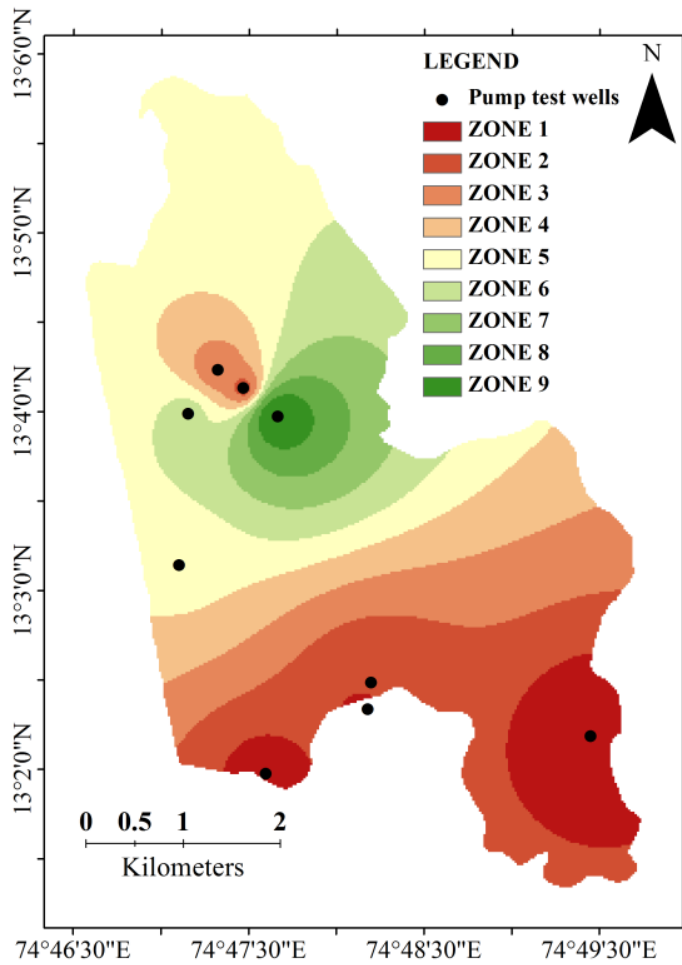


Fig.3.24 Aquifer property zonation map of sub-basins 1 and 2

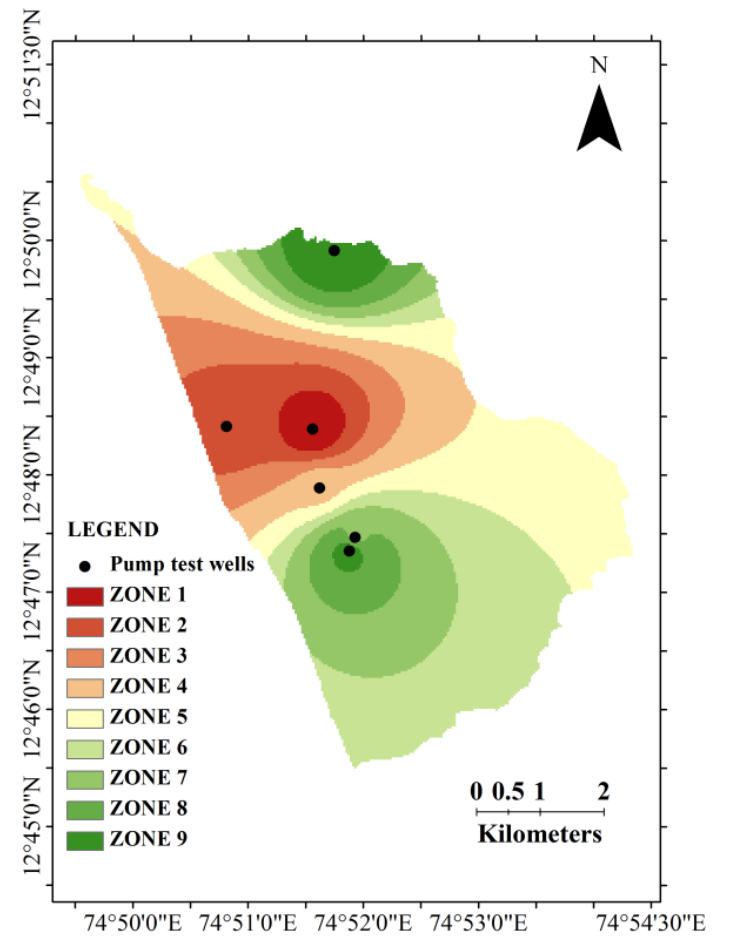
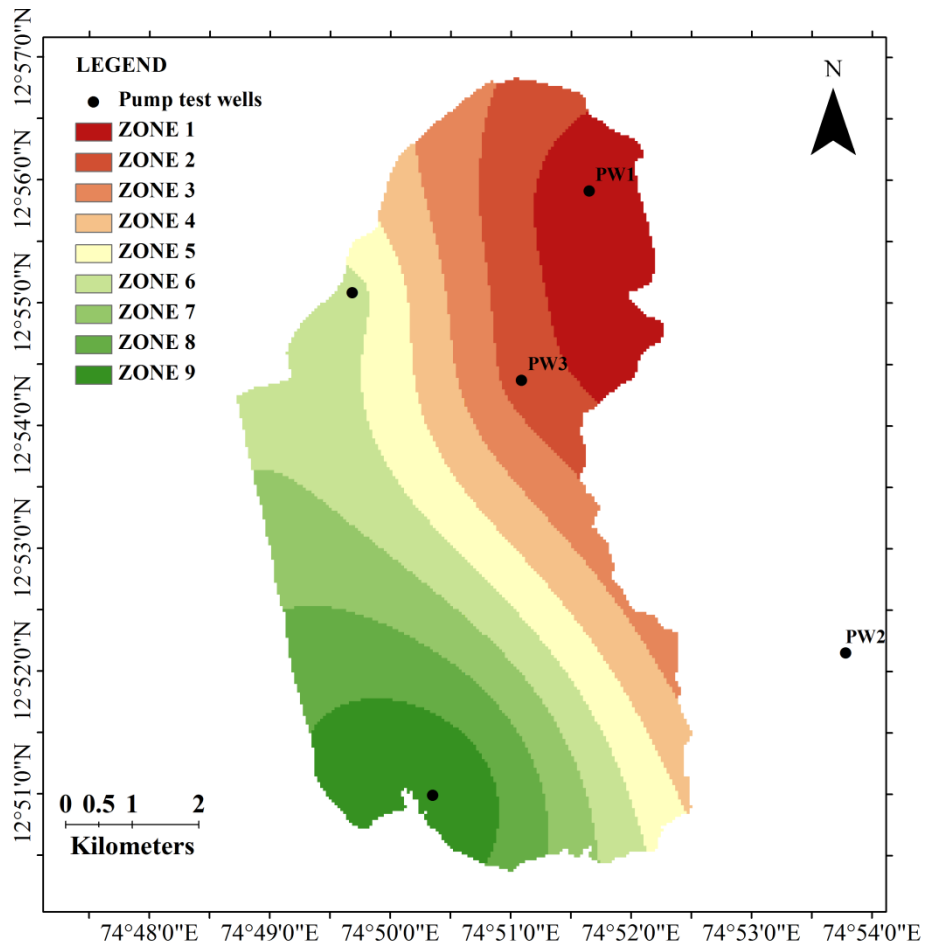


Fig.3.25 Aquifer property zonation map of sub-basins 3 and 4

3.5 CLOSURE

Aquifer characterization is a necessary execution required for any groundwater study. Therefore, in the present study, bore-log data, vertical electrical sounding information and lithology maps procured from reliable sources are used and in addition to the pumping tests that are also carried out. As per the study, it is found that, the basin is predominantly an unconfined aquifer with depth ranging from 12m to 30m. The lateritic formation is topped by sand followed by the top soil and beneath the laterite, a huge mass of gneiss is detected upto a depth of about 90m.

Since all the three wells considered for pumping test are shallow, (less than 10 m depth), the methods most suitable for a shallow unconfined aquifer are used. In the process, Theis (1935) method, Nueman (1974) method and Tartakovsky Nueman (2007) methods are chosen for the analysis of pumping test data to find the transmissivity and storage parameters. The results obtained by all three methods closely agree with each other. The parameters obtained by Nueman (1974) method are adopted as an addition to the database in the modeling study in the following chapters. This is because, the assumptions made in this method are much similar to the type of aquifer under study and the circumstances under which the test is carried out. Based on the available data, the four sub-basins are divided into 9 aquifer zones each with transmissivity ranging from 10 to 1440 m²/day.

CHAPTER 4

GROUNDWATER FLOW MODEL

4.1 GENERAL

Groundwater model development is a process where hydrogeological conditions are simulated using mathematical equations which are solved using a computer program. First of all, the conceptual model for the study area is formulated using the available geological and hydro-geological data, including the spatial and temporal distribution of groundwater draft / recharge. In the present study, a modular three dimensional finite difference ground water flow model MODFLOW 2000 (Harbaugh et al., 2000) is used to simulate the groundwater flow. This model as implemented in the GMS (Groundwater Modeling System) package, version 10.0.1 is used in this work. The easy-to-use interface offered by this modeling package is specifically designed to enhance the modeling productivity and minimize the complexities associated in the modeling process. The GMS is comprehensive graphical user environment for performing groundwater simulations and have been used by several hydrologists earlier (Kushwaha et al., 2009; Ahmed and Umar, 2009 and Gates, 2002) to understand and manage various types of groundwater issues. The GMS interface is developed by Aquaveo, LLC in Provo, Utah. The output from the flow model is the hydraulic head along with the water budget. The MODFLOW program was originally written using FORTRAN 66 (McDonald and Harbaugh, 1988).

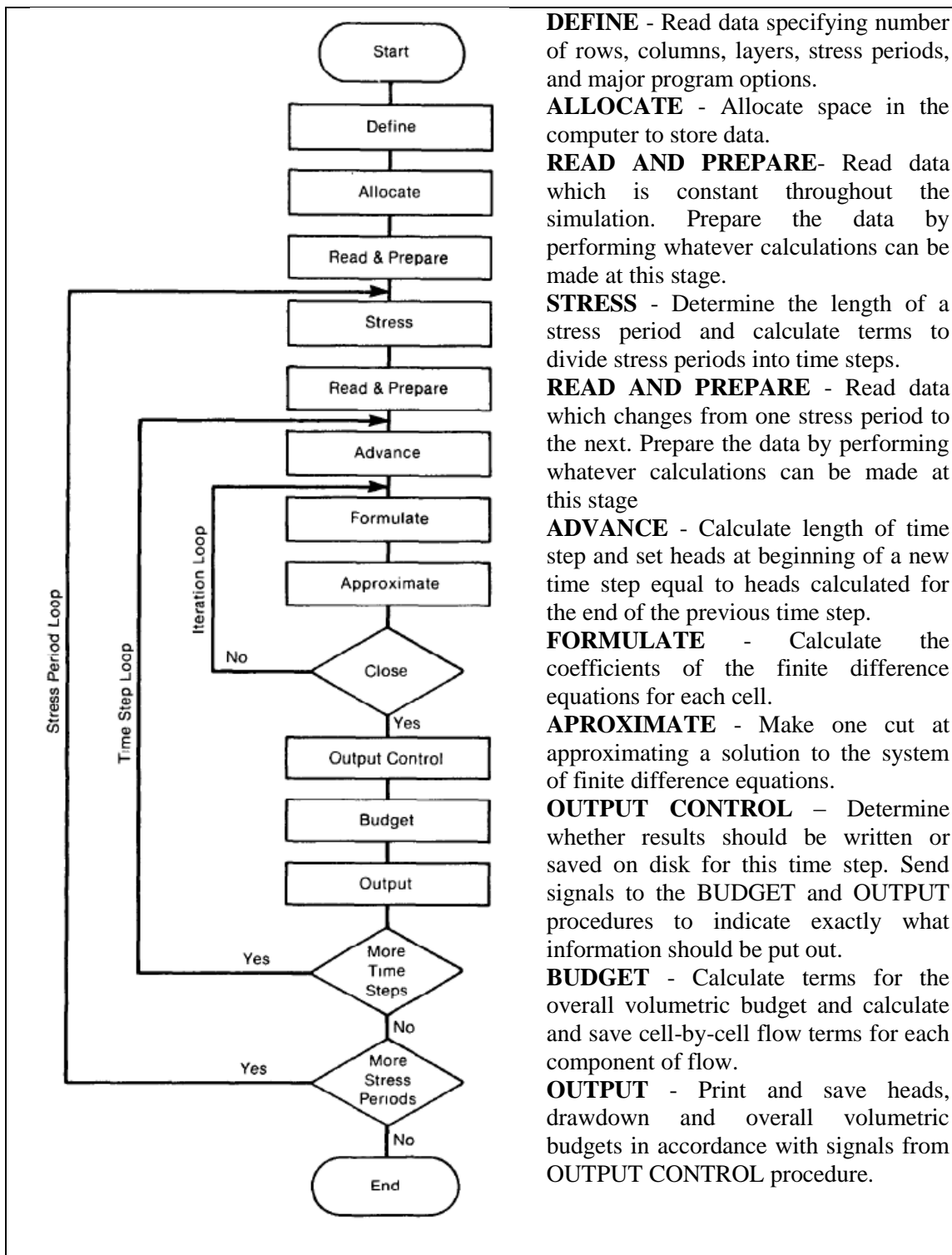
The groundwater flow simulation of the aquifer system in this study is carried out in two stages. Initially, a steady state water level for the month of October 2007 is adopted for the steady state calibration of the hydraulic conductivity, as well as for getting an estimate of the aquifer's water balance. In the next step, transient conditions between years 2011-2013 are used to calibrate the specific yield, hydraulic conductivity and other aquifer parameters. The two year simulation period is divided into 24 monthly stress periods with daily time step. A stress period represents a period of time during which all model stresses remain constant e.g. recharge, groundwater

abstraction or discharge to rivers. The stress periods can be divided into one or more time-steps. The sensitivity test is also carried out parallel to the calibration process, with a focus on estimating the influence of input parameters on the simulated heads.

4.2 OVERALL PROGRAM STRUCTURE

There are four modularization entities in MODFLOW-2000 computer program structure, namely procedures, packages, modules and process. This can be better illustrated with the help of a flow chart (fig.4.1). Each rectangle in fig.4.1 is termed a procedure. Prior to entering the stress loop, the program executes three procedures which pertain to the simulation as a whole. The “define” procedure is used to specify the size of the model, the type of simulation (transient or steady state), the number of stress periods, the hydrologic options, and the solution scheme. The “allocate” procedure is used to assign memory space required by the program. The “read and prepare” procedure reads the data that are not functions of time. The work within the procedures is performed by individual subroutines, or modules, called by the main program. The modular structure of the computer program consists of a main program and a series of highly independent subroutines called "modules". The modules are grouped into packages, which deals with a specific feature of the hydrologic system which is to be simulated. Table.4.1 lists the MODFLOW packages used for the flow simulation in the present work, with a brief description of the package operation. A process is a part of the code that solves a fundamental equation by a specified numerical method.

The finite difference equation (4.1) is solved to yield the head at each node. The iterative solution procedure is used to solve for the heads for each time step. Thus, within a simulation, there are three nested loops viz; a stress period loop, within which there is a time step loop, which in turn contains an iteration loop. The concise review of mathematical theory, concepts and governing equations of MODFLOW are provided in the subsequent sections.



DEFINE - Read data specifying number of rows, columns, layers, stress periods, and major program options.

ALLOCATE - Allocate space in the computer to store data.

READ AND PREPARE- Read data which is constant throughout the simulation. Prepare the data by performing whatever calculations can be made at this stage.

STRESS - Determine the length of a stress period and calculate terms to divide stress periods into time steps.

READ AND PREPARE - Read data which changes from one stress period to the next. Prepare the data by performing whatever calculations can be made at this stage

ADVANCE - Calculate length of time step and set heads at beginning of a new time step equal to heads calculated for the end of the previous time step.

FORMULATE - Calculate the coefficients of the finite difference equations for each cell.

APROXIMATE - Make one cut at approximating a solution to the system of finite difference equations.

OUTPUT CONTROL - Determine whether results should be written or saved on disk for this time step. Send signals to the BUDGET and OUTPUT procedures to indicate exactly what information should be put out.

BUDGET - Calculate terms for the overall volumetric budget and calculate and save cell-by-cell flow terms for each component of flow.

OUTPUT - Print and save heads, drawdown and overall volumetric budgets in accordance with signals from OUTPUT CONTROL procedure.

Fig. 4.1 Flow chart for the overall program structure of MODFLOW (McDonald and Harbaugh, 1988)

Table. 4.1 The MODFLOW packages used for groundwater flow simulation

Package name	Description	Reference
Basic (BAS)	The tasks that are part of the model as a whole, such as; specification of boundaries, determination of time-step length, establishment of initial conditions, and printing of results are carried out.	McDonald and Harbaugh(1988)
Layer-Property Flow (LPF)	Performs the cell by cell flow calculations. The input to this package includes layer types and cell attributes such as specific yield and hydraulic conductivity	Harbaugh et al., (2000)
Well (WEL)	The well recharge rate (negative sign indicates discharge) can be defined using parameters. It is a head independent package. Adds terms representing flow to wells to the finite difference equations.	McDonald and Harbaugh(1988)
Recharge (RCH)	The Recharge flux can be defined using parameters. It is a head independent package. Adds terms representing areally distributed recharge to the finite difference equations.	McDonald and Harbaugh(1988)
River (RIV)	The riverbed conductance can be defined using parameters. It is a head dependent package. Adds terms representing flow to rivers to the finite difference equations.	McDonald and Harbaugh(1988)
Drain (DRN)	The drain conductance can be defined using parameters. Adds terms representing flow to drains to the finite difference equations.	McDonald and Harbaugh(1988)

Time-Variant Specified-Head (CHD)	It allows parameters to define the specified head.	Leake and Prudic (1991)
Preconditioned Conjugate Gradient (PCG2)	Method for solving the simultaneous equations resulting from the finite-difference method. It is a solver package.	Hill(1990)

4.3 GOVERNING EQUATION

Three dimensional movement of constant density groundwater through a porous media is described by the following parabolic partial differential equation, called groundwater flow equation (McDonald and Harbaugh,1988)

$$\frac{\partial}{\partial x} \left(K_{xx} \frac{\partial h}{\partial x} \right) + \frac{\partial}{\partial y} \left(K_{yy} \frac{\partial h}{\partial y} \right) + \frac{\partial}{\partial z} \left(K_{zz} \frac{\partial h}{\partial z} \right) - W = S_s \frac{\partial h}{\partial t} \quad (4.1)$$

where,

x, y, z =cartesian coordinates aligned along the major axes of hydraulic conductivities K_{xx} , K_{yy} , and K_{zz}

h = potentiometric head (L)

S_s =specific storage of the porous material (L^{-1})

t =time (T)

W =volumetric flux per unit volume and represents sources and sinks of water (T^{-1}).

The right hand side of the equation (4.1) is zero for steady state condition. The equation when combined with boundary and initial conditions, describes transient three dimensional groundwater flow in a heterogeneous and anisotropic medium. The groundwater flow process solves the above equation using the finite difference method in which, the groundwater flow system is divided into a grid of cells (fig. 4.2). For each cell, there is a single point, called a node, at which head is calculated. The finite difference equation for each cell is defined as (McDonald and Harbaugh, 1988):

$$\begin{aligned}
& CR_{i,j-\frac{1}{2},k}(h_{i,j-1,k}^m - h_{i,j,k}^m) + CR_{i,j+\frac{1}{2},k}(h_{i,j+1,k}^m - h_{i,j,k}^m) \\
& + CC_{i-\frac{1}{2},j,k}(h_{i-1,j,k}^m - h_{i,j,k}^m) + CC_{i+\frac{1}{2},j,k}(h_{i+1,j,k}^m - h_{i,j,k}^m) \\
& + CV_{i,j,k-\frac{1}{2}}(h_{i,j,k-1}^m - h_{i,j,k}^m) + CV_{i,j,k+\frac{1}{2}}(h_{i,j,k+1}^m - h_{i,j,k}^m) \\
& + P_{i,j,k}h_{i,j,k}^m + Q_{i,j,k} = SS_{i,j,k}(DEL R_j \times DEL C_i \times THICK_{i,j,k}) \frac{h_{i,j,k}^m - h_{i,j,k}^{m-1}}{t^m - t^{m-1}} \quad (4.2)
\end{aligned}$$

where

$h_{i,j,k}^m$ = head at cell i,j,k at time step m (L);

CV, CR and CC= hydraulic conductances, between node i,j,k and a neighbouring node (L²/T)

$P_{i,j,k}$ = sum of co-efficients of head from source and sink terms

$Q_{i,j,k}$ = sum of constants from source and sinks terms, with $Q_{i,j,k} < 0.0$ for flow out of the groundwater system and $Q_{i,j,k} > 0.0$ for flow in (L³/T)

$SS_{i,j,k}$ = specific storage (L⁻¹)

$DEL R_j$ = cell width of column j in all rows (L)

$DEL C_i$ = cell width of row i in all columns (L)

$THICK_{i,j,k}$ = vertical thickness of cell i,j,k (L)

t^m = time at time step m (T).

To designate hydraulic conductance between nodes, as opposed to hydraulic conductance within a cell, the subscript notation “1/2” is used. For example $CR_{i,j+\frac{1}{2},k}$ represents the conductance between nodes i, j, k and i, j+1, k. For steady state stress periods, the storage term and therefore the right hand side of equation (4.2) is set to zero.

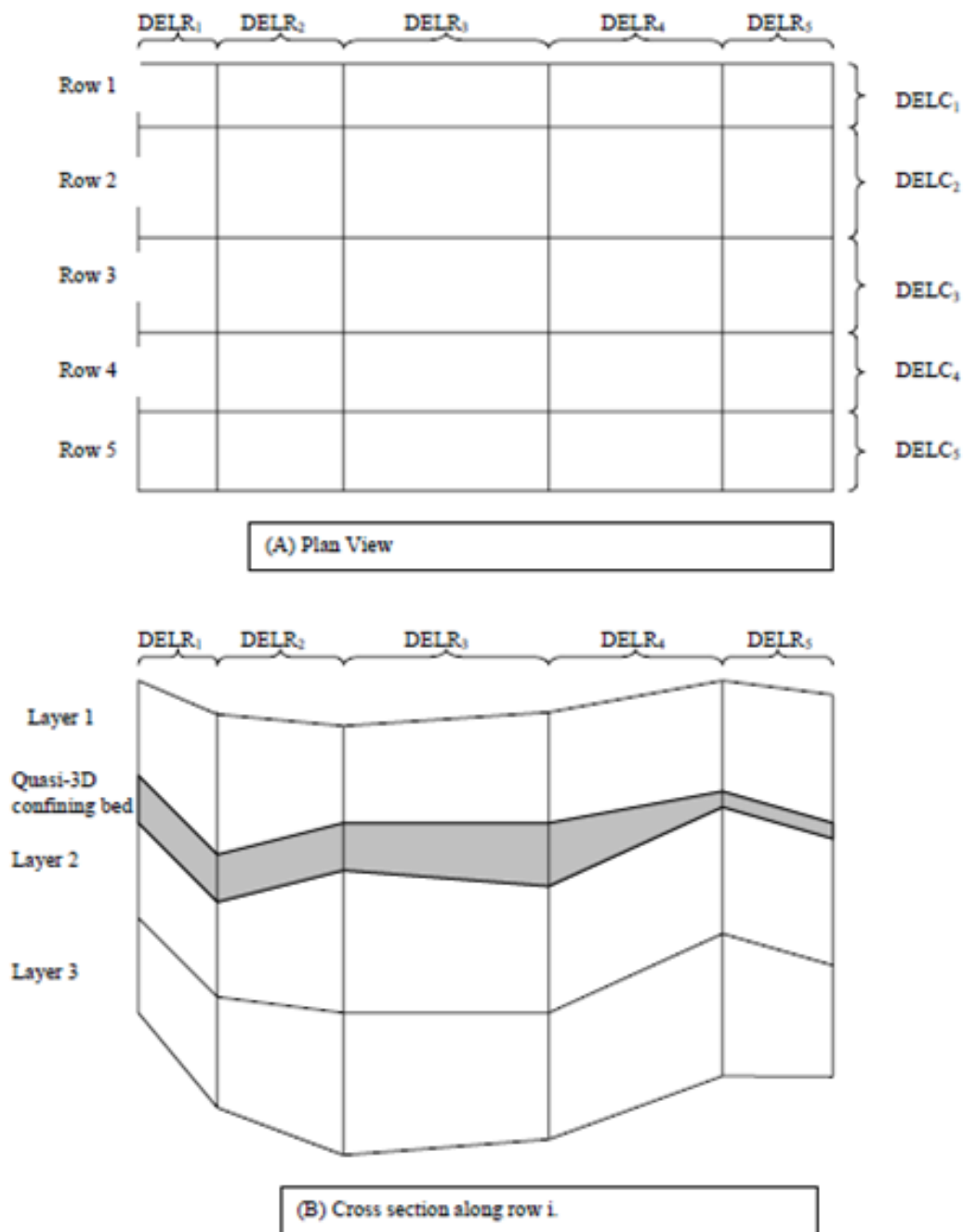


Fig.4.2 Finite difference grid (Harbaugh et al.,2000)

4.4 MODELING APPROACH

The conceptual model design is an essential step in model design, as it aids in understanding the formation of the problem physically that would further assist in determining the modeling approach. This approach simplifies the field problem and stacks the required field data in a well organised manner for easy analysis of the

aquifer system. In addition, a conceptual model is very useful for identifying knowledge or data gaps that must be filled before a quantitative model can be constructed.

The specific steps involved in groundwater flow and solute transport modeling as applied in the present study is illustrated in fig.1.1. However, discretization of model domain, sources and sinks, initial and boundary conditions assigned to the model in addition various input parameter in contemplation to groundwater flow model are discussed in this section.

4.4.1 Data

The data collected related to groundwater table and salinity in the study area are listed in table 4.2.

Table 4.2 Availability of water level and salinity data in the study area

Sl No.	Period	Data intensity	Available for	Source
1	2005 to 2014	Seasonal	All sub-basins	CGWB and DMG Govt. of Karnataka*
2	2011 to 2013	Fortnightly	All sub-basins	Shivanagouda (2015)
3	2005 to 2007	Monthly	Sub-basin 2	Vyshali (2008)
4	2013 to 2014	Monthly	Sub-basin 3	Sylus (2015)

***Salinity data unavailable**

4.4.2 Discretization of the basin

The complex river network (fig.1.5, chapter 1), involving two major rivers present in the study area are dealt by dividing the whole area into four sub-basins and each is modeled separately. The physical boundary of each basin is represented by rivers on its north and south, sea towards the west and representative ridge line along the east. Hence, the conceptual model in this study requires the design of four unique aquifer systems. Each one is defined as an unconfined aquifer, with the vertical thickness based on the hydro-geological properties and geological stratigraphy of the basin, where the model elevations range between -30m to 90m.

Spatial discretization

The model of each sub-basin has two dimensional grids in the horizontal plane with an approximate cell dimension of 100×100m. The vertical section is represented by a single grid of varying dimension. The digital elevation model (fig.1.3, chapter 1) is interpolated to the top elevation of the model grid. The base of the model layer is set at -30m (with respect to mean sea level), which corresponds to the base of the shallow unconfined aquifer. The spatial discretization of model for 4 sub-basins is shown in table.4.3.

Temporal discretization

The time steps have a very important role to play in analysing groundwater system. The time step length depends on the dynamic character of the hydrologic process to be modeled. In the present study, the aquifer system is modeled for transient state with daily time step. Prior to transient run, steady state simulation is also performed to set up initial groundwater head for the transient simulation. The monthly data on the hydrologic stresses (Pumping rate, river bed conductance, river stage and recharge rate) are assigned to the model.

Table. 4.3 Model discretization

Sub-basin	Origin (UTM WGS 1984, zone 43)		Number of cells		Number of active cells	Surface elevation (m)
	x-direction	y-direction	x-direction	y-direction		
1	4,75,646 E	14,39,602 N	65	95	2,587	0 to 60
2	4,76,680 E	14,26,495 N	100	200	3,962	0 to 70
3	4,79,268 E	14,17,538 N	76	144	6,551	0 to 90
4	4,80,653 E	14,09,944 N	96	103	3,786	0 to 70

4.4.3 Hydrologic sources and sinks

The continuity equation, which states that, the sum of all flows into and out of the cell must be equal to the rate of change in storage within the cell is basically the concept

involved in the development of the groundwater flow equation. Hence, the equation as stated earlier involves all inflows and outflows into a representative finite model domain of the aquifer, with well-known external and internal hydrologic sources (recharge) and sinks (draft). The sinks are analysed as negative sources. In this study, sources include recharge, mainly from rainfall and groundwater extractions from agricultural pumping wells act as sinks.

Groundwater recharge

Generally, recharge is estimated as a portion of the effective rainfall. Recharge is usually hard to be quantified correctly, as it varies spatially, depending on factors such as soil type, land use and topography. The concept of recharge coefficient is used in the present numerical simulation. The recharge coefficient is defined as the ratio of the recharge to the precipitation. The areally distributed recharge to the groundwater system is simulated using the recharge (RCH) package.

The natural recharge from rainfall replenishes the aquifer to the saturation level, through infiltration and percolation to the sub-surface soil layers every year due to the copious monsoon rains (June to September) to the extent of about 3000mm. The Groundwater Estimation Committee (GEC,1997) recommends the recharge coefficient value as 7% for lateritic formations. Also, as per the studies executed by Udaykumar (2008) for a part of the study area, the recharge coefficient appropriate to this area is 8% to 26.5%. The recharge estimation is done based on the rainfall records observed at the meteorological station at the National Institute of Technology Karnataka, Surathkal, India. The recharge is assigned on the uppermost active (wet) layer of the model for each vertical column of grid cell and is modified and fine tuned within the specified range during the calibration.

Abstractions from agricultural wells

The wells which withdraw water from the aquifer at a specified rate during a given stress period are simulated using the well (WEL) package in MODFLOW. The well discharge is handled in the Well Package by specifying the rate, Q , at which, each

individual well removes water from the aquifer, during each stress period. The negative values of Q are used to indicate well discharge.

Groundwater in the study area is extensively used for irrigation, industrial and domestic purposes during the lean period. A total of 587, 730, 835 and 996 wells are introduced in the agricultural area of sub-basin 1, 2, 3 and 4 respectively, based on the village wise installation of irrigation pump set data supplied by the Mangalore Electricity Supply Company Limited. To identify the agricultural area, the LULC map (fig.1.7) of the area is used.

In the absence of actual well draft data, the draft per well is assigned based on the water requirement of crops, i.e. evapo-transpiration of 7mm/day, 6mm/day and 5mm/day during the pre-monsoon (February to May), monsoon (June to September) and post-monsoon (October to January) periods respectively as estimated by Kumar (2010). The village-wise data of freshwater draft considered are presented in table.4.4. The village map of Dakshina Kannada district procured from the KSRSAC (Karnataka State Remote Sensing Applications Centre) is used to develop a village map for the present study area (fig.4.3A and B). Also, the major drafts by the New Mangalore Port ($2000 \text{ m}^3/\text{day}$) and the National Institute of Technology, Karnataka ($350 \text{ m}^3/\text{day}$) are considered during the simulation.

Table 4.4. Village-wise details of pumping rates

	Village	Area (km ²)	No. of wells	Well draft (m ³ /day)		
				Pre-monsoon	Monsoon	Post-monsoon
SUB-BASIN-1	Mulki	8.18	259	11.60	13.93	16.25
	Sasihitlu	1.50	04	137.94	165.53	193.12
	Padupampbur	1.36	56	8.90	10.69	12.47
	Bellairu	2.35	19	45.43	54.52	63.60
	Pavanje	1.80	29	22.82	27.38	31.95
	Haleyangadi	1.78	62	10.52	12.63	14.73
	Thokuru	3.60	91	14.54	17.45	20.36
	Koikude	2.51	25	36.96	44.35	51.74
	Kermal	0.45	14	11.86	14.23	16.61
	Attur	0.18	05	13.08	15.70	18.31
	Panja	1.12	23	17.91	21.49	25.07
SUB-BASIN-2	Sasihitlu	11.12	28	154.04	184.85	215.66
	Pavanje	0.50	05	21.37	25.64	29.92
	Chellairu	3.54	243	5.034	6.04	7.05
	Madhya	1.99	100	6.55	7.86	9.17
	Bala	1.19	02	179.21	215.05	250.90
	Thokur-62	6.95	06	412.85	495.42	578
	Kuthethur	1.53	13	37.43	44.92	52.41
	Hosabettu	2.68	127	7.14	8.57	10
	Panambur	8.68	202	15.40	18.48	21.56
	Baikapmady	0.85	04	59.22	71.07	82.91
SUB-BASIN-3	Mangalore (M.Corp +OG)	56	835	24.30	29.16	34.02
SUB-BASIN-4	Mangalore	1.23	11	40.99	49.18	57.38
	Kudugu	7.51	108	25.53	30.64	35.75
	Peramannuru	3.43	65	19.38	23.25	27.13
	Munnuru	0.60	38	5.82	6.99	8.15
	Someshwara	7.93	118	24.69	29.63	34.57
	Kotekar	10.26	385	9.79	11.75	13.71
	Belma	0.38	13	10.77	12.92	15.08
	Talapady	2.51	137	6.72	8.07	9.41
	Kinya	1.98	85	8.57	10.28	12
Manjanady	0.56	36	5.70	6.83	7.97	

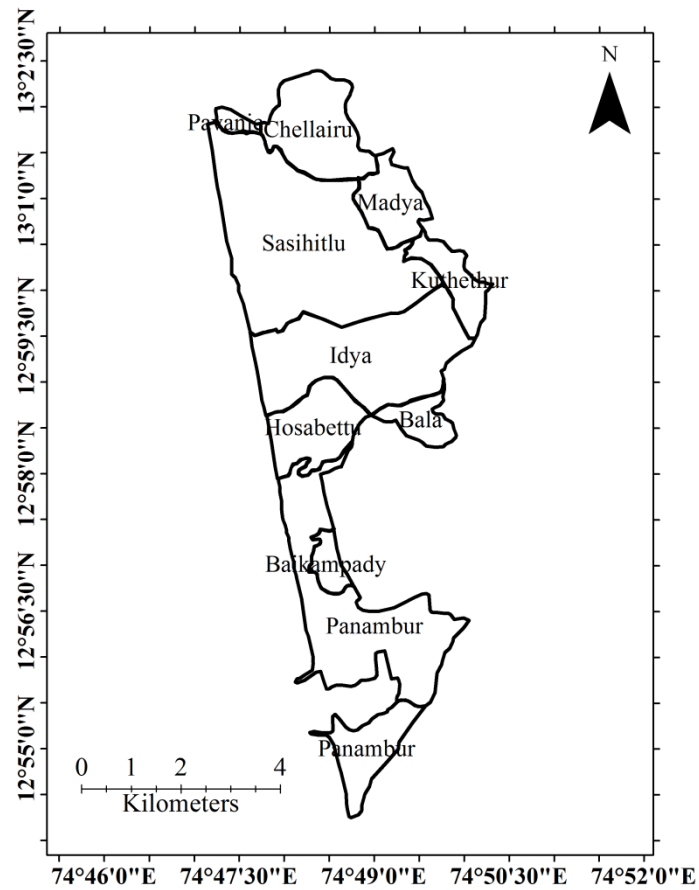
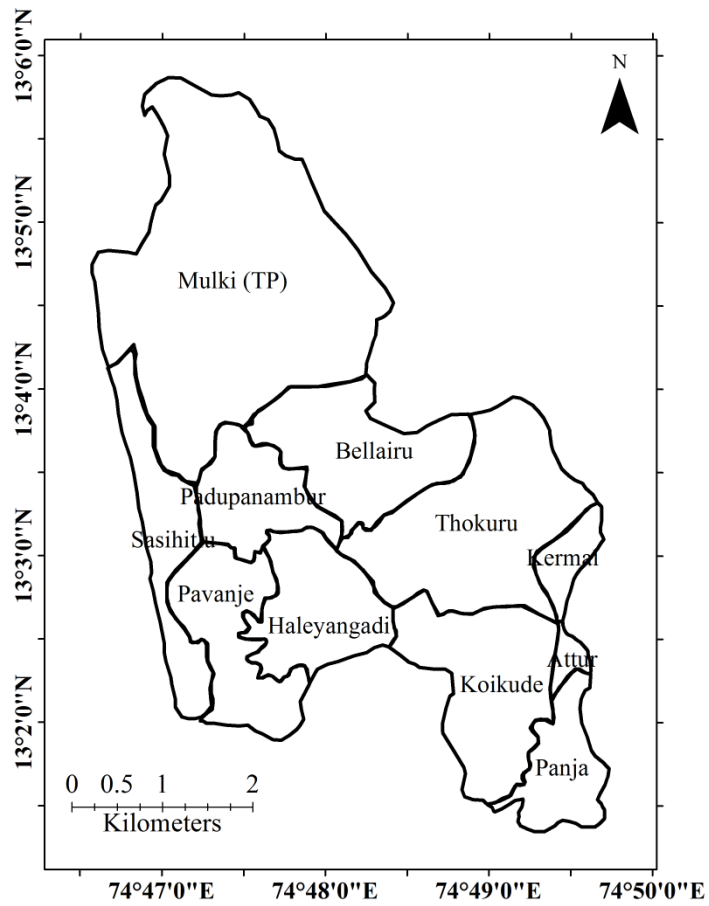


Fig. 4.3A Village map of sub-basin 1, and 2

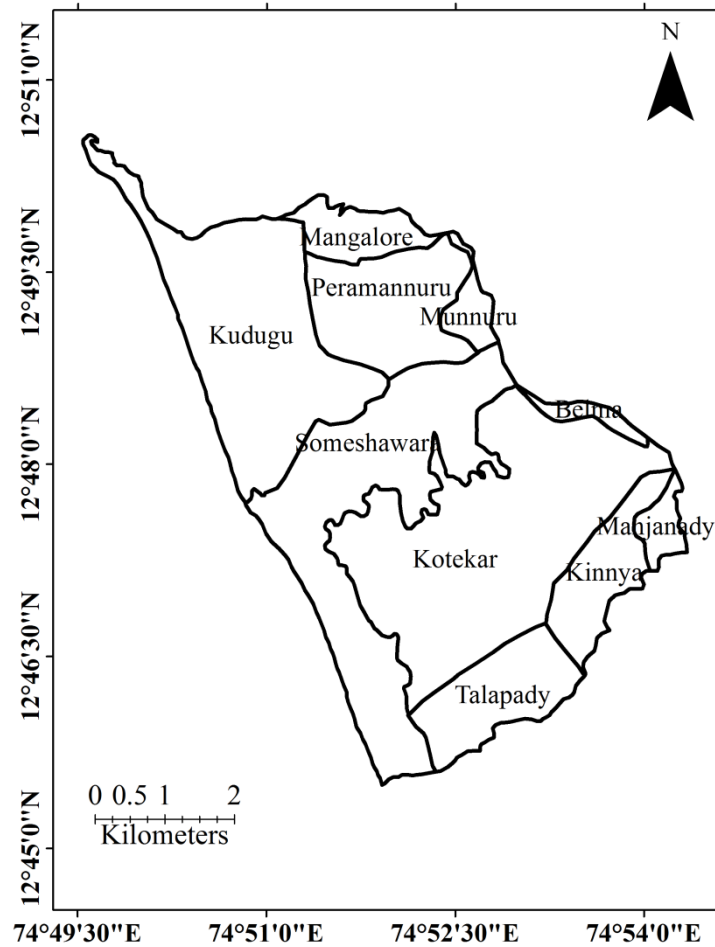


Fig. 4.3B Village map of sub-basin 4

4.4.4 Boundary conditions

The boundaries are mathematically classified into three categories namely; Dirichlet (constant head or concentration), Neumann (specific flux), and Cauchy (head-dependent flux or mixed boundary condition). Apart from these, the physical features such as surface water bodies (rivers, drains, stream etc), pumping or injection wells and physical processes such as evapotranspiration and recharge that impose boundary conditions on the groundwater regime are implemented to equation (4.1) through source/ sink terms. The discretization of all the sub-basins 1, 2, 3 and 4 with the applied boundary conditions is shown in figures 4.4, 4.5, 4.6 and 4.7.

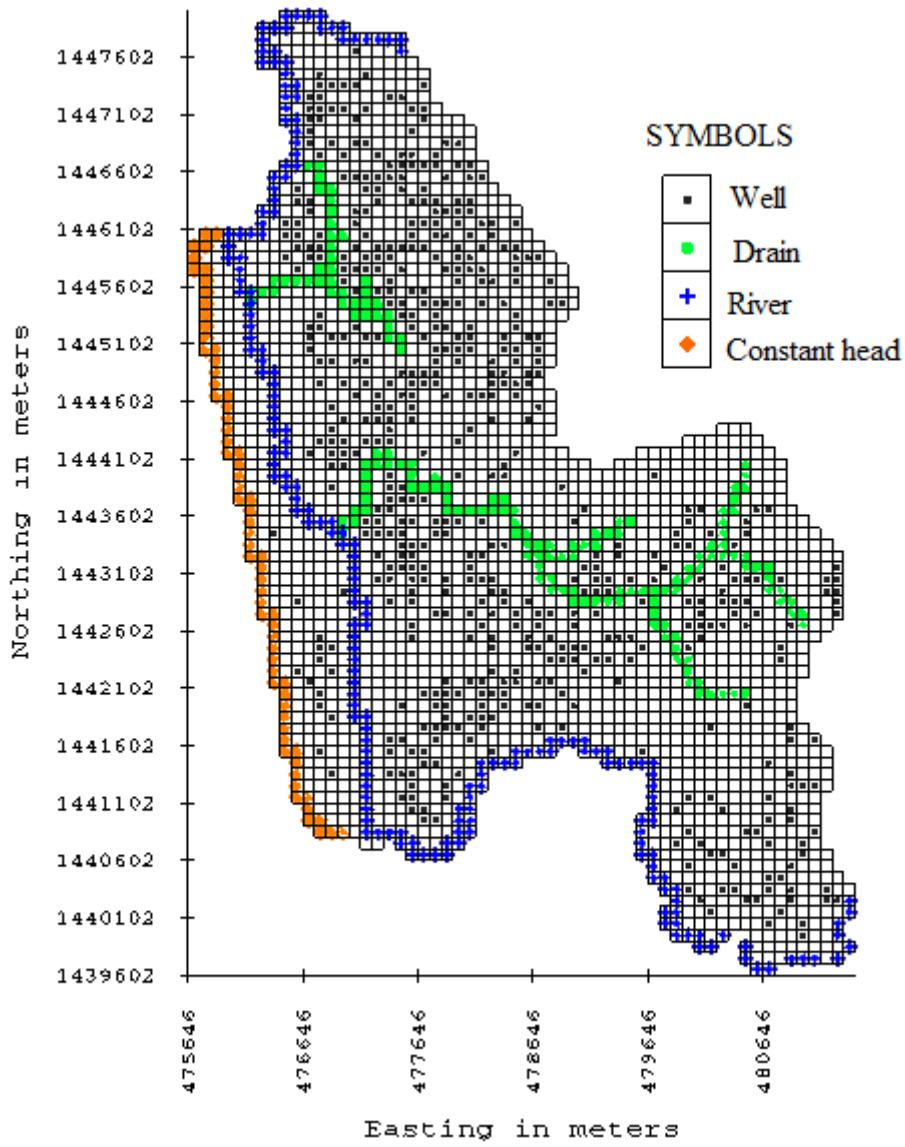


Fig. 4.4 Model representation of sub-basin 1

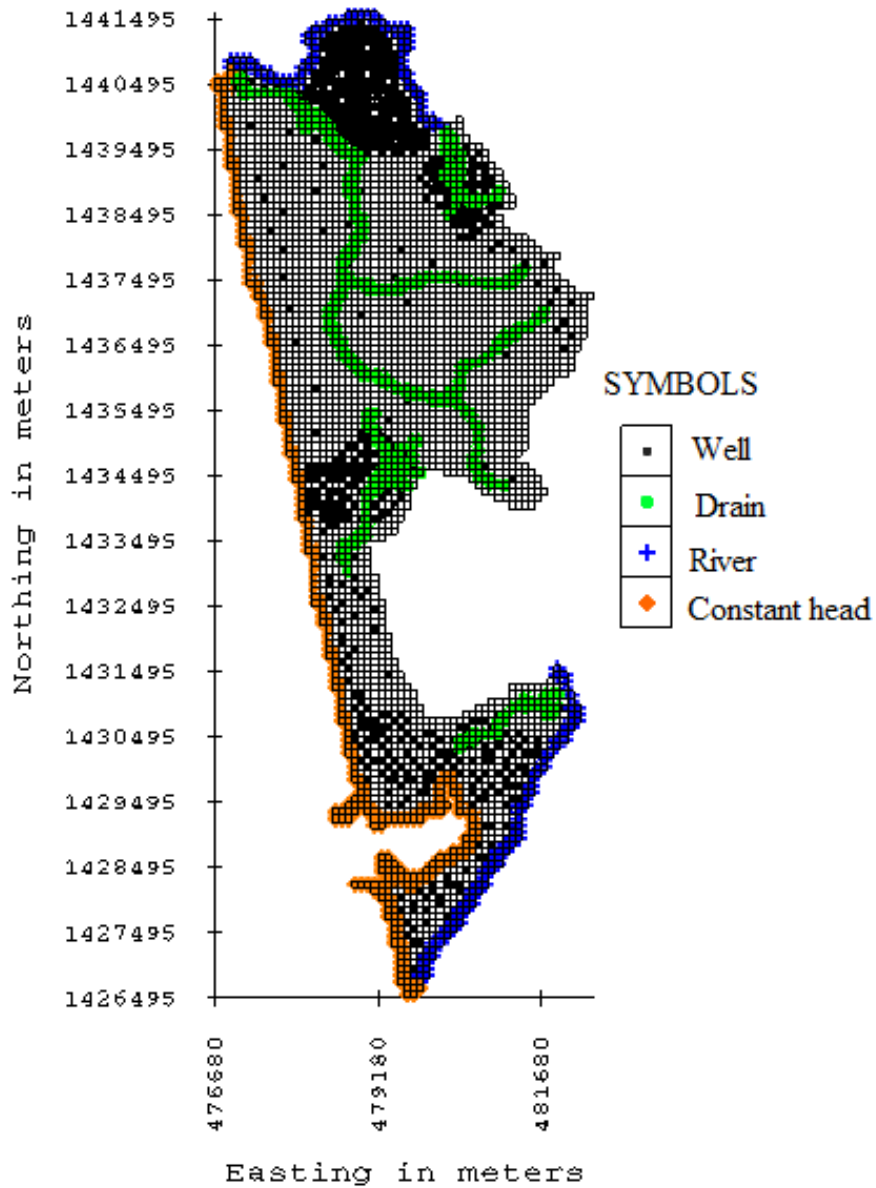


Fig.4.5 Model representation of sub-basin 2

Dirichlet boundary

The Dirichlet boundary is also called as type I boundary. The head or concentration value may vary from point to point or as a function of time and is treated as a known quantity in the solution of the equation. A Dirichlet boundary condition of constant head equal to 0 m above mean sea level (AMSL) is assigned at the western boundary for each of the model, which corresponds to the Arabian sea coastline. The time variant specified head (CHD) package of MODFLOW is used to simulate the

Dirichlet boundary condition. The starting and the end node of the arc representing the western boundary (coastline) are assigned a value equal to zero. The effect of tidal fluctuation is neglected because of very high computational requirements. However, since the effect of tidal fluctuations on groundwater levels is limited to areas very close to the coast (less than 500m or so), it's effect on saltwater intrusion can be neglected when compared to groundwater pumping effects (Narayan et al., 2007).

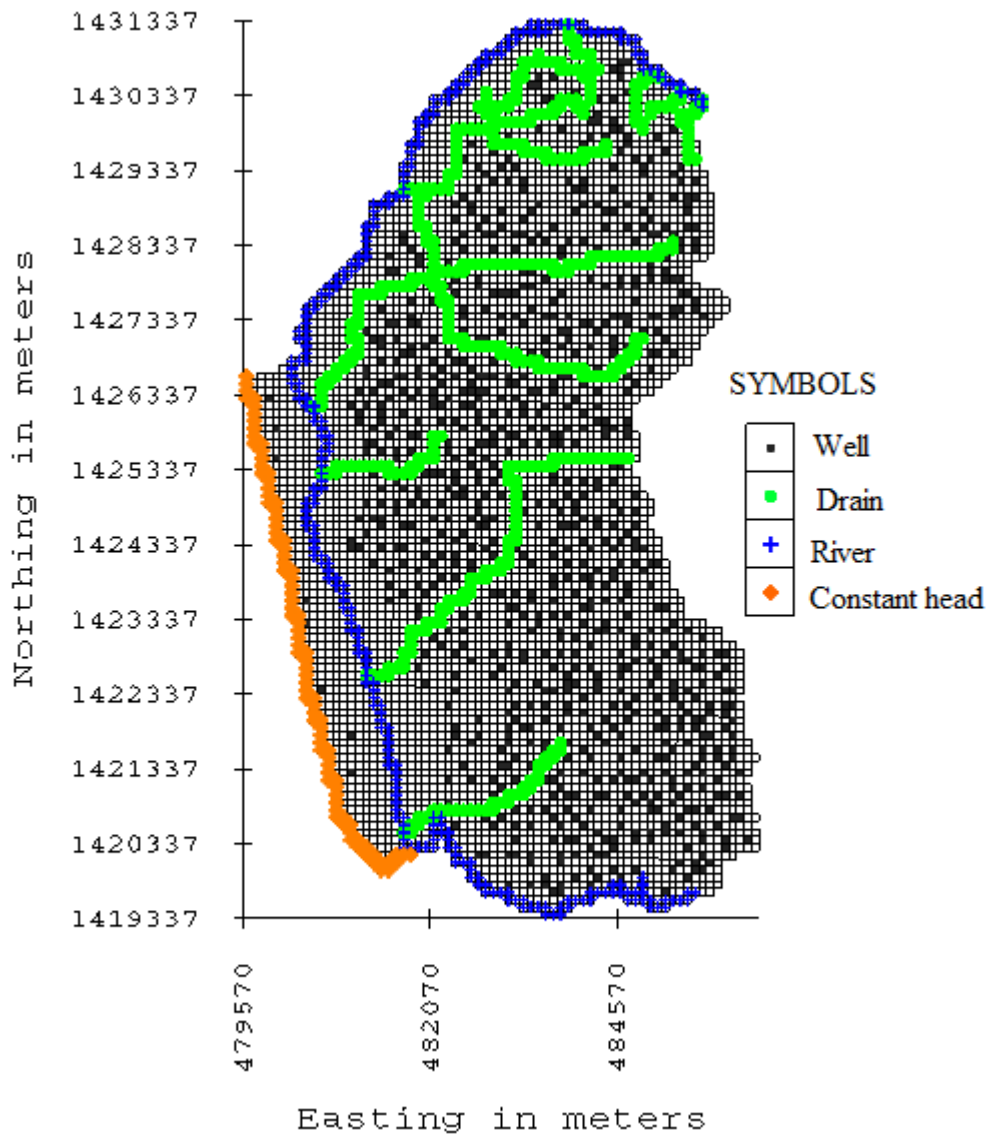


Fig. 4.6 Model representation of sub-basin 3

Neumann boundary

The Neumann boundary, also referred as type II boundary represents the condition in which the gradient of the dependent variable is specified normal to the boundary. In terms of ground-water flow, this boundary condition results in a specified flux of water into or out of the modeled area and in terms of solute transport, the concentration gradient is specified normal to the boundary. An impermeable boundary (commonly called a no-flow boundary) is simulated by specifying cells for which a flow equation is not solved. Additionally, the flow between a no-flow cell and an adjacent cell is zero. No-flow cells are used to delete the portion of the array of cells beyond the aquifer boundary. It is used in the eastern part of the model to simulate the watershed boundary of the aquifer.

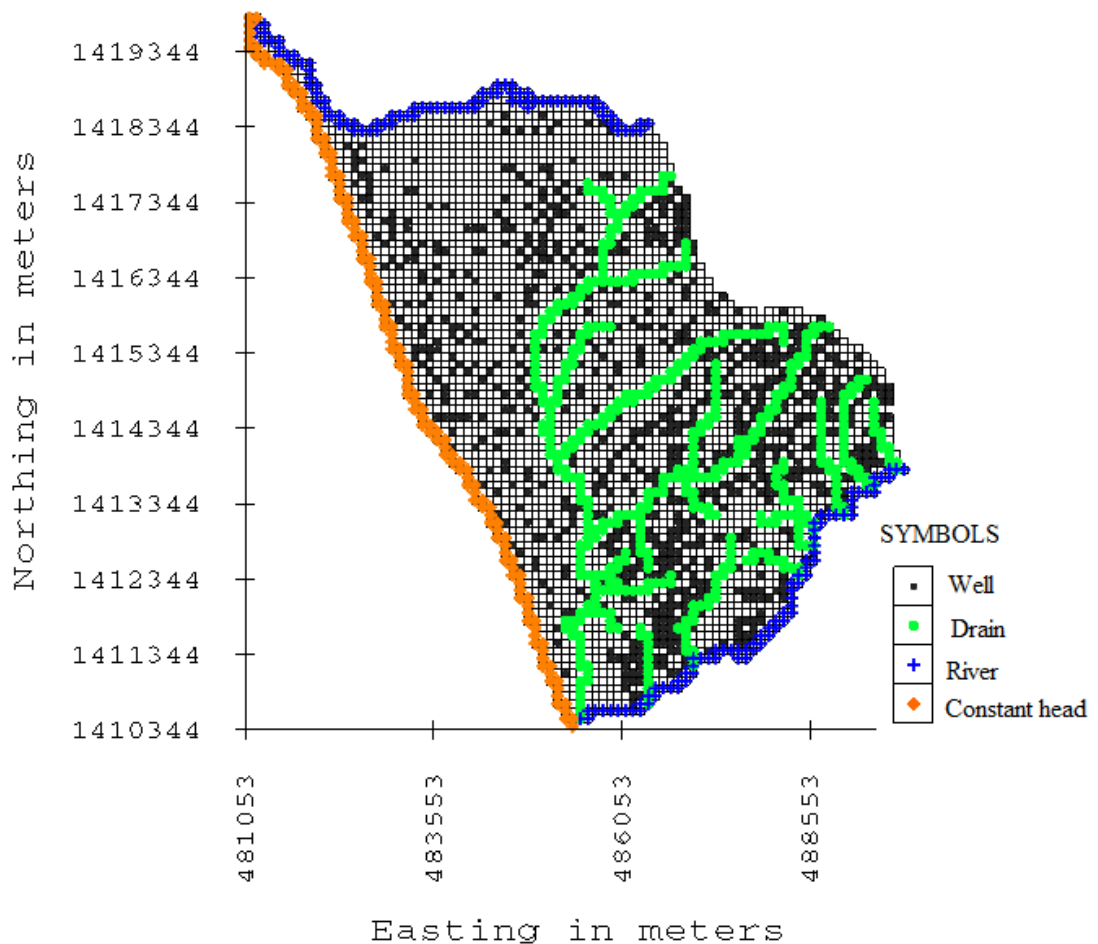


Fig.4.7 Model representation of sub-basin 4

Cauchy boundary

Cauchy boundary, also referred to as type III boundary represents a head-dependent flow condition for the simulation of flow (Anderson and Woessner, 1992). With the Cauchy boundary for flow, a control head is specified, but this control head prevails at some hydraulic separation from the boundary. The head on the boundary itself is calculated in the simulation, but is linked to the control head through a conductance term, which may represent, for example, the semi permeable material on the bed of a stream or the local head loss through convergent flow into a drain. The flow (Q_b), into or from a head dependent flow boundary is calculated as:

$$Q_b = COND(h_c - h_{i,j,k}) \quad (4.3)$$

where

$COND$ = conductance term,

h_c = specified control head, and

$h_{i,j,k}$ = calculated head at the boundary cell, which is linked through the conductance term.

The RIV and DRN involve limiting values of head beyond which the flow value (Q_b); takes on a fixed value, making these nonlinear variations of the head-dependent flux boundary condition.

The exact geometry and properties of a river channel cannot be represented in detail in a model grid (Rushton, 2007). Hence, the river-aquifer interaction is represented by river conductance. This is incorporated in an equation relating the river-aquifer flow to the difference between the elevation of the water surface in the river and groundwater head at the appropriate node in river package of MODFLOW. The rivers on the northern and southern boundary of each of the sub-basins are represented by arc feature and assigned as river boundary, using the river (RIV) package of MODFLOW. This is used to simulate the effects of flow between surface water features and groundwater systems. The real river as shown on fig.4.8 (A) is

conceptualized as shown in fig.4.8 (B) in MODFLOW. In the River package, the user specifies two elevations. One represents the elevation of the bottom of the river bed and the other represents the head in the river. If the head in the cell connected to the river drops below the bottom of the river bed, water enters the groundwater system from the river at a constant rate. If the head is above the bottom of the river, water will either leave or enter the ground water system depending on whether the head is above or below the head in the river. A conductance term will be multiplied by the difference between the head in the cell and the head in the river to determine the flux.

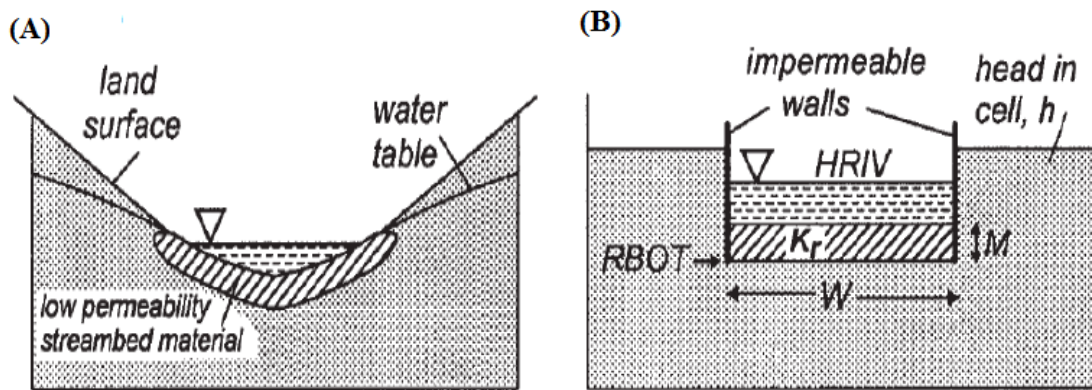


Fig.4.8 Representation of river in MODFLOW

The RIV package input file requires the following information for each grid cell containing a River boundary;

- (i) River Stage: The free water surface elevation of the surface water body. This elevation may change with time.
- (ii) Riverbed Bottom: The elevation of the bottom of the seepage layer (bedding material) of the surface water body.
- (iii) Conductance: A numerical parameter representing the resistance to flow between the surface water body and the groundwater caused by the seepage layer (riverbed).

The river bed elevation of -2 m with respect to mean sea level (msl) is assigned to the node at the river mouth (Radheshyam, 2009) where the river discharges into the sea and is gradually elevated away from the coast with a bed slope of 1 in 6000 for

Gurupur and Nethravathi rivers and bed slope of 1 in 3000 for the rest of the rivers. The river stage data is obtained from the Minor Irrigation Department and <http://www.india.wris.nrsc.gov.in>. The monthly river stage values are reduced to the model elevation and are assigned at the start and end nodes of the rivers. The river bed conductance value (*CRIV*) is defined by the equation:

$$CRIV = \frac{K_r LW}{M} \quad (4.4)$$

where; K_r = hydraulic conductivity of the river bed material. Based on the field observations the river bed material was found to be fine to medium sand, which is also evident from the studies carried out by Kumar (2011). The hydraulic conductivity for fine sand is 2.5m/day and that of medium sand is 12m/day (Todd and Mays 2005); L = length of the reach in the cell, which is automatically calculated by the software; W = width of the river, which is measured using google earth and average values are assigned; M = river bed thickness, assigned as 1m.

The drain (DRN) package of MODFLOW is used to simulate the effect of drainage network in the model. The inputs required are the reference head and conductance. The drain is assumed to be 1.5m deep from the surface and 3m wide. The drain is considered active only during the monsoon season. In drain boundaries, water can only leave the groundwater system through the drain cell, but it never re-enters to the groundwater system. That is, drains remove water from the aquifer as long as the water table is above the elevation of the drain and if the water table falls below the elevation of the drain, the drain has no effect.

4.4.5 Initial conditions

The starting values assigned for the dependent variable, such as freshwater head for groundwater flow and concentration for the solute transport are represented by initial conditions. In the present application, the steady state calibration is carried out for October 2007 and the simulated water levels are assigned as initial condition for the transient simulation.

4.5 MODEL CALIBRATION

The model calibration is a process in which the hydraulic parameters are varied until the simulated values of groundwater heads match the observed groundwater heads, thus improving the accuracy of the model. The model parameters are varied either manually or automatically during calibration process. In the present study, Parameter Estimation (PEST) version 12.2 (Doherty, 2004) is used to calibrate the model. PEST works by using a template file containing parameters to be estimated. Before carrying out calibration by PEST, parameters are varied by trial and error method and the model is run several times to obtain the approximate range of parameter values, which is then used as input for PEST. Moriasi et al. (2007) provided a comprehensive review of various model evaluation techniques (statistical and graphical) available to facilitate model evaluation in terms of the accuracy of simulated data compared to measured data. Each method has its own advantages and disadvantages, hence it is desirable to use a combination of different evaluation methods for better estimation of model results. In this work, the model simulated and measured groundwater head are compared using the following four methods:

- Slope and y-intercept: The scatter plot of observed and model simulated values are plotted with x and y axis having the same intervals and a 1:1 trend line (or 45° line) is fitted diagonally at point (0,0) across the plot area. This line has a slope of 1 and y-intercept of 0 indicating that the model perfectly reproduces the magnitudes of measured data (Willmott, 1981). Hence, the alignment of the scatter plot with the 45° line reveals the reliability of the model results.
- Coefficient of determination (R^2): Describes the degree of co-linearity between simulated and measured data and the proportion of the variance in measured data explained by the model. R^2 ranges from 0 to 1, with higher values indicating less error variance, and typically values greater than 0.5 are considered acceptable (Santhi et al., 2001 and Van Liew et al., 2003).
- Root mean square error (RMSE): RMSE indicate the error between simulated and measured data. RMSE values of 0 indicate a perfect fit. It is calculated as,

$$RMSE = \sqrt{\frac{1}{n} \sum (Y^{obs} - Y^{sim})^2} \quad (4.5)$$

- Nash-Sutcliffe efficiency (NSE): A method recommended for model evaluation by the ASCE (1993) is most commonly used in hydrological applications. This determines the relative magnitude of the residual variance compared to the measured data variance and is calculated as,

$$NSE = 1 - \left[\frac{\sum (Y^{obs} - Y^{sim})^2}{\sum (Y^{obs} - Y^{mean})^2} \right] \quad (4.6)$$

where Y^{obs} =observed data, Y^{sim} = model simulated data, Y^{mean} = mean of the observed data and n is the total number of observations.

NSE values between 0 and 1 are generally viewed as acceptable for model performance and values ≤ 0.0 indicated unacceptable performance.

4.5.1 Observation wells

The observed groundwater heads used for transient calibration of the model are obtained from the water levels measured at 29 observation wells on fortnightly basis (Shivanagouda, 2015) for a period of 2 years (2011-13). However, Google Earth imagery is used to establish the elevation of well location by the investigator in the study. An average error of +1.4m was estimated and need to be corrected accordingly. To further minimize the errors involved, DGPS (Differential Geographic Positioning System) survey is conducted in the present work in order to recalculate hydraulic head from measured groundwater depths.

Differential Geographic Positioning System

Differential Geographic Positioning System a technique developed in the early 1980s is a method of improving the accuracy of the receiver by adding a local reference station to augment the information available from the satellites. Accuracy upto

centimetre resolution is generally possible with this technique, whereas the non-DGPS can only achieve a resolution of a few meters. For the present study Trimble® Juno® 3 series handheld instruments along with tripod stand is used.

Differential GPS is conducted with the utilization of two receivers, one that is stationary and set up at a precisely known location (base or reference receiver) and another that is roving around making position measurements. The stationary receiver compares its calculated GPS location with the actual location based on satellite signals and computes the error associated with the unknown rover position. Since the base station is fixed, the difference between the measurement of the base and the rover receivers is used to create an error correction vector. The precise location of the rover can then be calculated by applying the error correction over all the satellite data. The data that is captured is post-processed on a computer using special processing software. In the present work Trimble® Business Center Software ver.1.10 is used. The details of the observation wells in the study area are given in Table 4.5 and the locations are shown in Fig. 1.2 (chapter 1)

Table 4.5 Details of observation wells

Well No.	Location		Well Depth (m)	Elevation of well head (m)
	Latitude	Longitude		
1	12° 45' 49"	74° 52' 23"	2.90	4.42
2	12° 46' 37"	74° 51' 51"	6.90	7.00
3	12° 47' 36"	74° 51' 27"	12.30	15.96
4	12° 49' 15"	74° 51' 32"	14.40	14.09
5	12° 50' 00"	74° 51' 34"	2.90	4.89
6	12° 49' 55"	74° 51' 43"	3.95	6.39
7	12° 49' 45"	74° 52' 13"	4.60	5.03
8	12° 50' 58"	74° 51' 17"	9.50	10.15
9	12° 50' 55"	74° 51' 39"	5.30	6.96
10	12° 51' 56"	74° 51' 57"	5.30	11.70
11	12° 52' 16"	74° 51' 50"	4.90	11.77

12	12° 53' 59"	74° 50' 40"	9.20	12.56
13	12° 55' 16"	74° 49' 50"	5.10	7.09
14	12° 55' 35"	74° 50' 20"	5.10	15.32
15	12° 56' 49"	74° 50' 28"	2.70	3.07
16	12° 56' 45"	74° 48' 54"	7.90	6.10
17	12° 57' 25"	74° 48' 25"	5.90	3.80
18	12° 58' 34"	74° 48' 12"	6.40	5.07
19	12° 59' 14"	74° 48' 18"	19.00	16.02
20	12° 59' 55"	74° 47' 50"	7.30	7.53
21	13° 00' 57"	74° 47' 35"	9.20	6.60
22	13° 01' 28"	74° 47' 19"	5.10	3.29
23	13° 01' 42"	74° 47' 32"	5.00	2.50
24	13° 01' 57"	74° 47' 51"	9.00	6.68
25	13° 02' 07"	74° 47' 37"	2.30	3.68
26	13° 03' 29"	74° 47' 50"	6.10	10.00
27	13° 03' 59"	74° 47' 50"	5.20	11.00
28	13° 05' 03"	74° 47' 20"	8.30	8.50
29	13° 05' 44"	74° 47' 08"	2.30	1.80

4.5.2 Steady state calibration

The aquifer is said to attain steady state during a time period when the flows get balanced and the water levels do not change over that period of time. Such condition may quite possibly arise at more than one time period. In practice, unless the aquifer system is analysed much beyond in time for past data it is very difficult to get the actual steady state condition. A limitation of data availability in the present region restricts such precedent investigation. Therefore, based on preliminary investigation the aquifer system was found to be in near steady state condition during October 2007. It is taken up to run and calibrate the model under steady state for this period and the calibrated hydraulic conductivity distribution and over all porosity is obtained. The head obtained there off is assigned as the starting head for the transient simulation.

The groundwater head obtained from steady state simulation is compared with the observation record of 11 wells (Vyshali, 2008) for sub-basin 2 and that available from the Central Ground Water Board and the Department of Mines and Geology, Govt. of Karnataka for the rest of the sub-basins. Altogether, a total of 18 available observation well records are used in the steady state calibration process.

The values of statistical parameters obtained as an indication of model performance are; co-efficient of correlation (r) = 0.947, co-efficient of determination (R^2) = 0.896, and root mean square error (RMSE) = 0.984. A scatter plot of the simulated versus the observed heads is shown in Figure 4.9. The plot reveals that the model fits the observed groundwater heads rather well, as all points are lying close to the diagonal line.

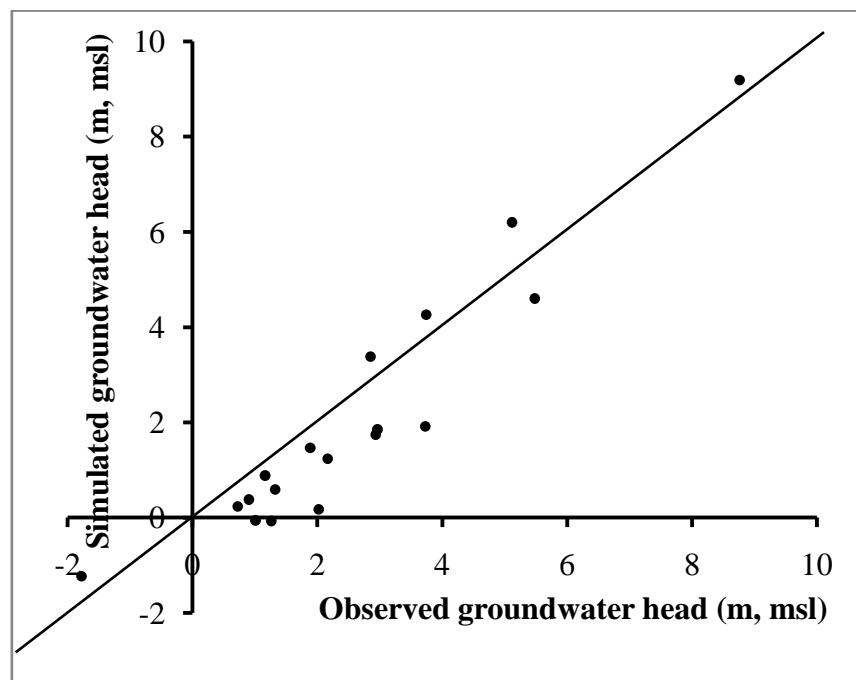


Fig.4.9 Scatter plot of steady state calibration

4.5.3 Transient calibration

The transient calibration is carried out from September 2011 to August 2013. The total simulation period of two years has been divided into 24 stress periods. Daily time step has been considered for the transient simulation applying all the hydro-geologic conditions of the same period. Calibration is carried out accounting for the

spatial variability of the aquifer parameters and the seasonal performance of the model. Apart from the aquifer parameters already calibrated in the steady state model, such as the hydraulic conductivity and porosity, the transient calibration requires the specification of the specific yield (S_y) as well. After successful calibration, the values of horizontal hydraulic conductivity and specific yield of the unconfined aquifer is estimated to be in the range 1.85m/day to 49.5 m/day and 0.006 to 0.281 respectively. The zone wise calibrated aquifer parameters are presented in table 4.6 and 4.7.

Table. 4.6 Optimal parameter values obtained after seasonal calibration

<i>Parameters</i>	<i>Value</i>
Hydraulic conductivity of the river bed material (m/day)	10
Recharge co-efficient (%)	20
Porosity (%)	30
Horizontal anisotropy	1

Table. 4.7 Zonewise parameter values obtained after seasonal calibration

Zone	<i>SUB-BASIN 1</i>		<i>SUB-BASIN 2</i>	
	Hydraulic conductivity (m/day)	Specific yield	Hydraulic conductivity (m/day)	Specific yield
1	2.12	0.006	4.5	0.0255
2	3.5	0.010	6.39	0.037
3	5.01	0.012	7.33	0.1305
4	6.096	0.013	9.5	0.065
5	9.656	0.029	10.5	0.12
6	11.192	0.073	11	0.1275
7	14.89	0.095	24.45	0.134
8	25.12	0.097	43.5	0.281
9	32.18	0.105	49.5	0.1405
Zone	<i>SUB-BASIN 3</i>		<i>SUB-BASIN 4</i>	
	Hydraulic conductivity (m/day)	Specific yield	Hydraulic conductivity (m/day)	Specific yield
1	1.85	0.012	4	0.052
2	9.00	0.03	4.5	0.07

3	10.29	0.0612	5.26	0.08
4	14.9	0.102	6.5	0.092
5	19.25	0.114	7.5	0.1
6	23.44	0.132	8.25	0.101
7	27.35	0.2172	8.75	0.1075
8	31.38	0.225	10	0.10275
9	35.87	0.24	14	0.1131

The R^2 , RMSE and NSE values for all months of the calibration period for the flow output are listed in table 4.8. Table 4.8 conveys that the model performance is satisfactory as the parameters are well within the acceptable ranges. However, the model performance during the monsoon (June to Sept) is not up to the mark, with all the three evaluation techniques showing deviation from the desired levels. This could be due to greater inter mixing of river water with seawater, additional later inflow/outflow during these months, which is not well addressed by the model. The RMSE values are approximately ≤ 1 m, except that for the monsoon season. This is satisfactory for the kind of model developed with the execution of scarcely available input data in the most logical approach.

Further, the model performance is tested with a graphical method and scatter plot of selected months in post-monsoon, monsoon and pre-monsoon are presented in fig.4.10 and fig. 4.11 for the sub-basins 1 to 4 respectively. Here, the scatter plot of the measured and simulated values of groundwater head for the pre-monsoon, monsoon and the post-monsoon seasons are exhibited for all the four sub-basins. The graphs show a convincingly good agreement with the observed and simulated groundwater heads. However, for the monsoon season, the model tends to underestimate the groundwater head, as few point appear below the 1:1 line. The reason for this is already discussed earlier. The well hydrograph for the observed and simulated water levels for few selected wells are presented in fig.4.12 which confirms a reasonably good match.

Table 4.8 Groundwater flow model efficiency values on monthly basis during 2011-13

<i>SUB-BASIN 1</i>				<i>SUB-BASIN 2</i>				<i>SUB-BASIN 3</i>				<i>SUB-BASIN 4</i>			
Month	R²	RMSE (m)	NSE	Month	R²	RMSE (m)	NSE	Month	R²	RMSE (m)	NSE	Month	R²	RMSE (m)	NSE
Oct	0.967	0.700	0.927	Oct	0.599	0.877	0.523	Oct	0.902	0.853	0.889	Oct	0.891	0.865	0.862
Nov	0.953	1.047	0.823	Nov	0.609	0.804	0.579	Nov	0.969	0.606	0.941	Nov	0.898	0.980	0.708
Dec	0.985	1.001	0.852	Dec	0.698	0.667	0.587	Dec	0.923	0.908	0.866	Dec	0.896	1.076	0.720
Jan	0.988	0.904	0.865	Jan	0.697	0.716	0.517	Jan	0.910	0.769	0.890	Jan	0.904	1.094	0.483
Feb	0.973	0.911	0.876	Feb	0.738	0.774	0.727	Feb	0.900	0.858	0.883	Feb	0.917	0.947	0.563
Mar	0.976	1.025	0.834	Mar	0.655	0.836	0.633	Mar	0.912	0.896	0.857	Mar	0.902	0.983	0.472
Apr	0.988	0.998	0.845	Apr	0.785	0.708	0.751	Apr	0.928	0.890	0.806	Apr	0.917	0.748	0.570
May	0.972	1.005	0.816	May	0.712	0.824	0.687	May	0.929	1.036	0.694	May	0.810	0.722	0.495
Jun	0.720	1.608	0.588	Jun	0.530	1.558	0.330	Jun	0.826	2.410	0.216	Jun	0.573	2.323	0.350
Jul	0.867	1.097	0.865	Jul	0.509	2.178	0.245	Jul	0.869	2.347	0.162	Jul	0.713	2.422	0.446
Aug	0.935	1.110	0.830	Aug	0.675	0.807	0.595	Aug	0.878	1.126	0.808	Aug	0.667	2.166	0.646
Sept	0.771	1.440	0.755	Sept	0.577	1.446	0.314	Sept	0.777	1.569	0.619	Sept	0.703	2.422	0.571

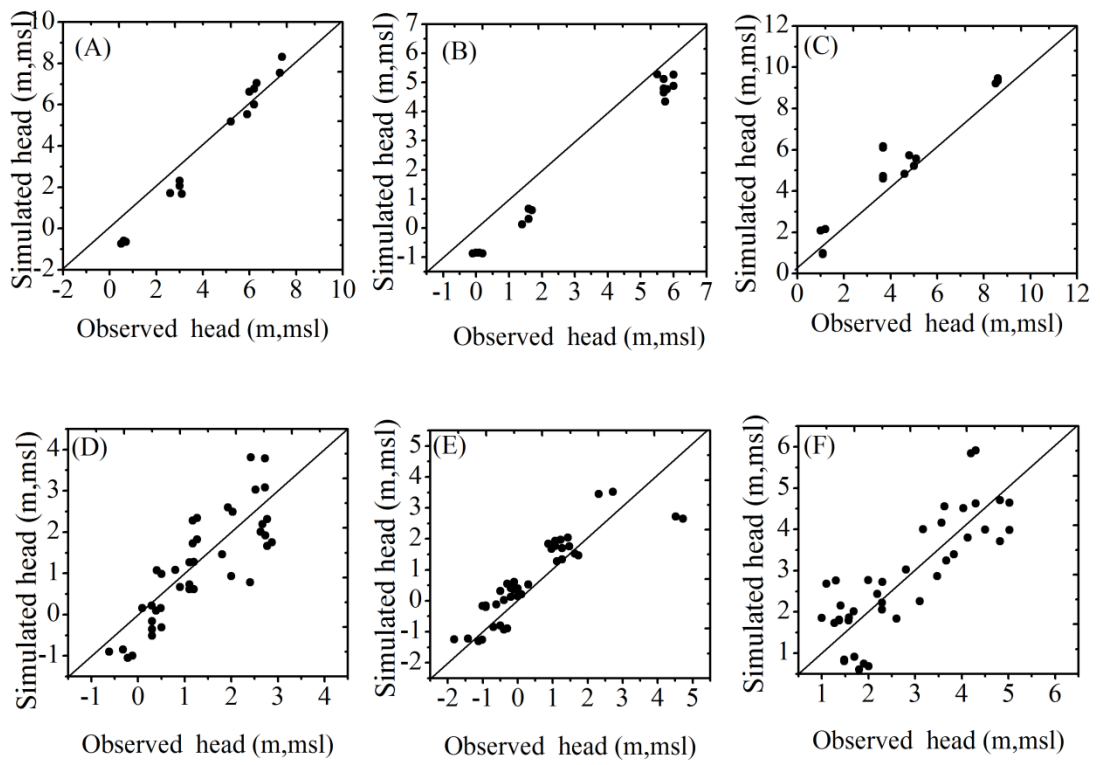


Fig. 4.10 Simulated and observed groundwater heads(2011-13) for(A)post-monsoon, (B) pre-monsoon and (C) monsoon seasons of sub-basin 1 and that for sub-basin 2 (D), (E) and (F) respectively.

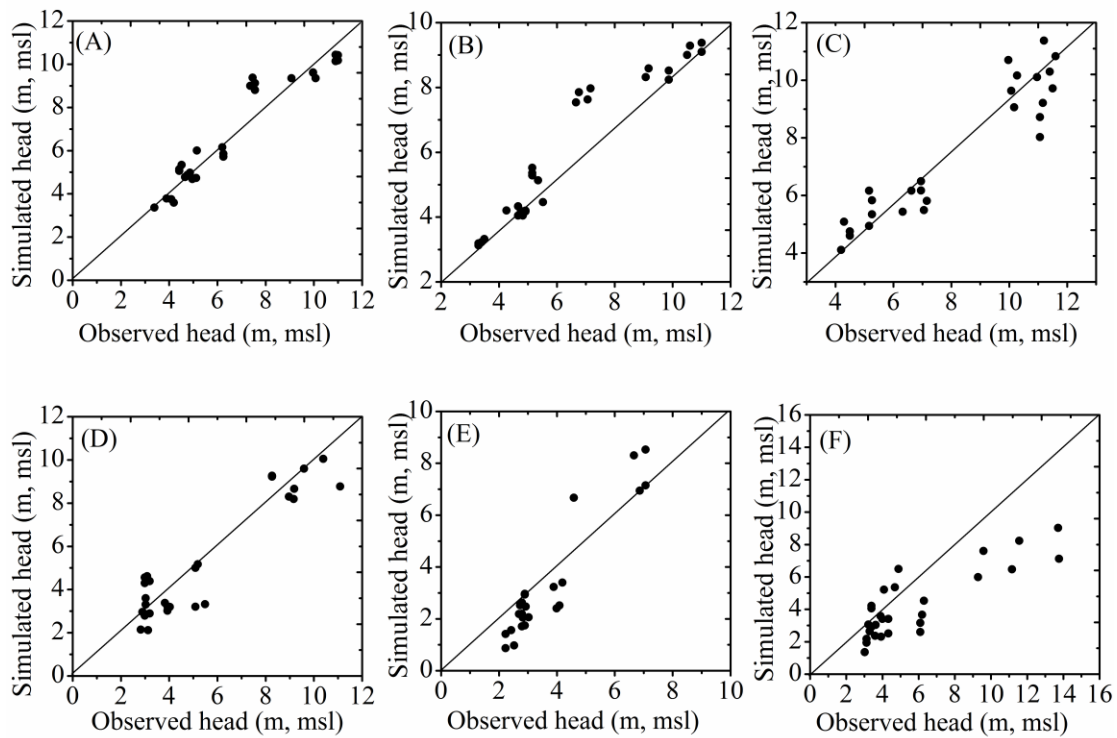


fig. 4.11 Simulated and observed groundwater heads(2011-15)for (A)post-monsoon, (B) pre-monsoon and (C) monsoon seasons of sub-basin 3 and that of sub-basin 4 (D), (E) and (F) respectively

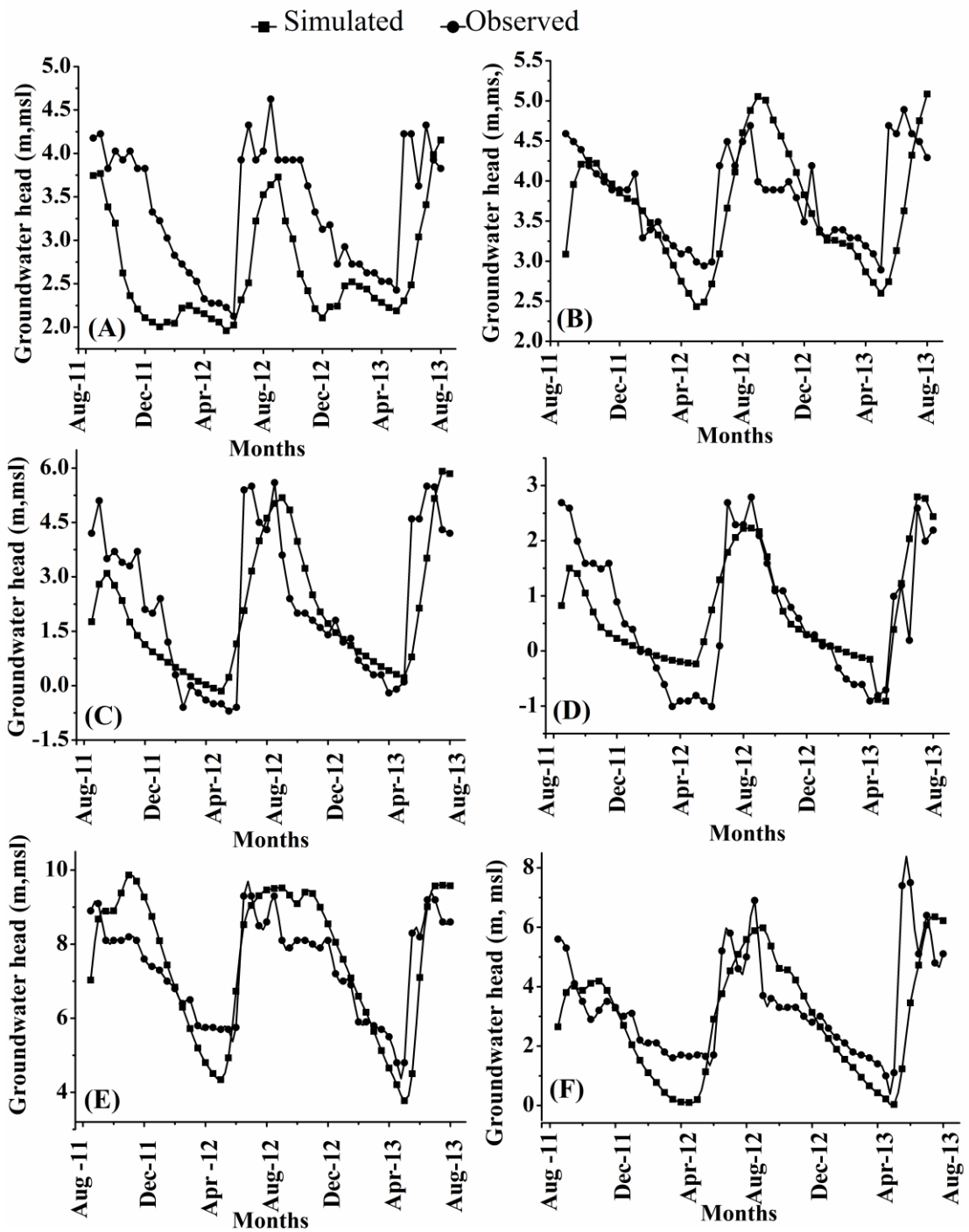


Fig.4.12 Simulated and observed groundwater heads during the calibration period for (A) well no.7 (B) well no.8 (C) well no.21 (D) well no.22 (E) well no.26 and (F) well no.28

Figures 4.13 to 4.16 show the calibrated groundwater flow pattern for the months of May (summer) and August (monsoon) of 2013. The water table map for August can be compared with that of aquifer zonation map. Here, the high water table potential zones coincide with that of low hydraulic conductivity zones and similarly, the low water table potential zones coincide with the zones of high hydraulic conductivity. Overall, the simulation results of all the sub-basins show a similar trend with the groundwater table gradually increasing from the coastline and the rivers towards the landward side (high elevated area). The water table rises to maximum elevation of about 43m (above msl) in sub-basin1 and 3. This could be because of greater drainage density. However, the areal extent of sub-basin 3 is more than twice that of sub-basin 1. The maximum water table elevation ranges from about 12m to 20 m (above msl) in rest of the sub-basins. It is clearly evident from the figures that the month of May is visibly drier than the month of August, with the lowest groundwater level contour moving towards inland by about 200m to 900m in comparison with that during the monsoon.

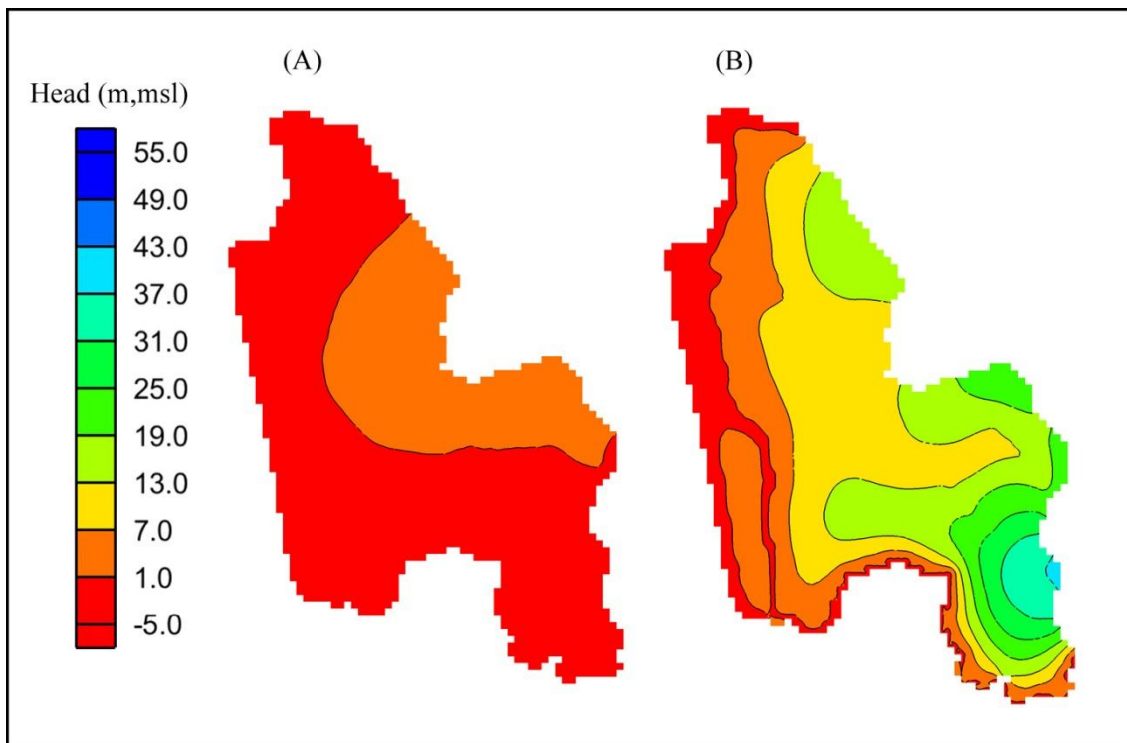


Fig.4.13 Groundwater flow contours for (A) May 2013 and (B) August 2013 for sub-basin 1

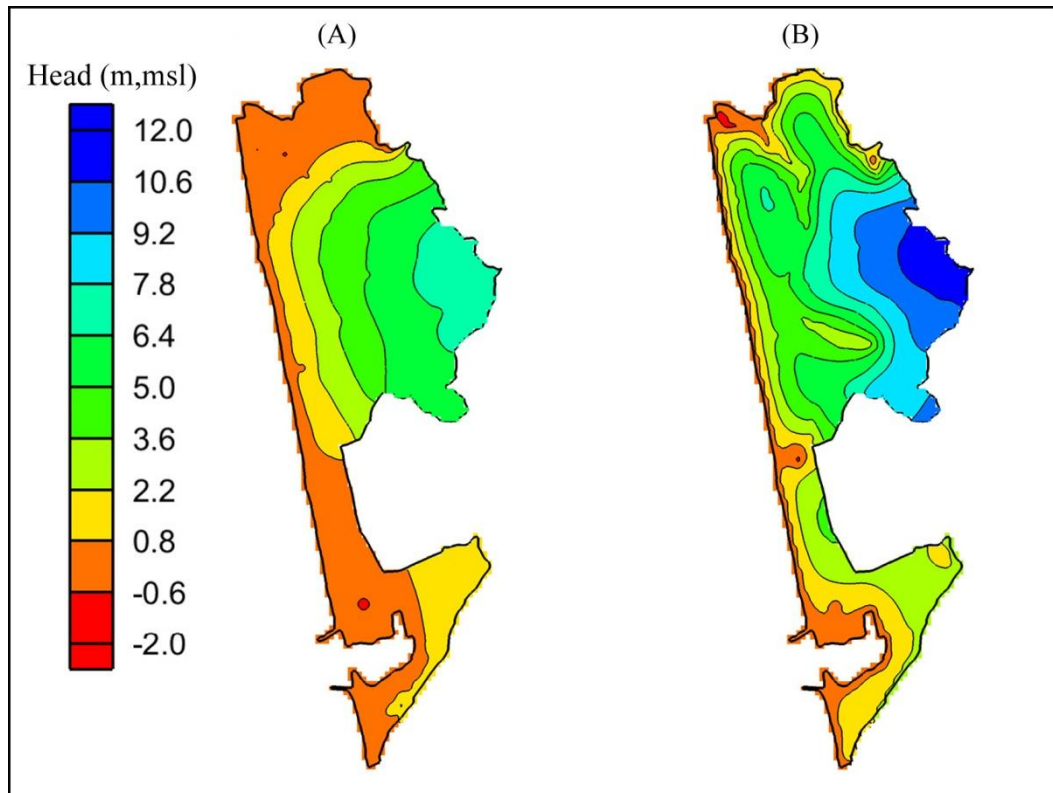


Fig.4.14 Groundwater flow contours for (A) May 2013 and (B) August 2013 for sub-basin 2

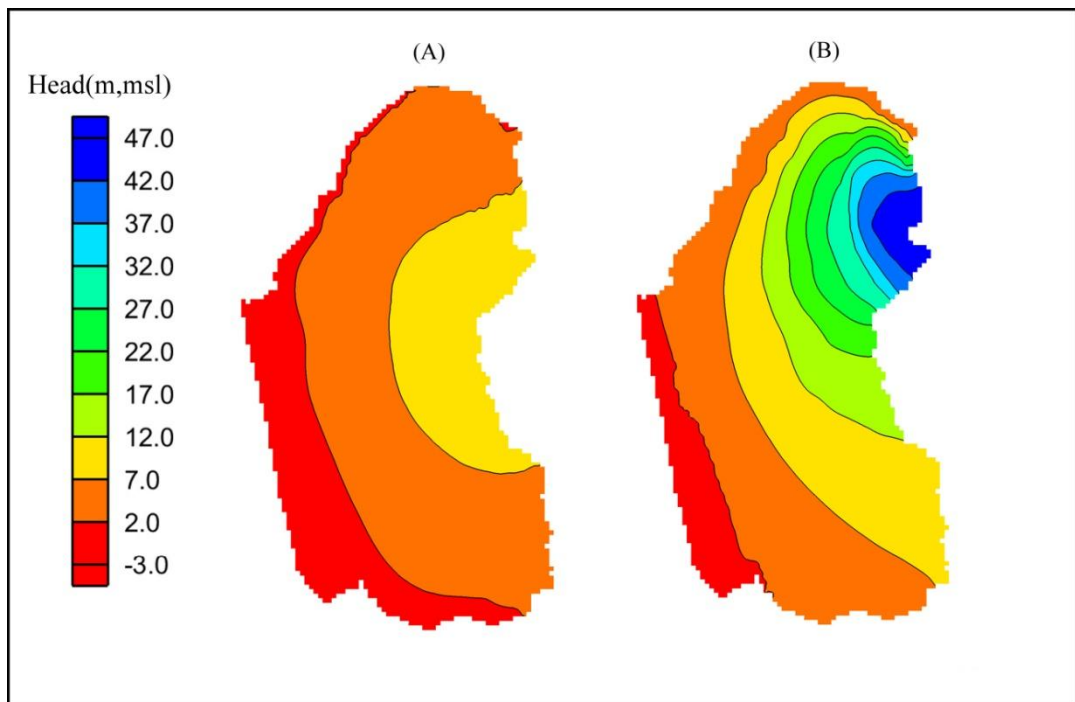


Fig.4.15 Groundwater flow contours for (A) May 2013 and (B) August 2013 for sub-basin 3

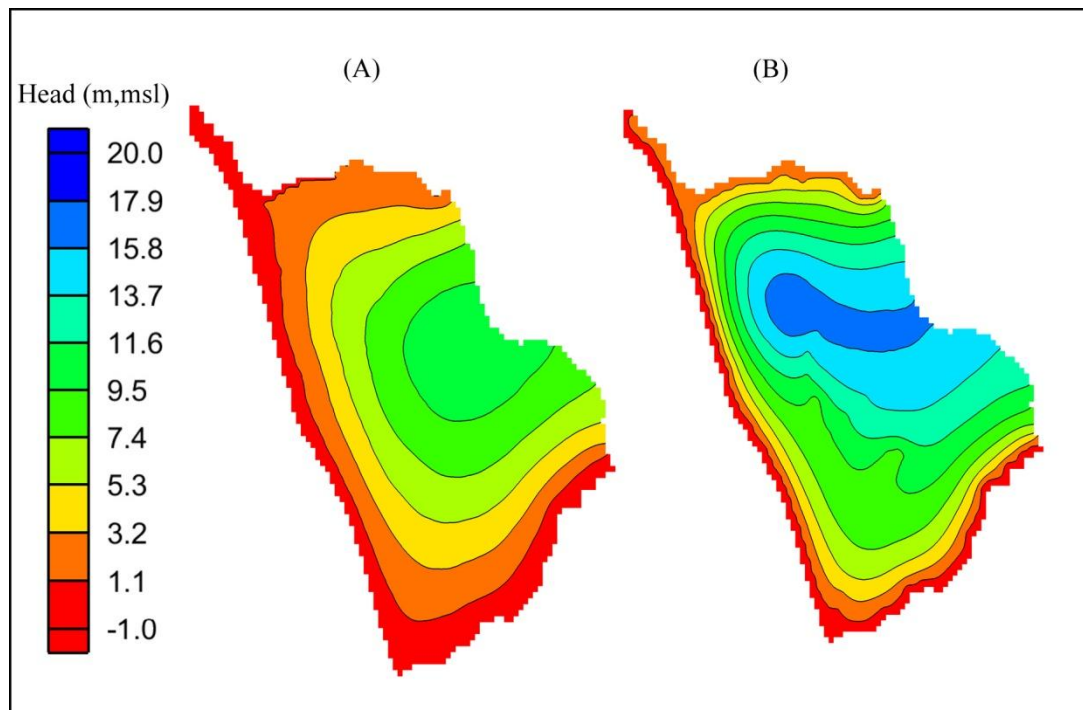


Fig.4.16 Groundwater flow contours for (A) May 2013 and (B) August 2013 for sub-basin 4

4.6 MODEL VALIDATION

It is important to check the authenticity of the model before applying it for predictive scenario simulation through the validation process. The validation is carried out for a period of one year during 2013-14 subsequent to the calibration run.

A total of 10wells monitored by the Central Ground Water Board and the Department of Mines and Geology, Govt. of Karnataka are used for validation purpose except that for sub-basin3. The water level data observed at 8 well locations on monthly basis (Sylus, 2015) is used to validate the groundwater flow model of sub-basin 3. The measured water level (meters below ground level) is converted to groundwater head (meters above mean sea level) using the grid elevation at the location of the well.

The R^2 , RMSE and NSE values obtained after analysing the observed and calibrated groundwater head at various observation points is provided in table 4.9 for each sub-basin. And the results are found to be consistent with that of the calibration results and therefore the model can be considered reliable for future predictions. To perceive the agreement between the observed and simulated groundwater head data during the

validation period, combined scatter plot of all 4 sub-basins is presented in fig.4.17. The trend as seen from the fig.4.17 is pretty persuasive.

Table.4.9 Groundwater flow model efficiency values during the period 2013-14

	R²	RMSE (m)	NSE
<i>SUB-BASIN 1</i>	0.749	1.380	0.608
<i>SUB-BASIN 2</i>	0.915	1.242	0.839
<i>SUB-BASIN 3</i>	0.703	1.011	0.622
<i>SUB-BASIN 4</i>	0.989	1.183	0.974

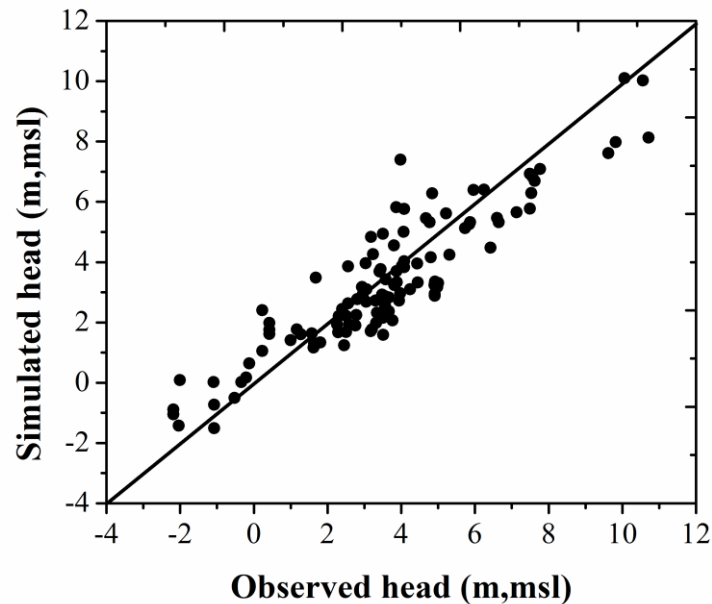


Fig. 4.17 Simulated and observed groundwater heads(2013-14)for (A) sub-basin-1 (B) sub-basin-2 (C) sub-basin-3(D)sub-basin-4

4.7 MODEL APPLICATIONS

4.7.1 Water balance

The groundwater mass balance simulation package, ‘ZONEBUDGET’ estimates the budget of volumetric flow rate of water in the whole system using the results from the MODFLOW. It uses cell-by-cell flow data in order to calculate the net inflows and outflows for a cell. The water budget of the model is presented schematically in fig.4.18. The rainfall recharge, contribution from the rivers and sea and storage due to

aquifer properties form the inflow into the aquifer. The aquifer loses water due to pumping, discharge to the sea, river and drains. Table 10 presents the volumetric water budget during the monsoon (August) and summer (May). In both cases, the water movement into and out of the aquifer system can be considered dynamically stable, with the percentage discrepancy between the two being zero in all sub-basins except sub-basin 1 and 3 which are being negligibly small.

More than 75% of available water is being discharged to the sea during the wet season compared to that during the dry season throughout the coastline. During the dry periods, the volume of water flowing out of the aquifer along the coastline is much lesser than the flow into the aquifer indicating higher probability of seawater intrusion. Since the rivers are tidal in nature, they contribute considerably to the aquifer system even during the non-monsoon months with saline water. The table also exhibits that the major input (>72%) into the aquifer is through rainfall recharge. It is also well established from the table that the drains are active only during the monsoon season and run dry during rest of the year.

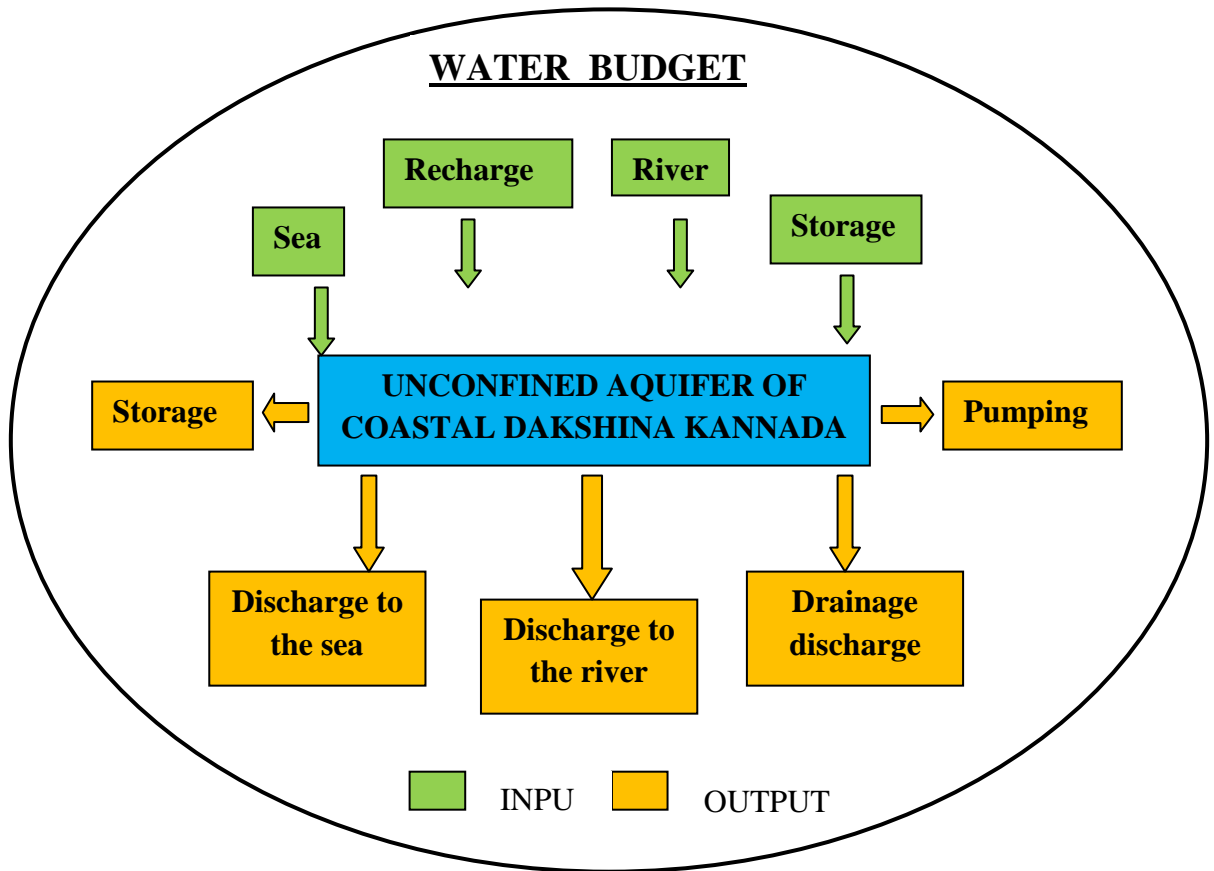


Fig.4.18 Schematic representation of water budget of the coastal aquifer of Dakshina Kannada

Table.4.10 Volumetric water budget

Sub-basin	Water balance components (m ³ /day)	Maximum head position (August)		Minimum head position (May)	
		In	Out	In	Out
1	Storage	244.02	8521.25	10288.75	0.78
	Constant Head	0.29	4841.11	1170.27	0
	Wells	0	10950.28	0	12774.72
	Drains	0	45345.84	0	0
	River leakage	4204.71	65361.49	10621.87	8965.88
	Recharge	130521.98	0	0	0
	Total	134970.99	135019.97	22080.89	21741.37
	<i>In - out</i>		48.98		339.53
<i>% Discrepancy</i>		0.04		1.55	
2	Storage	508.40	42448.91	20348.28	0
	Constant Head	276.35	70980.34	2605.82	12582.62

	Wells	0	18631.16	0	21344.80
	Drains	0	77776.83	0	0
	River leakage	30799.39	14233.62	12273.99	1300.32
	Recharge	192488.80	0	0	0
	Total	224072.94	224070.87	35228.08	35227.75
	<i>In - out</i>	2.07		0.34	
	<i>% Discrepancy</i>	0.00		0.00	
3	Storage	0	126574.08	60866.38	0
	Constant Head	0	28433.08	1305.72	2487.41
	Wells	0	24348.60	0	28406.70
	Drains	0	16746.83	0	0
	River leakage	102930.49	195572.05	117193.73	148416.16
	Recharge	288713.17	0	0	0
	Total	391643.67	391674.65	179365.84	179310.27
	<i>In - out</i>	30.98		55.57	
<i>% Discrepancy</i>	0.008		0.03		
4	Storage	0	73115.09	34505.04	0.00
	Constant Head	81.32	36471.98	3.37	8249.82
	Wells	0	15966.13	0	18627.28
	Drains	0	22205.98	0	0
	River leakage	16743.60	57974.34	12950.58	20581.07
	Recharge	188914.60	0	0	0
	Total	205739.53	205733.50	47458.98	47458.16
	<i>In - out</i>	6.01		0.82	
<i>% Discrepancy</i>	0.00		0.00		

4.7.2 Aquifer-river interaction

The river-aquifer interaction plays an important role in sustainably managing water resources. In MODFLOW (McDonald and Harbaugh, 1988), the River package simulates the effects of flow between surface water features and groundwater systems. It is assumed that, the measurable head losses between the river and the aquifer are limited to those across the riverbed itself. It is also presumed that the model cell underlying the stream remains fully saturated. The aquifer-river interaction is based on the concept that the low permeability riverbed material governs the loss from a river. The equation for flow between the river and the aquifer is derived based upon two cases:

- (i) The groundwater head is above the bottom of the river bed (fig.4.19a) - A case of varying flow depending on the groundwater head and river surface elevation.

$$QRIV = CRIV(HRIV - h) \quad h > RBOT \quad (4.7)$$

- (ii) The groundwater head is below the bottom of the river bed (fig.4.19b), a case where the river losses to the aquifer independent of the groundwater head.

$$QRIV = CRIV(HRIV - RBOT) \quad h \leq RBOT \quad (4.8)$$

where,

$QRIV$ = flow between river and the aquifer

$CRIV$ = river bed conductance as given by equation (4.4)

$HRIV$ =river water elevation

$RBOT$ = elevation of the bottom of river bed

h =groundwater head in the cell

These two cases are represented graphically in fig.4.19 (c).The flow is zero when h is equal to the water level in the stream ($HRIV$). For higher values of h , flow is negative (into the stream) and for lower values of h , flow is positive (into the aquifer). This positive flow increases linearly as h decreases (horizontal line AB in fig.4.19c), until h reaches $RBOT$, thereafter, the flow remains constant (inclined line BC in fig 4.19c).

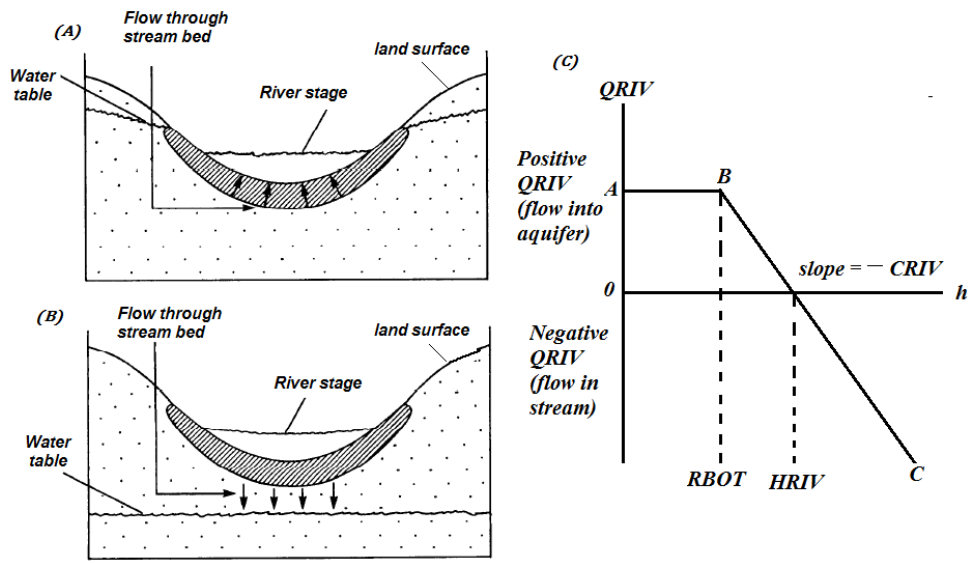


Fig.4.19 Representation of river–aquifer interaction in MODFLOW

The bar charts of river flow rate during the calibration period (2011-13) are presented in figures 4.20 to 4.23. The bar charts show a considerable amount of river flow getting discharged out of the aquifer system into the sea (5,000 to 2,00,000 m³/day), except that for sub-basin 2 (from Shambhavi and Pavanje rivers). The bar chart representing sub-basin 1 (fig.4.20) indicates that, there is a high river flow rate out of the aquifer during June to September (85,000 m³/day) and comparatively very low inflow rate (5,000 m³/day). This is causing the river water to flow out of the aquifer without much percolation into the aquifer. However, during the non-monsoon seasons, there is marginal difference between the river inflow and outflow rates, both varying within 10,000 m³/day. This indicates that, there is equal interaction between the river and aquifer system in the non-monsoon season. During this period, river channel carries backwater from the sea with considerable amount of salinity. Hence, salinity present in the river water may be seeping into the aquifer, contributing to the increase in groundwater salinity.

Sub-basin 2 (between rivers Pavanje and Gurupur) exhibits a complete change in the trend of river flow rate into and out of the aquifer system. In this case, (fig.4.21) greater river flow into the aquifer (30,469 m³/day) is observed during monsoon season. It is also established that river Gurupur contributes significantly to the aquifer due to the fact that, the area surrounding the river is a low lying area.

The bar chart representing sub-basin 3 (fig.4.22), which is also associated with river Gurupur (southern bank) and northern bank of river Nethravathi shows river flow of 67,965 to 1,18,405 m³/day into the aquifer. The bar chart representing sub-basin 4 (fig.4.23) shows a constant rate of river flow into the aquifer (approx.10,000 m³/day), which is mainly due to river Nethravathi, which is a major river of the region.

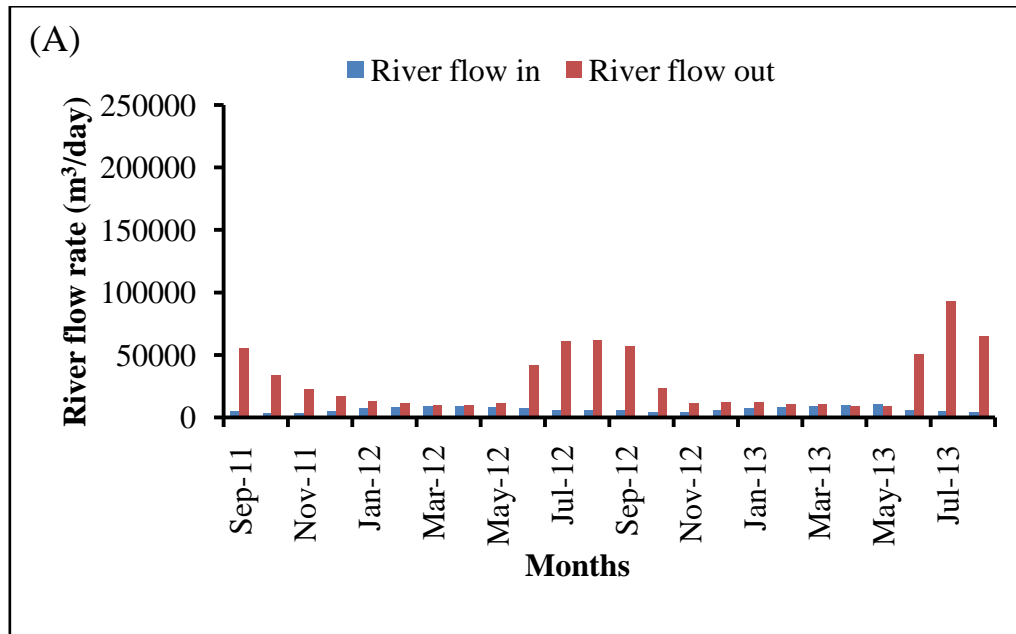


Fig.4.20 River flow rate during the calibration period (2011-13) in sub-basin 1

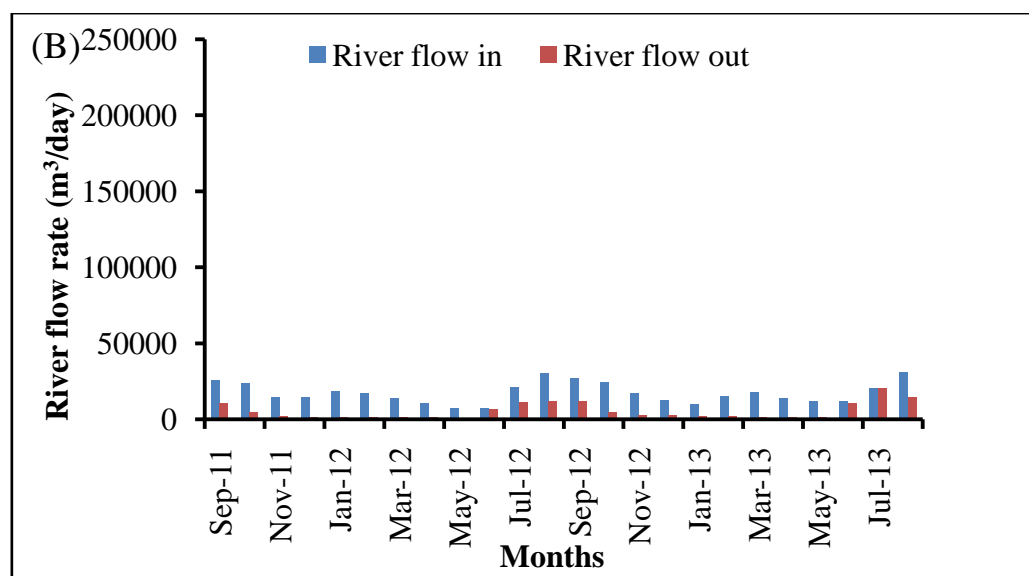


Fig.4.21 River flow rate during the calibration period (2011-13) in sub-basin 2

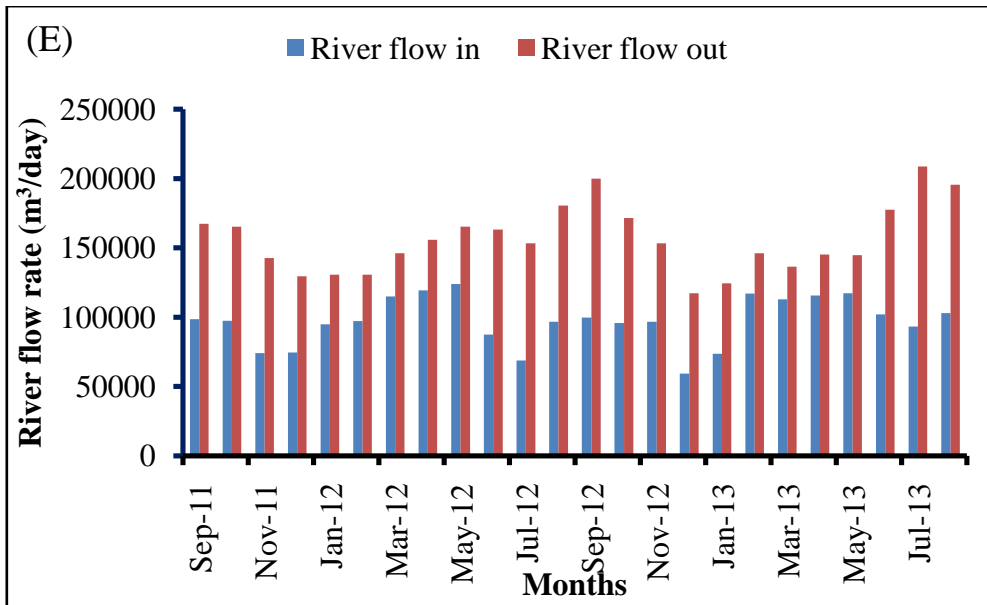


Fig.4.22 River flow rate during the calibration period (2011-13) in sub-basin 3

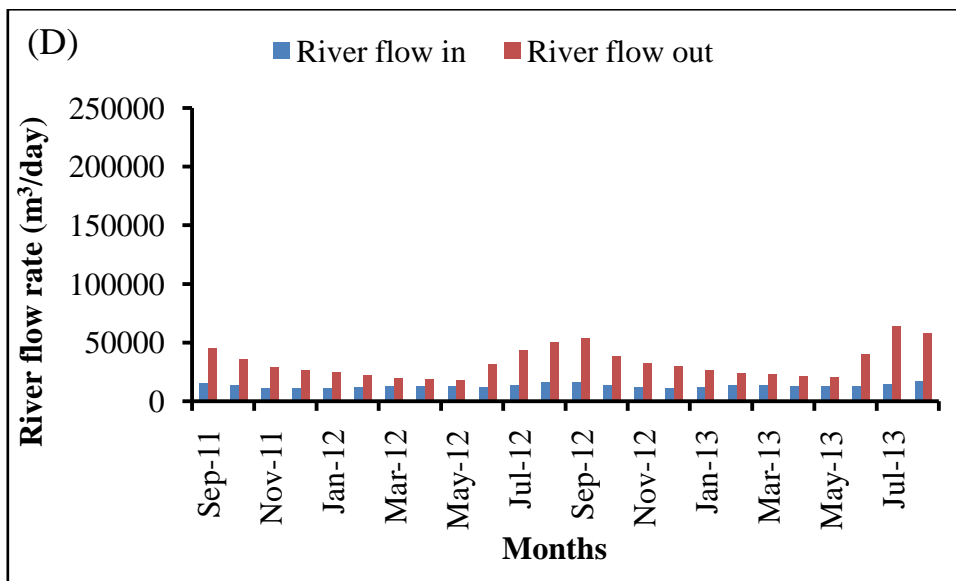


Fig.4.23 River flow rate during the calibration period (2011-13) in sub-basin 4

4.8 SENSITIVITY ANALYSIS

4.8.1 General

Since the intense database used in a groundwater model requires considerable scrutiny of appropriateness of parameters, sensitivity analysis is an essential part of modeling applications (Ting et al., 1998). The sensitivity analysis quantifies the uncertainty in estimating aquifer parameters, stresses and boundary conditions in a calibrated model (Senthil Kumar and Elango, 2004). In the present study, the flow and transport parameters are systematically varied within appropriate ranges and applied in the model to learn their influence on the model results. The sensitivity of the water table to a particular parameter in the calibrated solution is assessed in the model output.

4.8.2 Methodology

In the present study, the sensitivity analysis is carried out by two methods. The first method is applied to demonstrate the zone-wise model sensitivity and the second method is employed to show the model sensitivity as put forth by the observation wells. In the first method, the parameters and stresses are decreased and increased by 25%, 50% and 75% each in the calibrated model applicable for all sub-basins. The mean absolute error (MAE) between the simulated and observed groundwater heads is calculated for all the set of results obtained for the changed parameter values as well as that for the calibrated parameters. A dot graph of mean absolute error (MAE) against the percentage increase and decrease in the parameter is plotted (Palma and Bentley, 2007) to compare their effect on the model. This analysis is performed on all 29 observation well data individually.

In the second method, each of the hydraulic conductivity, specific yield and recharge rate are increased and decreased by 25%, 50% and 75% in the calibrated model of all the sub-basins. Meanwhile, the sensitivity here is expressed by a dimensionless index SI, which is the ratio of the relative (absolute) change of model output $|\Delta y|/y_0$ and the relative change of an input parameter $\Delta x/x_0$, i.e. $SI = (|\Delta y|/y_0) / (\Delta x/x_0)$ (Lenhart et al., 2002; Arlai et al., 2006). The calculated sensitivity indices are ranked into four

classes, as shown in table 4.11 and this ranking is used to assess the calculated sensitivities.

Table.4.11 Ranking of sensitivity classes (Lenhart et al., 2002)

Class	Index	Sensitivity
I	$0.00 \leq I \leq 0.05$	Small to neglect
II	$0.05 \leq I \leq 0.20$	Medium
III	$0.20 \leq I \leq 1.00$	High
IV	$ I \geq 1.00$	Very high

4.8.3 Results and discussion

The hydraulic conductivity, specific yield, recharge rate and the river bed conductance values, which are known to have significant impacts on the simulated heads are tested for sensitivity. Since the sensitivity analysis was very exhaustive, the dot graph of MAE versus percentage change in the flow parameters and hydrological stresses for one zone each in all the four sub-basins are shown in figures 4.24 to 4.27. The table representing the statistical results of sensitivity classes for each observation well are presented in Appendix-1. The plot of sensitivity index as a function of percentage change in hydraulic conductivity, specific yield and recharge rate for well no.4 is shown in fig.4.28.

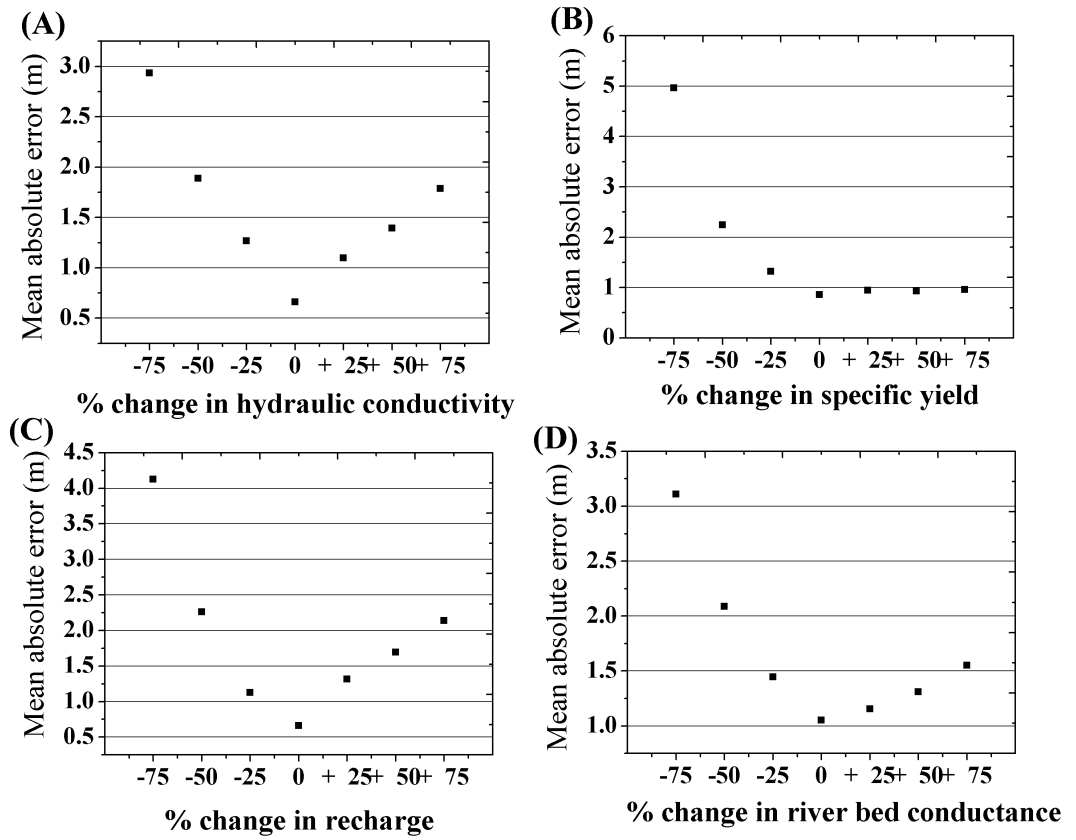


Fig.4.24. Dot plot for zone 7 of sub-basin 1 considering (A) hydraulic conductivity (B) specific yield (C) recharge (D) river bed conductance

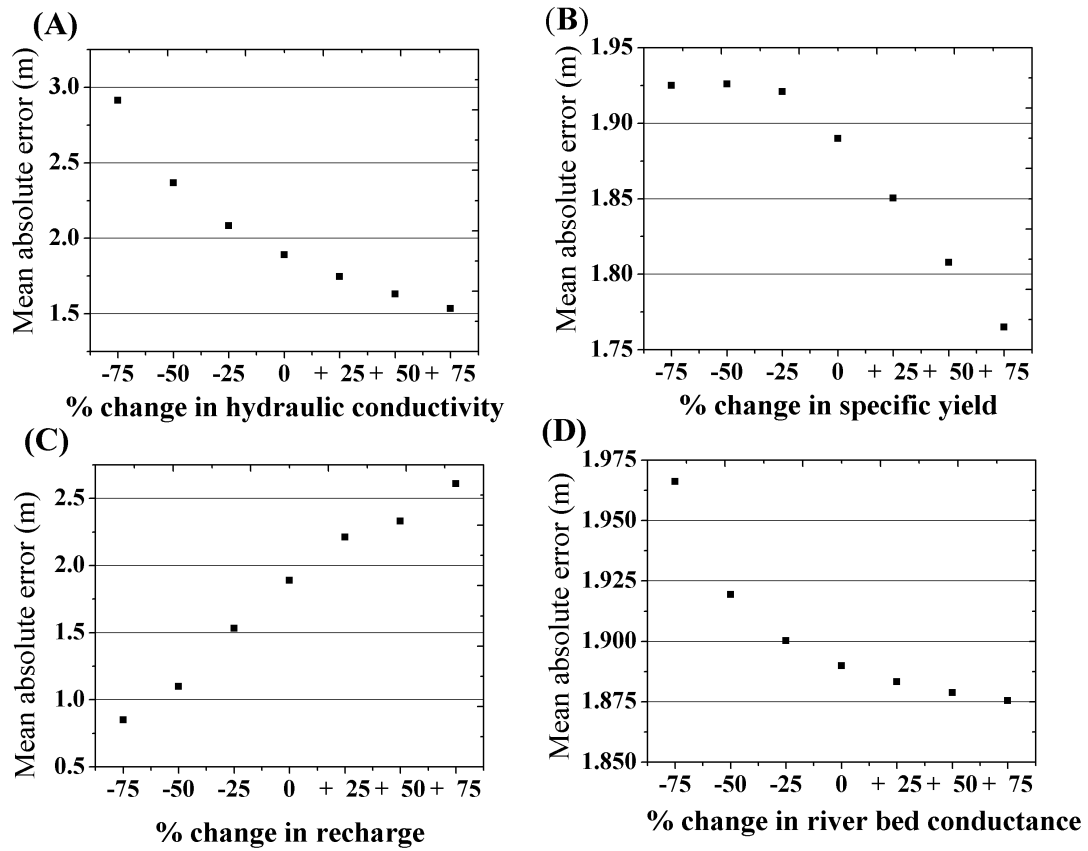


Fig. 4.25. Sensitivity analysis for zone 4 of sub-basin 2 considering (a) hydraulic conductivity; (b) specific yield; (c) recharge; (d) river bed conductance

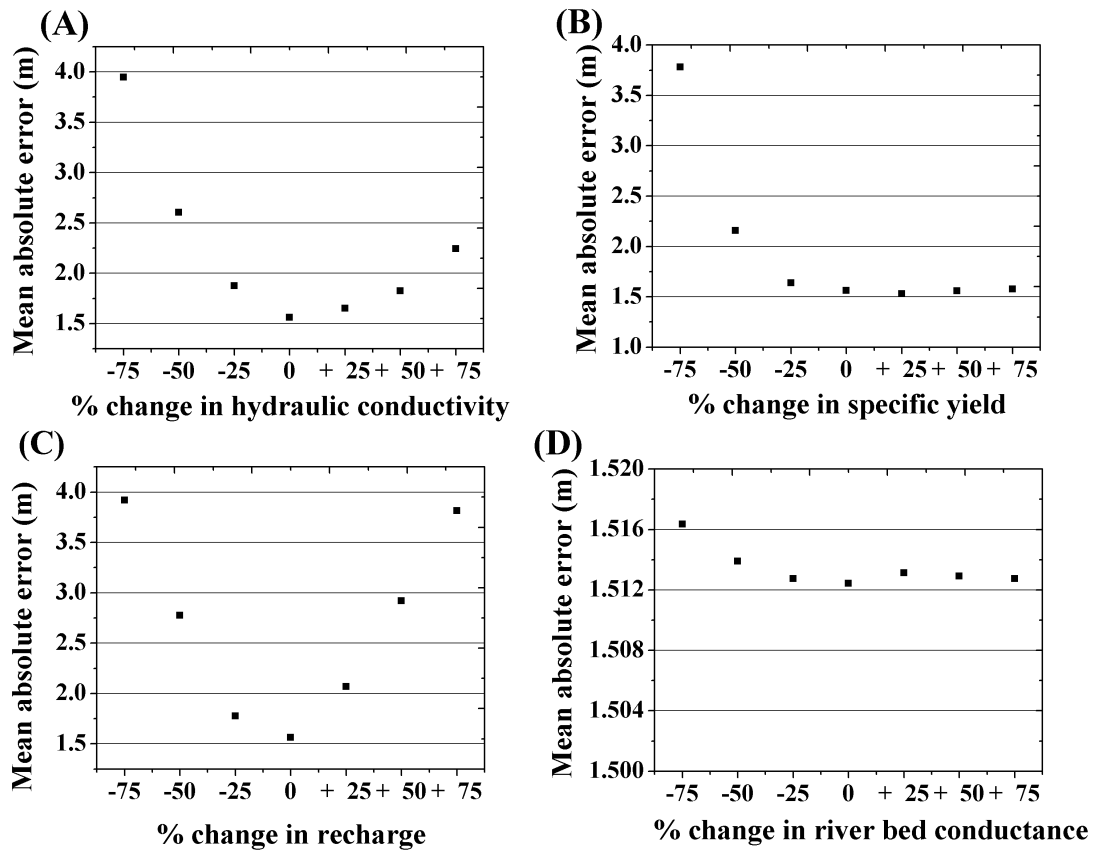


Fig. 4.26 Sensitivity analysis for zone 5 of sub-basin 3 considering (a) hydraulic conductivity; (b) specific yield; (c) recharge; (d) river bed conductance

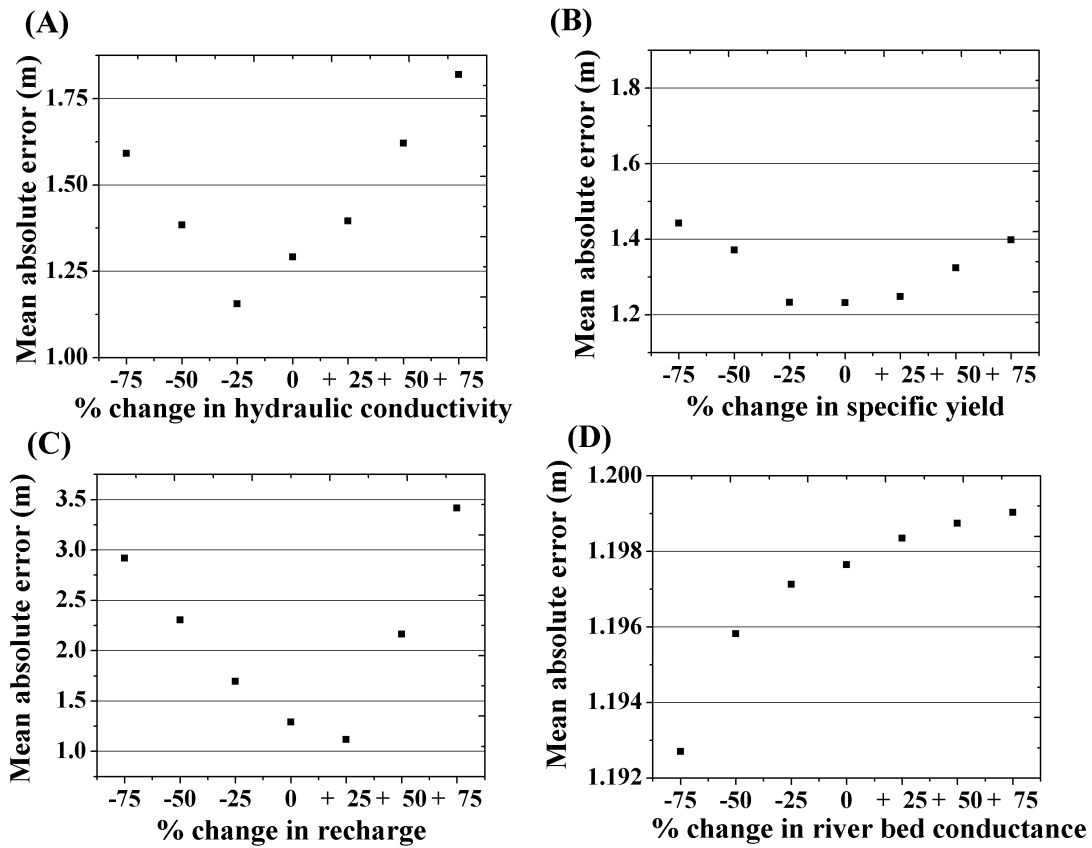


Fig. 4.27 Sensitivity analysis for zone 7 of sub-basin 4 considering (a) hydraulic conductivity; (b) specific yield; (c) recharge; (d) river bed conductance

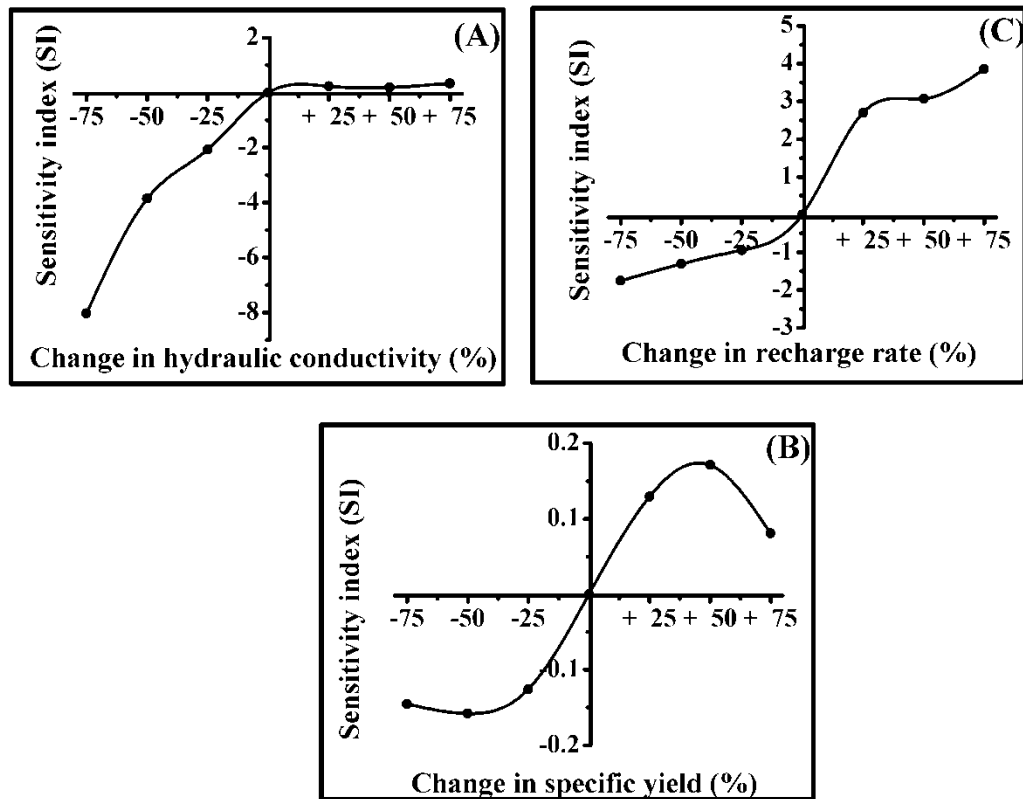


Fig. 4.28 Plot of sensitivity index (SI) as a function of percentage change in (A) hydraulic conductivity (B) specific yield and (C) recharge rate

4.8.3.1 Parameter sensitivities

An attempt is made to analyse the sensitivity of the aquifer system to two important input parameters namely hydraulic conductivity and specific yield in the zones of the study area where the observation wells exist.

Hydraulic conductivity

It is found that, small percentage of change in hydraulic conductivity causes a considerable change in the hydraulic head all through the study. Hence, it may be considered as the most sensitive parameter in the analysis. But, when the sensitivity of the hydraulic conductivity is analysed in detail with respect to each zone, it was found that, zone5 in sub-basin 1, 9 and 1 in sub-basin 2, 5 and 4 in sub-basin 3 and zones 8 and 9 in sub-basin 4 react less to the change in hydraulic conductivity in comparison

to the other zones of the study area. This may be because, the observation wells representing these zones are located adjacent to the rivers and the results are likely to be influenced by the difference between river water elevation and the water table. The lesser the difference, lesser will be the sensitivity of the parameter. The sensitivity indices are higher for lower values of hydraulic conductivity than to higher values. Hence, it is understood that, the model is sensitive to lower values of hydraulic conductivity than to higher values (fig.4.28 A). Accordingly, the area with well numbers 7, 14, 15, 22, 24, 25 and 29 which are beside the river boundary can be categorised into sensitivity class I and II with small to medium model sensitivity to hydraulic conductivity. The rest of the area comes under the high and very high sensitivity class (III and IV).

Specific yield

It is learnt that, the system barely reacts even to large changes in specific yield in sub-basins 2 and 4, hence may be considered as the insensitive parameter. However, it was observed that, the water table shows a considerable rise in most of the zones only when the specific yield is decreased by 75%. For example, in sub-basin 1 - zone numbers 5 and 7; in sub-basin 3 - most of the zones (4, 5, 6 and 7) are showing this characteristic. This behaviour of the aquifer system could be due to the river that traverses into these two sub-basins (1 and 3) with dense river network which are absent in the other two sub-basins (2 and 4). The sensitivity ranking method also agrees that, the sub-basins 2 and 4 are insensitive to the specific yield. Whereas, the aquifer system of sub-basin 3 responds unevenly to the changes in the specific yield values. However, sub-basin 1 and wells that are close to the river boundary are sensitive to lower values of specific yield. Therefore, specific yield is a sensitive parameter in sub-basins 1 and 3, whereas, highly insensitive in sub-basins 2 and 4 (Fig.4.28 B).

4.8.3.2 Aquifer sensitivity to the hydrological stresses

The sensitivity of the system to the applied hydrological stresses, namely areal recharge rate and river bed conductance are analysed by conducting a similar exercise with an increase and decrease in the calibrated parameter values.

Recharge rate

The areal recharge due to precipitation considered in the present study was found to be the most sensitive parameter. The recharge rate has a considerable effect on the system in areas with a shallow water table. It was found that, due to the lateral inflow in zones (zone 5 in sub-basin 1, zone 9 and 1 in sub-basin 2, zone 5 and 4 in sub-basin 3 and zone 9 and 8 in sub-basin 4) near the recharging rivers, the effect of rainfall recharge was reduced. The sensitivity class of the model due to recharge rate can be categorised into III and IV, with sensitivity index increasing beyond 0.20 and 1.00 over the entire aquifer. Also, the model is extremely sensitive to the higher values of recharge rate as compared to lower values (fig.4.28 C). Well number 15, which is very close to the river boundary, has a minor effect due to change in recharge rate.

River leakage

There was no significant influence of river bed conductance on the water table elevation except in sub-basin 1. The sub-basin 1 is smallest among all the sub-basins with dense river network. The influence of river bed conductance on the water table is exceptionally notable here. However, zone 9 in sub-basin 2 which is adjoining the river Gurupur, is more susceptible to river bed conductance. This may be because of higher discharge in the river, with river stage attaining a height of 3.40 m above sea level (13 year average) in the month of July. Additionally, clay layer was found in the area at relatively shallow depths.

4.9 CLOSURE

Increasing demand for freshwater along the seacoast stresses the need for better management of freshwater resources. The numerical groundwater simulation using MODFLOW is carried out for effective assessment of groundwater resources in a tropical, coastal aquifer. The study is focused on a shallow, lateritic, unconfined aquifer, with good groundwater potential. This kind of study gives useful insights into the coastal processes and river–aquifer interactions, with quantitative estimates.

The calibration results are analysed for consistency using graphical as well as analytical methods. As per the analysis, there exists a reasonably good correlation (R^2

= 0.60 to 0.99) between the simulated and observed water levels, except for the monsoon months. The RMSE and NSE (≥ 0.5) values also follow the same tendency. However, the summer months give good results, which are more critical for the investigation on seawater intrusion. Thus, the model illustrates the importance of seasonable variability throughout the year because, things change dramatically between the seasons.

After successful calibration, recharge co-efficient of 20% of rainfall, porosity of 30% and river bed conductance of 10 m/day are obtained as suitable parameters. The calibrated values of various hydraulic properties of the aquifer are within the range established by the earlier studies. Also, the values of horizontal hydraulic conductivity and specific yield of the unconfined aquifer is estimated to be in the range 1.85m/day to 49.5 m/day and 0.006 to 0.281 respectively. The model is also validated with reasonable accuracy ($R^2 > 0.70$) for future applications.

The water budget analysis confirms the accuracy of the model and reveals the water movement strategy and the volume of water exchange across the aquifer the boundaries. The water budget study also reveals the possible saltwater intrusion into the low lying areas during the dry periods. The river-aquifer interaction study carried out in the present work indicates that, a good amount of river water is lost into the sea throughout the year, expect for the river Gurupur which is surrounded by low lying and marshy area.

The results of sensitivity analysis clearly shows that, the overall aquifer system is sensitive to hydraulic conductivity and recharge rate. The model is sensitive to lower values of hydraulic conductivity and higher values of recharge rate. The results also show that, specific yield is a sensitive parameter for sub-basin 1 and 3 and insensitive over the rest of the area. Also, it is observed that, the lateral movement of water from the river causes the adjoining area to respond differently to changes in the parameters than away from it. No significant influence of river bed conductance on the water table elevation was noticed over in the entire area except that in sub-basin 1 and zones adjacent to the river flow.

SOLUTE TRANSPORT MODEL

5.1 GENERAL

The modeling of variable density groundwater flow and solute transport in a coastal aquifer system is an intricate process in comparison with the regular solute transport modeling. This is due to the fact that large density variations in the saline groundwater arise due to the non-uniform distributions of highly concentrated solutes in the coastal aquifers. This density variation also has an effect on the groundwater flow movement. In the constant-density groundwater flow and solute transport modeling, the flow is not affected by the subsequent concentration of the transport equation. For variable density flow and transport, the groundwater flow equation and the solute transport equation are coupled with each other by an equation of state for the density as a function of the solute concentration.

In the past few decades, solutions to these complex governing equations are sought using numerical techniques [(SUTRA code (Voss, 1984), HST3D code (Kipp, 1986), SEAWAT (Guo and Bennett, 1998) and MOCDENS3D (Essink, 1998)] that enables in-depth three dimensional modeling of freshwater-seawater interactions. SEAWAT model is extensively used by researchers all over the world to explore both hypothetical and site specific cases (Chang and Clement, 2013; Praveena et al., 2011; Vandenbohede et al., 2014; Cobaner et al., 2012; Lin et al., 2009; Gates et al., 2002; El-Kadi et al., 2014; Qahman and Larabi, 2006; Bauer et al., 2006) to assess the sustainable use of groundwater resources in the coastal aquifers and predict the freshwater–saltwater interface. In the present investigation, SEAWAT package is used for solute transport modeling.

5.2 CONCEPTS AND PRINCIPLES OF SEAWAT

5.2.1 Basic description of the model

SEAWAT is a coupled version of MODFLOW (Harbaugh et al., 2000) and MT3DMS (Zheng and Wang, 1999; Zheng, 2006) designed to simulate three dimensional, variable-density ground-water flow and multi-species transport. The coupling is necessary in order to account for the effects of density differences due to mixing of high salt concentrations in seawater with freshwater in the coastal groundwater system. The Variable-Density Flow (VDF) process in SEAWAT is based on the constant-density Ground-Water Flow (GWF) process of MODFLOW-2000. The VDF process uses the familiar and well established MODFLOW methodology to solve the variable-density ground-water flow equation (Langevin et al., 2003). The MT3DMS (A Modular Three Dimensional Multispecies Transport Model) which is a part of SEAWAT, referred to as the Integrated MT3DMS Transport (IMT) Process, solves the solute transport equation. Both the flow and transport equations are solved during one SEAWAT time step.

However, the MODFLOW is modified in the SEAWAT version, in a way that fluid mass is conserved instead of fluid volume and the Darcy's equation is solved to obtain the variable density flow in terms of an equivalent freshwater head. The Darcy's law which describes the fluid flow in the porous medium and the equations of continuity that relates the fluid mass conservation and solute advection–diffusion are solved simultaneously in the process.

In MT3DMS, MT3D stands for the Modular 3-Dimensional Transport model, and MS denotes the Multi-species structure for accommodating add-on reaction packages. It is based on the assumption that changes in the concentration field will not affect the flow field significantly (Zheng and Wang, 1999). MT3DMS computer program uses a modular structure similar to MODFLOW (McDonald and Harbaugh, 1988) and consists of a main program and a large number of highly independent subroutines, called modules, which are grouped into a series of “packages.” The MT3DMS packages deals with a single aspect of the transport simulation. The transport packages used in the present study are listed in table 5.1 with a brief description of

their operation. The solution scheme of third order TVD (ULTIMATE) is used in advection package and modified incomplete Cholesky pre-conditioner is used in GCG (Generalized Conjugate Gradient) solver in the current transport simulation.

Table. 5.1 The MT3DMS packages used for transport simulation in the study

Package name	Description	Reference
Basic transport (BTN)	Handles basic tasks that are required by the entire transport model. Among these tasks are definition of the problem, specification of the boundary and initial conditions, determination of the step size, preparation of mass balance information, and printout of the simulation results.	Zheng and Wang (1999)
Flow Model Interface (FMI)	FMI Interfaces with a flow model. The FMI package prepares heads and flow terms in the form needed by the transport model.	Zheng and Wang (1999)
Generalized Conjugate Gradient Solver (GCG)	If the GCG solver is selected, dispersion, sink/source, and reaction terms are solved implicitly without any stability constraints.	Zheng and Wang (1999)
Advection (ADV)	Solves the concentration change due to advection with an explicit scheme or formulates the coefficient matrix of the advection term for the matrix solver.	Zheng and Wang (1999)
Dispersion (DSP)	Solves the concentration change due to dispersion with the explicit finite difference method.	Zheng and Wang (1999)
Source/Sink Mixing (SSM)	Solves the concentration change due to sink/source mixing explicitly or formulates the coefficient matrix of all sink/source terms for the matrix solver.	Zheng and Wang (1999)
Utility (UTL)	Contains utility modules that are called upon by primary modules to perform such general-purpose tasks as input/output of data arrays.	Zheng and Wang (1999)

5.2.2 Generalized program structure of SEAWAT

The mixing of saltwater in coastal aquifer system is a complex process due to the non-uniform distribution of high concentration solute. Due to this increased concentration of solute, large density variation arise in the saline groundwater, which in turn affects the flow of groundwater in coastal aquifers. Hence, in the variable-density flow and transport, the groundwater flow equation and the solute transport equation are coupled with each other by an equation of state for the density as a function of the solute concentration. The simulation is less complicated in the constant-density groundwater flow and solute transport modeling as the flow is unaffected by the consequent concentration solution of the transport equation.

SEAWAT is one of the widely used codes to simulate saltwater intrusion (Werner et al., 2013). The generalized flow chart of the SEAWAT program is replicated in fig.5.1. Here, the coupling between flow and transport is performed through a synchronous time stepping approach that cycles between MODFLOW solutions of the flow equation and MT3DMS solutions of the transport equation using an iterative computational process.

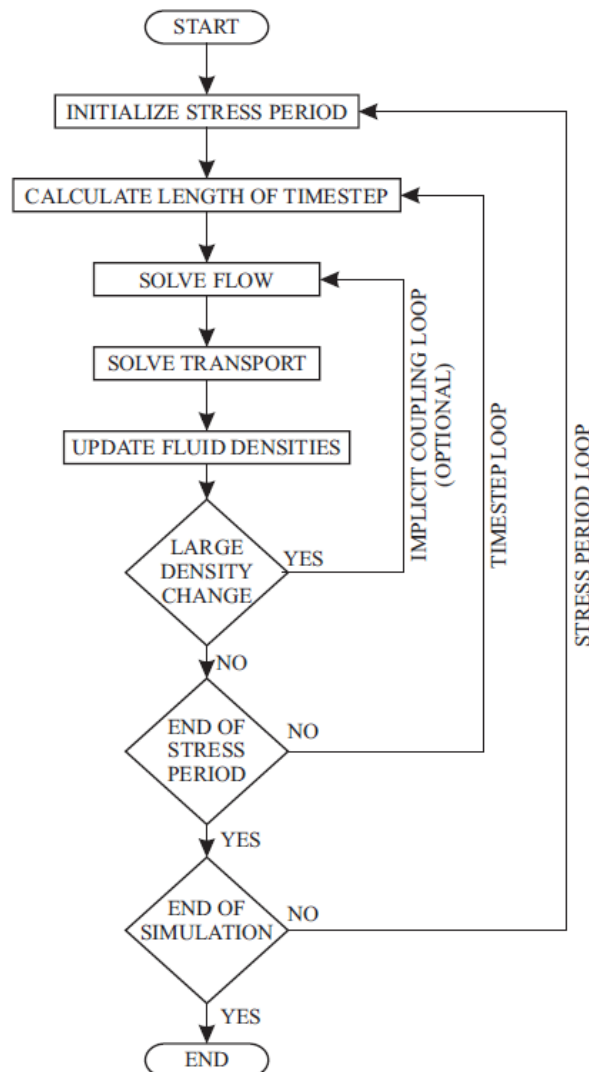


Fig.5.1 Generalized flow chart of SEAWAT program (Guo and Langevin, 2002)

5.2.3 The concept of equivalent fresh water head

The SEAWAT model is developed on the concept of equivalent fresh water head. This concept is considered due to the fact that, the saltwater-freshwater interface is the region where non-uniform fluid densities exist because of different saltwater concentrations. Hence, all the equations are written in terms of equivalent freshwater head (h_f), whose effective value depends on the local variable density at the location. This concept is better understood with a simple experimental setup, (fig.5.2) as explained by Guo and Langevin (2002).

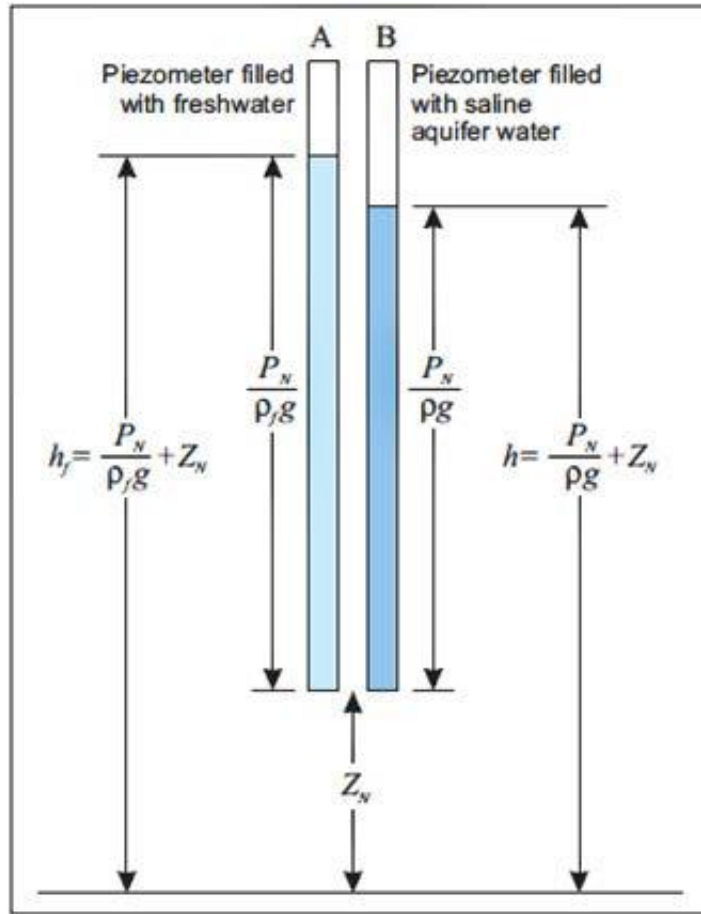


Fig.5.2 Experimental setup to illustrate the concept of equivalent freshwater head (Guo and Langevin, 2002).

This setup consists of two piezometers open to a given point N in an aquifer, containing saline water. The piezometer A contains freshwater and is equipped with a mechanism that prevents saline water in the aquifer from mixing with freshwater. The piezometer B contains water identical to that present in the saline aquifer at point N . The elevation of the water level in piezometer A above the datum is the freshwater head at point N , given by

$$h_f = \frac{P_N}{\rho_f g} + Z_N \quad (5.1)$$

Where

h_f = the equivalent freshwater head [L], P_N =the pressure at point N [$ML^{-1}T^{-2}$],

ρ_f = the density of freshwater [ML^{-3}], g = the acceleration due to gravity [LT^{-2}] and

Z_N = the elevation of point N above datum [L].

The equivalent saltwater head expressed in terms of saline aquifer is the level in piezometer B above datum, given by

$$h_f = \frac{P_N}{\rho g} + Z_N \quad (5.2)$$

Where

h = head [L], ρ = the density of saline groundwater at point N [ML^{-3}].

Equations (5.1) and (5.2) can be expressed in terms of pressure at point N (P_N) and replacing Z_N with a more general datum Z as;

$$P_N = \rho_f g (h_f - Z) \quad (5.3)$$

$$P_N = \rho g (h_f - Z) \quad (5.4)$$

Equating equations (5.3) and (5.4), relation between the total head and equivalent freshwater head and vice versa can be obtained.

$$h_f = \frac{\rho}{\rho_f} h - \frac{\rho - \rho_f}{\rho_f} Z \quad (5.5)$$

$$h = \frac{\rho_f}{\rho} h_f - \frac{\rho - \rho_f}{\rho} Z \quad (5.6)$$

In the SEAWAT model, the equation (5.6) is employed, wherein the total head h appearing in the Darcy equation and the pressure P in the groundwater balance equation are written in terms of the equivalent freshwater head h_f . Thereby, the basic structure of the fundamental equations remains intact allowing use of the MODFLOW software with relatively little modifications as in SEAWAT model.

5.2.4 Governing equation

The governing equation for the variable density flow in terms of freshwater head as per the concept of equivalent freshwater head discussed in section 5.2.3 is expressed as follows (Guo and Langevin, 2002);

$$\begin{aligned} & \frac{\partial}{\partial \alpha} \left\{ \rho K_{f\alpha} \left[\frac{\partial h_f}{\partial \alpha} + \frac{\rho - \rho_f}{\rho_f} \frac{\partial Z}{\partial \alpha} \right] \right\} + \frac{\partial}{\partial \beta} \left\{ \rho K_{f\beta} \left[\frac{\partial h_f}{\partial \beta} + \frac{\rho - \rho_f}{\rho_f} \frac{\partial Z}{\partial \beta} \right] \right\} + \frac{\partial}{\partial \gamma} \left\{ \rho K_{f\gamma} \left[\frac{\partial h_f}{\partial \gamma} + \frac{\rho - \rho_f}{\rho_f} \frac{\partial Z}{\partial \gamma} \right] \right\} \\ & = \rho S_f \frac{\partial h_f}{\partial t} + \theta \frac{\partial \rho}{\partial C} \frac{\partial C}{\partial t} - \bar{\rho} q_s \end{aligned} \quad (5.7)$$

where α, β, γ = orthogonal coordinate axes, aligned with the principal directions of permeability; $K_{f\alpha}, K_{f\beta}, K_{f\gamma}$ = equivalent freshwater hydraulic conductivities in the three coordinate directions, respectively [LT⁻¹]; ρ = fluid density [ML⁻³]; ρ_f = density of freshwater [ML⁻³]; h_f = equivalent freshwater head [L]; Z = elevation above datum of the centre of the model cell [L]; S_f = equivalent freshwater specific storage [L⁻¹]; θ = effective porosity [dimensionless]; C = solute concentration [ML⁻³]; $\frac{\partial \rho}{\partial C}$ = density of water entering from a source or leaving through a sink [ML⁻³]; q_s = volumetric flow rate of sources or sinks per unit volume of aquifer [T⁻¹] and t = time [T]. The preconditioned conjugate-gradient (PCG2) package is used to solve the flow equation.

The solute mass is transported in porous media by the flow of groundwater (advection), molecular diffusion, and mechanical dispersion. MT3DMS is used to solve the solute transport in groundwater by the SEAWAT code with the following partial differential equation (Zheng and Bennett, 2002):

$$\frac{\partial C}{\partial t} = \nabla \cdot (D \cdot \nabla C) - \nabla \cdot (\vec{v} C) - \frac{q_s}{\theta} C_s + \sum_{k=1}^N R_k \quad (5.8)$$

where, D = hydrodynamic dispersion coefficient [L²T⁻¹]; ν = fluid viscosity [LT⁻¹]; C_s = solute concentration of water entering from sources or leaving through sinks [ML⁻³] and $R_k (k=1, 2, \dots, N)$ = rate of solute production or decay in reaction k of N different reactions [ML⁻³T⁻¹].

For a coupled variable density flow and solute transport simulation, fluid density is assumed to be a function only of solute concentration and the effects of pressure and temperature on fluid density are ignored (Langevin et al., 2003). A linear equation of state is used by the SEAWAT to convert solute concentration to fluid density as:

$$\rho = \rho_f + \frac{\partial \rho}{\partial C} C \quad (5.9)$$

where, $\frac{\partial \rho}{\partial C}$ = slope of the equation, whose value is entered by the user and depends on the units used for the simulation. For example, in the present simulation, the concentration and density of seawater are defined as 35 kg/m³ and 1025 kg/m³ respectively. The freshwater is considered as the reference fluid with zero concentration and density equal of 1000 kg/m³. Therefore, the value of $\frac{\partial \rho}{\partial C}$ is set to 0.7143, which is approximately the change in fluid density divided by the change in solute concentration for freshwater and seawater. The solution scheme of third order TVD (ULTIMATE) is used in advection package. The limitations of the model applicability are stated in the SEAWAT-2000 documentation (Langevin et al., 2003).

5.3 APPLICATION TO THE STUDY AREA

5.3.1 Similarity with the groundwater flow model

The SEAWAT model entails the MODFLOW model within its basic conceptual model structure. In fact, the SEAWAT model is developed by incorporating the transport parameters through the MT3DMS model and density parameters to the originally developed groundwater flow model. Thereby, the structure of both these models are learnt to be identical. Hence the SEAWAT model setup for the study area as executed in GMS (Groundwater modeling system) software is directly reliant on that of the groundwater flow model (MODFLOW) set-up presented in Chapter 4. Hence, the comprehensive description of SEAWAT model development is omitted in this chapter. In this context, it is also important to note that the domain discretization, hydrologic sources and sinks and boundary conditions as adopted for the constant density model as described in section 4.4 (chapter 4) are incorporated in the SEAWAT model during the simulation of transient dynamics of the saltwater-freshwater interface in the study area.

5.3.2 Boundary conditions

SEAWAT model in fact, requires the concentration of total dissolved solids (TDS) which determines the density of the saline fluid, rather than the chloride concentrations. Hence, total dissolved solid (TDS) is used as an indicator of salinity

(Langevin and Zygnerski, 2013; Qahman and Larabi, 2006 and Cobaner et al., 2012) in the solute transport model.

Apart from the boundary conditions assigned to the conceptual groundwater flow model described in section 4.4.4 (chapter 4), additional boundary conditions also have to be applied for the resolution of the solute transport equation in the model domain. The first one is the Dirichlet boundary condition with constant concentration (TDS) of 35 kg/m^3 to seawater is specified to the model cells along the western boundary (Arabian sea). The second one is the Neumann boundary condition assigned to the rivers with a TDS values of 35 kg/m^3 during non-monsoon (October to May) months. The TDS value of 17.5 kg/m^3 is considered during monsoon (June to September) considering the quantum of mixing of freshwater and seawater as per the guidelines given by Lin et al. (2009). This value is assigned to account for the salinity carried by the backwater flow from the sea. Also, the field studies conducted by Harshendra (1991) have shown that, the chloride concentration of river water is enormously high starting from October as compared with the period from June to September. The salinity introduced due to the infiltration of contaminant water from the rainfall recharge is neglected, due to its very little effect compared to the seawater intrusion.

5.3.3 Initial conditions

The TDS is one of the indicators of salinity in solute transport model. The measured TDS in the observation wells during September 2011 is interpolated for each of the sub-basins using ArcGIS 9.3 to obtain the spatial distribution of TDS concentration. This is assigned to each cell as initial concentration for the transport model.

5.3.4 Transport and density parameters

In addition to the aquifer parameters, the solute transport parameter, namely the hydrodynamic dispersivity is essential in solving the solute transport equation (5.8). This is initially assigned as per available data which are adjusted by trial and error method at the time of model calibration. As per Fetter (2000), the longitudinal dispersion is much larger than the transversal dispersion for transport simulations. Also, the horizontal transverse dispersivity of $1/10^{\text{th}}$ of the longitudinal dispersivity is suggested by Cobaner et al., (2012). The longitudinal dispersivity values ranging

between 15 to 150m is arrived at by Bhosale and Kumar (2001) under similar aquifer conditions, which is used as a range for calibration process. The molecular diffusion is an insensitive parameter and it can be ignored in the salinity calibration (Langevin et al., 2008). The diffusion coefficient used is $8.64 \times 10^{-5} \text{m}^2/\text{day}$.

5.4 MODEL CALIBRATION

5.4.1 Calibration for flow parameters

Since the calibrated aquifer parameters obtained from the MODFLOW model run are directly implemented in the SEAWAT run, it is very important to authenticate the SEAWAT model through calibration. This step is vital to gain assurance in the variable-density flow and transport model results. Here, this is performed by comparing the groundwater head values obtained by the constant density model with that of the variable density model. It was found that the SEAWAT simulates the aquifer system with nearly the same accuracy as that of the MODFLOW. To demonstrate this, the results of both MODFLOW and SEAWAT transient simulation (2011-13) for one of the sub-basins are presented in fig.5.3. It is well understood that, the groundwater head contours of the both the simulation have an almost identical pattern with very slight variation. This statement is true for the rest of the sub-basins, for both steady state and transient simulations. Therefore, no further assessment is carried to validate the SEAWAT.

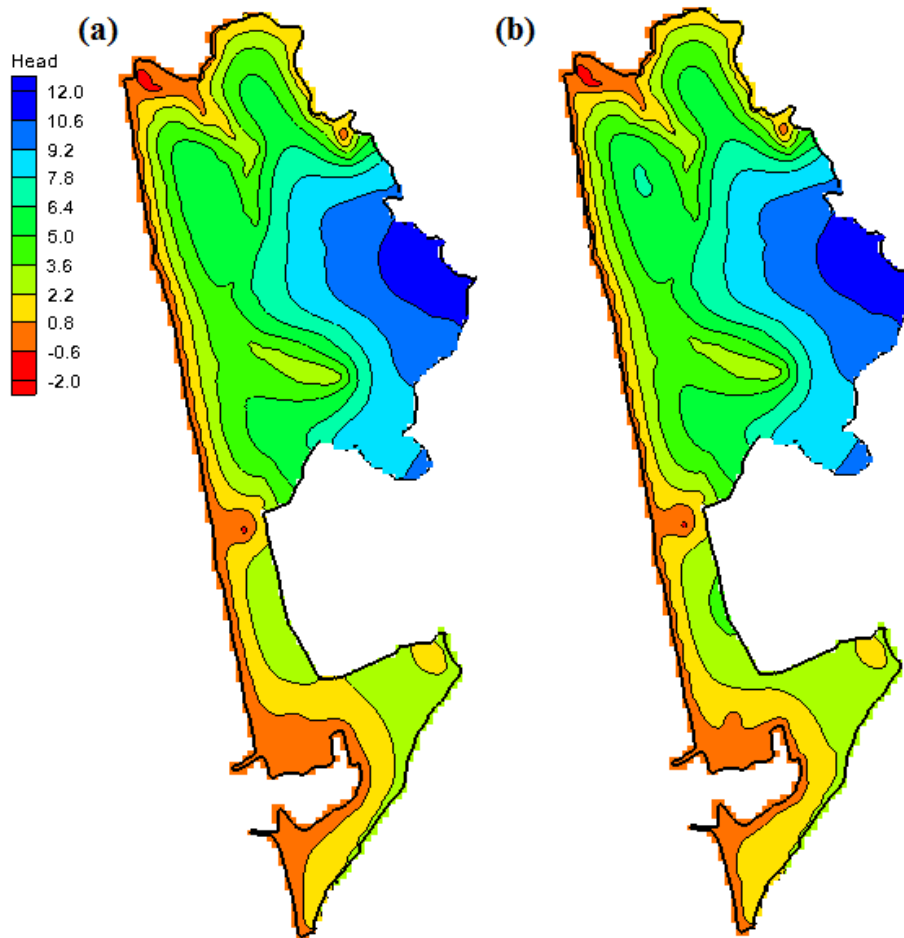


Fig.5.3 Simulated groundwater heads at the end of the transient calibration by (a) MODFLOW and (b) SEAWAT

5.4.2 Calibration for transport parameters

The calibration of transport parameters is performed similar to that of the flow parameters as elaborated in section 4.5 (chapter 4). 29 observations well data (Shivanagouda, 2015) on TDS values measured on fortnightly basis for a period of 2011 to 2013 is used to calibrate the model. However, steady state calibration is not carried out due to non-availability of quality data. Furthermore, the accuracy of the seasonal performance of the solute transport model is also carried out using the same four model evaluation techniques used for the flow model. Apart from the aquifer parameters calibrated in the MODFLOW, the dispersivity parameter is calibrated in the SEAWAT model by varying the values within the range specified in section 5.3.4 by trial and error method.

Transient calibration

The transport parameters obtained after successful calibration are presented in table 5.2. The R^2 , RMSE and NSE values on monthly basis are listed in table 5.3. Table 5.3 shows that, the model performance is satisfactory, as the values are well within the acceptable ranges. Again, similar to that of the flow simulation, the model performance during the monsoon (June to Sept) is not very convincing. It is quite possibly due to the same reasons applicable to that of the MODFLOW simulation. Also, the observed TDS data of wells that are very close to the river or close to both the river and the sea do not match well with the simulated results. This could be because of the complex river-aquifer interaction which is not well addressed by the model due to scarce data in this regard.

The results obtained by the graphical method for selected months of post-monsoon, monsoon and pre-monsoon months for sub-basin 1 and 2 are shown in fig. 5.4 and that for sub-basin 3 and 4 are shown in fig. 5.5. The graphs show a convincingly good agreement with the observed and simulated groundwater heads, except that during the monsoon season. A considerable deviation in TDS value is seen in the plot for the sub-basin 1 even during the pre-monsoon season. It could be possibly due to the behaviour of well no. 25 which surrounds clayey layer with compaction as shown in fig. 1.6. This permits lesser saltwater intrusion into the location than predicted through the model. Hence, observed salinity is less than predicted salinity.

Table 5.2 Solute transport parameters

Parameters	Value
Hydraulic conductivity of river bed material (m/day)	10
Recharge co-efficient (%)	20
Effective porosity (%)	30
Longitudinal dispersivity (m)	35
Transverse dispersivity (m)	3.5
Molecular diffusion co-efficient (m ² /day)	8.64×10^{-5}

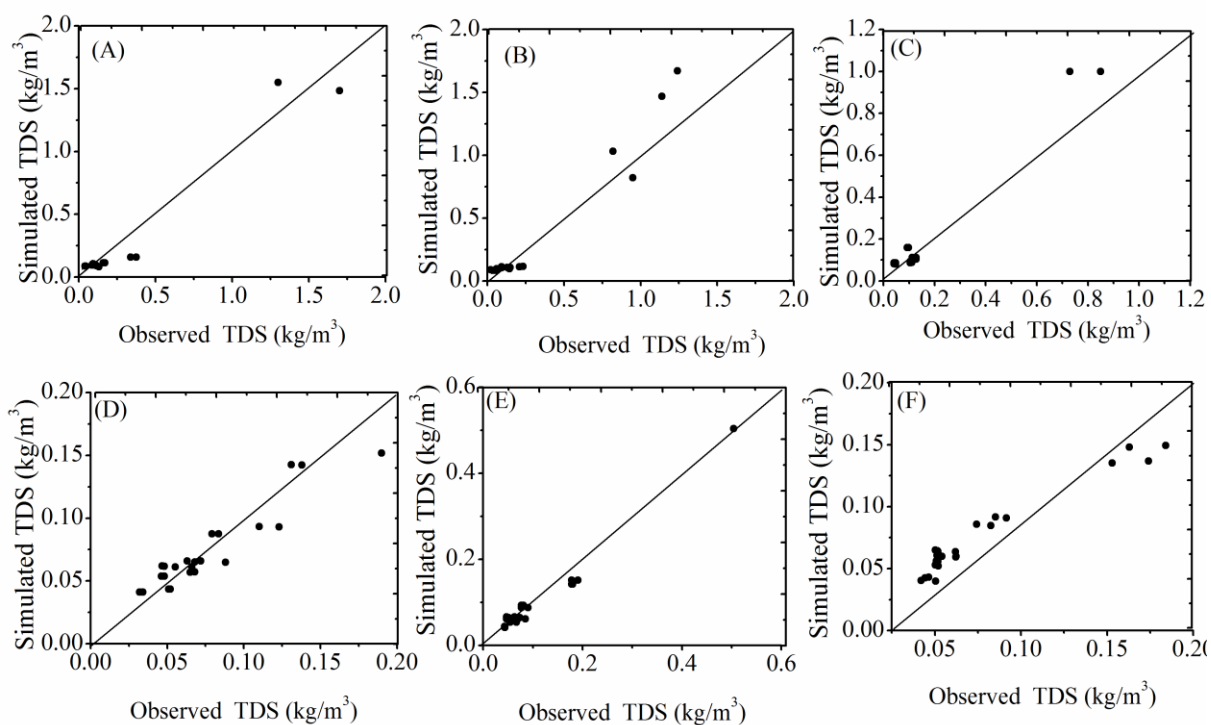


Fig. 5.4 Simulated and observed TDS values (2011-13) during (A) post-monsoon, (B) pre-monsoon and (C) monsoon seasons of sub-basin 1 and that of sub-basin 2 (D), (E) and (F) respectively.

Table 5.3 SEAWAT model efficiency values on monthly basis during 2011-13

<i>SUB-BASIN 1</i>				<i>SUB-BASIN 2</i>				<i>SUB-BASIN 3</i>				<i>SUB-BASIN 4</i>			
Month	R²	RMSE (m)	NSE	Month	R²	RMSE (m)	NSE	Month	R²	RMSE (m)	NSE	Month	R²	RMSE (m)	NSE
Oct	0.851	0.039	0.807	Oct	0.866	0.021	0.807	Oct	0.715	0.050	0.506	Oct	0.864	0.050	0.856
Nov	0.940	0.105	0.941	Nov	0.869	0.021	0.817	Nov	0.649	0.048	0.543	Nov	0.674	0.088	0.673
Dec	0.877	0.177	0.808	Dec	0.921	0.044	0.513	Dec	0.775	0.048	0.773	Dec	0.797	0.148	0.574
Jan	0.988	0.219	0.669	Jan	0.833	0.017	0.824	Jan	0.778	0.048	0.745	Jan	0.792	0.118	0.785
Feb	0.991	0.192	0.946	Feb	0.956	0.086	0.313	Feb	0.697	0.104	0.420	Feb	0.906	0.158	0.887
Mar	0.955	0.141	0.864	Mar	0.643	0.062	0.311	Mar	0.780	0.064	0.776	Mar	0.950	0.200	0.899
Apr	0.961	0.174	0.605	Apr	0.970	0.017	0.787	Apr	0.664	0.054	0.540	Apr	0.810	0.264	0.728
May	0.790	0.226	0.770	May	0.530	0.103	0.554	May	0.792	0.064	0.784	May	0.946	0.257	0.901
Jun	0.881	0.182	0.874	Jun	0.567	0.094	0.217	Jun	0.769	0.077	0.676	Jun	0.826	0.350	0.776
Jul	0.943	0.099	0.801	Jul	0.950	0.013	0.907	Jul	0.759	0.052	0.130	Jul	0.524	0.083	0.415
Aug	0.672	0.071	0.497	Aug	0.943	0.011	0.927	Aug	0.724	0.054	0.213	Aug	0.603	0.062	0.561
Sept	0.677	0.046	0.537	Sept	0.934	0.001	0.931	Sept	0.723	0.056	0.458	Sept	0.560	0.076	0.470

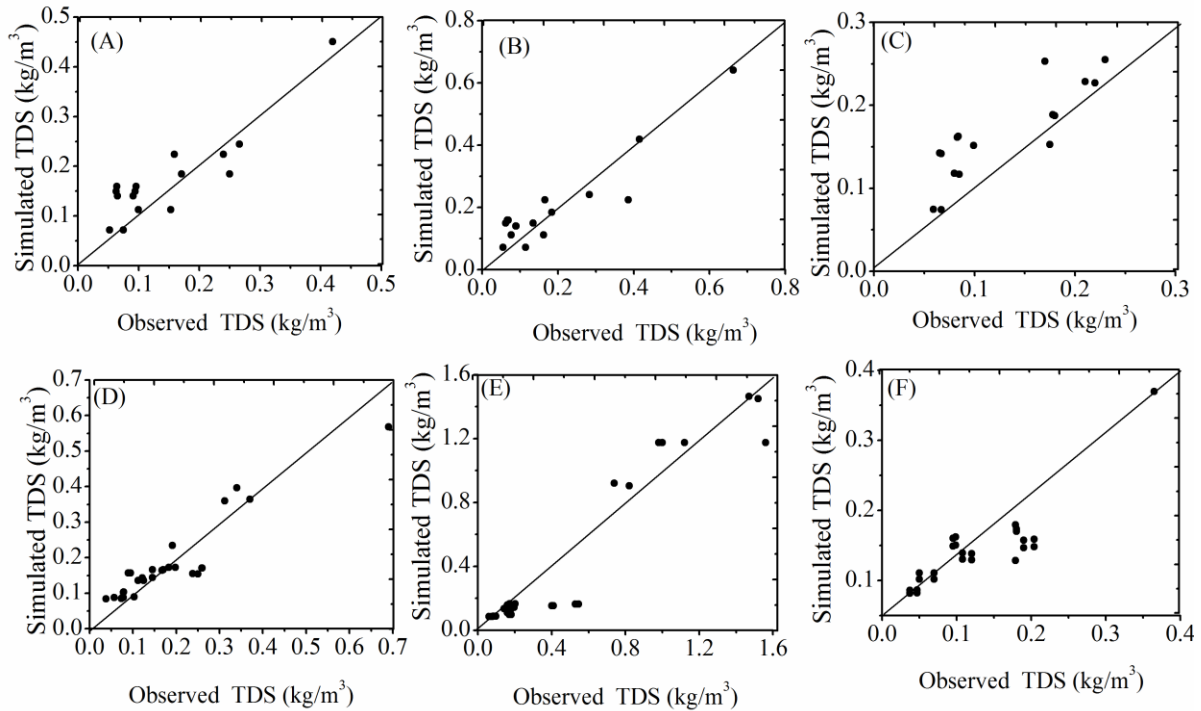


Fig. 5.5 Simulated and observed TDS values (2011-13) during (A) post-monsoon, (B) pre-monsoon and (C) monsoon seasons of sub-basin 3 and that of sub-basin 4 (D), (E) and (F) respectively.

Figs. 5.6 show the plan view of the simulated salinity distribution across the study area for sub-basins 1, 2, 3, 4 during the month of May 2013. From the figures, we can see a similar pattern of salinity distribution in all the four sub-basins. Also, an important point to be noted from these figures is that, the rivers that surround the system on the north and the south sides contribute equally as that of the sea in bringing in salinity into the aquifer. This seems to be more critical in the south of the sub-basin 2, perhaps because of the harbour in the adjoining area.

Another important observation that can be made from these figures is that, the red colour that spreads all over the area indicating a salinity variation from 0 to 3.5 kg/m³. The TDS values are predominantly within 0.5 kg/m³ throughout the year, except that for well nos. 1, 15 and 25 (Shivanagouda, 2015). It is essential to note that, all these

wells are very close to the rivers (less than 300 m). This can be observed in fig.1.2. Well no.1, 15 and 25 are near the rivers Talapady, Gurupur and Pavanje respectively.

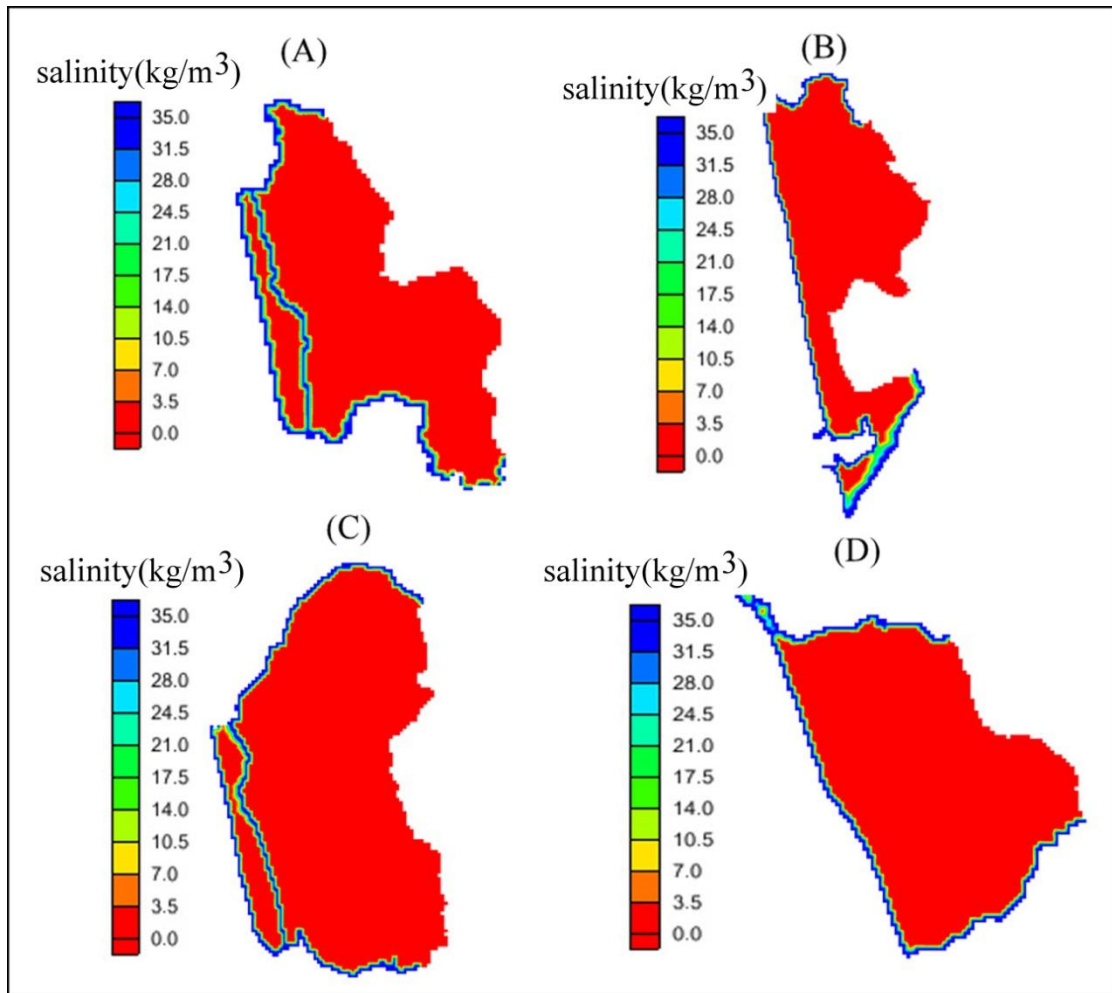


Fig.5.6 Plan view of the simulated salinity distribution in the study area during the month of May 2013

However the progress of salinity ingress towards the landward side during the simulation period in the area does seem to pose a threat to the groundwater quality. To understand the future implications, under various stress scenarios, parametric studies are carried out and are presented in the following chapter.

5.5 MODEL VALIDATION

In order to apply the calibrated solute transport model for future saltwater intrusion scenarios, validation of the model is carried out for a one year period during 2013-14.

However, due to the limited water quality data, data from at least one well each in all the sub-basins obtained from the observation wells maintained by Central Ground Water Board, Govt. of Karnataka and water quality data of 8 wells for sub-basin 3 (Sylus, 2015) on monthly basis are used to validate the model. As per the observation made on all these 12 wells, the salinity level persists within 0.4 kg/m^3 all through the season. Hence, no further scrutiny is done and the model is affirmed validated.

5.6 SENSITIVITY ANALYSIS

The sensitivity analysis has also been carried out to assess the effects of the hydrodynamic dispersion coefficient D on the performance of the density-dependent solute transport. This study is important, since in most cases, the dispersivity value is not known in a real aquifer. The sensitivity analysis of the hydrodynamic dispersion is performed by executing various simulations with 25%, 50% and 75% increase in longitudinal dispersivity values. In such simulations, the horizontal transverse dispersivity of $1/10^{\text{th}}$ of the longitudinal dispersivity is assigned as discussed in section 5.3.4.

The salinity distribution simulated by the SEAWAT for the year 2013 with 25%, 50% and 75% increased values of longitudinal dispersivity are illustrated in the fig.5.7. The movement of the salinity contour is similar all through the coastline and hence only an illustration of a part of coastline is shown in fig.5.7. It could be observed from the figures that, the simulated movement of the seawater intrusion into the landward side shows lesser sensitivity to the dispersivity value. The movement of the farthest salinity contour is as small as 10m for every increase of 25% of the dispersivity values.

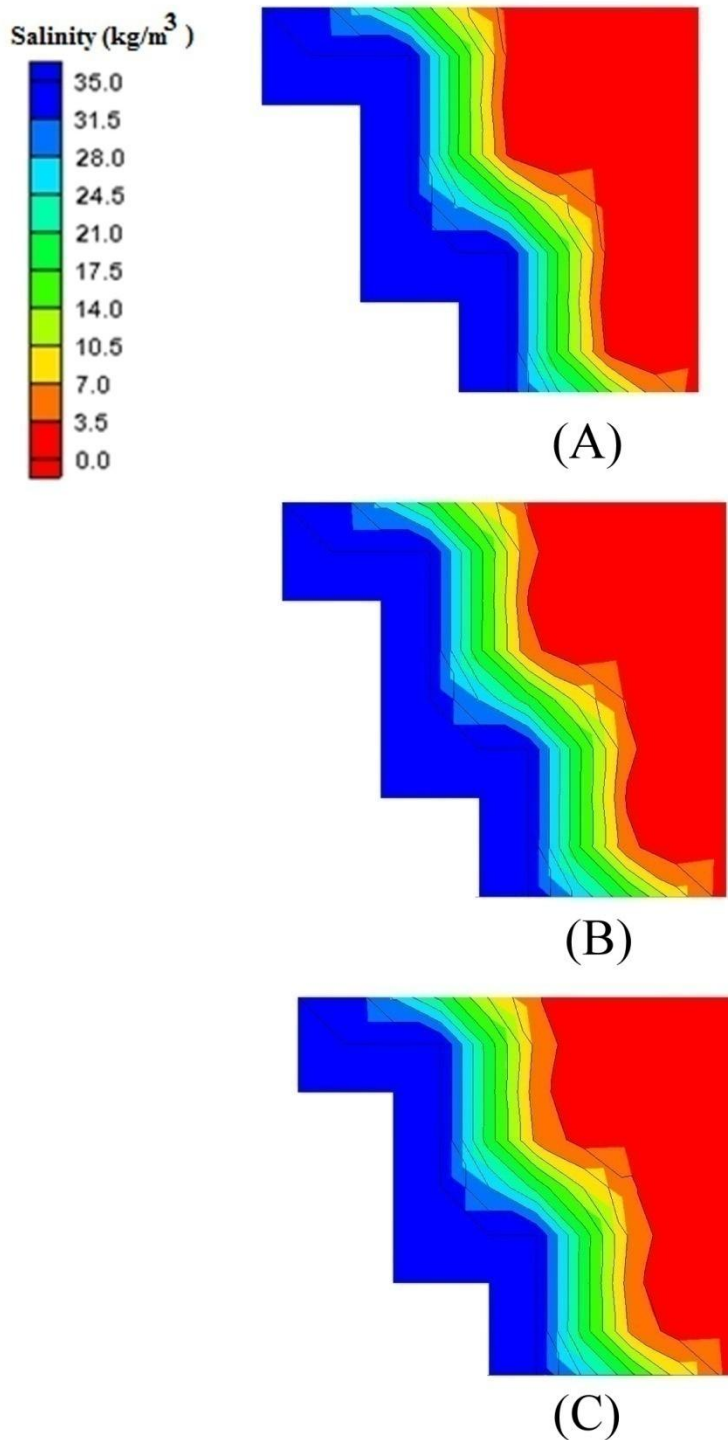


Fig. 5.7 Spatial distribution of saline concentration as simulated by SEAWAT along a part of the coastline during the year 2013 for increase of the longitudinal dispersivity by (A) 25% (B) 50% (C) 75%

5.7 CLOSURE

The variable density groundwater flow model, SEAWAT is successfully applied to simulate the saltwater intrusion in the study area. Since the SEAWAT model involves the same model structure as that of MODFLOW, with minor changes, the model domain remains the same. In the SEAWAT model, flow and density parameters are introduced to bring in the concept of equivalent fresh water head.

The calibration and validation of the model are carried out with reasonable accuracy (with $NSE \geq 0.5$). It is also admitted that, the performance of the model is not up to the mark during the period of interaction between the aquifer and river flow during the monsoon. The reasons for this are discussed in the context of the constant density flow model performance. In addition to the flow parameters calibrated earlier, transport parameters are standardised for the study area through the calibration process.

The model results show that, the rivers that surround the study area on either side contribute significantly to salinity as that of sea. This is because, the rivers are tidal in nature and carry saline water beyond October till May. However, under the current scenario, the aquifer system of the study area remains safe with $TDS < 1000$ ppm all over basin except a few regions very close to saltwater source. Well nos. 1, 15 and 25 which are located within 300m near the river tend to bring in high salinity (TDS greater than 500 ppm) during the pre-monsoon season as per the observed data. This is confirmed by the SEAWAT results as well.

The sensitivity analysis result shows that, the aquifer is found to be insensitive to the solute transport parameter, dispersivity.

CHAPTER 6

PREDICTIVE SIMULATIONS

6.1 GENERAL

In exercise of the powers conferred by the Environment (Protection) Act, 1986, the Government of India has declared the coastal stretches of the country and the water spread upto its territorial water limit as Coastal Regulation Zone (CRZ). With this, there is restriction setting up and expansion of any industry, operations or processes and manufacture or handling or storage or disposal of hazardous waste (www.moef.nic.in/downloads/public.../CRZ-Notification-2011.pdf). This notification is planned to ensure several aspects such as livelihood security to the fisherman communities and other local communities living in the coastal areas, to conserve and protect coastal stretches, their unique environment and to promote development through sustainable manner in view of natural hazards in the coastal areas, sea level rise due to global warming etc. According to the regulation, withdrawal of groundwater and construction related activities within 200m of high tide line (HTL) is prohibited, except for the areas which are inhabited by the local communities and only for their use. In the area between 200m-500m, withdrawal of groundwater shall be permitted manually through open wells for drinking, horticulture, agriculture and fisheries where no other source of water is available. Also, restrictions for such withdrawal may be imposed by the Authority designated by the State Government and Union territory Administration in the areas affected by sea water intrusion.

The area considered for the present study has an equal impetus to agricultural and industrial activities. The demand for groundwater would certainly increase in future, as the population growth and the industrial development in the area are taking an exponential trend. The area also shelters several educational institutes, New Mangalore Port and many small scale industries. Unplanned and uncontrolled withdrawal of groundwater resources may lead to drastic lowering of groundwater

table and hence adversely affecting the groundwater quality. This in turn, causes harmful effects on the domestic use, vegetation, industries, and other activities. As per the rainfall trend analysis carried out for the region (Shetkar and Mahesha, 2011), it was found that, the annual and seasonal rainfall trends of 14 weather stations are decreasing at a rate of 6–18% of average annual rainfall of 3,900 mm over a 100-year period.

With this background, the present work explores the feasible study of the effects of various stress scenarios on the aquifer for the period 2014-34 using the numerical simulation. Hence, this study investigates the response of the aquifer for increased pumping rates, decreased recharge rates and sea level rise in terms of the potential of groundwater and extent of lateral movement of seawater intrusion. The density dependent flow and transport model SEAWAT is used for the purpose. Specifically, the calibrated SEAWAT model is employed to simulate the effects of various near-future scenarios on the groundwater quantity and quality of the aquifer system.

6.2 DESCRIPTION OF THE SCENARIOS

In the previous chapters, the MODFLOW and SEAWAT are calibrated and have been used to investigate the seasonal variability of groundwater, salinity distribution, aquifer-river interactions and water balance under transient conditions during the period 2011-13. In this chapter, the SEAWAT is applied to simulate the groundwater flow and solute transport for future anticipated groundwater development in the study area. The following are the scenarios considered for simulation:

Scenario 1- :The present abstraction rate, calibrated recharge rate and no sea level rise. The existing level of groundwater utilization is listed in table 4.4 (chapter 4). The calibrated recharge rate for the region is 20% of rainfall. This scenario is basically the real time simulation of the present conditions for another 20 years i.e. upto the year 2034. Optimistically, the present conditions are presumed to prevail for another two decades. This scenario is conservative in estimating the groundwater utilization which is based on the crop evaporation data in view of lack of groundwater draft data from each well both with respect to quantity and time.

Scenario 2: This simulation considers decrease in recharge rate by 50% in view of anticipated decrease in rainfall resulting from climate change and low pervious soil. As per the studies conducted in the nearby aquifer, recharge co-efficient could be as low as 8% (Udaykumar, 2008). The recharge into the aquifer not only depends on the rainfall, but also on the soil characteristics and aquifer characteristics. Taking into account such possibilities which could cause a deliberate decrease of recharge rate, this scenario is taken up for simulation. In this scenario, the model is run for a 20 years period with 50% decrease in recharge rate i.e. 10% of rainfall amount.

Scenario 3 -Increase in the rate of groundwater utilization. Since, it becomes crucial to know the behaviour of the aquifer system to increased pumping, this scenario is introduced. In this simulation, it is also assumed that, the aquifer is getting recharged due to rainfall (with a recharge co-efficient of 0.20). Three separate cases are considered with 50%, 100% and 150% increase in pumping rate for the wells listed in table 4.4 (chapter 4). These simulations are indicated as case 1, case 2 and case 3 respectively.

Scenario 4 -Increase in abstraction rate together with decrease in recharge rate. This is the worst possible scenario with increased draft and decreased recharge. Here again, groundwater draft is increased by 50%, 100% and 150% along with 50% reduction in recharge rate i.e. 10% of rainfall amount. These are case 1, case 2 and case 3 of scenario 4 respectively.

Scenario 5 - Increase in abstraction rate together with decrease in recharge rate and accounting for sea level rise. The average global sea level rise over the second half of the 20th century was 1.8 ± 0.3 mm/year. It is likely of the order of 2 to 3mm/year during early 21st century as a consequence of global warming (IPCC, 2008). Several attempts were made to study the effect of sea level rise on saltwater intrusion into coastal aquifer. Most of the studies conducted in coastal aquifers have concluded that, groundwater extraction and decrease in recharge rate are predominant drivers of seawater intrusion when compared to sea level rise (Loaiciga et al., 2012; Narayan et al., 2007; Bobba, 2002; Green and MacQuarrie, 2014).

As per the studies conducted on the Indian coast (Unnikrishnan et al., 2007 and INCCA, 2010) a sea level rise of about 1mm/ year to 1.3 mm/ year is estimated. To account for the effect of sea level rise in the study area, scenario 4 with 1mm/year sea level rise was considered.

6.3 RESULTS AND DISCUSSION

The calibrated model is used to predict the spatial and temporal impacts of all the 5 scenarios on the aquifer's vulnerability to saltwater intrusion for 20 years period. The WHO recommends permissible TDS limit of 500 mg/L and excessive limit of 1,500 mg/l for drinking purpose. Therefore, the seawater intrusion is studied with respect to the lateral movement of the 1.5 kg/m³ iso-line from the coastline and the river boundaries. Similarly, the salt tolerance limits for the plants and vegetable range from TDS equal to 3kg/m³ to 10kg/m³ (Comte et al., 2014).

6.3.1 Temporal impacts of scenario simulation on the aquifer

The four sub-basins react more or less alike to the various scenario simulations. The response of the aquifer system during the 20 year simulation period is illustrated by presenting comparative graphs for water table elevation and groundwater salinity at few locations in the study area.

Impacts on water table

The variation of groundwater table through the 20 year simulation period for the 4 scenarios considered are depicted for a crucial location (x = 479,720 E and y = 1,429,951 N), in sub-basin 2 which is at a distance of 1000m from the seacoast boundary and approximately 750m from the Gurupur river. The temporal variation of water table is presented for the summer month of May (fig.6.1) and the monsoon month of September (fig.6.2) at this location for various scenarios.

When all the 4 scenarios (fig.6.1A) are compared, water table is seen to fall by 0.3m and 0.6 m for scenario 3 (case 3) and scenario 4(case 3) from that of scenario 1 respectively. The water table gradually reduces by 0.15m by the end of 20 year period for scenario 2 simulation from that of scenario 1. The plot for the month of May for

the scenario 3 (case 3) as seen in fig.6.1B shows a noticeable fall in the water table by the middle of the simulation period. All the cases of scenario 4 show a decline of 0.1 m by the end of the simulation period (fig.6.1C).

The plot for the month of September (fig.6.2) shows the direct effect of 50% reduction in recharge with water table falling by 0.25m throughout the simulation period. This effect is not seen in plot of water table for the month of May, because no recharge is assigned during the non-monsoon period. The effect of pumping in scenario 3 and 4 show a similar variation through 20 years as that of May.

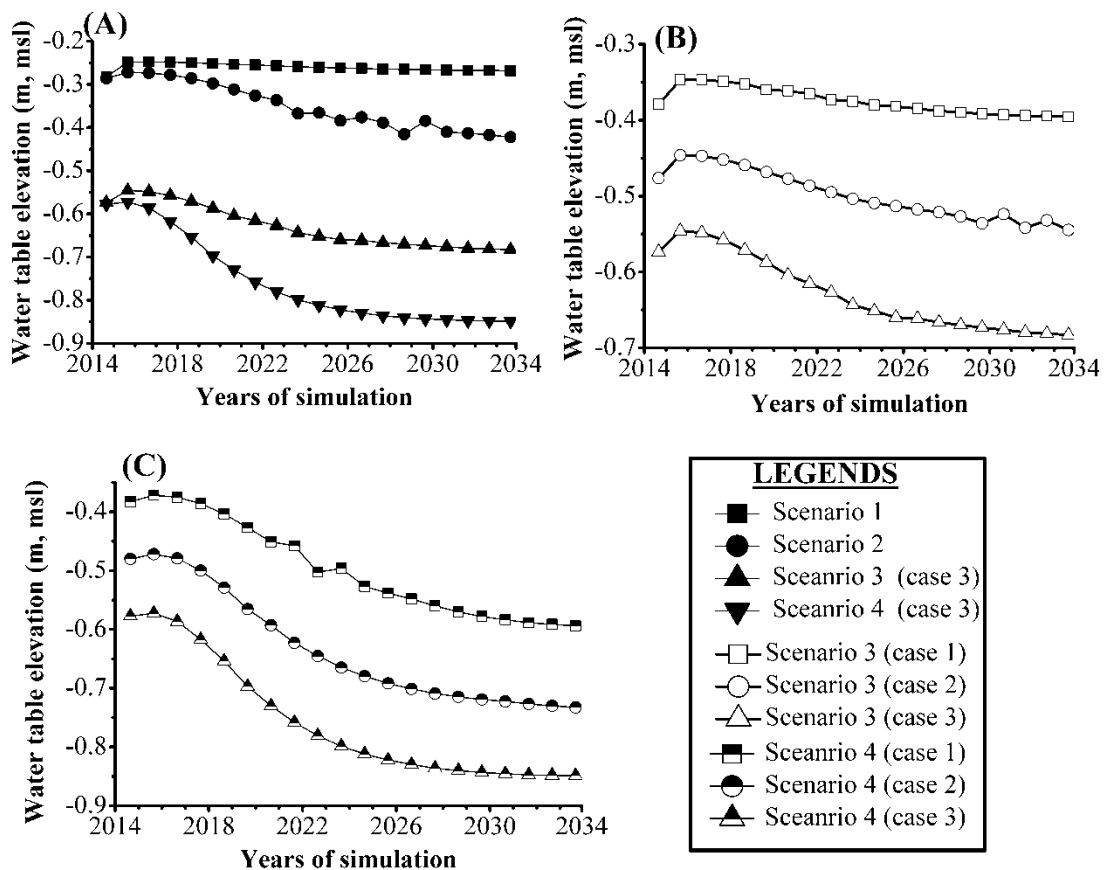


Fig.6.1 Variation of groundwater table over 20 year period during the month of May.

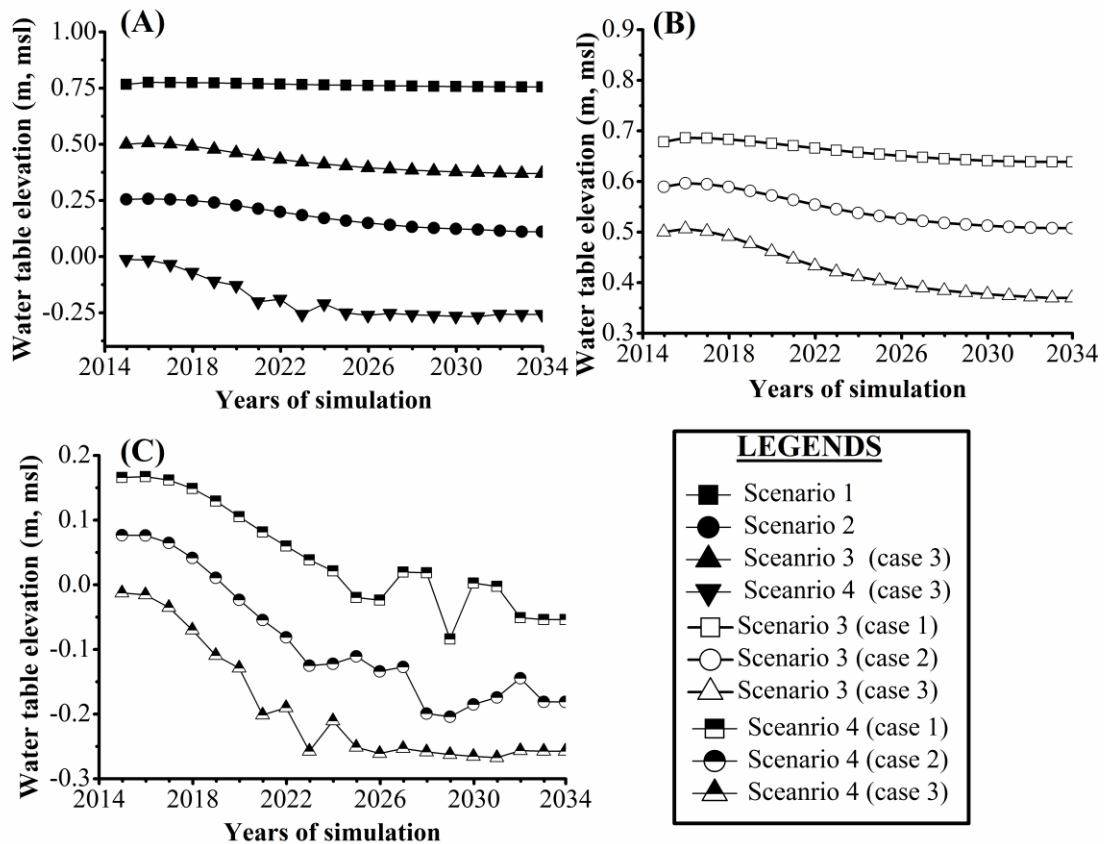


Fig.6.2 Variation of groundwater table over 20 year period for the month of September

The estimated water table elevation during the 20 year simulation is plotted at a grid 700m from the coastline and 300m from river Shambhavi and is shown in fig. 6.3.

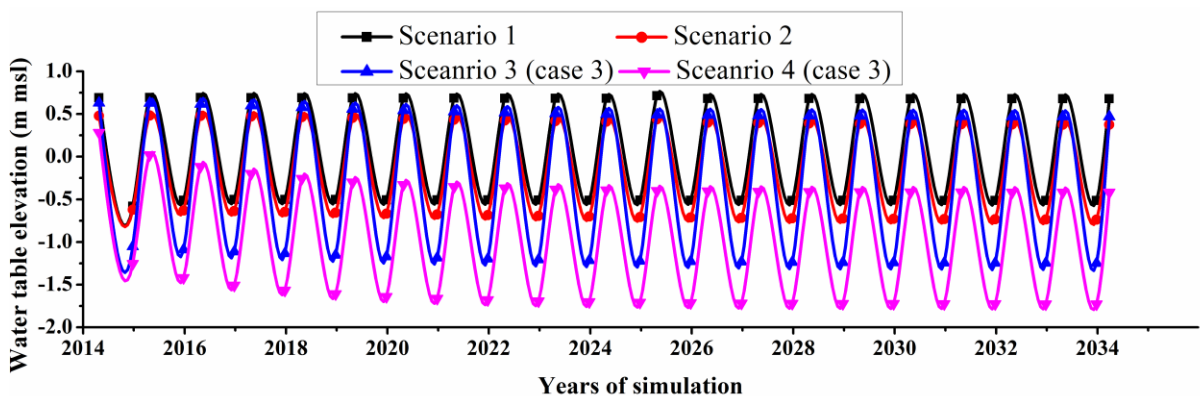


Fig.6.3 Variation of water table elevation over 20 year period at a grid 700m from the coastline and 300m from river Shambhavi

Impacts on salinity

The variation of salinity with time over a simulated period of 20 years at the same location in sub-basin 2 is presented in fig.6.4 (A) for scenarios 1 to 4. This graph shows that, the decrease in recharge rate (scenario 2) alone can raise the TDS to 1.5kg/m^3 in the first 8 years of simulation and thereafter increases to 14 kg/m^3 by the end of 20 years of simulation. However, with the present rate of groundwater utilization and recharge rate, the aquifer can be considered safe for the next 16 years with $\text{TDS} < 1.5\text{ kg/m}^3$, which reaches a TDS of 1.82 kg/m^3 by the end of 20 years. The quality of groundwater remains safe for drinking purpose ($\text{TDS} < 1.5\text{ kg/m}^3$) till next 6 years, 8 years, 6 years, 5 years, 4 years, 4 years and 3 years for different cases of scenario 2 to scenario 4 respectively. The groundwater quality is deprived for cultivation ($\text{TDS} > 10\text{kg/m}^3$) by the next 14 years, 13 years, 9 years, 7 years and 6 years for scenario, scenario 3 (case 3) and case 1, 2 and 3 of scenario 4 respectively.

Every 50% increase in groundwater utilization (fig.6.4B) causes the salinity to increase steeply with every year of simulation till the end of 20 year period. Finally, decrease in recharge rate further with increase in withdrawal rate is suspected to have a serious impact on the aquifer system. As only 50% increase in groundwater utilization rate combined with reduction in recharge rate (fig.6.4C) causes the salinity to rise above $\text{TDS} = 1.5\text{ kg/m}^3$ in the fifth year of simulation itself. However, it is found that, the system reaches steady state by about 20 years. Hence, except scenario 1 and scenario 3 (case 1), the remaining scenarios lead to the salinity above the drinking water standards, with 6 years of operation.

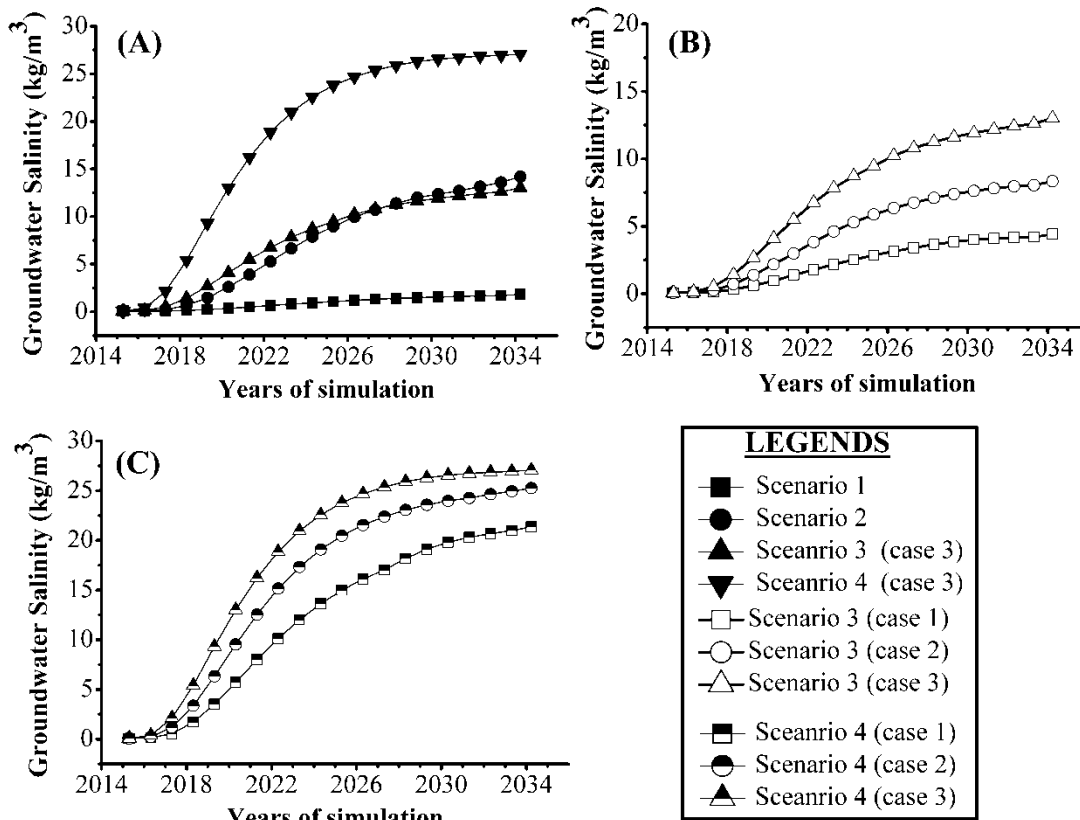


Fig.6.4 Variation of groundwater salinity over 20 year period for different scenario simulations

6.3.2 Spatial impacts of scenario simulation on the aquifer

Impacts on water table

The water table elevation and groundwater salinity at the observation wells simulated for all the scenarios considered are listed in table 6.1 to 6.4 for the all the 4 sub-basins respectively. The table indicates that, the water table falls by an average of 3.0m, 1.5m, 4.23m and 3.67m in sub- basins 1, 2, 3 and 4 respectively due to the decrease in recharge rate (ie scenario 2) compared to scenario 1. But the saltwater ingress is not prominent due to this scenario (scenario 2), except that near the areas close to the river boundary.

Table.6.1 Water table elevation (with respect to mean sea level) and groundwater salinity due to different scenario simulations for sub-basin 1 at the end of simulation

Description	Well no.	Scenario 1	Scenario 2	Scenario 3			Scenario 4		
				case1	case 2	case 3	case1	case2	case3
Water table elevation (m)	25	3.98	2.24	3.49	3.99	3.47	2.05	1.48	0.92
	26	8.76	4.03	7.94	6.71	5.19	2.00	-0.40	-3.21
	27	7.97	2.71	6.45	4.68	2.68	0.46	-2.20	-5.32
	28	6.31	3.50	5.81	5.33	4.81	2.87	1.78	0.27
	29	1.02	0.58	0.99	0.95	0.91	0.54	0.48	0.38
Groundwater salinity (kg/m ³)	25	3.57	10.60	3.69	7.62	11.69	11.72	17.61	21.41
	26	0.03	0.05	0.03	0.03	0.03	0.04	0.04	7.43
	27	0.03	0.04	0.03	0.03	0.03	0.04	0.04	2.10
	28	0.04	0.06	0.04	0.04	0.18	0.21	7.19	19.09
	29	0.40	0.43	0.40	0.51	1.50	1.56	2.83	7.43

Table.6.2 Water table elevation (with respect to mean sea level) and groundwater salinity due to different scenario simulations for sub-basin 2 at the end of simulation

Description	Well no.	Scenario 1	Scenario 2	Scenario 3			Scenario 4		
				case1	case 2	case 3	case1	case2	case3
Water table elevation (m)	15	1.52	1.36	1.50	1.49	1.47	1.40	1.33	1.31
	16	2.72	1.23	2.42	2.24	2.05	1.04	0.84	0.65
	17	3.01	1.46	2.84	2.67	2.49	1.26	1.05	0.83
	18	4.39	2.14	3.95	3.42	2.78	1.15	-0.36	-1.83
	19	4.56	2.74	4.27	3.91	3.27	1.17	-1.41	-3.73
	20	4.46	2.33	4.25	3.84	3.19	1.40	0.09	-1.12
	21	5.27	2.38	4.92	4.53	4.07	1.73	0.90	0.08
	22	1.79	0.78	1.64	1.49	1.34	0.60	0.44	0.30
	23	1.11	0.30	1.04	0.98	0.92	0.22	0.15	0.07
	24	1.54	1.02	1.48	1.40	1.30	0.90	0.72	0.59
Groundwater salinity (kg/m ³)	15	5.70	13.20	7.15	8.68	10.21	14.82	16.18	17.25
	16	0.02	0.03	0.02	0.02	0.02	0.03	0.03	0.03
	17	0.05	0.08	0.05	0.05	0.05	0.08	0.08	0.08
	18	0.03	0.05	0.03	0.03	0.03	0.05	1.30	18.57
	19	0.02	0.04	0.02	0.02	0.02	0.04	0.04	1.28
	20	0.02	0.03	0.02	0.02	0.02	0.03	2.62	21.48
	21	0.02	0.03	0.02	0.02	0.02	0.05	0.24	4.45
	22	7.60	18.46	12.80	17.88	22.24	25.99	30.01	31.58
	23	0.03	0.05	0.03	0.03	0.03	0.05	0.06	0.08
	24	1.26	1.57	1.88	5.05	8.11	11.01	20.96	26.88

Table 6.3 Water table elevation (with respect to mean sea level) and groundwater salinity due to different scenario simulations for sub-basin 3 at the end of simulation

Description	Well no.	Scenario 1	Scenario 2	Scenario 3			Scenario 4		
				case1	case 2	case 3	case1	case2	case3
Water table elevation (m)	8	5.58	1.87	4.17	3.02	1.66	0.47	-1.00	-2.54
	9	5.31	2.14	4.14	3.20	2.09	1.01	-0.22	-1.47
	10	10.08	3.23	7.74	5.50	2.95	0.54	-2.43	-5.67
	11	9.45	2.95	7.15	4.97	2.49	0.35	-2.49	-5.62
	12	8.83	3.14	6.76	5.01	2.97	0.98	-1.35	-3.72
	13	4.74	3.36	4.38	4.12	3.80	3.03	2.61	0.23
	14	6.33	4.02	5.92	5.47	4.95	3.48	2.92	2.33
Groundwater salinity (kg/m ³)	8	0.05	0.08	0.05	0.05	0.05	0.08	0.08	0.08
	9	0.05	0.09	0.05	0.05	0.05	0.11	6.63	13.22
	10	0.05	0.08	0.05	0.05	0.05	0.08	0.08	0.08
	11	0.05	0.08	0.05	0.05	0.05	0.08	0.08	0.08
	12	0.04	0.07	0.04	0.04	0.04	0.07	0.07	0.24
	13	0.05	0.08	0.05	0.05	0.05	0.14	7.59	16.05
	14	0.05	0.08	0.05	0.05	0.05	0.08	0.98	10.10

Table 6.4 Water table elevation (with respect to mean sea level) and groundwater salinity due to different scenario simulations for sub-basin 4 at the end of simulation

Description	Well no.	Scenario 1	Scenario 2	Scenario 3			Scenario 4		
				case1	case 2	case 3	case1	case2	case3
Water table elevation (m)	1	3.96	1.67	3.59	3.17	2.66	1.12	0.55	-0.03
	2	5.92	2.54	5.37	4.70	3.82	1.59	0.60	-0.45
	3	9.40	4.54	9.30	8.34	6.20	2.16	-0.44	-3.30
	4	13.11	3.87	8.11	6.69	5.23	2.35	0.76	-0.93
	5	5.45	3.48	4.83	4.46	4.12	3.21	2.82	2.50
	6	6.74	3.57	5.81	5.14	4.52	3.06	2.52	1.92
	7	4.24	3.49	4.07	3.90	3.73	3.30	3.01	2.81
Groundwater salinity (kg/m ³)	1	0.05	0.10	0.05	0.05	0.05	0.10	0.10	0.10
	2	0.05	0.09	0.05	0.05	0.05	0.09	0.09	1.75
	3	0.04	0.06	0.04	0.04	0.05	0.05	0.05	0.05
	4	0.05	0.08	0.05	0.05	0.05	0.08	0.08	0.08
	5	0.08	0.16	0.08	0.08	0.09	0.68	10.73	17.56
	6	0.05	0.08	0.05	0.05	0.05	0.09	2.44	12.37
	7	1.20	1.37	1.20	1.20	1.20	2.16	12.76	15.96

With the increase in pumping rate by 50%, 100% and 150%, the water table falls by an average of <1m each, except in sub-basin 3, wherein the water table falls by about 1.5m for simulation of each case of scenario 3. This could be because of steep terrain of sub-basin 3. A steepness of 30.07°, as compared to 20° in the other 3 sub-basins is reported as calculated by the spatial analyst tool in ArcGIS. However, the water table goes below mean sea level (negative water table) in about 60% to 80% of the study area when case 2 and 3 of scenario 4 is simulated, which is not desirable. To substantiate the results, the spatial distribution map of water table contour for scenario 1, 2, 3 (case 3) and 4 (case 3) are presented in fig.6.5 to 6.8. The simulated heads show significant spatial variability over the period due to the application of various scenarios. There is no difference in the end effect between scenario 4 and scenario 5.

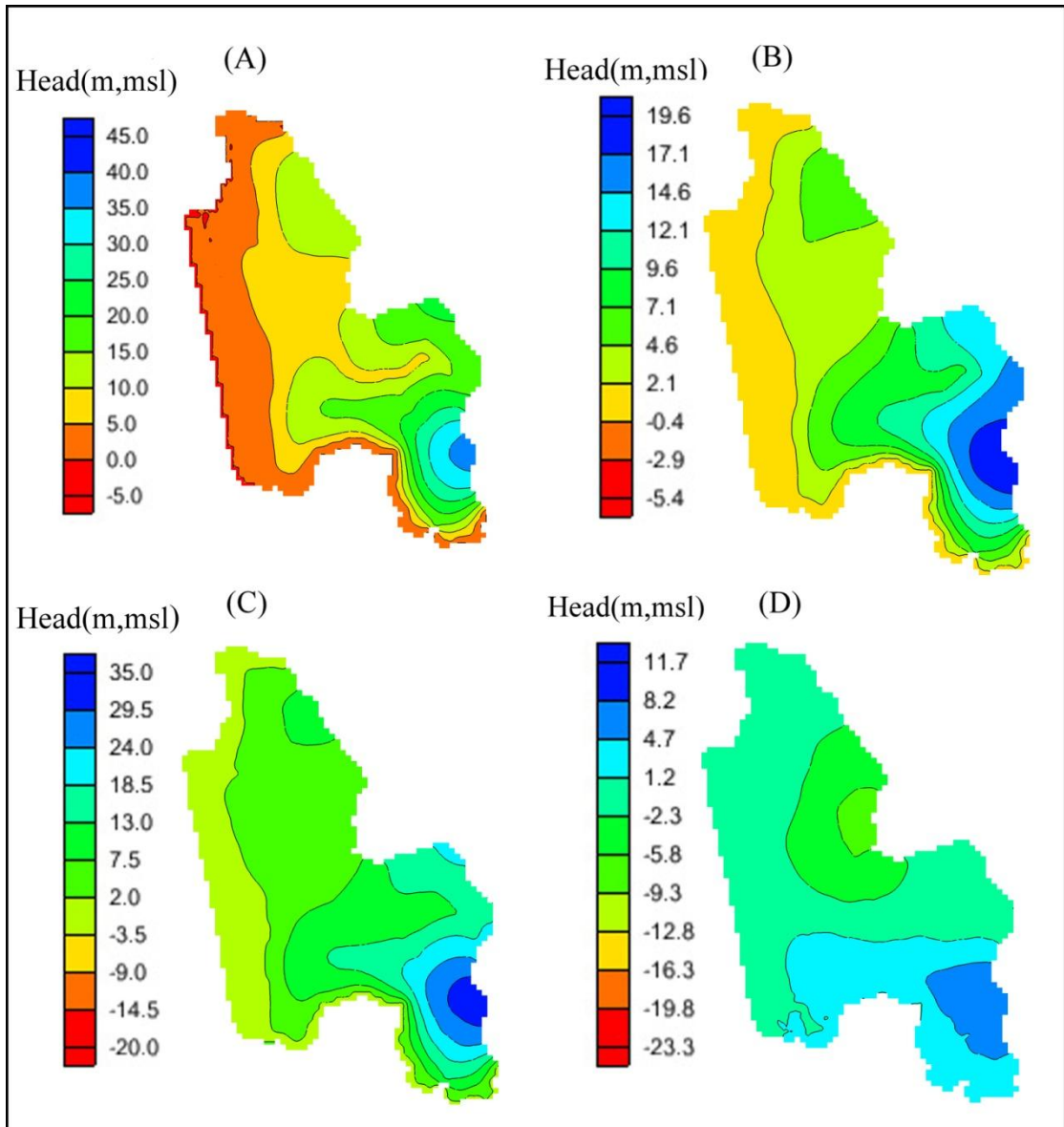


Fig. 6.5 Spatial distribution of water table in sub-basin 1 for (A) scenario 1 (B) scenario 2 (C) scenario 3 (case 3) (D) scenario 4 (case 3) at the end of 20 year simulation

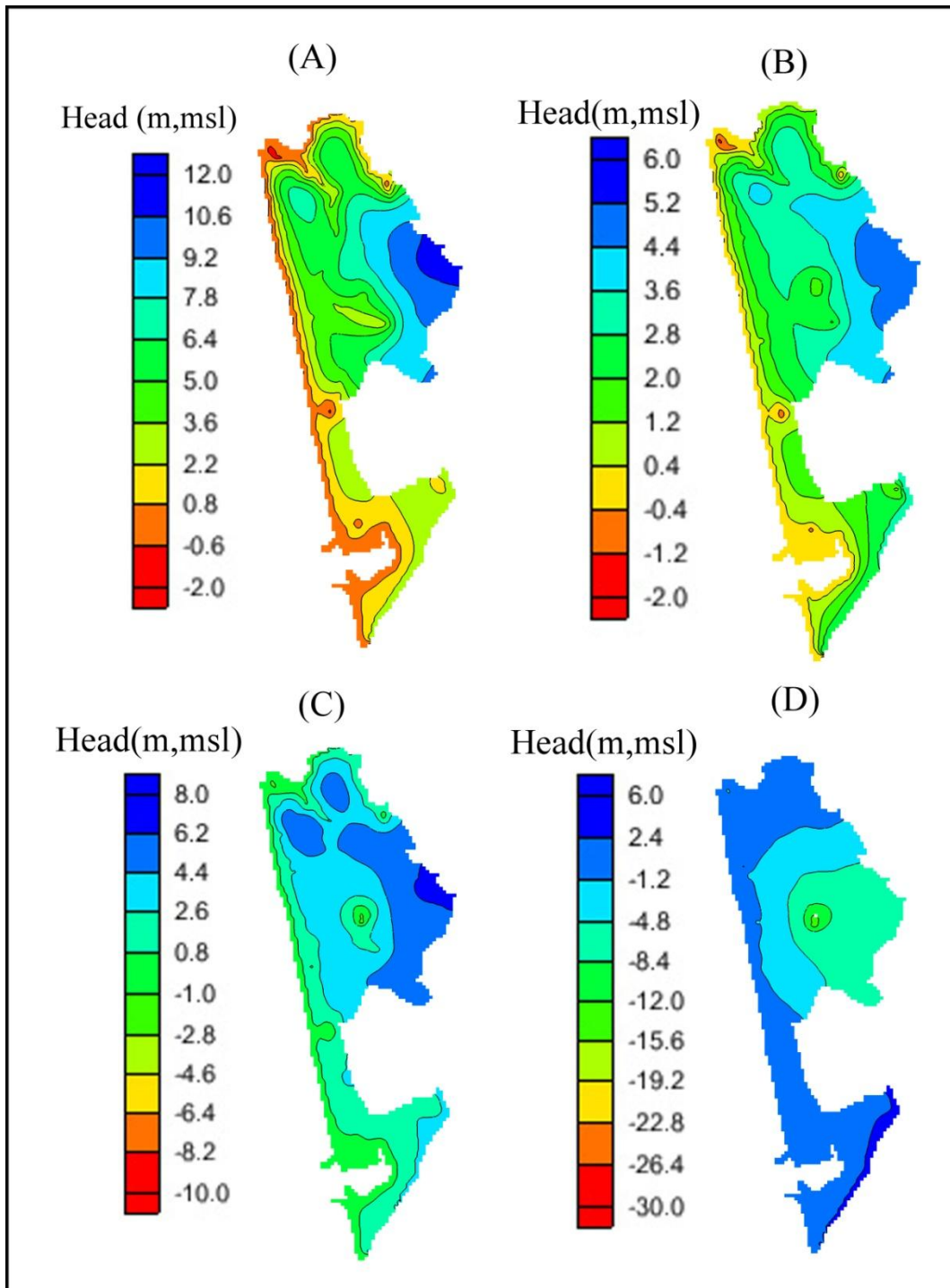


Fig. 6.6 Spatial distribution of water table in sub-basin 2 for (A) scenario 1 (B) scenario 2 (C) scenario 3 (case 3) (D) scenario 4 (case 3) the end of 20 year simulation

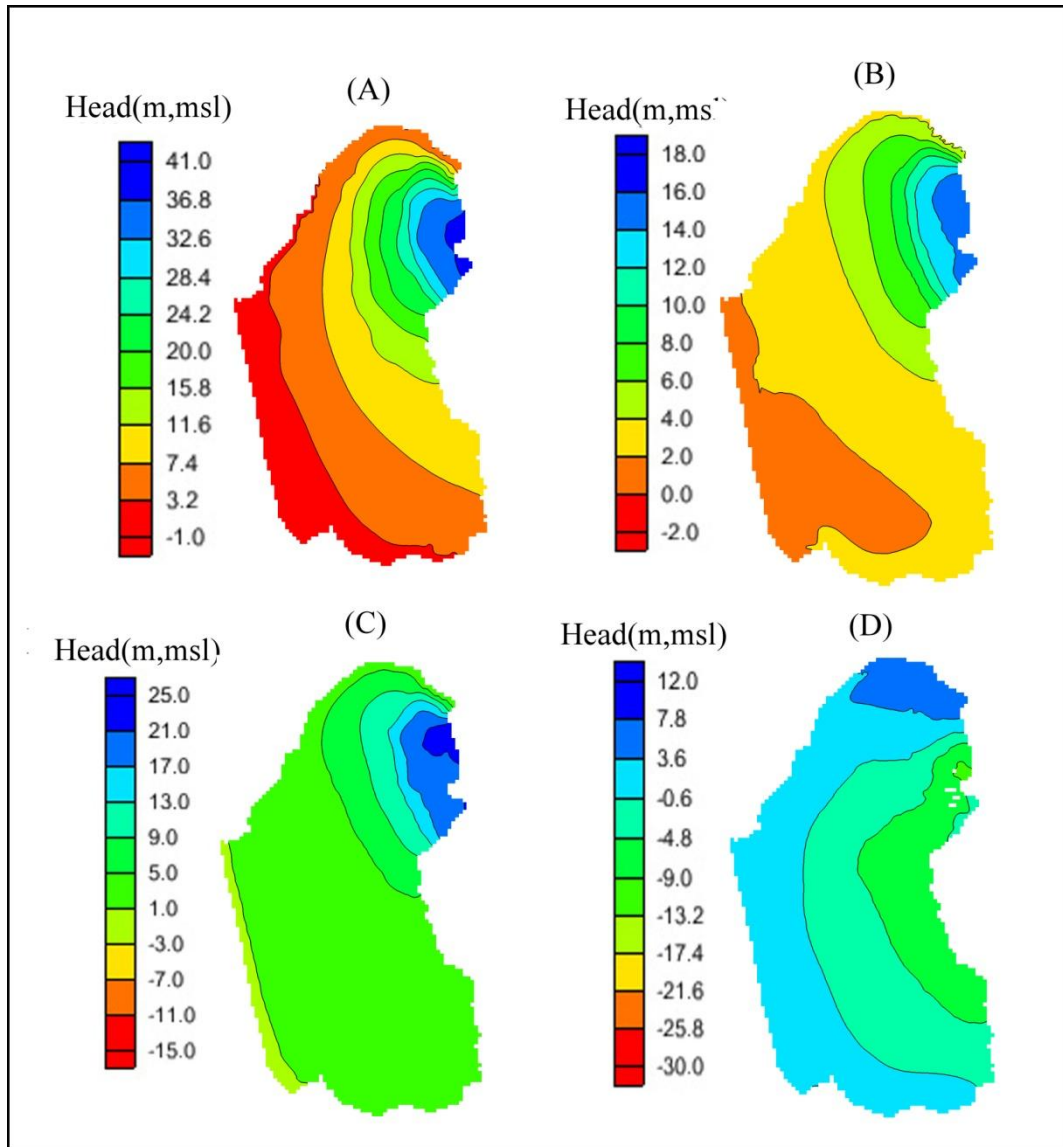


Fig. 6.7 Spatial distribution of water table in sub-basin 3 for (A) scenario 1 (B) scenario 2 (C) scenario 3 (case 3) (D) scenario 4 (case 3) the end of 20 year simulation

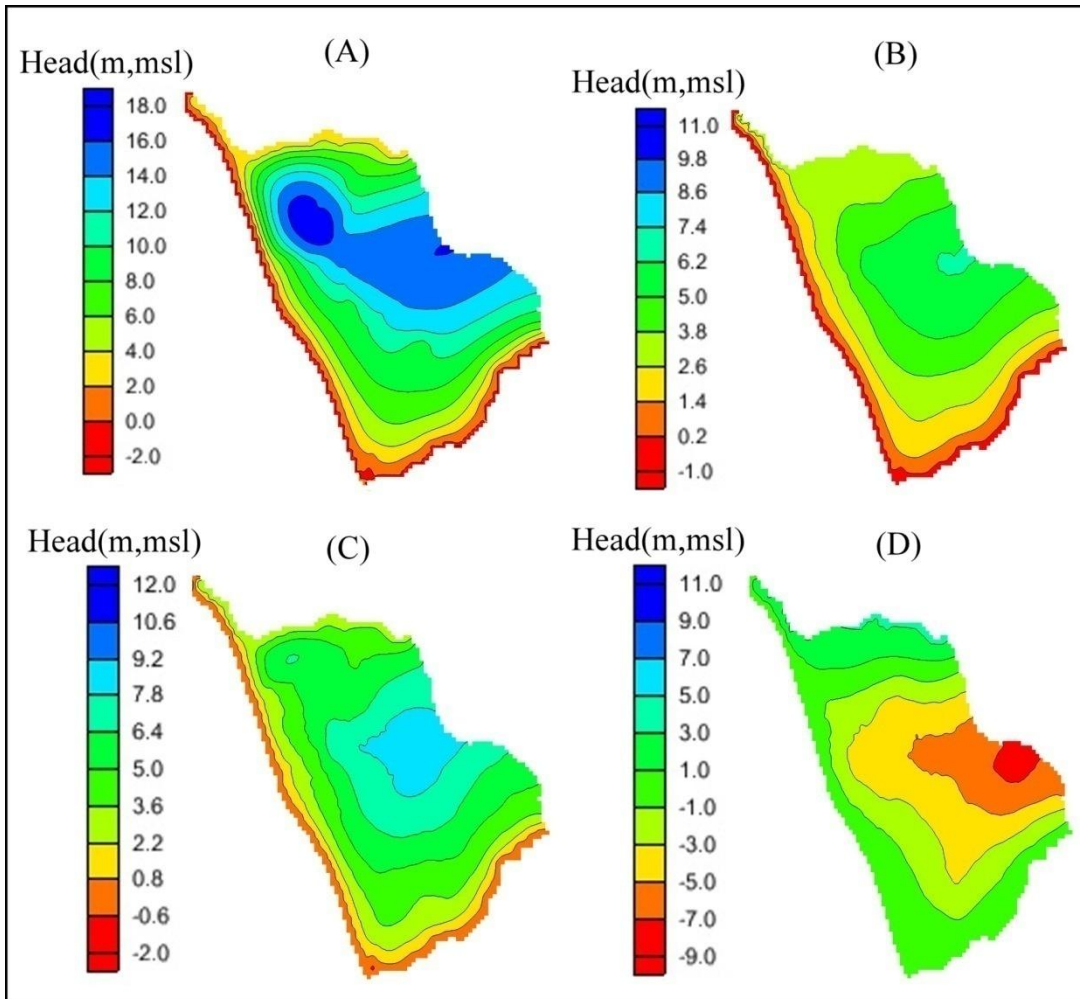


Fig. 6.8 Spatial distribution of water table in sub-basin 4 for (A) scenario 1 (B) scenario 2 (C) scenario 3 (case 3) (D) scenario 4 (case 3) the end of 20 year simulation

It is noticed from the simulation that, regional sea level rise incorporated into the simulation has no impact on the groundwater dynamics of the aquifer. It is evident by comparing the results of scenario 4 and 5.

The decline in water table elevations for scenarios 3 and 4 are evident compared to scenarios 1 and 2. Due to 50% decrease in recharge rate (scenario 2), the maximum water table elevation (during wet period) falls by about 1m whereas the minimum water table elevation (during dry period) coincides with that of scenario 1. This is because, recharge due to rainfall is not applicable during the non-monsoon period. Interestingly, when the pumping rate is increased by 150% (that is in scenario 3), the

maximum water table elevation coincides with that of scenario 2, but, the minimum water table elevation falls by about 1.5m. This indicates that the increased pumping rate during the wet period is compensated by recharge due to rainfall. However, in the case of scenario 4, the maximum water table falls further by about 1.3m.

Impacts on salinity

The spatial movement of the salinity contours are analysed for each sub-basin separately. The salinity distribution maps of sub-basin1, 2, 3 and 4 for scenario 1, scenario 2, scenario 3 (case 3) and scenario 4 (case 3) are shown in fig.6.9 to 6.12.

From the salinity values listed in tables 6.1 to 6.4, as well as from the fig.6.8 to 6.11, it can be shown that, the area coming under the influence of river and sea (< 500m) are prone to seawater intrusion ($TDS > 1.5 \text{ kg/m}^3$) when the model is simulated for the present condition (Scenario 1). The remaining scenarios aggravate the situation further, except the ones in the vicinity of Talapady river. The areas away from the river and sea by more than 500m to about 1000m come under the influence of seawater ingress ($TDS > 1.5 \text{ kg/m}^3$) only due to the simulation of scenario 4 (case 2 and 3) and safe for rest of the cases. In the areas close to the river boundary and sea boundary, water remains to be safe for potable use ($TDS < 1.5 \text{ kg/m}^3$) up to scenario 2 and scenario 3 (case 1 and 2). For other scenarios, water is found to be affected by salinity (TDS close to 3 kg/m^3).

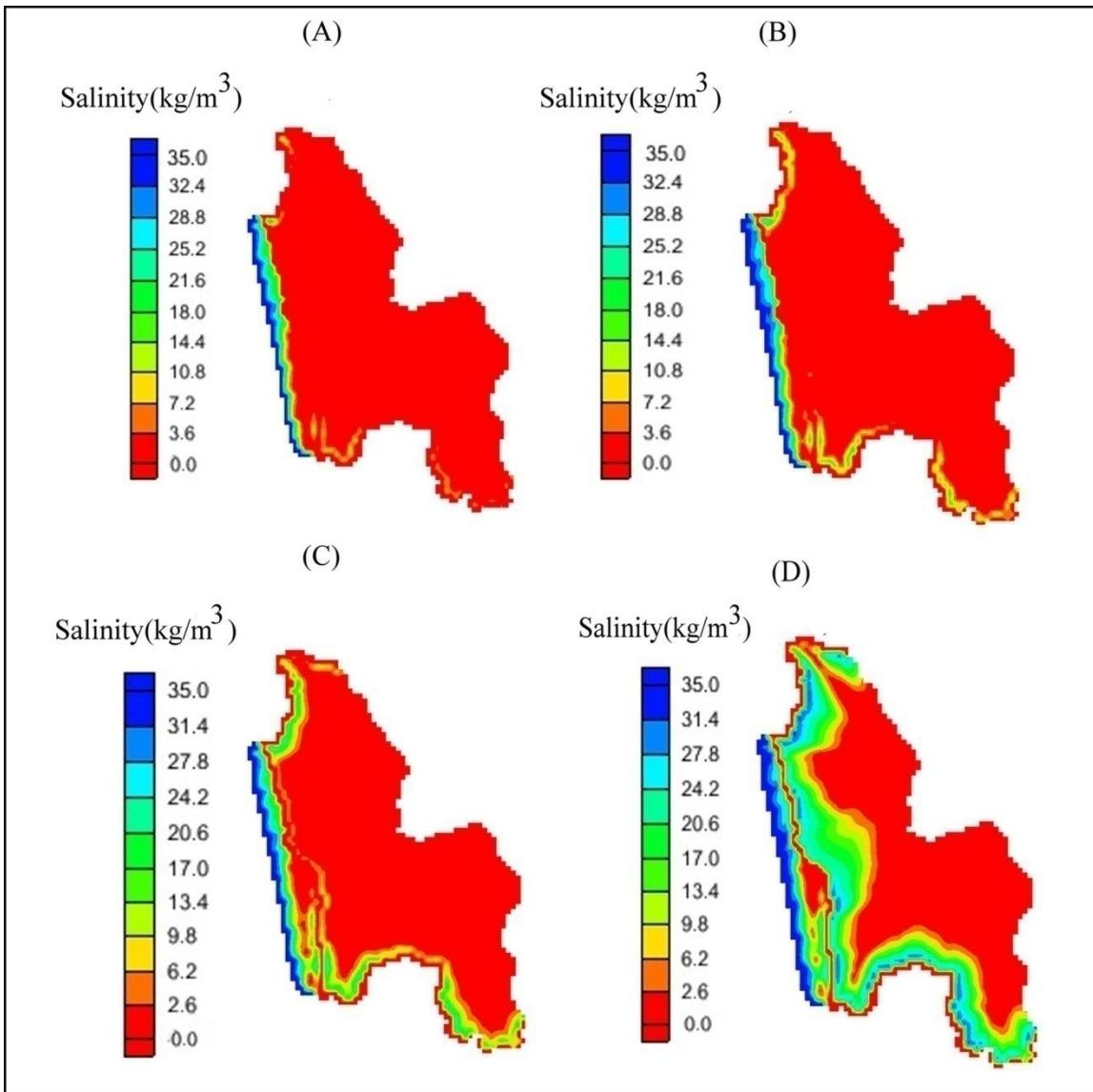


Fig.6.9 Spatial distribution of salinity in sub-basin 1 for (A) scenario 1 (B) scenario 2 (C) scenario 3 (case 3) (D) scenario 4 (case 3) at the end of 20 year simulation

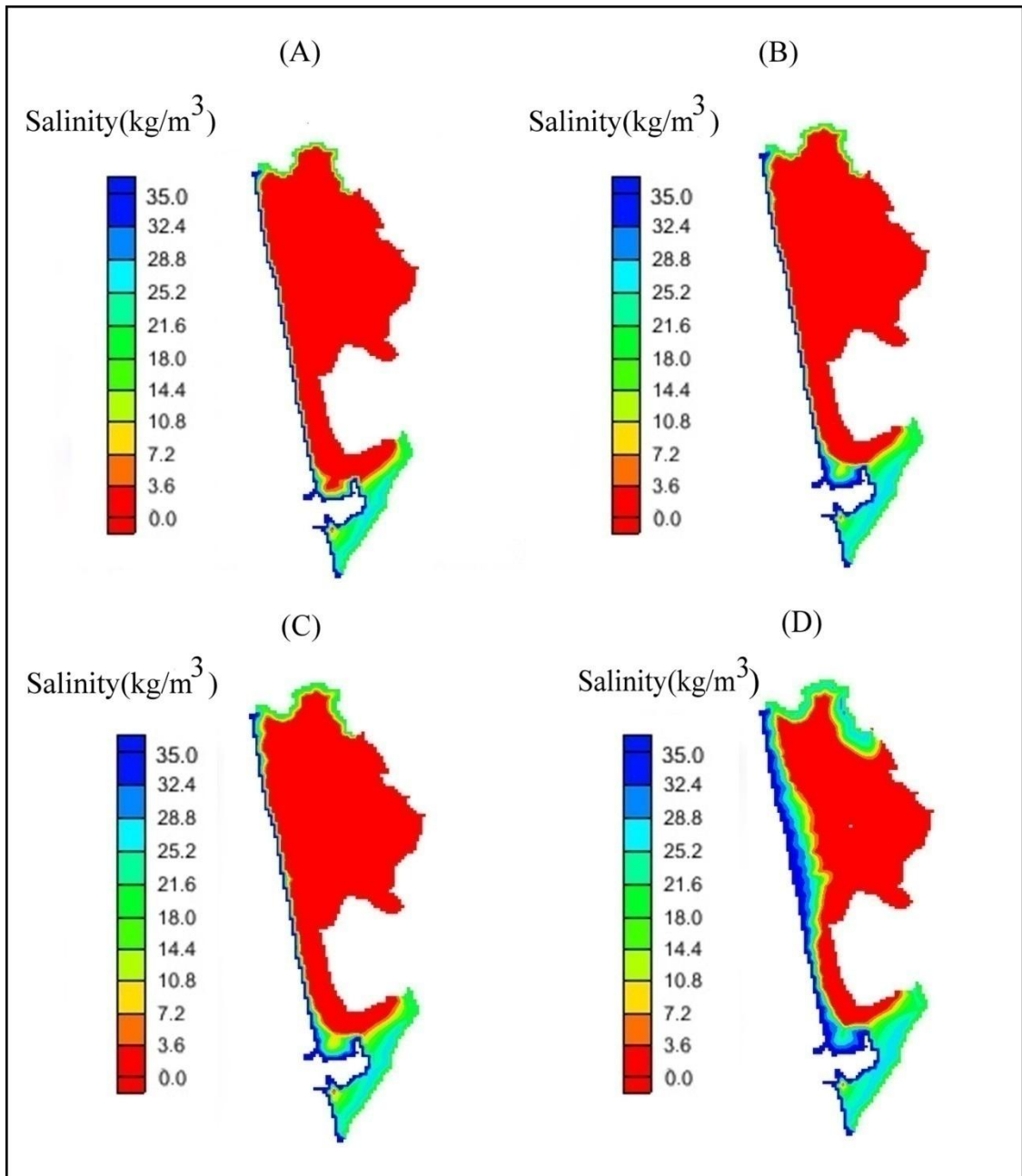


Fig.6.10 Spatial distribution of salinity in sub-basin 2 for (A) scenario 1 (B) scenario 2 (C) scenario 3 (case 3) (D) scenario 4 (case 3) at the end of 20 year simulation

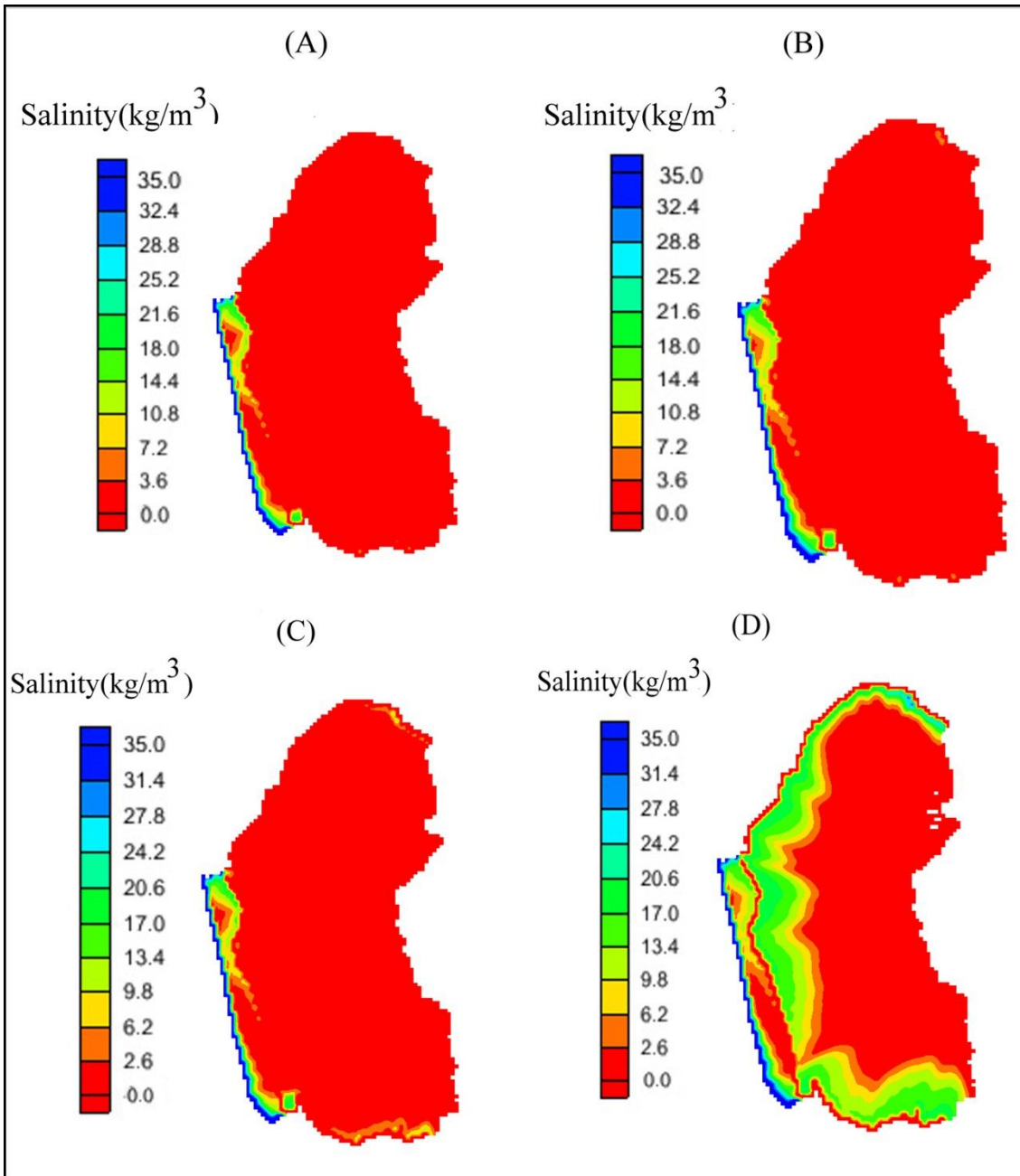


Fig.6.11 Spatial distribution of salinity in sub-basin 3 for (A) scenario 1 (B) scenario 2 (C) scenario 3 (case 3) (D) scenario 4 (case 3) at the end of 20 year simulation

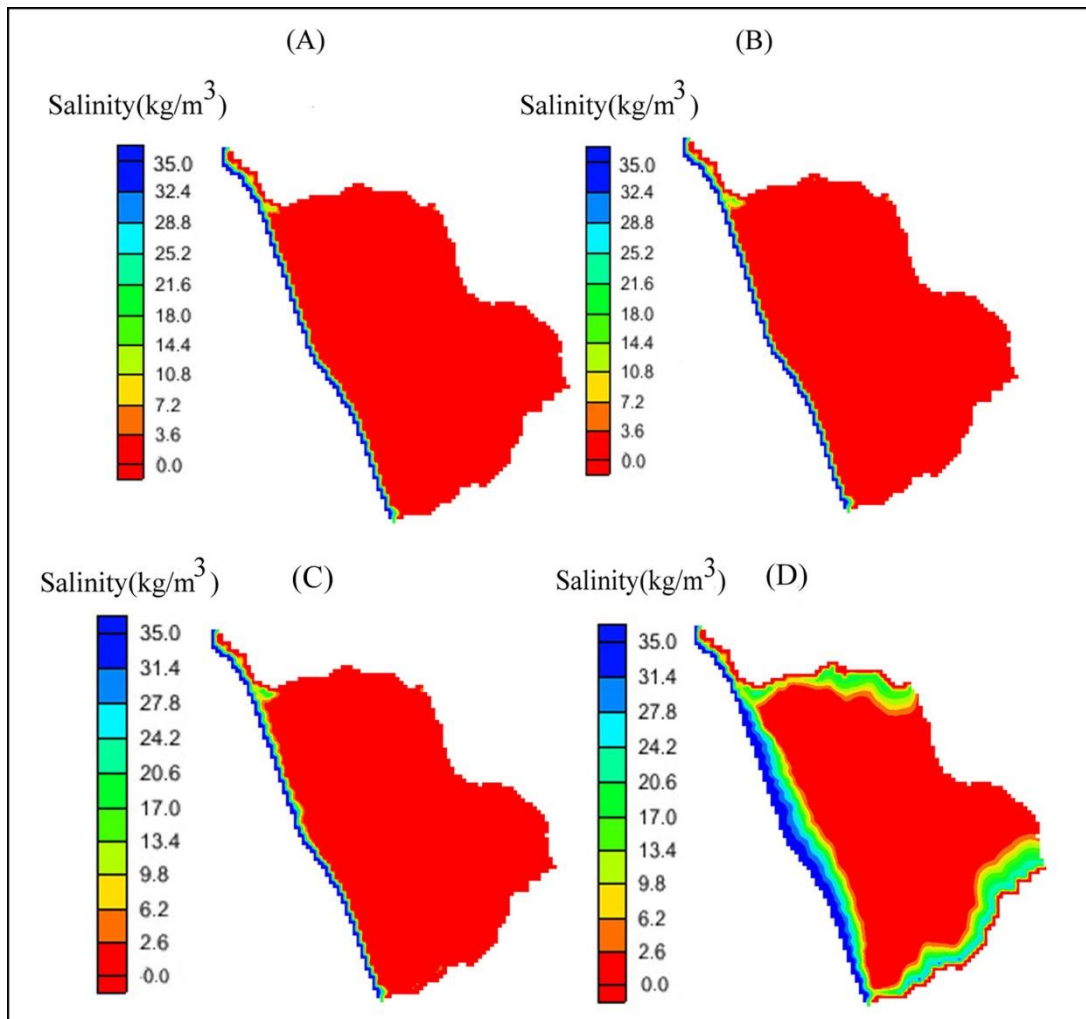


Fig.6.12 Spatial distribution of salinity in sub-basin 4 for (A) scenario 1 (B) scenario 2 (C) scenario 3 (case 3) (D) scenario 4 (case 3) at the end of 20 year simulation

6.4 Variation of salinity and water table across the study area

To study the effect of various scenarios on the water table and advancement of salinity into the aquifer from the coastline alone, a plot of hydrograph and salinity at every 200m distance from the coastline is plotted. Fig.6.13 shows the salinity plot for different scenario simulation at every 200m. From the figure it is evident that, the aquifer close to the coastline (beyond 200m) is safe ($TDS < 1.5 \text{ kg/m}^3$) against seawater intrusion for scenarios 1, 2 and 3. Only due to scenario 4 (case 2 and 3), the seawater intrudes beyond 600 m to 1200m making the aquifer unfavourable for drinking purpose. The seawater further intrudes into the coastal aquifer after 17 years and 10

years of simulations of scenario 4 (case 2) and scenario 4 (case 3) respectively. The hydrograph plot agrees with this behaviour of the aquifer, with water table falling below mean sea level for the simulation of case 2 and 3 of scenario 4 in the month of September (fig.6.14) either. The water table in the summer month of May (fig.6.15) is lower than the monsoon month of September due to fact that, the non-monsoon periods do not receive any recharge due to the scanty rainfall.

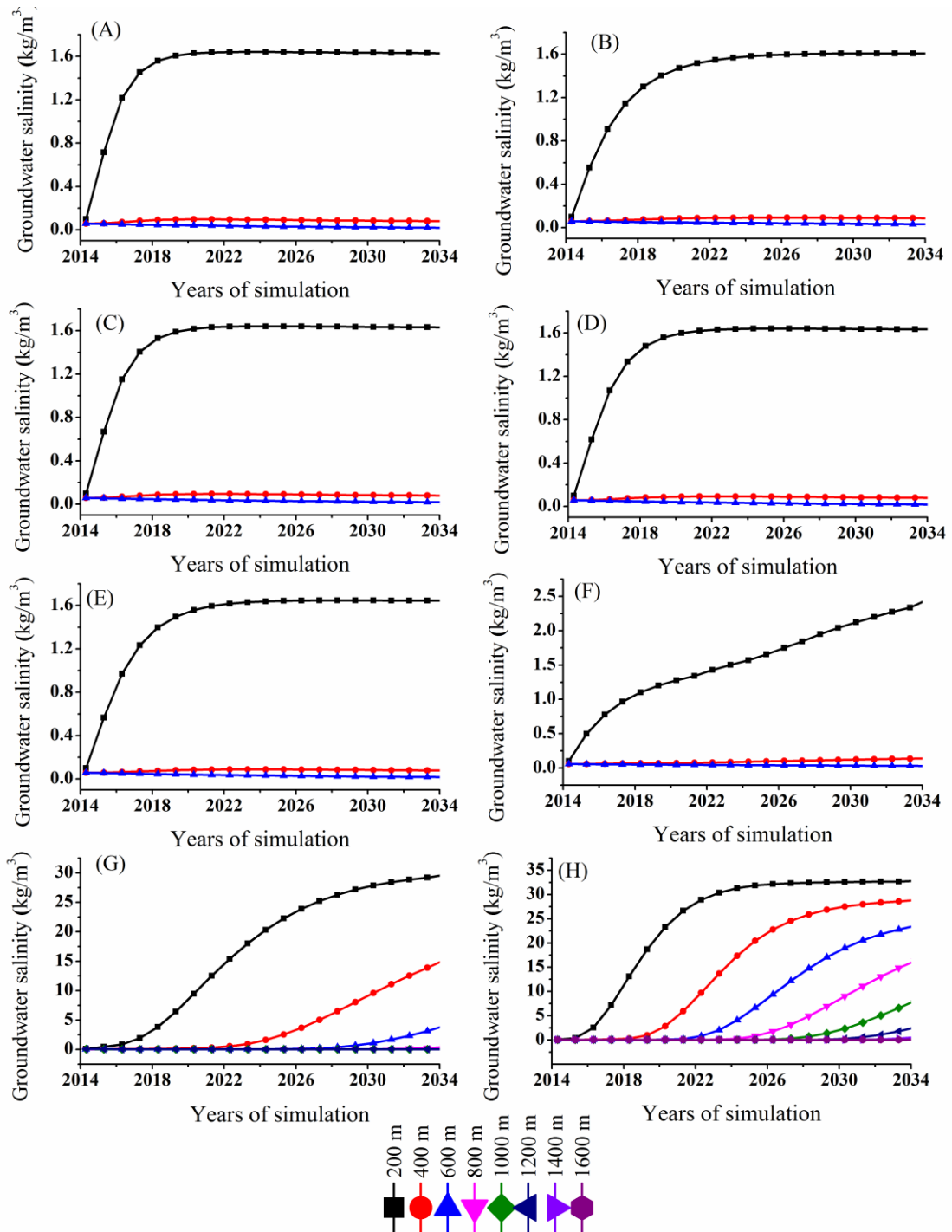


Fig.6.13 Salinity profile at the end of 20 year simulation period along every 200m interval from the coastline for simulation of (A) scenario 1 (B) scenario 2 (C) scenario 3 (case 1) (D) scenario 3 (case 2) (E) scenario 3 (case 3) (F) scenario 4 (case 1) (G) scenario 4 (case 2) (H) scenario 4 (case 3)

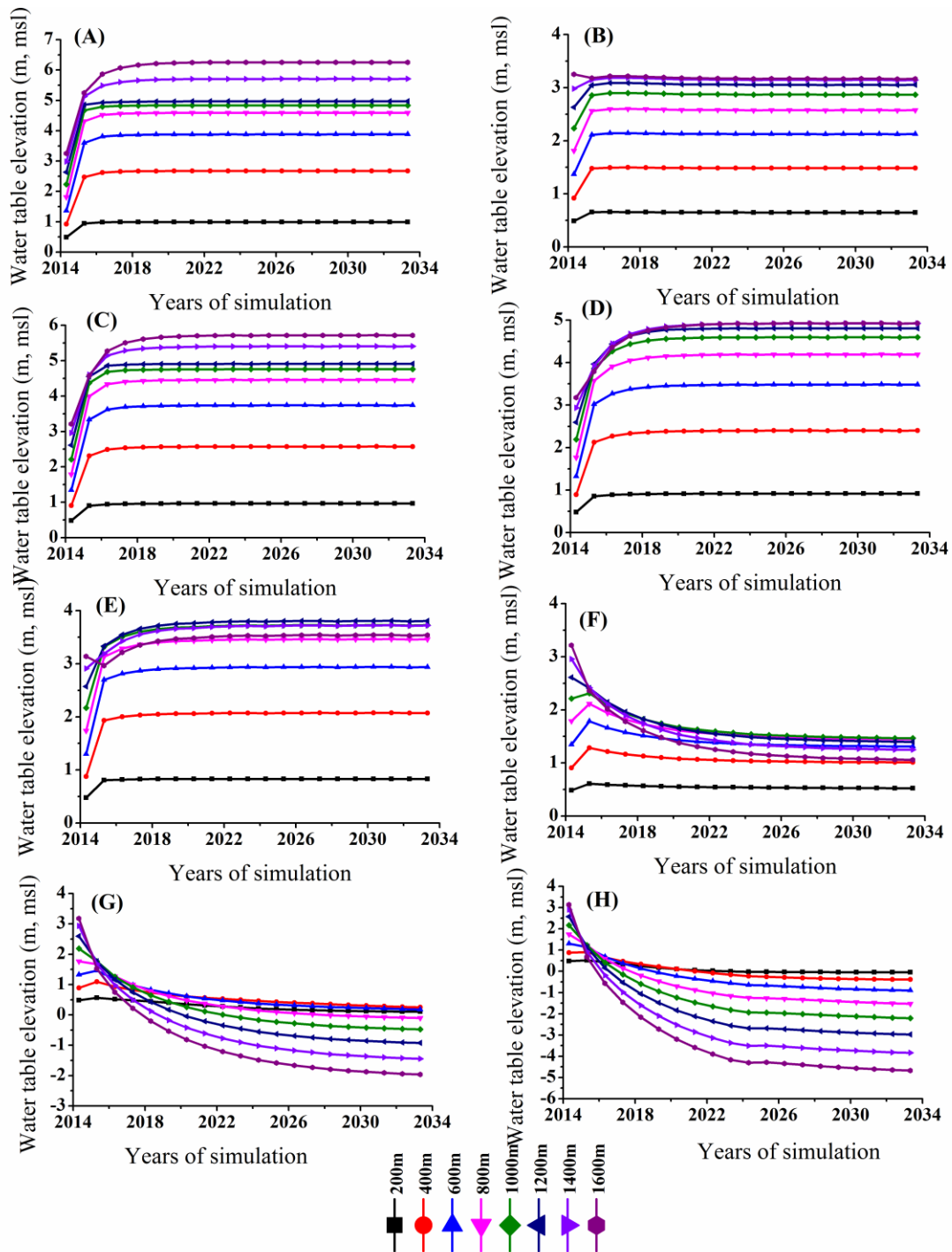


Fig.6.14 Water table profile at the end of 20 year simulation period along every 200m interval from the coastline during the month of September for the simulation of (A) scenario 1 (B) scenario 2 (C) scenario 3 (case 1) (D) scenario 3 (case 2) (E) scenario 3 (case 3) (F) scenario 4 (case 1) (G) scenario 4 (case 2) (H) scenario 4 (case 3)

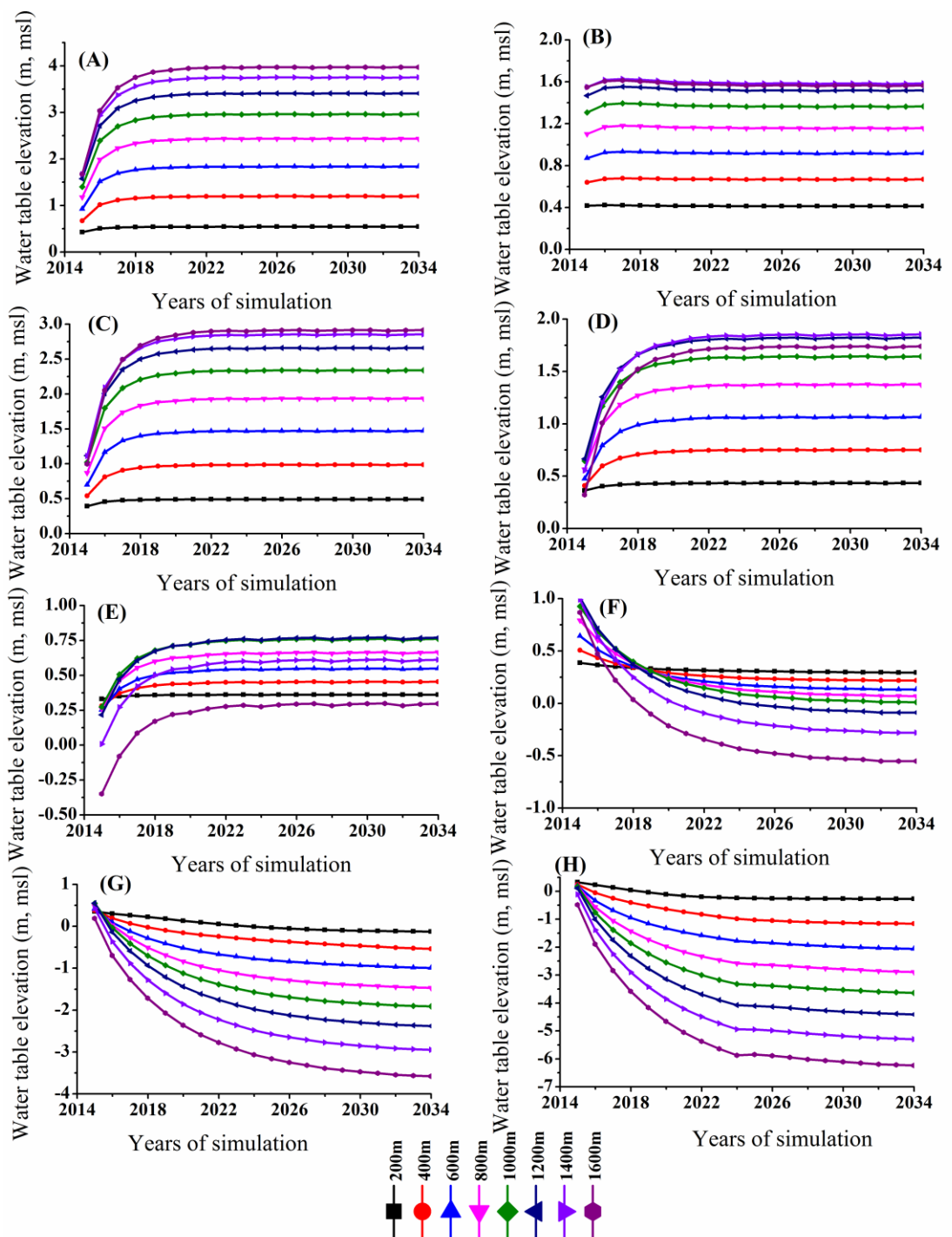


Fig.6.15 Water table profile at the end of 20 year simulation period along every 200m interval from the coastline during the month of May for the simulation of (A) scenario 1 (B) scenario 2 (C) scenario 3 (case 1) (D) scenario 3 (case 2) (E) scenario 3 (case 3) (F) scenario 4 (case 1) (G) scenario 4 (case 2) (H) scenario 4 (case 3)

6.5 Percentage area affected by seawater intrusion

The percentage area affected by saltwater intrusion due to different anticipated scenarios are estimated in fig.6.16. It is evident from the figure that, the affected area significantly increases for scenario 4 compared to scenario 1.

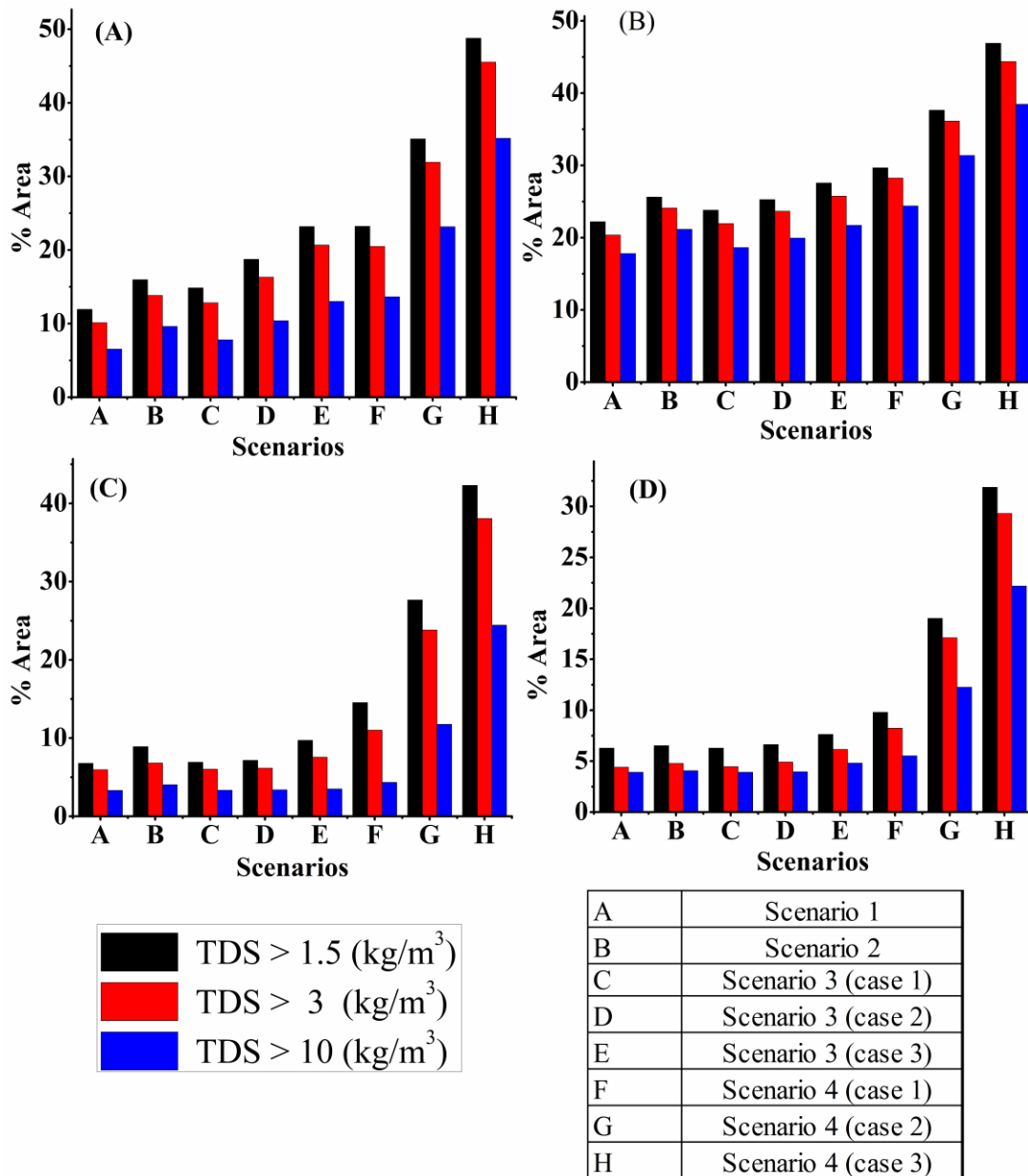


Fig.6.16 Bar graph of percentage area affected by seawater intrusion due to different anticipated scenarios in (A) sub-basin 1 (B) sub-basin 2 (C) sub-basin 3 (D) sub-basin 4

Therefore, scenario 4 (case 3) is considered to be the most unfavourable conditions, rendering 35 % to 45% of the total area unfit for drinking purpose ($TDS > 1.5\text{kg/m}^3$). However, with the present stress conditions continuing for the next 20 years, less than 10% of the total area is predicted to be with $TDS > 1.5\text{ kg/m}^3$, which is considered to be not an alarming situation. But, overdraft by three times the present rate i.e. scenario 3 (case 3) may increase this area beyond 10% for sub-basins 1 and 2. The basins 3 and 4 show their sensitiveness to seawater ingress only due to scenario 4.

6.6 CLOSURE

The calibrated and validated SEAWAT model is applied to evaluate the overall regional impact on the aquifer for five scenarios. The simulation is executed for a reasonably longer period of 20 years (2014-34). The scenarios are planned keeping in view the possible stresses that could be exerted on the aquifer due to exponential growth rate of the region. The effect of sea level rise (1mm/year) due to anticipated climate change effects on the aquifer system is considered. Altogether, this study is framed in such a way that, the combinations of different recharge and pumping activities can be analysed with respect to the aquifer response in the future. Such a study would be of immense importance in the view of utilizing groundwater in a planned and optimal manner, thereby maintaining a sustainable development of groundwater.

The affect of scenario simulation on the aquifer is analysed in different aspects, considering the temporal and spatial variation and variation across a horizontal cross section and finally percentage area suitable for drinking water purpose.

The study reveals that areas within 500m from the river and sea are influenced by seawater intrusion ($TDS > 3\text{kg/m}^3$) except around the Talapady river and continue to aggravate in each scenario. But, the worst case combination of reduced recharge rate with increased pumping rates has a serious impact on the aquifer system with water table sinking below mean sea level in about 60 to 80% of the study area. In this case, seawater intrudes ($TDS > 1.5\text{kg/m}^3$) more than 2km inland from the tidal river and sea making more than 25% of the aquifer water unsuitable for drinking.

Finally, the simulation results show that, anticipated sea level rise has negligible impact on groundwater level and salinity.

CHAPTER 7

SUMMARY AND CONCLUSIONS

The coastal areas have a very fragile freshwater resource base that affects the economy, agriculture and other activities. In many coastal areas, growth of human settlements together with the development of agricultural, industrial and tourist activities have led to the over-exploitation of aquifers. Such over-exploitation induces seawater intrusion in coastal region and there by resulting in the degradation of the quality of groundwater. The problem may be aggravated by the anticipated rise in sea level associated with global warming. Hence, groundwater resources in coastal aquifers will have to be managed in a sustainable manner to overcome the challenges.

The present study is considered up with the focus on the above issue by taking up the simulation of the shallow, coastal aquifer involving seawater and freshwater interactions for the present and future anticipated groundwater developments. The numerical simulation was carried out using SEAWAT. In addition, aquifer characterization was also arrived at through the field tests. The results obtained from the investigation may be useful for scientific assessment of freshwater resources under similar conditions worldwide.

The major conclusions drawn from the investigation are presented below:

AQUIFER CHARACTERIZATION

For the purpose of investigation, the entire basin is divided into four sub-basins depending on the hydraulic boundaries. Pumping tests, bore log and vertical electrical sounding tests were used to evaluate the aquifer parameters.

1. The data from various bore log and VES investigations in the study area confirms that, the basin is predominantly an unconfined aquifer with depth ranging from 12m to 30m. Also, the lateritic formation is topped by sand followed by the top

soil. Beneath the laterite, a huge mass of hard rock material (gneiss) is detected upto a depth of about 90m.

2. The aquifer parameters ie. transmissivity and specific yield evaluated from the pumping tests using Neuman's method range from 15.44 m²/day to 271.40 m²/day and 0.001 to 0.2432 respectively. Compared to other methods of estimation, Neuman's method was found to be more appropriate for the study area. The, aquifer is found to be having moderate to good groundwater potential.

GROUNDWATER FLOW MODEL

The model is built with a finite difference grid size of 100m×100m in the horizontal plane. In the vertical plane, the model follows the top elevation interpolated with the DEM generated. Based on the field tests, the bottom of the model is set at -30m (with respect to mean sea level). Apart from evaluating the seasonal performance of the model with respect to the calibrated parameters, an effort was made to evaluate the spatial distribution of water table, river aquifer interaction and water budget analyses.

1. The RMSE values are usually ≤ 1 m, except that for the monsoon season. This is reasonable for the kind of model developed with the execution of scarcely available input data in the most logical approach.
2. The NSE ≥ 0.5 (except during the monsoon months) demonstrates the ability of the model to simulate the monthly groundwater table with reasonable accuracy both during the calibration and validation process.
3. The values of horizontal hydraulic conductivity and specific yield of the unconfined aquifer is estimated to be in the range 1.85m/day to 49.50 m/day and 0.006 to 0.281 and these values agree with the range established by the aquifer characterization studies carried out earlier. Also, recharge co-efficient of 20% of rainfall, porosity of 30% and river bed conductance of 10 m/day are obtained as appropriate parameters during the calibration process.
4. The spatial distribution of the water table generated by the model for all the four sub-basins are comparable with that of the transmissivity map developed by

krigging technique of interpolation of transmissivity values obtained by different studies. The comparison indicates that, high water table zones coincide with that of low hydraulic conductivity zones and vice versa.

5. The river-aquifer interaction study carried out from the water budget output indicates that, there is greater interaction between the river and aquifer system in the non-monsoon season. During this season, the tidal river carries backwater from the sea, possibly inducing the salinity into the aquifer. It is also established from the river-aquifer interaction study that, river Gurupur contributes significantly to the aquifer of sub-basin 2 may be because, the adjoining area is a low lying land.
6. During the application of MODFLOW, the mass budget shows negligible discrepancy between inflow and outflow ensuring the efficacy of the model. The model also estimates huge flow (75% of available water) out of the aquifer into the sea /river during the monsoon to the extent of 5,000 m³/day to 2,00,000 m³/day, highlighting the perviousness of the aquifer. The river-aquifer interaction indicates constant inflow into the system from the tidal rivers during January to May indicating potential threat of saltwater contamination.

SOLUTE TRANSPORT MODEL

The simulation carried out using MODFLOW incorporated into MT3DMS with SEAWAT model for the area leads to following conclusions:

1. The calibration results show that, the ability of the model to simulate salinity is reasonably good with $NSE \geq 0.5$. The model was performing better during the non-monsoon season than during the monsoon season.
2. Longitudinal dispersivity of 35m, transverse dispersivity of 3.5m and molecular diffusion co-efficient of $8.64 \times 10^{-5} \text{m}^2/\text{day}$ are achieved during calibration of transport model.
3. The calibration results indicate that, the study area remains safe against seawater intrusion (TDS < 1500 ppm) for the present scenario of groundwater draft.

However, the locations very close to the saline source (<500m) tend to bring in salinity of the order >1500 ppm throughout the year, which is confirmed by the observations.

4. From the results, it was also evident that, the tidal behaviour of the rivers play an equally significant role as that of the sea in causing seawater intrusion into the aquifer especially during October to May.
5. The management of freshwater aquifers within 1 km from the sea is of prime importance for sustainability against seawater intrusion. It can be concluded from the study that, areas in and around the industrial area, Panambur, are most sensitive to seawater intrusion because of the influence of the sea and the river water salinity.

SENSITIVITY ANALYSIS

The response of the coastal aquifer to various flow parameters (recharge rate, horizontal hydraulic conductivity, specific yield, and river bed conductance) and transport parameter (longitudinal dispersivity) is also investigated. The conclusions drawn based on this study are:

1. The sensitivity analysis results clearly show that, the model is sensitive to lower values of hydraulic conductivity (0.46 m/day to 12.40 m/day) and higher values of recharge rate (28 mm/day). Specific yield was found to be a sensitive parameter for sub-basin 1 and 3. This could be due to the presence of higher drainage density across the basin unlike sub-basin 2 and 4.
2. Except for sub-basin 1 and the zones adjacent to the river flow, no significant influence of river bed conductance on the groundwater table is noticed.
3. The aquifer was found to be least sensitive to dispersivity, with the movement of salinity contour by just 10m for every increase in 25% of the dispersivity value.

PREDICTIVE SIMULATION

The SEAWAT was applied to simulate the future anticipated scenarios of increase in groundwater draft and sea level rise. The conclusions drawn based on 20 year simulation are:

1. The anticipated sea level rise of 1mm/year along the coastline has negligible influence on groundwater and salinity of the study area.
2. The topography of sub-basin 3 plays a role in falling water table compared to relatively flatter other sub-basins. The water table falls by about 1.5m for every 50% increase in the groundwater utilization rate in sub-basin 3, which is less than 1 m in the rest of the basins.
3. The simulation results show that, the wells within 500m from the sea and rivers are highly saline with $TDS > 3\text{kg/m}^3$ which was also confirmed with field observations. Hence, any developments in the region should be totally avoided.
4. The water table falls below mean sea level in about 60 to 80% of the study area, due to steep increase in groundwater draft (2 to 3 times present withdrawal rate) coupled with decreased recharge rate.
5. The water table indicates a considerable depletion for 50% reduction in recharge rate spatially. However, at that point of time, seawater ingress doesn't advance proportionally except that near the river and sea boundary. This could be due to lag in the response of seawater intrusion for falling water table.
6. With the existing groundwater draft, aquifer is safe for the regions beyond 500m from saline source. In these cases, water salinity is within a range of $TDS < 1.5\text{ kg/m}^3$.
7. The aquifer was also found to be sustainable against seawater intrusion ($TDS < 1.5\text{ kg/m}^3$) for scenarios 2, 3 and scenario 4 (case 1) beyond 600m from the sea and river.

8. The decrease in recharge rate causes a severe threat to the groundwater quality compared to doubling of groundwater draft in about 15 years of operation. Increase in groundwater draft by 2 to 3 times along with 50% decrease in recharge rate causes TDS=1.5kg/m³ line progressing upto 1 to 2 km from sea as well from the river boundary.

LIMITATIONS OF THE STUDY

1. In the present work, the domain is considered to vertically homogeneous up to the bottom.
2. The model performance during the monsoon (June to Sept) is not up to the mark, with all the three evaluation techniques showing deviation from the desired levels. There could be greater interaction / increased inflow between river water with seawater during these months, which is not well addressed by the model.
3. The model was validated at a few locations only due to the non-availability of spatially and temporally spread field observations.
4. The recharge considered in the model is during the period of monsoon (June to September). Any additional recharge during other period is not accounted in the model.
5. The locations of pumping wells are fixed as per the available data. And while carrying predictive simulations, the pumping rate is increased uniformly for all the wells.

SCOPE FOR FUTURE STUDIES

1. Effort could be made to refine the three dimensional model incorporating all the relevant details of sub-strata.
2. The database of the wells in the regions for withdrawal rate, water level and quality could be maintained for a sufficiently longer period for better calibration and validation of numerical simulations.

REFERENCES

- Abdulla, F. and Al-Assad, T. (2006). "Modeling of groundwater flow for Mujib aquifer, Jordan." *J. Earth Sys. Sci.*, 115(3), 289-297.
- Abdulla, F. A., Al-Khatib, M. A. and Al-Ghazzawi, Z. D. (2000). "Development of groundwater modeling for the Azraq Basin, Jordan." *Environ. Geol.*, 40, 1-2.
- Abdalla, O.A.E. (2009). "Groundwater modeling in semiarid Central Sudan: adequacy and long-term abstraction." *Arab J. Geosci.*, 2, 321–335.
- Adrian, D., Werner, J.D., Ward, L. K., Morgan, C. T., Simmons, N. I., Robinson, M. D. and Teubner, M. D. (2012). "Vulnerability indicators of seawater intrusion." *Ground Water*, 50 (1), 48-58.
- Aggarwal, R., Sondhi, S. K., Jain, A. K. and Kaushal, M. P. (2005). "Groundwater simulation model for South-West Punjab." *IE(I) Journal –AG*, 86(2),18-23.
- Ahmed, I. and Umar, R. (2009). "Groundwater flow modelling of Yamuna–Krishniinterstream, a part of central Ganga Plain Uttar Pradesh." *J. Earth Sys. Sci.*, 118 (5), 507–523.
- Allow, K. A. (2012). "The use of injection wells and a subsurface barrier in the prevention of seawater intrusion:a modelling approach." *Arab J. Geosci.*, 5, 1151-1161.
- Al-Salamah, I. S., Ghazaw, Y. M. and Ghumman, A. R. (2011). "Groundwater modeling of Saq Aquifer Buraydah Al Qassim for better water management strategies." *Environ. Monit. Assess.*, 173(1-4), 851-860.

- Amer, A. M. (1995). "Saltwater intrusion in coastal aquifers." *Proc., Int. Conf. on Water Resources Management in Arid Countries*, Muscat, 521–529. In: Shamma, M. I and Jacks, G. (2007). "Seawater intrusion in the Salalah plain aquifer, Oman." *Environ. Geol.*, 53, 575–587.
- Anderson, M. and Woessner, W. (1992). "Applied groundwater modeling simulation of flow and advective transport.", *Academic Press*, San Diego, CA, 381pp.
- Antonellini, M., Allen, D. M., Mollema, P. N., Capo, D. and Greggio, N. (2015). "Groundwater freshening following coastal progradation and land reclamation of the Po Plain, Italy." *Hydrogeol J.*, 23(5), 1009-1026.
- Arlai, P., Koch, M. and Koontanakulvong, S. (2006). "Statistical and stochastic approaches to assess reasonable calibrated parameters in a complex multi-aquifer system", In: *Proc. of CMWR XVI - Computational Methods in Water Resources*, Copenhagen, Denmark.
- Asghar, M. N., Prathapar, S. A. and Shafique, M. S. (2002). "Extracting relatively fresh groundwater from aquifers underlain by salty groundwater." *Agr. Water Manag.*, 52, 119–137.
- Ataie-Ashtiani, B., Volker, R. E. and Lockington, D. A. (1999). "Tidal effects of seawater intrusion in unconfined aquifers." *J. Hydrol.*, 216, 17-31.
- Ayenu, T., Demlie, M. and Wohnlich, S. (2008). "Application of Numerical Modeling for Groundwater Flow System Analysis in the Akaki Catchment, Central Ethiopia." *International Association for Mathematical Geology*, 40, 887–906.

- ASCE, 1993. "Criteria for evaluation of watershed models." *J. Irrigation Drainage Eng.*, 119(3), 429-442.
- Bauer, P., Held, R. J., Zimmermann, S., Linn, F. and Kinzelbach, W. (2006). "Coupled flow and salinity transport modelling in semi-arid environments: The Shashe river valley, Botswana." *J. Hydrol.*, 316, 163-183.
- Bear, J., Cheng, A .H.D., Sorek. S., Ouazar, D. and Herrera, I. (1999). "Seawater intrusion in coastal aquifers: concepts, methods and practices." *Theory and Applications of Transport in Porous Media*, 14. Kluwer, Dordrecht, Netherlands.
- Bhosale, D.D. and Kumar, C.P. (2001). "Simulation of seawater intrusion in Ernakulam coast ." (<http://www.angelfire.com/nh/cpkumar/publication/ernac.pdf>), Dec. 8, 2013.
- Bobba, A. G. (2002). "Numerical modelling of salt-water intrusion due to human activities and sea-level change in the Godavari Delta, India." *Hydrolog. Sci. J*, 47, 67-80.
- Boulton, N. S. (1954). "Unsteady radial flow to a pumped well allowing for delayed yield from storage." *Intern. Assoc. Sci. Hydrol. Rome. Publ.* 37, 472-477.
- Boulton, N. S. (1963). "Analysis of data from non-equilibrium pumping tests allowing for delayed yield from storage." *Proc., Inst. Civ. Eng., USA*, 26, 469-482.
- Boulton, N. S. (1970). "Analysis of data from pumping tests in unconfined anisotropic aquifers." *J. Hydrol.*, 10, 369-378.

- Boulton, N. S. and Pontin, J. M. A. (1971), “An extended theory of delayed yield from storage applied to pumping tests in unconfined anisotropic aquifers.” *J. Hydrol.*, 14, 53–65.
- Boulton, N. S. and Streltsova, T. D. (1975). “The drawdown near an abstraction well of large diameter under non-steady conditions in an unconfined aquifer.” *J. Hydrol.*, Vol. 30, 29-46.
- Brunner, P., Hendricks, F. H. J., Kgotlhang, L., Bauer-Gottwein, P. and Kinzelbach, W. (2006). “How can remote sensing contribute in groundwater modeling?.” *Hydrogeol J.*, 15(1), 5–18.
- Camp, V. M., Mjemah, I. C., Al Farrah, N. and Walraevens, K. (2013). “Modeling approaches and strategies for data-scarce aquifers: example of the Dar es Salaam aquifer in Tanzania.” *Hydrogeol J.*, 21(2), 341-356.
- Carrera, J., Hidalgo, J. J., Slooten, L. J. and Vázquez-Suñé, E. (2010). “Computational and conceptual issues in the calibration of seawater intrusion models.” *Hydrogeol J.*, 18(1), 131-145.
- Chaaban, F., Darwishe, H., Louche, B., Battiau-Queney, Y., Eric Masson., El Khattabi, J. and Carlier, E. (2012). “Geographical information system approach for environmental management in coastal area (Hardelot-Plage, France).” *Environ. Earth Sci.*, 65,183–193.
- Chang, S. W. and Clement, T. P. (2013). “Laboratory and numerical investigation of transport processes occurring above and within a saltwater wedge.” *J. Contam. Hydrol.*, 147, 14-24.
- Chekirbane, A., Tsujimura, M., Kawachi, A., Isoda, H., Tarhouni, J. and Benalaya, A. (2015). “3D simulation of a multi-stressed coastal aquifer, northeast of

Tunisia: salt transport processes and remediation scenarios." *Environ. Earth Sci.*, 73(4), 1427-1442.

Cobaner, M., Yurtal, R., Dogan, A., and Motz, L. H. (2012). "Three dimensional simulation of seawater intrusion in coastal aquifers: A case study in the Goksu deltaic plain." *J. Hydrol.*, 262-280.

Comte, J. C., Join, J. L., Banton, O. and Nicolini, E. (2014). "Modelling the response of fresh groundwater to climate and vegetation changes in coral islands." *Hydrogeol. J.*, 22(8), 1905-1920.

Cooper, H. H. Jr., Kohout, F. A., Henry, H. R. and Glover, R. E. (1964). "Sea water in coastal aquifers." *US Geol Surv Water Supply*, 1613-1626.

Coppola, E. A., Anthony, J. R., Mary M. P., Ferenc, S. and Vincent, W. U. (2005). "A neural network model for predicting aquifer water level elevations." *Ground Water*, 43(2), 231-241.

Custodio, E. and Galofre, A. (1992). "Study and modeling of saltwater intrusion into aquifers." *Proc. of the saltwater intrusion meeting*, Barcelona, Spain. CIMNE Publisher.

CGWB (2008). Central Groundwater Board. "Groundwater resources and development potential of Dakshina Kannada district, Karnataka." (AAP 2004-2005), *Govt. of India, Ministry of Water Resources*, South western region, Bangalore.

CGWB (2012), Central Ground Water Board. "Groundwater information booklet, Dakshina Kannada district, Karnataka." *Govt. of India, Ministry of Water Resources*, South western region, Bangalore, pp-18.

- Dagan, G. (1967). "A method of determining the permeability and effective porosity of unconfined anisotropic aquifers." *Water Resour. Res.*, 3(4), 1059-1071.
- De Louw, P. G., Eeman, S., Siemon, B., Voortman, B. R., Gunnink, J., Van Baaren, E. S. and Essink, O.G. (2011). "Shallow rainwater lenses in deltaic areas with saline seepage." *Hydrol. Earth Syst. Sci.*, 15, 3659-3678.
- Diersch, H.J.G (2006). "FEFLOW 5.3: Finite element subsurface flow and transport simulation system user manual version 5.3." Berlin Germany: WASY GmbH Institute for Water Resources Planning and Systems Research. In: Loaiciga, H. A., Pingel, T. J. and Garcia, E. S. (2012). "Seawater intrusion by sea-level rise: Scenarios for the 21st century." *Ground Water*, 50 (1), 37-47.
- Doherty, J. (2004). "PEST- Model Independent Parameter Estimation, User manual." Watermark Numerical Computing.
- Duffield, G. M. (2007). "AQTESOLV for Windows Version 4.5 User's Guide." *Hydro SOLVE, Reston, VA.*
- Dufresne, D. P. and Drake, C.W. (1999). "Regional groundwater flow model construction and wellfield site selection in a karst area, Lake City, Florida." *Eng.Geol.*, 52, 129–139.
- El-Bihery, M. A (2009). "Groundwater flow modeling of Quaternary aquifer Ras Sudr, Egypt." *Environ. Geol.*, 58, 1095–1105.
- El-Kadi, A. I., Tillery, S., Whittier, R. B., Hagedorn, B., Mair, A., Ha, K. and Koh, G. W. (2014). "Assessing sustainability of groundwater resources on Jeju Island, South Korea, under climate change, drought, and increased usage." *Hydrogeol. J.*, 22(3), 625-642.

- Essink, G.H.P. (1998). "MOC3D adapted to simulate 3D density-dependent groundwater flow." In: *Proc. of the MODFLOW'98 Conference Golden, CO, USA*, 291-303.
- Essink, G. O. (2001). "Improving fresh groundwater supply: problems and solutions." *Ocean Coast. Manage.*, 44, 429–449.
- Feseker, T. (2007). "Numerical studies on saltwater intrusion in a coastal aquifer in northwestern Germany." *Hydrogeol. J.*, 15, 267-279.
- Freeze, R. A and Cherry, J. A. (1979). "Groundwater", Prentice-Hall Inc., Eaglewood N.J.
- Fried, J. J. and Combamous, M. A. (1971). "Dispersion in porous media." *Adv. Hydrosci.*, 7, 420-435.
- Gates, T. K., Burkhalter, J., John, W. L., James, C. V. and Broner, I. (2002). "Monitoring and Modeling Flow and Salt Transport in a Salinity-Threatened Irrigated Valley." *J. Irrig. Drain. Eng.*, 128(2), 87-99.
- Geyh, M. A. and Soefner, B. (1996). "Groundwater mining study by simplified collection in the Jakarta Basin aquifer, Indonesia." *Isotopes in Water Resources Management*. IAEA, *The International Atomic Energy Agency*, Vienna, 174–176. In: Shamma, M. I. and Jacks, G. (2007). "Seawater intrusion in the Salalah plain aquifer, Oman." *Environ. Geol.*, 53, 575–587.
- Gholami, V., Zabihollah, Y and Hosseinali, Z, R. (2010). "Modeling of Ground Water Salinity on the Caspian Southern Coasts." *Water Resour. Manag.*, 24, 1415–1424.

- Giambastiani, M. B., Antonellini, M., Essink, G. H. and Stuurman, R. J. (2007). "Saltwater intrusion in the unconfined coastal aquifer of Ravenna (Italy): A numerical model." *J. Hydrol.*, 340, 91-104.
- Green, N.R. and MacQuarrie, K. T. B (2014). "An evaluation of the relative importance of the effects of climate change and groundwater extraction on seawater intrusion in coastal aquifers in Atlantic Canada." *Hydrogeol. J.*, 22, 609-623.
- Guo, W. and Bennett, G. D. (1998). "SEAWAT version 1.1—A computer program for simulations of ground water flow of variable density." *A report prepared by Missimer International Inc.*
- Guo,W and Langevin,C.D (2002). "User's Guide to SEAWAT: A Computer Program for Simulation of Three-Dimensional Variable-Density Ground-Water Flow." U.S. Geological Survey *Techniques of Water Resources Investigations of the USGS, Book 6, Chapter A7*, 87.
- GEC (1997). "Groundwater Resource Estimation Methodology." *Report of the Groundwater Resource Estimation Committee*, Ministry of Water Resources, Government of India, New Delhi.
- Harbaugh, A. W., Banta, E. R., Hill, M. C. and McDonald, M. G. (2000). "MODFLOW-2000, the U.S. Geological Survey Modular Ground-Water Model—User guide to modularization concepts and the ground-water flow process." *U.S. Geological Survey, Open-File Report 00-92*.
- Harshendra, K. (1991). "Studies on water quality and soil fertility in relation to crop yield in selected river basins of D.K. District of Karnataka State." Ph.D. Thesis, Mangalore University, Karnataka, India.

- Haque , Al Mamunul, M., Jahan, C.S., Mazumder, Q.H., Nawaz, S.M.S., Mirdha, G.C., Mamud, P and Adham, M.I. (2012). “Hydrogeological Condition and Assessment of Groundwater Resource Using Visual Modflow Modeling, Rajshahi City Aquifer, Bangladesh.” *J. Geol. Soc. India*, 79, 77-84.
- Hill, M. C. (1990). “Preconditioned conjugate-gradient 2 (PCG2), a computer program for solving ground-water flow equations”. Department of the Interior, US Geological Survey, 90-4048.
- INCCA (2010). “Indian Network for Climate Change Assessment 2010 Climate change and India: A 4X4 Assessment sectoral and regional analysis for 2030s.” *Ministry of Environment & Forests Government of India*. (<http://www.moef.nic.in/downloads/public-information/fin-rpt-incca.pdf>) (April 17, 2015).
- IPCC (2008). “Intergovernmental Panel on Climate Change.” *Technical Paper VI- Climate Change and Water*, Bates B.C, Kundzewicz S. Wu and J.P Palutik of, Eds, 210 pp. (<http://www.ipcc.ch/pdf/technical-papers/climate-changewater-en.pdf>) (August 4, 2014).
- Jacob, C. E. (1963). “Correction of drawdowns caused by a pumped well tapping less than the full thickness of an aquifer.” *Methods of determinig permeability, transmissivity and drawdown*. US Geol. Survey, Water-Supply paper, 272-282.
- Jayappa, K. J. (1991). "A textural and mineralogical study of the beach sands between Talapady and Surathkal." *J. Geotech. Soc. India*, 37, 151-163.
- Juckem, P.F, Hunt, R.J. and Anderson, M. P. (2006). “Scale effects of hydrostratigraphy and recharge zonation on base flow.” *Ground Water*, 44 (3), 362- 370.

- Karant, K. R. (1987). "Ground water assessment: development and management." Tata McGraw-Hill Education.
- Kelbe, B. E., Grundling, A. T. and Price, J. S. (2016). "Modelling water-table depth in a primary aquifer to identify potential wetland hydrogeomorphic settings on the northern Maputaland Coastal Plain, KwaZulu-Natal, South Africa." *Hydrogeol. J.*, 1-17.
- Kerrou, J., Renard, P., Cornaton, F. and Perrochet, P. (2013). "Stochastic forecasts of seawater intrusion towards sustainable groundwater management: application to the Korba aquifer (Tunisia)." *Hydrogeol. J.*, 21(2), 425-440.
- Kerrou, J., Renard, P. and Tarhouni, J. (2010). "Status of the Korba groundwater resources (Tunisia): observations and three-dimensional modelling of seawater intrusion." *Hydrogeol. J.*, 18(5), 1173-1190.
- Kipp, K. L. Jr. (1973). "Unsteady flow to partially penetrating, finite radius well in an unconfined aquifer." *Water Resour. Res.*, 9(2), 448-462.
- Kipp, K. L. (1986). "HST3D—A computer code for simulation of heat and solute transport in 3D ground water flow systems." *US Geological Survey, Water resources Investigations*. Report 86-4095.
- Kopsiaftisa, G., Mantoglou, A. and Giannoulou, P. (2009). "Variable density coastal aquifer models with application to an aquifer on Thira Island." *J. Desal.*, 237, 65-80.
- Kruseman, G.P. and Ridder, N. A. (1994). "Analysis and Evaluation of Pumping Test Data (2nd ed.)", Publication 47, *Intern. Inst. for Land Reclamation and Improvement*, Wageningen, The Netherlands, 370p.

- Kumar, R.B.C. (2010). "Modelling regional actual evapotranspiration over Netravathi basin using satellite data". M.Tech. Thesis, National Institute of Technology Karnataka, Surathkal, Mangalore, India.
- Kumar, A., Jayappa, K.S. and Deepika, B. (2011). "Application of remote sensing and geographic information system in change detection of the Netravati and Gurpur river channels, Karnataka, India." *Geocarto Int.*, 25 (5), 397–425.
- Kushwaha, R. K., Pandit, M.K. and Rohit, G. (2009). "MODFLOW Based Groundwater Resource Evaluation and Prediction in Mendha Sub-Basin, NE Rajasthan." *J. Geol. Soc. India*, 74, 449-458.
- Lachaal, F., Mlayah, A., Be´dir, M., Tarhouni, J. and Christian, L. (2012). "Implementation of a 3-D groundwater flow model in a semi-arid region using MODFLOW and GIS tools:The Ze´ramdine–Be´ni Hassen Miocene aquifer system (east–central Tunisia)." *Comput. Geosci.*, 48, 187-198.
- Langevin, C. D. (2003). "Simulation of submarine groundwater discharge to a marine estuary:Biscayne Bay,Florida." *Ground Water*, 41 (6), 758-771.
- Langevin, C .D., Shoemaker, WB. and Guo, W. (2003). "MODFLOW-2000, the U.S. Geological Survey Modular Ground-Water Model", *Documentation of the SEAWAT-2000 version with the variable density flow process (VDF) and the integrated MT3DMS Transport Process (IMT)*. USGS Open-File Report 03-426.
- Langevin, C., Thorne, D., Dausman, A., Sukop, M. and Guo, W. (2008). "SEAWAT Version 4: A Computer Program for Simulation of Multi-Species Solute and Heat Transport." *U.S. Geological Survey Techniques and Methods*, Book 6, Chapter A22.

- Langevin, C.D. and Guo, W. (1999). "Improvements to SEAWAT, a variable density modeling code." *Eos Trans*, 80(46), F-373.
- Langevin, C. D. and Guo, W. (2006). "MODFLOW/MT3DMS–Based Simulation of Variable-Density Ground Water Flow and Transport." *Ground Water*, 44(3), 339-351.
- Langevin, C. D. and Zygnerski, M. (2013). "Effect of sea-level rise on saltwater intrusion near a coastal well field in Southeastern Florida." *Ground Water*, 51 (5), 781-803.
- Leake, S. A. and Prudic, D. E. (1991). "Documentation of a computer program to simulate aquifer-system compaction using the modular finite-difference ground-water flow model." *US Department of the Interior*, US Geological Survey.
- Lenhart, T., Eckhardt, K., Fohrer, N. and Frede, H. G. (2002). "Comparison of two different approaches of sensitivity analysis." *Phys.Chem. Earth*, 27(9-10), 645-654.
- Li, W., Liu, Z., Guo, H., Li, N. and Kang, W. (2011). "Simulation of a groundwater fall caused by geological discontinuities." *Hydrogeol. J.*, 19, 1121–1133.
- Lin, J.J., Snodsmith, B. and Zeng, C. (2009). "A modeling study of seawater intrusion in Alabama Gulf coast, USA." *Environ. Geol.*, 57, 119-130.
- Lin, Y.C. and Medina, Jr. M. A. (2003). "Incorporating transient storage in conjunctive stream–aquifer modelling." *Adv. Water Resour.*, 26, 1001–1019.

- Liu, C. W., Yen-Lu, C., Shien-Tsung, L., Gin-Jie, Lin. and Cheng-Shin, J. (2010). "Management of High Groundwater Level Aquifer in the Taipei Basin." *Water Resour. Manag.*, 24, 3513–3525.
- Loaiciga, H. A., Pingel, T. J. and Garcia, E. S. (2012). "Seawater intrusion by sea-level rise: Scenarios for the 21st century." *Ground Water*, 50 (1), 37-47.
- Lokesh, K. N. (1997). "Some principles and methods for mineral exploration: An overview." National Seminar on Emerging Technology in Surface Mining and Environmental Challenges, Dept. of Mining Engineering, Karnataka Regional Engineering College, Surathkal, India, 63–66.
- Louwyck, A., Vandenbohede, A., Bakker, M. and Lebbe, L. (2014). MODFLOW procedure to simulate axisymmetric flow in radially heterogeneous and layered aquifer systems. *Hydrogeol. J.*, 22(5), 1217-1226.
- Mahesha, A and Lakshmikant, P. (2014). "Saltwater intrusion in coastal aquifers subjected to freshwater pumping." *J.Hydrol.Engg., ASCE*, 17 , 448-456.
- Mahesha, A., Vyshali, Lathashri, U. A. and Ramesh, H. (2012). "Parameter estimation and vulnerability assessment of coastal unconfined aquifer to saltwater intrusion." *J.Hydrol.Engg., ASCE*, 17 (8), 933-943.
- Manghi, F., Dennis, W., Jack, S. and Moshrik, R. H. (2012). "Groundwater Flow Modeling of the Arlington Basin to Evaluate Management Strategies for Expansion of the Arlington Desalter Water Production." *Water Resour. Manag.*, 26, 21–41.
- Mao, X.S., Jia, J.S., Liu, C.M. and Hou, Z.M. (2005). "A simulation and prediction of agricultural irrigation on groundwater in well irrigation area of the piedmont of Mt. Taihang, North China." *Hydrol. Process*, 19(10), 2071–2084.

- Martinez-Santos, P., Ramon, M. L. and Pedro, E. M. (2008). "Vulnerability assessment of groundwater resources: A modelling-based approach to the Mancha Occidental aquifer, Spain." *Environ. Model. Softw.*, 23, 1145-1162.
- Mathias, S. A. and Butler, A. P. (2006). "Linearized Richards' equation approach to pumping test analysis in compressible aquifers." *Water Resour. Res.*, 42(6).
- McDonald, M. G. and Harbaugh, A.W. (1988). "A modular three dimensional finite-difference groundwater flow model." *USGS Open File Report*, 83-875.USGS, Washington, D.C.
- Moench, A. F. (1995). "Combining the Neuman and Boulton models for flow to a well in an unconfined aquifer." *Ground Water*, 33(3), 378-384.
- Mollema, P. N., & Antonellini, M. (2013). Seasonal variation in natural recharge of coastal aquifers. *Hydrogeol. J*, 21(4), 787-797.
- Moriasi, D. N., Arnold, J. G., Van Liew, M. W., Bingner, R. L., Harmel, R. D. and Veith, T. L. (2007). "Model evaluation guidelines for systematic quantification of accuracy in watershed simulations." *Trans. Asabe*, 50(3), 885-900.
- Moustadraf, J., Razack, M. and Sinan, M. (2008). "Evaluation of the impacts of climate changes on the coastal Chaouia aquifer, Morocco, using numerical modelling." *Hydrogeol. J*, 16, 1411-1426
- Narasimhan, T. N. and Zhu, M. (1993). "Transient flow of water to a well in an unconfined aquifer-applicability of some conceptual models." *Water Resour. Res.*, 29 (1), 179-191.

- Narayan, K. A., Schleeberger, C. and Bristow, K. L. (2007). "Modelling seawater intrusion in the Burdekin Delta irrigation area, North Queensland, Australia." *Agric. Water Manage.*, 89, 217-228.
- Neuman, S.P. (1972). "Theory of flow in unconfined aquifers considering delayed response of the water table." *Water Resour. Res.*, 8(4), 1034-1044.
- Neuman, S.P. (1974). "Effects of partial penetration on flow in unconfined aquifers considering delayed aquifer response." *Water Resour. Res.*, 10(2), 303-312.
- Neuman, S.P. (1975). "Analysis of pumping test data from anisotropic unconfined aquifers considering delayed gravity response." *Water Resour. Res.*, 10(2), 303-312
- Nowbuth, M. D., Rambhojun, P and Bhavana, U. (2012). "Numerical groundwater flow and contaminant transport modeling of the southern aquifer, Mauritius." *Earth Sci. India*, 5(3), 79-91.
- NBSS&LUP. (1998). "National Bureau of soil survey and land use planning (Indian council of agricultural research). Soils of Karnataka for optimising land use." *State soil survey, department of agriculture*, Bangalore, Karnataka. NBSS Publ.47.
- Palma, H.C. and Bentley, L.R. (2007). "A regional-scale groundwater flow model for the Leon-Chinandega aquifer, Nicaragua." *Hydrogeol. J.*, 15, 1457-1472.
- Panagopoulos, G. (2012). "Application of MODFLOW for simulating groundwater flow in the Trifilia karst aquifer, Greece." *Environ. Earth Sci.*, 6, 425-438.
- Park, S. U., Kim, J. M., Yum, B. W. and Yen, G. T. (2012). "Three-dimensional numerical simulation of saltwater extraction schemes to mitigate seawater

intrusion due to groundwater pumping in a coastal aquifer system." *J. Hydrol. Engg., ASCE*, 17, 10-22.

Perkins, S. P. and Marios, S. (1999). "Development of a comprehensive watershed model applied to study stream yield under drought conditions." *Ground Water*, 37(3), 418-426.

Pinder, G. F., Cooper, H. H. Jr. (1970). "A numerical technique for calculating the transient position of the saltwater front." *Water Resour Res*, 9, 1657–1669.

Pisinaras.V., Petalas. C., Tsihrintzis.V.A. and Zagana. E. (2007). "A groundwater flow model for water resources management in the Ismarida plain, North Greece." *Environ. Model. Assess.*, 12, 75-89.

Post, V.E.A. (2011). "A new package for simulating periodic boundary conditions in MODFLOW and SEAWAT." *Comput Geosci.*, 37, 1843–1849.

Praveena, S. M., Abdulla, M. H., Aris, A. Z., Yik, L. C. and Bidin. (2011). "Numerical modeling of seawater intrusion in Manukan Island Aquifer." *Resear. World Appl .Sci. J*, ISSN 1818-4952.

Qahman, K. and Larabi, A. (2006). "Evaluation and numerical modeling of seawater intrusion in the Gaza aquifer (Palestine)." *Hydrogeol. J.*, 14, 713-728.

Radheshyam, B.(2009). "Study of coastal processes and solution to erosion problems in the vicinity of Netravathi-Gurupur river estuary - A modelling approach." Ph.D. thesis, National Institute of Technology, Karnataka, Surathkal, India.

Rahnama, M.B. and Zamzam, A. (2011). "Quantitative and qualitative simulation of groundwater by mathematical models in Rafsanjan aquifer using MODFLOW and MT3DMS." *Arab. J. Geosci*, DOI 10.1007/s12517-011-0364-x.

- Ranganna, G., Gurappa, K, M., Gajendragad, M, R. and Chandrakantha, G. (1986). “Hazardous effects of groundwater pollution and mitigative measures thereof.” *Report submitted by Department of Applied Mechanics and Hydraulics, NITK, Surathkal to the Department of Environment, Government of India*,128.
- Rao, B. N. (1974). "Geotechnical investigations of the marine deposits in the Mangalore harbor project." *Indian Geotech. J*, 4 (1), 78-92.
- Rao. S.V.N , Murty, B. S., Thandaveswara, B.S. and Sreenivasulu .V. (2005). “Planning Groundwater Development in Coastal Deltas with Paleo Channels.” *Water Resour. Manag.*, 19, 625–639.
- Rajgopalan, S. P., Prabhashankar, P. N. and Balakrishnan, V. (1983). “Pumping test and analysis data of open wells in the coastal tract of Kozikode district”, *GW/R-56/83*. Centre for Water Resour. Develop. Mgmt. Kozikode, Kerala, 43.
- Rao, S. V. N., Sreenivasulu, V., Bhallamudi, S. M., Thandaveswara, B. S. and Sudheer, K. P. (2004). “Planning groundwater development in coastal aquifers/Planification du développement de la ressource en eau souterraine des aquifères côtiers.” *Hydrolog. Sci. J.*, 49(1), 155-170.
- Reeve, A.S., Warzocha. J., Glaser, P.H. and Siegel.D.I. (2001). “Regional groundwater flow modeling of the Glacial Lake Agassiz Peatlands, Minnesota.” *J. Hydrol.*, 243, 91–100.
- Rejani. R, Madan K. Jha , Panda.S.N and Mull. R (2008). “Simulation modeling for efficient groundwater management in Balasore Coastal Basin, India.” *Water Resour. Manag.*, 22, 23–50.

- Rojas, R. and Dassargues, A. (2007). "Groundwater flow modelling of the regional aquifer of the Pampa del Tamarugal, northern Chile." *J. Hydrol*, 15, 537–551.
- Rozell, D. J. and Wong, T. F. (2010). "Effects of climate change on groundwater resources at Shelter Island, New York State, USA." *Hydrogeol J* , 18(7), 1657-1665.
- Rushton, K. (2007). "Representation in regional models of saturated river–aquifer interaction for gaining/losing rivers." *J. Hydrol*, 334(1), 262-281.
- Sakiyan, J. and Yazicigil, H. (2004). "Sustainable development and management of an aquifer system in western Turkey." *Hydrogeol J*, 12, 66–80.
- Sanford, W. E. and Konikow, L. F. (1985). "A two-constituent solute-transport model for ground water having variable density." *US Geol Surv Water Resour Invest Rep.* 85-4279.
- Santhi, C. J. G., Arnold, J. R., Williams, W. A., Dugas, R., Srinivasan. and Hauck, L.M. (2001). "Validation of the SWAT model on a large river basin with point and nonpoint sources." *J. Am. WaterResour. Assoc.*,37(5), 1169-1188.
- Santhosh, K.C. (2011). "Groundwater flow and transport modeling of Pavanje basin using GMS." M.Tech, Thesis, Department of Applied Mechanics & Hydraulics, National Institute of Technology Karnataka, Surathkal, Mangalore.
- Sanz, D., Santiago, C., Eduardo, C., Andres, S., Juan, J. G. A., Salvador, P. and Alfonso, C. (2011). "Modeling aquifer–river interactions under the influence of groundwater abstraction in the Mancha Oriental System (SE Spain)." *Hydrogeol. J*, 19, 475–487.

- Sedki, A. and Ouazar, D. (2011). "Simulation-Optimization Modeling for Sustainable Groundwater Development: A Moroccan Coastal Aquifer Case Study." *Water Resour. Manag*, 25, 2855–2875.
- Segol, G. and Pinder, G. F. (1976). "Transient simulation of saltwater intrusion in southeastern Florida." *Water Resour. Res.*, 12, 65–70.
- Senthilkumar, M. and Elango, L. (2004). "Three-dimensional mathematical model to simulate groundwater flow in the lower Palar River basin, southern India." *Hydrogeol. J*, 12(2), 197-208.
- Senthilkumar, M. and Elango, L. (2011). "Modelling the impact of a subsurface barrier on groundwater flow in the lower Palar River basin, southern India." *Hydrogeol. J*, 19, 917–928.
- Shammas, M.I. and Thunvik, R. (2009). "Predictive simulation of flow and solute transport for managing the Salalah coastal aquifer, Oman." *Water Resour. Manag.*, 23(3), 2941-2963.
- Sherif, M. (1999). "Seawater intrusion in the Nile delta aquifer-An overview." 296-308. <http://aquas.igme.es/igme/publica/tiac-02/EGIPTO-Ipdf>>(June5,2006)
- Sherif, M., Kacimov, A., Javadi, A. and Ebraheem, A. A. (2012). "Modeling groundwater flow and seawater intrusion in the coastal aquifer of Wadi Ham, UAE." *Water Resour. Manag.*, 26, 751-774.
- Shetkar, R. V. (2008). "Studies on the efficacy of vented dams as water harvesting structures across the river Netravathi of D.K. district, Karnataka." Ph.D. thesis, National Institute of Technology, Karnataka, Surathkal, India.

- Shetkar, R.V. and Mahesha, A. (2011). "Tropical, seasonal river basin development: Hydrogeological analysis." *J. Hydrol. Engg., ASCE*, 16(3), 280-291.
- Shivanagouda. H. S. (2015). "Studies on aquifer characterization and seawater intrusion vulnerability assessment of coastal Dakshina Kannada district, Karnataka." Ph.D. Thesis, National Institute of Technology Karnataka, Surathkal India,184.
- Simpson, M. J. (2004). "SEAWAT-200:Variable –density flow processes and integrated MT3DMS transport processes." *Ground Water*, 42(5), 642-645.
- Sindhu, G., Ashitha, M., Jairaj, P.G. and Rajesh, R. (2012). "Modelling of Coastal Aquifers of Trivandrum". *Proc. Engineering*, 38, 3434 – 3448.
- Singh, S. K. (2006). "Semi-analytical model for drawdown due to pumping a partially penetrating large diameter well", *J. Irrig. Drain., ASCE*, 133(2), 155-161.
- Srikantiah, H. R. (1987). "Laterite and lateritic soils of west coast of India." In B. T. *Proc. 9th South-east Asian Geotechnical Conference*. Asian Institute of Technology: Bangkok, Thailand,159-169.
- Sudhir, K., Subrata, H. and Singhal, D. C. (2011). "Groundwater Resources Management through Flow Modeling in Lower Part of Bhagirathi - Jalangi Interfluve, Nadia, West Bengal." *J. Geol Soc India.*, 78, 587-598.
- Suresh, B. D. S., Atul, K. S., Mauricio, A. N. and Eduardo, M. (2008). "Hydraulic response of a tidally forced coastal aquifer, Pontal do Parana, Brazil." *Hydrogeol. J*, 16, 1427–1439.
- Surinaidu, L., Gurunadha, V.V.S. and Ramesh, G. (2011). "Assessment of groundwater inflows into Kuteshwar Limestone Mines through flow modeling

study, Madhya Pradesh, India.” *Arab. J Geosci.* DOI 10.1007/s12517-011-0421-5

Sylus, K. J. and Rahesh, H. (2015). “The Study of Sea Water Intrusion in Coastal Aquifer by Electrical Conductivity and Total Dissolved Solid Method in Gurpur and Netravathi River Basin.” *Aquatic Proc.* (Elsevier), 4, 57-64
DOI:[10.1016/j.aqpro.2015.02.009](https://doi.org/10.1016/j.aqpro.2015.02.009)

Takounjou, F.A., Gurunadha, V.V.S, Ndam, N. J., Sigha, N .L. and Ekodeck, G.E. (2009). “Groundwater flow modelling in the upper Anga’a river watershed, Yaounde, Cameroon.” *Afr. J Environ. Sci. Technol.*, 3 (10), 341-352.

Tartakovsky, G. D. and Neuman, S. P. (2007). “Three-dimensional saturated-unsaturated flow with axial symmetry to a partially penetrating well in a compressible unconfined aquifer.” *Water Resour. Res.*, 43(1).

Theis, C.V (1935). “The Relation between lowering the piezometric surface and the rate and duration of discharge of a well using ground water storage.” *Trans Am. Geophys.Union.*, 2, 519-524.

Ting, C. S., Kerh, T. and Liao, C. J. (1998). “Estimation of groundwater recharge using the chloride mass-balance method, Pingtung Plain, Taiwan. *Hydrogeol. J.*, 6(2), 282-292.

Todd, D. K. (1959). “Ground water hydrology.” Wiley, New York

Todd, D.K. and Mays, L. W. (2005). “Groundwater hydrology.” 3rd edition, John Wiley and Sons, New York, 93.

- Udayakumar, G. (2008). "Subsurface barrier for water conservation in lateritic formations", Ph.D. thesis, Department of Applied Mechanics & Hydraulics, National Institute of Technology, Karnataka, Surathkal, India, 88-92.
- Unnikrishnan, A. S. and Shankar, D. (2007). "Are sea-level-rise trends along the coasts of the north Indian Ocean consistent with global estimates?". *Global and Planet. Change*, 57(3), 301-307.
- Van Liew, M. W., Arnold, J.G and Garbrecht, J.D. (2003). "Hydrologic simulation on agricultural watersheds: Choosing between two models." *Trans. ASAE* 46(6), 1539-1551.
- Vandenbohede, A., Houtte. E.V. and Lebbe, L. (2009). "Sustainable groundwater extraction in coastal areas: a Belgian example." *J. Environ. Geol.*, 57, 735–747.
- Vandenbohede, A., Mollema, P. N., Greggio, N. and Antonellini, M. (2014). "Seasonal dynamic of a shallow freshwater lens due to irrigation in the coastal plain of Ravenna, Italy." *Hydrogeol. J.*, 22(4), 893-909.
- Varni, M.R and Usunoff, E. J (1999). "Simulation of regional-scale groundwater flow in the Azul River basin, Buenos Aires Province, Argentina." *Hydrogeol. J.*, 7, 180–187.
- Volker, A. (1983). "Rivers of SE Asia: their regime, utilisation and regulation." *Hydrology of humid tropical regions*, 140, 127–138.
- Voss, C. (1984). "*SUTRA*: A finite-element simulation model for saturated-unsaturated fluid-density-dependent groundwater flow with energy transport or chemically-reactive single-species solute transport." *U.S. Geol. Surv. Water Resour. Invest. Rep. 84-4369*, USA.

- Vyshali. (2008). Studies on saltwater intrusion in the coastal D.K district, Karnataka.Ph.D. Thesis, Department of Applied Mechanics & Hydraulics, National Institute of Technology Karnataka, Surathkal, Mangalore, India. 52-72
- Wang, S., Jingli, S., Xianfang, S., Yongbo, Z., Zhibin, H. and Xiaoyuan, Z. (2008). “Application of MODFLOW and geographic information system to groundwater flow simulation in North China Plain, China.” *Environ. Geol.*, 55, 1449–1462.
- Webb, M. D. and Howard, K. W. F. (2011). "Modelling the transient response of saline intrusion to rising sea-levels." *Ground Water*, 49 (4), 560-569.
- Weiss, M. and Gvirtzman, H. (2007). “Estimating ground water recharge using flow models of perched karstic aquifers.” *Ground Water*, 45(6), 761-773.
- Werner, A. D., Bakker, M., Post, V. E., Vandenbohede, A., Lu, C., Ataie-Ashtiani, B. and Barry, D. A. (2013). “Seawater intrusion processes, investigation and management: recent advances and future challenges.” *Adv. Water Resour.*, 51, 3-26.
- Willmott, C. J. (1981). “On the validation of models.” *Physical Geography* 2, 184-194.
- Xi, H., Qi, F., Wei, L., Jian, H. S., Zongqiang, C. and Yonghong, Su. (2010). “The research of groundwater flow model in Ejina Basin, Northwestern China.” *Environ. Earth Sci.*, 60, 953–963.
- Xu , G. H., Zhongyi, Q. and Luis, S. P. (2011) “Using MODFLOW and GIS to Assess Changes in Groundwater Dynamics in Response to Water Saving Measures in

- Irrigation Districts of the Upper Yellow River Basin.” *Water Resour. Manag.*, 25, 2035–2059.
- Yang, J. S., Son, M. W., Chung, E. S. and Kim, I. H. (2015). “Prioritizing Feasible Locations for Permeable Pavement Using MODFLOW and Multi-criteria Decision Making Methods.” *Water Resour. Manag.*, 29(12), 4539-4555.
- Yang, Q., Wenxi, L. and Yanna, F. (2011). “Numerical Modeling of Three Dimension Groundwater Flow in Tongliao (China).” *Proc. Engineering*, 24, 638 – 642.
- Yeh, G., Cheng, J. and Cheng, H. (1994). “3DFEMFAT: A 3-dimensional finite element model of density-dependent flow and transport through saturated-unsaturated media, version 2.0.” *Technical Report*, Dept. of Civil and Environ. Eng., Pennsylvania State Univ., University Park, PA.
- Zheng, C. (2006). “MT3DMS v5.2 supplemental user’s guide.” Department of Geological Sciences, University of Alabama, *Technical Report*, U.S. Army Engineer Research and Development Center.
- Zheng, C. and Bennett, G. D. (1995). “Applied contaminant transport modeling, theory and practice.” Van Nostrand Reinhold.
- Zheng, C. and Bennett, G. D. (2002). “Applied contaminant transport modeling.”, Vol. 2, New York, Wiley-Interscience.
- Zheng, C. and Wang, K. (1999). “A modular three dimensional multispecies transport model for simulation of advection, dispersion and chemical reactions of contaminants in groundwater systems.” *Contract Report SERD99-1*, U.S. Army Corps of Engineers, United States.

Zhou, P., Li, G., Lu, Y. and Li, M. (2014). “Numerical modeling of the effects of beach slope on water-table fluctuation in the unconfined aquifer of Donghai Island, China.” *Hydrogeol. J.*, 22(2), 383-396.

Zume, J. and Tarhule, A. (2008). “Simulating the impacts of groundwater pumping on stream–aquifer dynamics in semiarid northwestern Oklahoma, USA.” *Hydrogeol. J.*, 16, 797–810.

APPENDIX I

Table 1 Sensitivity index calculation for hydraulic conductivity

Well No	Change in hydraulic conductivity (%)	Absolute residual mean (m)	$ \Delta y /y_0$	$\Delta x/x_0$	Sensitivity index	Sensitivity class
1	-75	1.19	0.38	-0.75	-0.51	High
	-50	0.84	0.03	-0.50	-0.05	Medium
	-25	0.76	0.11	-0.25	-0.45	High
	Calibrated	0.86				
	25	0.93	0.09	0.25	0.35	High
	50	1.03	0.20	0.50	0.40	High
	75	1.12	0.31	0.75	0.41	High
2	-75	1.59	0.23	-0.75	-0.31	High
	-50	1.38	0.07	-0.50	-0.14	Medium
	-25	1.16	0.10	-0.25	-0.42	High
	Calibrated	1.29				
	25	1.40	0.08	0.25	0.32	High
	50	1.62	0.26	0.50	0.51	High
	75	1.82	0.41	0.75	0.54	High
3	-75	2.46	0.22	-0.75	-0.29	High
	-50	2.30	0.14	-0.50	-0.27	High
	-25	2.16	0.07	-0.25	-0.26	High
	Calibrated	2.02				
	25	1.96	0.03	0.25	0.12	Medium
	50	1.96	0.03	0.50	0.06	Medium
	75	2.04	0.01	0.75	0.01	Small to neglect
4	-75	10.61	6.03	-0.75	-8.04	Very high
	-50	4.42	1.93	-0.50	-3.85	Very high
	-25	2.29	0.52	-0.25	-2.07	Very high
	Calibrated	1.51				
	25	1.60	0.06	0.25	0.23	High
	50	1.66	0.10	0.50	0.20	High
	75	1.89	0.25	0.75	0.34	High
5	-75	2.35	1.91	-0.75	-2.55	Very high
	-50	1.05	0.30	-0.50	-0.61	High
	-25	0.73	0.09	-0.25	-0.36	High
	Calibrated	0.81				
	25	0.63	0.22	0.25	0.88	High
	50	0.65	0.20	0.50	0.40	High
	75	0.67	0.17	0.75	0.22	High
6	-75	3.59	3.90	-0.75	-5.20	Very high

	-50	1.75	1.38	-0.50	-2.77	Very high
	-25	1.09	0.48	-0.25	-1.94	Very high
	Calibrated	0.73				
	25	0.64	0.13	0.25	0.52	High
	50	0.58	0.20	0.50	0.40	High
	75	0.58	0.21	0.75	0.28	High
7	-75	0.73	0.04	-0.75	-0.05	Medium
	-50	0.48	0.36	-0.50	-0.72	High
	-25	0.52	0.31	-0.25	-1.25	Very high
	Calibrated	0.75				
	25	0.66	0.12	0.25	0.48	High
	50	0.74	0.02	0.50	0.03	Small to neglect
	75	0.80	0.07	0.75	0.09	Medium
8	-75	1.27	0.20	-0.75	-0.26	High
	-50	0.92	0.13	-0.50	-0.26	High
	-25	0.88	0.16	-0.25	-0.65	High
	Calibrated	1.06				
	25	1.24	0.18	0.25	0.70	High
	50	1.53	0.45	0.50	0.90	High
	75	1.80	0.71	0.75	0.94	High
9	-75	1.55	0.89	-0.75	-1.19	Very high
	-50	0.87	0.06	-0.50	-0.12	Medium
	-25	0.61	0.26	-0.25	-1.03	Very high
	Calibrated	0.82				
	25	0.73	0.11	0.25	0.45	High
	50	0.91	0.10	0.50	0.20	High
	75	1.12	0.37	0.75	0.49	High
10	-75	2.41	1.04	-0.75	-1.39	Very high
	-50	1.25	0.06	-0.50	-0.12	Medium
	-25	0.83	0.30	-0.25	-1.19	Very high
	Calibrated	1.18				
	25	1.82	0.54	0.25	2.18	Very high
	50	2.48	1.11	0.50	2.22	Very high
	75	3.06	1.60	0.75	2.13	Very high
11	-75	2.54	1.66	-0.75	-2.22	Very high
	-50	1.43	0.51	-0.50	-1.01	Very high
	-25	0.97	0.02	-0.25	-0.09	Medium
	Calibrated	0.95				
	25	1.57	0.65	0.25	2.60	Very high
	50	2.17	1.28	0.50	2.55	Very high
	75	2.70	1.84	0.75	2.45	Very high
12	-75	3.94	1.52	-0.75	-2.03	Very high
	-50	2.60	0.67	-0.50	-1.33	Very high
	-25	1.88	0.20	-0.25	-0.80	High
	Calibrated	1.56				

	25	1.65	0.06	0.25	0.24	High
	50	1.83	0.17	0.50	0.34	High
	75	2.24	0.44	0.75	0.58	High
13	-75	0.69	0.44	-0.75	-0.59	High
	-50	0.48	0.61	-0.50	-1.21	Very high
	-25	0.58	0.53	-0.25	-2.10	Very high
	Calibrated	1.23				
	25	0.89	0.27	0.25	1.10	Very high
	50	1.03	0.17	0.50	0.33	High
	75	1.15	0.07	0.75	0.09	Medium
14	-75	1.61	0.06	-0.75	-0.08	Medium
	-50	1.19	0.31	-0.50	-0.61	High
	-25	1.18	0.31	-0.25	-1.24	Very high
	Calibrated	1.71				
	25	1.50	0.12	0.25	0.48	High
	50	1.68	0.02	0.50	0.04	Small to neglect
	75	1.84	0.08	0.75	0.10	Medium
15	-75	1.41	0.09	-0.75	-0.12	Medium
	-50	1.36	0.05	-0.50	-0.10	Medium
	-25	1.32	0.02	-0.25	-0.09	Medium
	Calibrated	1.30				
	25	1.28	0.01	0.25	0.05	Small to neglect
	50	1.27	0.02	0.50	0.03	Small to neglect
	75	1.28	0.01	0.75	0.02	Small to neglect
16	-75	1.55	1.08	-0.75	-1.44	Very high
	-50	1.11	0.49	-0.50	-0.99	High
	-25	0.89	0.19	-0.25	-0.76	High
	Calibrated	0.75				
	25	0.65	0.13	0.25	0.51	High
	50	0.58	0.22	0.50	0.44	High
	75	0.54	0.28	0.75	0.37	High
17	-75	1.76	1.53	-0.75	-2.04	Very high
	-50	1.14	0.64	-0.50	-1.28	Very high
	-25	0.85	0.23	-0.25	-0.92	High
	Calibrated	0.69				
	25	0.61	0.12	0.25	0.50	High
	50	0.56	0.19	0.50	0.38	High
	75	0.54	0.23	0.75	0.31	High
18	-75	2.49	0.56	-0.75	-0.75	High
	-50	2.01	0.26	-0.50	-0.52	High
	-25	1.76	0.11	-0.25	-0.42	High
	Calibrated	1.59				

	25	1.47	0.08	0.25	0.32	High
	50	1.37	0.14	0.50	0.28	High
	75	1.29	0.19	0.75	0.26	High
19	-75	3.66	0.30	-0.75	-0.41	High
	-50	3.21	0.15	-0.50	-0.29	High
	-25	2.97	0.06	-0.25	-0.24	High
	Calibrated	2.80				
	25	2.66	0.05	0.25	0.20	High
	50	2.55	0.09	0.50	0.18	Medium
	75	2.44	0.13	0.75	0.17	Medium
20	-75	2.91	0.54	-0.75	-0.72	High
	-50	2.37	0.25	-0.50	-0.50	High
	-25	2.08	0.10	-0.25	-0.41	High
	Calibrated	1.89				
	25	1.75	0.08	0.25	0.30	High
	50	1.63	0.14	0.50	0.27	High
	75	1.53	0.19	0.75	0.25	High
21	-75	2.90	1.11	-0.75	-1.48	Very high
	-50	1.97	0.44	-0.50	-0.87	High
	-25	1.59	0.16	-0.25	-0.64	High
	Calibrated	1.37				
	25	1.22	0.11	0.25	0.44	High
	50	1.11	0.19	0.50	0.39	High
	75	1.02	0.26	0.75	0.35	High
22	-75	1.41	2.69	-0.75	-3.58	Very high
	-50	0.69	0.81	-0.50	-1.62	Very high
	-25	0.49	0.27	-0.25	-1.06	Very high
	Calibrated	0.38				
	25	0.39	0.03	0.25	0.11	Medium
	50	0.41	0.07	0.50	0.14	Medium
	75	0.43	0.13	0.75	0.17	Medium
23	-75	0.63	0.19	-0.75	-0.26	High
	-50	0.53	0.31	-0.50	-0.62	High
	-25	0.69	0.11	-0.25	-0.46	High
	Calibrated	0.78				
	25	0.83	0.07	0.25	0.26	High
	50	0.86	0.11	0.50	0.22	High
	75	0.89	0.14	0.75	0.19	Medium
24	-75	0.89	0.11	-0.75	-0.14	Medium
	-50	0.94	0.05	-0.50	-0.11	Medium
	-25	0.97	0.02	-0.25	-0.07	Medium
	Calibrated	0.99				
	25	1.01	0.01	0.25	0.05	Medium
	50	1.02	0.02	0.50	0.05	Medium
	75	1.03	0.03	0.75	0.05	Medium
25	-75	7.12	5.42	-0.75	-7.23	High

	-50	3.06	1.76	-0.50	-3.51	High
	-25	1.86	0.68	-0.25	-2.73	High
	Calibrated	1.11				
	25	1.14	0.03	0.25	0.11	Medium
	50	1.06	0.04	0.50	0.08	Medium
	75	1.09	0.02	0.75	0.03	Small to neglect
26	-75	2.54	1.49	-0.75	-1.98	Very high
	-50	1.46	0.43	-0.50	-0.85	High
	-25	1.18	0.16	-0.25	-0.62	High
	Calibrated	1.02				
	25	1.48	0.45	0.25	1.79	Very high
	50	1.70	0.67	0.50	1.33	Very high
	75	1.92	0.88	0.75	1.17	Very high
27	-75	2.93	3.45	-0.75	-4.60	Very high
	-50	1.89	1.86	-0.50	-3.73	Very high
	-25	1.27	0.92	-0.25	-3.68	Very high
	Calibrated	0.66				
	25	1.10	0.67	0.25	2.67	Very high
	50	1.39	1.11	0.50	2.22	Very high
	75	1.79	1.71	0.75	2.28	Very high
28	-75	2.65	1.52	-0.75	-2.03	Very high
	-50	1.41	0.33	-0.50	-0.67	High
	-25	1.16	0.10	-0.25	-0.39	High
	Calibrated	1.05				
	25	1.24	0.18	0.25	0.71	High
	50	1.35	0.28	0.50	0.56	High
	75	1.46	0.39	0.75	0.52	High
29	-75	1.29	0.58	-0.75	-0.77	High
	-50	0.87	0.07	-0.50	-0.13	Medium
	-25	0.81	0.01	-0.25	-0.06	Medium
	Calibrated	0.82				
	25	0.85	0.04	0.25	0.15	Medium
	50	0.87	0.06	0.50	0.13	Medium
	75	0.89	0.08	0.75	0.11	Medium

Table 2 Sensitivity index calculation for specific yield

Well No	Change in specific yield (%)	Absolute residual mean (m)	$ \Delta y /y_0$	$\Delta x/x_0$	Sensitivity index	Sensitivity class
1	-75	0.99	0.15	-0.75	-0.20	Medium
	-50	0.94	0.09	-0.50	-0.19	Medium
	-25	0.83	0.04	-0.25	-0.14	Medium
	Calibrated	0.86				
	25	0.82	0.05	0.25	0.20	Medium

	50	0.81	0.05	0.50	0.11	Medium
	75	0.82	0.04	0.75	0.05	Medium
2	-75	1.44	0.12	-0.75	-0.16	Medium
	-50	1.37	0.06	-0.50	-0.12	Medium
	-25	1.23	0.05	-0.25	-0.18	Medium
	Calibrated	1.29				
	25	1.25	0.03	0.25	0.14	Medium
	50	1.32	0.03	0.50	0.05	Medium
	75	1.40	0.08	0.75	0.11	Medium
3	-75	2.22	0.10	-0.75	-0.13	Medium
	-50	1.84	0.09	-0.50	-0.19	Medium
	-25	1.94	0.04	-0.25	-0.17	Medium
	Calibrated	2.02				
	25	2.08	0.03	0.25	0.11	Medium
	50	2.09	0.03	0.50	0.07	Medium
	75	2.11	0.04	0.75	0.05	Medium
4	-75	1.67	0.11	-0.75	-0.15	Medium
	-50	1.63	0.08	-0.50	-0.16	Medium
	-25	1.46	0.03	-0.25	-0.13	Medium
	Calibrated	1.51				
	25	1.46	0.03	0.25	0.13	Medium
	50	1.64	0.09	0.50	0.17	Medium
	75	1.42	0.06	0.75	0.08	Medium
5	-75	1.08	0.34	-0.75	-0.45	High
	-50	0.85	0.05	-0.50	-0.10	Medium
	-25	0.72	0.11	-0.25	-0.44	High
	Calibrated	0.81				
	25	0.59	0.27	0.25	1.08	Very high
	50	0.56	0.31	0.50	0.62	High
	75	0.53	0.34	0.75	0.45	High
6	-75	1.48	1.02	-0.75	-1.36	Very high
	-50	1.06	0.45	-0.50	-0.90	High
	-25	0.88	0.20	-0.25	-0.82	High
	Calibrated	0.73				
	25	0.74	0.01	0.25	0.05	Small to neglect
	50	0.73	0.00	0.50	0.01	Small to neglect
	75	0.73	0.00	0.75	0.01	Small to neglect
7	-75	0.87	0.16	-0.75	-0.21	High
	-50	0.63	0.16	-0.50	-0.33	High
	-25	0.59	0.21	-0.25	-0.85	High
	Calibrated	0.75				
	25	0.58	0.22	0.25	0.89	High
	50	0.57	0.24	0.50	0.47	High

	75	0.57	0.24	0.75	0.32	High
8	-75	1.19	0.12	-0.75	-0.17	Medium
	-50	1.15	0.08	-0.50	-0.17	Medium
	-25	1.02	0.04	-0.25	-0.14	Medium
	Calibrated	1.06				
	25	1.01	0.05	0.25	0.18	Medium
	50	1.01	0.04	0.50	0.09	Medium
	75	1.01	0.04	0.75	0.06	Medium
9	-75	2.01	1.45	-0.75	-1.93	Very high
	-50	1.08	0.31	-0.50	-0.62	High
	-25	0.76	0.07	-0.25	-0.28	High
	Calibrated	0.82				
	25	0.51	0.38	0.25	1.51	Very high
	50	0.45	0.45	0.50	0.89	High
	75	0.41	0.50	0.75	0.66	High
10	-75	4.07	2.46	-0.75	-3.28	Very high
	-50	1.96	0.66	-0.50	-1.32	Very high
	-25	1.37	0.16	-0.25	-0.64	High
	Calibrated	1.18				
	25	1.11	0.06	0.25	0.23	High
	50	1.07	0.09	0.50	0.18	Medium
	75	1.05	0.11	0.75	0.14	Medium
11	-75	4.07	3.28	-0.75	-4.37	Very high
	-50	2.02	1.12	-0.50	-2.23	Very high
	-25	1.39	0.46	-0.25	-1.84	Very high
	Calibrated	0.95				
	25	0.98	0.02	0.25	0.10	Medium
	50	0.88	0.08	0.50	0.15	Medium
	75	0.82	0.14	0.75	0.19	Medium
12	-75	3.78	1.42	-0.75	-1.89	Very high
	-50	2.16	0.38	-0.50	-0.76	High
	-25	1.64	0.05	-0.25	-0.19	Medium
	Calibrated	1.56				
	25	1.53	0.02	0.25	0.09	Medium
	50	1.56	0.00	0.50	0.01	Small to neglect
	75	1.58	0.01	0.75	0.01	Small to neglect
13	-75	1.25	0.01	-0.75	-0.02	Small to neglect
	-50	0.96	0.22	-0.50	-0.44	High
	-25	0.81	0.34	-0.25	-1.37	Very high
	Calibrated	1.23				
	25	0.71	0.43	0.25	1.70	Very high
	50	0.68	0.45	0.50	0.89	High
	75	0.68	0.45	0.75	0.60	High

14	-75	1.98	0.16	-0.75	-0.21	High
	-50	1.62	0.05	-0.50	-0.10	Medium
	-25	1.45	0.15	-0.25	-0.60	High
	Calibrated	1.71				
	25	1.27	0.26	0.25	1.02	Very high
	50	1.23	0.28	0.50	0.56	High
	75	1.20	0.30	0.75	0.40	High
15	-75	1.25	0.03	-0.75	-0.04	Small to neglect
	-50	1.27	0.02	-0.50	-0.04	Small to neglect
	-25	1.29	0.01	-0.25	-0.03	Small to neglect
	Calibrated	1.30				
	25	1.30	0.01	0.25	0.02	Small to neglect
	50	1.31	0.01	0.50	0.02	Small to neglect
	75	1.31	0.01	0.75	0.02	Small to neglect
16	-75	0.77	0.03	-0.75	-0.04	Small to neglect
	-50	0.75	0.01	-0.50	-0.02	Small to neglect
	-25	0.74	0.00	-0.25	-0.02	Small to neglect
	Calibrated	0.75				
	25	0.75	0.00	0.25	0.00	Small to neglect
	50	0.76	0.02	0.50	0.03	Small to neglect
	75	0.77	0.03	0.75	0.04	Small to neglect
17	-75	0.72	0.03	-0.75	-0.04	Small to neglect
	-50	0.70	0.00	-0.50	-0.01	Small to neglect
	-25	0.70	0.00	-0.25	-0.01	Small to neglect
	Calibrated	0.69				
	25	0.70	0.00	0.25	0.02	Small to neglect
	50	0.71	0.02	0.50	0.04	Small to neglect
	75	0.71	0.03	0.75	0.04	Small to neglect
18	-75	1.66	0.04	-0.75	-0.06	Medium

	-50	1.69	0.06	-0.50	-0.12	Medium
	-25	1.65	0.03	-0.25	-0.13	Medium
	Calibrated	1.59				
	25	1.54	0.03	0.25	0.13	Medium
	50	1.49	0.06	0.50	0.13	Medium
	75	1.45	0.09	0.75	0.12	Medium
19	-75	2.79	0.00	-0.75	-0.01	Small to neglect
	-50	2.93	0.04	-0.50	-0.09	Medium
	-25	2.87	0.02	-0.25	-0.10	Medium
	Calibrated	2.80				
	25	2.74	0.02	0.25	0.09	Medium
	50	2.68	0.04	0.50	0.09	Medium
20	75	2.63	0.06	0.75	0.08	Medium
	-75	1.78	0.06	-0.75	-0.08	Medium
	-50	1.93	0.02	-0.50	-0.04	Small to neglect
	-25	1.92	0.02	-0.25	-0.07	Medium
	Calibrated	1.89				
	25	1.85	0.02	0.25	0.08	Medium
21	50	1.81	0.04	0.50	0.09	Medium
	75	1.76	0.07	0.75	0.09	Medium
	-75	1.56	0.13	-0.75	-0.18	Medium
	-50	1.42	0.04	-0.50	-0.07	Medium
	-25	1.39	0.02	-0.25	-0.06	Medium
	Calibrated	1.37				
22	25	1.35	0.02	0.25	0.07	Medium
	50	1.32	0.04	0.50	0.07	Medium
	75	1.29	0.06	0.75	0.08	Medium
	-75	0.47	0.22	-0.75	-0.30	High
	-50	0.44	0.15	-0.50	-0.30	High
	-25	0.43	0.11	-0.25	-0.44	High
23	Calibrated	0.38				
	25	0.40	0.04	0.25	0.18	Medium
	50	0.39	0.02	0.50	0.05	Medium
	75	0.40	0.03	0.75	0.05	Medium
	-75	0.94	0.21	-0.75	-0.28	High
	-50	0.84	0.08	-0.50	-0.16	Medium
24	-25	0.80	0.03	-0.25	-0.12	Medium
	Calibrated	0.78				
	25	0.76	0.02	0.25	0.09	Medium
	50	0.75	0.04	0.50	0.08	Medium
	75	0.74	0.05	0.75	0.07	Medium
	-75	1.29	0.30	-0.75	-0.40	High
24	-50	1.08	0.09	-0.50	-0.18	Medium
	-25	1.02	0.03	-0.25	-0.10	Medium

	Calibrated	0.99				
	25	0.98	0.01	0.25	0.04	Small to neglect
	50	0.98	0.01	0.50	0.02	Small to neglect
	75	0.98	0.01	0.75	0.02	Small to neglect
25	-75	1.38	0.24	-0.75	-0.32	High
	-50	1.37	0.23	-0.50	-0.47	High
	-25	1.36	0.23	-0.25	-0.92	High
	Calibrated	1.11				
	25	1.34	0.20	0.25	0.82	High
	50	1.33	0.20	0.50	0.40	High
26	-75	3.91	2.83	-0.75	-3.77	Very high
	-50	2.36	1.31	-0.50	-2.62	Very high
	-25	1.67	0.63	-0.25	-2.52	Very high
	Calibrated	1.02				
	25	1.06	0.04	0.25	0.15	Medium
	50	0.94	0.08	0.50	0.16	Medium
27	-75	4.96	6.53	-0.75	-8.71	Very high
	-50	2.24	2.40	-0.50	-4.81	Very high
	-25	1.32	1.00	-0.25	-3.99	Very high
	Calibrated	0.66				
	25	0.95	0.43	0.25	1.74	Very high
	50	0.93	0.41	0.50	0.83	High
28	-75	2.08	0.97	-0.75	-1.30	Very high
	-50	1.55	0.47	-0.50	-0.94	High
	-25	1.29	0.23	-0.25	-0.91	High
	Calibrated	1.05				
	25	1.08	0.02	0.25	0.09	Medium
	50	1.03	0.02	0.50	0.04	Small to neglect
29	-75	0.84	0.02	-0.75	-0.03	Small to neglect
	-50	0.83	0.01	-0.50	-0.02	Small to neglect
	-25	0.82	0.00	-0.25	-0.01	Small to neglect
	Calibrated	0.82				
	25	0.82	0.00	0.25	0.00	Small to neglect
	50	0.82	0.00	0.50	0.00	Small to neglect

	75	0.82	0.00	0.75	0.00	Small to neglect
--	----	------	------	------	------	------------------

Table 3 Sensitivity index calculation for recharge rate

Well No	Change in recharge rate (%)	Absolute residual mean (m)	$ \Delta y /y_0$	$\Delta x/x_0$	Sensitivity index	Sensitivity class
1	-75	1.94	1.26	-0.75	-1.68	Very high
	-50	1.50	0.75	-0.50	-1.50	Very high
	-25	1.08	0.25	-0.25	-1.02	Very high
	Calibrated	0.86				
	25	0.80	0.06	0.25	0.26	High
	50	0.97	0.13	0.50	0.27	High
	75	2.73	2.18	0.75	2.91	Very high
2	-75	2.92	1.26	-0.75	-1.68	Very high
	-50	2.30	0.78	-0.50	-1.57	Very high
	-25	1.69	0.31	-0.25	-1.24	Very high
	Calibrated	1.29				
	25	1.12	0.13	0.25	0.54	High
	50	1.16	0.10	0.50	0.20	High
	75	3.41	1.64	0.75	2.19	Very high
3	-75	3.83	0.89	-0.75	-1.19	Very high
	-50	2.77	0.37	-0.50	-0.74	High
	-25	2.16	0.07	-0.25	-0.27	High
	Calibrated	2.02				
	25	2.16	0.07	0.25	0.26	High
	50	2.34	0.15	0.50	0.31	High
	75	5.69	1.81	0.75	2.42	Very high
4	-75	3.50	1.32	-0.75	-1.76	Very high
	-50	2.49	0.65	-0.50	-1.30	Very high
	-25	1.86	0.23	-0.25	-0.94	High
	Calibrated	1.51				
	25	2.53	0.67	0.25	2.70	Very high
	50	3.82	1.53	0.50	3.07	Very high
	75	5.87	2.89	0.75	3.85	Very high
5	-75	0.85	0.06	-0.75	-0.08	Medium
	-50	0.69	0.14	-0.50	-0.28	High
	-25	0.62	0.24	-0.25	-0.95	High
	Calibrated	0.81				
	25	0.78	0.03	0.25	0.13	Medium
	50	0.96	0.18	0.50	0.37	High
	75	1.44	0.78	0.75	1.04	Very high
6	-75	0.86	0.17	-0.75	-0.23	High
	-50	0.55	0.25	-0.50	-0.50	High
	-25	0.53	0.28	-0.25	-1.12	Very high

	Calibrated	0.73				
	25	1.16	0.59	0.25	2.35	Very high
	50	1.58	1.15	0.50	2.31	Very high
	75	2.32	2.16	0.75	2.88	Very high
7	-75	1.00	0.33	-0.75	-0.44	High
	-50	0.85	0.13	-0.50	-0.27	High
	-25	0.70	0.07	-0.25	-0.26	High
	Calibrated	0.75				
	25	0.52	0.31	0.25	1.24	Very high
	50	0.51	0.33	0.50	0.66	High
	75	1.19	0.58	0.75	0.78	High
8	-75	2.60	1.46	-0.75	-1.95	Very high
	-50	2.02	0.91	-0.50	-1.82	Very high
	-25	1.44	0.36	-0.25	-1.45	Very high
	Calibrated	1.06				
	25	0.88	0.17	0.25	0.66	High
	50	1.19	0.12	0.50	0.24	High
	75	1.41	0.33	0.75	0.44	High
9	-75	2.08	1.53	-0.75	-2.04	Very high
	-50	1.46	0.77	-0.50	-1.54	Very high
	-25	0.86	0.05	-0.25	-0.19	Medium
	Calibrated	0.82				
	25	0.77	0.07	0.25	0.27	High
	50	1.20	0.46	0.50	0.91	High
	75	1.84	1.24	0.75	1.65	Very high
10	-75	4.85	3.12	-0.75	-4.16	Very high
	-50	3.59	2.05	-0.50	-4.09	Very high
	-25	2.32	0.97	-0.25	-3.89	Very high
	Calibrated	1.18				
	25	1.08	0.08	0.25	0.32	High
	50	1.93	0.64	0.50	1.29	Very high
	75	3.08	1.61	0.75	2.15	Very high
11	-75	4.36	3.58	-0.75	-4.77	Very high
	-50	3.18	2.34	-0.50	-4.68	Very high
	-25	2.01	1.11	-0.25	-4.43	Very high
	Calibrated	0.95				
	25	1.26	0.32	0.25	1.29	Very high
	50	2.06	1.16	0.50	2.33	Very high
	75	3.16	2.32	0.75	3.09	Very high
12	-75	3.92	1.51	-0.75	-2.01	Very high
	-50	2.78	0.78	-0.50	-1.55	Very high
	-25	1.78	0.14	-0.25	-0.55	High
	Calibrated	1.56				
	25	2.07	0.32	0.25	1.30	Very high
	50	2.92	0.87	0.50	1.74	Very high
	75	3.82	1.44	0.75	1.92	Very high

13	-75	1.65	0.34	-0.75	-0.45	High
	-50	1.32	0.07	-0.50	-0.14	Medium
	-25	0.98	0.21	-0.25	-0.82	High
	Calibrated	1.23				
	25	0.62	0.50	0.25	1.99	Very high
	50	0.58	0.53	0.50	1.06	Very high
	75	0.58	0.53	0.75	0.70	High
14	-75	2.61	0.53	-0.75	-0.71	High
	-50	2.03	0.19	-0.50	-0.38	High
	-25	1.57	0.08	-0.25	-0.33	High
	Calibrated	1.71				
	25	1.25	0.27	0.25	1.08	Very high
	50	1.22	0.29	0.50	0.58	High
	75	1.21	0.29	0.75	0.39	High
15	-75	1.37	0.06	-0.75	-0.08	Medium
	-50	1.29	0.01	-0.50	-0.01	Small to neglect
	-25	1.29	0.00	-0.25	-0.02	Small to neglect
	Calibrated	1.30				
	25	1.30	0.00	0.25	0.02	Small to neglect
	50	1.17	0.10	0.50	0.20	Medium
	75	1.17	0.10	0.75	0.13	Medium
16	-75	0.88	0.18	-0.75	-0.23	High
	-50	0.56	0.25	-0.50	-0.50	High
	-25	0.59	0.21	-0.25	-0.84	High
	Calibrated	0.75				
	25	0.96	0.29	0.25	1.16	Very high
	50	0.97	0.31	0.50	0.61	High
	75	1.22	0.64	0.75	0.85	High
17	-75	0.83	0.20	-0.75	-0.27	High
	-50	0.60	0.14	-0.50	-0.29	High
	-25	0.60	0.14	-0.25	-0.57	High
	Calibrated	0.69				
	25	0.89	0.28	0.25	1.13	Very high
	50	0.89	0.27	0.50	0.55	High
	75	1.09	0.58	0.75	0.77	High
18	-75	0.80	0.50	-0.75	-0.66	High
	-50	0.95	0.40	-0.50	-0.81	High
	-25	1.26	0.21	-0.25	-0.84	High
	Calibrated	1.59				
	25	1.90	0.19	0.25	0.77	High
	50	2.01	0.26	0.50	0.52	High
	75	2.29	0.44	0.75	0.58	High
19	-75	1.40	0.50	-0.75	-0.67	High

	-50	1.91	0.32	-0.50	-0.64	High
	-25	2.39	0.15	-0.25	-0.60	High
	Calibrated	2.80				
	25	3.18	0.13	0.25	0.53	High
	50	3.45	0.23	0.50	0.46	High
	75	3.79	0.35	0.75	0.47	High
20	-75	0.85	0.55	-0.75	-0.73	High
	-50	1.10	0.42	-0.50	-0.84	High
	-25	1.53	0.19	-0.25	-0.76	High
	Calibrated	1.89				
	25	2.21	0.17	0.25	0.68	High
	50	2.33	0.23	0.50	0.47	High
21	75	2.61	0.38	0.75	0.51	High
	-75	0.54	0.60	-0.75	-0.81	High
	-50	0.43	0.69	-0.50	-1.37	Very high
	-25	0.89	0.35	-0.25	-1.42	Very high
	Calibrated	1.37				
	25	1.88	0.37	0.25	1.48	Very high
22	50	2.17	0.58	0.50	1.16	Very high
	75	2.67	0.94	0.75	1.26	Very high
	-75	0.74	0.93	-0.75	-1.24	Very high
	-50	0.55	0.43	-0.50	-0.85	High
	-25	0.41	0.07	-0.25	-0.29	High
	Calibrated	0.38				
23	25	0.51	0.34	0.25	1.36	Very high
	50	0.63	0.63	0.50	1.26	Very high
	75	0.75	0.97	0.75	1.29	Very high
	-75	1.13	0.45	-0.75	-0.60	High
	-50	1.03	0.33	-0.50	-0.66	High
	-25	0.90	0.15	-0.25	-0.61	High
24	Calibrated	0.78				
	25	0.67	0.14	0.25	0.58	High
	50	0.71	0.09	0.50	0.18	Medium
	75	0.63	0.19	0.75	0.26	High
	-75	1.04	0.05	-0.75	-0.06	Medium
	-50	1.10	0.11	-0.50	-0.22	High
25	-25	1.04	0.05	-0.25	-0.19	Medium
	Calibrated	0.99				
	25	0.96	0.04	0.25	0.14	Medium
	50	1.03	0.03	0.50	0.07	Medium
25	75	1.00	0.00	0.75	0.01	Small to neglect
	-75	2.30	1.08	-0.75	-1.44	Very high
	-50	1.53	0.38	-0.50	-0.76	High
	-25	1.18	0.07	-0.25	-0.27	High
	Calibrated	1.11				

	25	1.77	0.60	0.25	2.39	Very high
	50	2.34	1.11	0.50	2.22	Very high
	75	2.99	1.70	0.75	2.27	Very high
26	-75	5.02	3.91	-0.75	-5.22	Very high
	-50	2.47	1.42	-0.50	-2.84	Very high
	-25	1.54	0.51	-0.25	-2.04	Very high
	Calibrated	1.02				
	25	1.30	0.27	0.25	1.07	Very high
	50	1.45	0.41	0.50	0.83	High
	75	1.70	0.66	0.75	0.88	High
27	-75	4.13	5.26	-0.75	-7.01	Very high
	-50	2.26	2.43	-0.50	-4.86	Very high
	-25	1.13	0.71	-0.25	-2.83	Very high
	Calibrated	0.66				
	25	1.31	0.99	0.25	3.97	Very high
	50	1.69	1.57	0.50	3.14	Very high
	75	2.14	2.24	0.75	2.99	Very high
28	-75	3.11	1.95	-0.75	-2.60	Very high
	-50	2.09	0.98	-0.50	-1.96	Very high
	-25	1.45	0.37	-0.25	-1.49	Very high
	Calibrated	1.05				
	25	1.16	0.10	0.25	0.39	High
	50	1.31	0.24	0.50	0.48	High
	75	1.55	0.47	0.75	0.63	High
29	-75	0.98	0.20	-0.75	-0.26	High
	-50	0.92	0.13	-0.50	-0.26	High
	-25	0.87	0.06	-0.25	-0.25	High
	Calibrated	0.82				
	25	0.80	0.02	0.25	0.09	Medium
	50	0.85	0.04	0.50	0.08	Medium
	75	0.85	0.04	0.75	0.06	Medium

PUBLICATIONS

International Journal Papers

- **Lathashri U.A** and A.Mahesha (2015) “Predictive simulation of seawater intrusion in a tropical, coastal aquifer”. **J. Environ. Engg., ASCE D 4015001** ([http://dx.doi.org/10.1061/\(ASCE\)EE.1943-7870.0001037](http://dx.doi.org/10.1061/(ASCE)EE.1943-7870.0001037)).
- **Lathashri.U.A** and A. Mahesha (2016) “Groundwater sustainability assessment in coastal aquifers”. *J. Earth. Syst. Sci.*, **SPRINGER (Accepted for publication)**

International Conference papers

- **Lathashri.U.A** and A. Mahesha (2015) “Simulation of Saltwater Intrusion in a Coastal Aquifer in Karnataka, India.”, *International Conference On Water Resources, Coastal And Ocean Engineering – ICWRCOE’2015*, National Institute of Technology Karnataka, Surathkal. *Published in Aquatic Procedia (Elsevier)*, 4, 700-705 DOI:[10.1016/j.aqpro.2015.02.090](https://doi.org/10.1016/j.aqpro.2015.02.090)
- **Lathashri.U.A** and A. Mahesha (2014) “Solute transport modeling of saltwater intrusion in coastal aquifers”, **International conference on Emerging trends in Engineering**, Department of Civil Engineering, NMAM Institute of Technology, Karnataka. ISBN: 978-93-83083-80-0.
- **Lathashri.U.A** and A. Mahesha (2014) “Solute transport modeling in tropical, coastal aquifer, a semi-conceptual approach”, **Fourth International conference on Hydrology and Watershed Management**, Centre for water resources, Institute of science and technology, JNTU, Hyderabad, Telangana state, India. ISBN: 978-81-8424-952-1.

RESUME

Name : Lathashri. U.A

Date of Birth : 09-12-1981

Address : Asst.Professor,
Department of Civil Engineering,
Manipal Institute of Technology,
Manipal, Udupi District,
Karnataka, India-5761

Mobile : (+91) 9483128565

Email(s) : ua.latha@gmail.com

Qualification : B.E. (Civil), M.Tech. (WRM)

Journal Publications : 2

No. of Conference Publications : 3

